Benthic-pelagic coupling and spatial dynamics of nutrient availability for benthic nuisance algae in the rocky nearshore zone of eastern Lake Erie

by

Joanna Majarreis

A thesis
presented to the University of Waterloo
in fulfillment of the
thesis requirement for the degree of
Doctor of Philosophy
in
Biology (Water)

Waterloo, Ontario, Canada, 2019

Examining Committee Membership

External Examiner	DR. HELENE CYR Associate Professor, University of Toronto
Supervisors	DR. RALPH E.H. SMITH Professor Emeritus, University of Waterloo
	DR. LEON BOEGMAN Associate Professor, Queen's University, Adjunct Professor, University of Waterloo
Internal Member	DR. ROLAND HALL Professor, University of Waterloo
Internal-external Member	DR. MICHAEL STONE Professor, University of Waterloo
Other Member(s)	DR. E. TODD HOWELL Research Scientist, Ontario Ministry of the Environment Adjunct Professor, University of Waterloo

AUTHOR'S DECLARATION

I hereby declare that I am the sole author of this thesis. This is a true copy of the thesis, including any required final revisions, as accepted by my examiners.

I understand that my thesis may be made electronically available to the public.

Abstract

Nuisance *Cladophora* growth in the nearshore during the summer growing season tends to imply nutrient, particularly phosphorus (P), enrichment in the benthos, especially where there is adequate light and hard substrate that would otherwise limit growth. Tributaries and dreissenid mussels are currently proposed as the main drivers of P to the nearshore fueling nuisance *Cladophora* growth, although other non-point sources may be important. How nutrients and Chl a are distributed in the nearshore may be a result of time of year in the growing season, proximity to the land-lake margin, proximity to the mouth of tributaries, and physical processes that might serve to enhance or reduce bottom mixing that provides seston to dreissenid mussels. Their relative effects may be modified by water motion, including prevailing currents, bottom turbulence, and boundary effects.

Nutrients and chlorophyll a (chla) bulk water samples were collected from the surface and near-bottom at stations using a 10L horizontal Van Dorn sampler in the northern nearshore of the East Basin of Lake Erie from during the *Cladophora* growing season (May-October) in 2013-2014, and in May 2015. The nearshore was divided into shallow (<10m deep) and deep (≥10m deep), in to make it relevant to nuisance *Cladophora* growth, which tends to grow to its highest biomass <10m. The full water column was profiled with YSI and FluroProbe sondes for specific conductivity, temperature, and chla. The bottom of the water column was profiled for horizontal water velocity using a down-looking ADCP, and temperature was measured using RBR temperature probes. This thesis specifically investigated horizontal and vertical patterns of nutrients and chla, and their potential sources. This thesis also estimated turbulent diffusive flux of Chl a down and SRP up from the lake bed, and compared these diffusive estimates to mussel-mediated assimilation flux estimates of chla, and with mussel excretion flux estimates of SRP.

The results in Chapter 2 suggested that nearshore SRP was above the threshold that *Cladophora* would be P limited (i.e. ≥2μg/L) in the nearshore. Nutrient and Chl a concentrations tended to be highest at stations closest to Grand River, and tended to be slightly higher in the early part of the season than the late part. *Cladophora* biomass tended to be highest at shallow stations located farther away from the mouth of the river. *Cladophora* may have grown to higher biomass at distal shallow stations because of enhanced light clarity in those regions, relative to the relatively turbid water from the river plume. Shallow stations tended to have higher values of nutrients and Chl a than deeper stations, but there were some exceptions, and this may be a reflection of non-point sources impacting the shallow nearshore more so than the deep nearshore. Sampling depth was not

significant in explaining nutrient variation in the nearshore; that is surface and bottom samples tended not to be significantly different. Syringe and tower filtration yielded different SRP concentration distributions, and the absolute differences ranged from very close to very large and reflected different temporal patters. Keeping in mind these important differences, syringe and tower filtration results on the whole exhibited similar direction and magnitude. Care must be taken when selecting a sampling method, especially if precise measurements are desired. However, if SRP trends are the goal, these two methods could be useful in showing patterns of SRP.

Chapter 3 found that stratification was actually common in the nearshore, and day-long profiling of the water column showed that onset of stratification is dynamic, at least at a 10m station. Stratification did not co-vary with strong patterns of coarse vertical water column heterogeneity, and the water column can appear to be relatively homogenous below the thermocline, at least in measures of specific conductivity and temperature. The relationship between grazing (TG) and mixing (TD) timescales, the estimated time in days for mussels to draw down near-bottom Chl a resulting in a gradient of depletion or the time in days for mixing to abolish near-bottom gradients, predicted that there should be many instances of Chl a depletion, but there were far fewer observations of this. Where near-bottom depletion gradients could be found, there was evidence of a relatively strong mussel influence on near-bottom Chl a depletion. Mussel biomass was positively correlated with the grazing time and with assimilation flux (areal feeding rate per square meter). Estimated assimilation flux was approximately an order of magnitude greater than estimated diffusive flux (the product of the gradient of near-bottom Chl a and diffusivity) at stations where significant near-bottom Chl a depletion was observed.

Chapter 4 demonstrated that mean diffusivity sampled under calm conditions in the nearshore at different station depths and times of the season is constrained to within a relatively consistent range. Estimated particulate phosphorus (PP) areal flux was greater than SRP areal flux, which in turn was greater than *Cladophora* areal uptake rates. There was a spatial disconnect between where the greatest biomass of *Cladophora* occurred and where the greatest biomass of mussels occurred. At some of the shallowest stations, estimated mussel diffusive SRP flux was not sufficient to support *Cladophora* growth locally. However, deeper stations do not have *Cladophora* due to light limitation, and there is SRP flux from the benthos in that area. Over the total nearshore area, mussels appear to produce enough SRP to support *Cladophora* biomass. PP flux was greater than SRP flux, and the fate of the remainder of the PP that is not converted to mussel tissue or excretia is still an unknown variable in benthic P-cycling. Diffusive SRP flux estimates were within the same range as

previously reported literature values and with estimates of assimilation flux that were ultimately estimated from Chl a profiles. This lends support to the idea of using Chl a profiles, which tend to be part of routine water quality monitoring cruises, to estimate of both Chl a fluxes into mussel beds and SRP fluxes out of them. Using Chl a profiles may be a less labour-intensive way to collect data with nearly the same accuracy as other more time-consuming methods to determine near-bottom fluxes.

Acknowledgements

I would first like to acknowledge that The University of Waterloo is situated on the Haldimand Tract, land promised to the Six Nations, which includes six miles on each side of the Grand River, and is on the traditional territory of the Attawandaron (Neutral), Anishnaabeg, and Haudenosaunee peoples.

I wouldn't have made it this far without the following people, who I gratefully acknowledge below. First, a thank you to my supervisors Drs. Ralph Smith and Leon Boegman. I thank you for your patience and guidance as I tried to learn near-bottom hydrodynamics on the fly and make sense of my very noisy data that seemed to want to defy nice, neat patterns. Many thanks to my committee members Dr. Todd Howell and Dr. Roland Hall, who I asked very random thesis-related questions at very random times, and who always helped me out when I had a question. Thank you to my Great Lakes Nutrient Initiative (GLNI) collaborators Dr. Dave Depew and Dr. Alice Dove. Discussing patterns that we had observed, and receiving and sharing data and ideas from you really helped make this work all the more nuanced. Thanks to Dr. Aidin Jabbari for helping me out with the parameterized structure function code. Many thanks too, to Dr. Veronique Hiriart-Baer for all the resources she put at my disposal. This work was supported by GLNI funding from Environment Canada, funding from the Ontario Ministry of the Environment, and Ontario Graduate Scholarships and UW President's Graduate Scholarships.

I cannot stress how thankful I am to Environment and Climate Change Canada's Technical Operations staff. I particularly thank Bob Rowsell for all his help in scheduling ship and personnel time, and Don Montrueil for creating specialized sampling apparatuses. The following people ferried me to my sampling sites, deployed my giant instrument-laden tripod off a boat too small to be doing that sort of thing, and were great company: Benoit Lalaonde, Adam Morden , Dan Abbey, Bruce Gray, Chris Duggan, Corey Treen, Carl Yanch, Jeremy Hicks, Josh, Cary Smith, and Joe Gabriel. Thanks to Jacqui Milne for coordinating sample collection and analysis. Thanks also to my field assistants over the years: Chris Ososki, Michael Funk, Joe Spohn, Kyla Bas, and James Cober.

Thank you to my friends Brenda, Kate, and Alannah, for being there to talk to about anything and everything. Thanks to Dr. Trent Hoover for encouraging me to do grad school all those years ago in the stream and riparian lab at UBC – here is that thesis acknowledgement I promised you (!). A special thank you to Dr. Laura Beecraft, who suffered through the PhD with me, cheered me on when I was ready to call it quits, and who made judicious use of "pompoms and newspaper whacks" to keep me motivated. A huge thank you to Dr. Christopher Kohar, for putting up with the 1%-of-the-year freak-outs without complaint, for all the matlab bailouts, hugs, love, and support of all kinds. Lastly, and certainly most importantly: thank you to my parents. I gratefully acknowledge their unfailing support and sacrifices made on my behalf, so that I could pursue all these post-graduate degrees and get a little farther in the world than they were able. I hope I am closer to fulfilling your immigrants' dream of a better life.

Dedication

This thesis is dedicated to my grandmothers: to Lola Iliang, for instilling a dedication to continual learning, and to Lola Fileng, who showed me that there is more than one way to make positive changes in the world.

Table of Contents

List of Figures

List of Tables

Chapter 1: General Thesis Introduction

The research described in this thesis was motivated in part by the ongoing challenge of designing and implementing nutrient loading controls that will protect aquatic environmental quality, particularly in the Laurentian Great Lakes. This work was part of a collaborative effort to better understand the sources of nutrient variation in the nearshore, and was supported in large part by the Great Lakes Nutrient Initiative (GLNI) program of Environment Canada and Climate Change. The program was a response to persistent problems with nuisance growth of the benthic alga *Cladophora* in many parts of the Great Lakes, resurgent problems of harmful phytoplankton blooms, and a change in the dominant sources of external nutrient loading that has taken place over the past five decades. Diffuse source nutrient loads (e.g. small to medium sized rivers, groundwater inputs, etc.) are now dominant in Great Lakes nutrient budgets (Dolan & Chapra, 2012) and are difficult to quantify and control. Defining and implementing acceptable nutrient loads is further complicated by the near-ubiquitous presence of the invasive benthic bivalve genus *Dreissena* (Mackie, 1991; Nalepa, Fanslow & Lang, 2009; Burlakova *et al.*, 2014). A major goal of this thesis was to better define the role of *Dreissena* in the cycling of phosphorus, the main limiting nutrient for *Cladophora* and harmful phytoplankton blooms, in Great Lakes nearshore zones where *Cladophora* problems and *Dreissena* effects are large (Hecky *et al.*, 2004). The approach taken was to quantify the fluxes of nutrients and particles associated with natural *Dreissena* populations *in situ*, and relate them to mussel population sizes and the spatiotemporal patterns of physical and chemical conditions in the study area. Such information can guide policy on external nutrient loads to account for the potential amplification of the impact of external loads caused by the mussels. It also, however, gives a comparatively novel picture of how the energetics (specifically food consumption and nutrient excretion) of *Dreissena* in nature compare to ideas based on lab experiments, and how the coupling of *Dreissena*-dominated benthic communities with the overlying plankton systems is affected by natural variations in the physical environment (notably mixing strength and thermal stratification). An additional

major goal was therefore to improve our ability to predict the strength and nature of benthic-pelagic interactions and to define critical aspects of the ecology of an important invasive organism in natural settings. The work was based in Lake Erie, which has a notable history of nutrient pollution, remediation, and sometimes spectacular water quality problems.

1.1 Eutrophication, management responses, and ecological outcomes in Lake Erie

Lake Erie is the smallest of the Laurentian Great Lakes by volume, and thus the most sensitive to external inputs. It is often subdivided into three basins (West, Central, and East), which are physically and chemically distinct from one another (Mortimer, 1987; Bolsegna & Herdendorf, 1993). Lake Erie's nutrient status has changed quite dramatically since the late 1950s, post-Great Lakes Water Quality Agreement (GLWQA), and through to the current time. By the mid 1960's Lake Erie showed considerable degradation in water quality indicators including concentrations of nutrients and chlorophyll a (an index of phytoplankton abundance (Beeton, 1969). There were severe cyanobacterial blooms over much of the West Basin and *Cladophora glomerata* blooms in nearshore zones of the Central and East Basins (Higgins *et al.*, 2005b; Depew *et al.*, 2011). Oxygen depletion in the deep waters of the central basin was severe and represented a significant loss of fish habitat as well as a potential source of internal nutrient loading (Charlton). With recognition of phosphorus as the key nutrient in controlling nuisance phytoplankton growth (Schindler, 1971, 1977), the binational Great Lakes Water Quality Agreement of 1972 set out limits for P loading to Lake Erie. P loading was decreased through improvements to municipal and industrial wastewater management, and both P concentrations and water quality indicators improved through the 1970's and 1980's (Makarewicz *et al.*, 1991). Phytoplankton abundance decreased and cyanobacterial blooms were greatly reduced (Makarewicz, 1993; Conroy *et al.*, 2005a b; Steffen *et al.*, 2014). Complaints by Lake Erie stakeholders about *Cladophora* decreased and its abundance was likely diminished, though data are limited (Higgins *et al.*, 2005b). The 1990's may have marked a high point in the success of controlling phytoplankton and *Cladophora* , with renewed deterioration in some areas becoming evident before the end of the decade and despite continued success in controlling

municipal and industrial P loads (Conroy *et al.*, 2005a; Dolan & McGunagle, 2005; Higgins *et al.*, 2005b; Chapra & Dolan, 2012; Stumpf *et al.*, 2012). Changes in the biology of the lake and in the dominant processes of external nutrient loading are thought to contribute to recent recurrence or worsening of some water quality problems.

Zebra mussels (*Dreissena polymorpha*) are believed to have established in the western parts of Lake Erie between 1985 and 1988 after introduction from Europe in the ballast water of sea-going cargo vessels (Mackie, 1991). The closely-related quagga mussel (*D. polymorpha)* was found shortly after and was likely in Lake Erie by 1989 (Mills *et al.* 1993). Both species were present and, in many areas, very abundant by 1991, with quaggas thriving in deeper waters and zebras in rocky nearshore zones (Dermott & Munawar, 1993). Quagga mussels have subsequently displaced zebras throughout most of Lake Erie and the other Great Lakes too (Mills *et al.*, 1996). Another pair of invaders, the round goby and the tube nosed goby, appeared and spread rapidly in the 1990s (Jude *et al.* 1992). These benthivorous fish have potential to limit dreissenid mussel populations (Ray & Corkum, 1997), and interactions have been inferred in some locations, but quagga mussels remained highly abundant and biomass-dominant in the benthos throughout much of Lake Erie to the time of the current study (Burlakova *et al.*, 2014, 2018). The ability of the mussels to retain and recycle nutrients, and to increase the clarity of the water column, has been suggested to contribute to blooms of phytoplankton and *Cladophora* that became resurgent some years after mussel colonization (Arnott & Vanni, 1996; Hecky *et al.*, 2004; Auer *et al.*, 2010; Higgins *et al.*, 2012).

As dreissenid mussels were making the Great Lakes their own, the patterns and processes of external nutrient loading were also changing. The now-dominant non-point inputs, which include surface runoff from water courses of all sizes, are widely believed to be the main driver of resurgent cyanobacterial blooms in western Lake Erie (Michalak *et al.*, 2013; Kane *et al.*, 2014; Scavia *et al.*, 2014). In this view, the widespread adoption of conservation tillage as an agricultural best management practice has had the ironic consequence of increasing the export of bioavailable phosphorus to receiving waters and has

indirectly fueled the renewed bloom problems (Baker *et al.*, 2014). Soils in many areas have also been receiving decades of fertilizer treatments that have led to very high P concentrations, and a legacy of high P export potential (Joosse & Baker, 2011). Weather, in conjunction with agricultural practices, may also play a role through heightened nutrient export during extreme or unseasonal precipitation events and through alterations of physical structure of the lake water column that favour phytoplankton bloom development (Michalak *et al.*, 2013).

Western Lake Erie, which receives a relatively large part of its water load from tributaries that drain intensely agricultural lands, is the most extreme example but there are other areas of the Great Lakes that are vulnerable to similar problems (e.g. Saginaw Bay of Lake Huron, Bay of Quinte in Lake Ontario, and parts of southern Lake Ontario and eastern Lake Huron). The east basin of Lake Erie, the object of study in this thesis, receives most of its water through advection from the central basin, which generally has oligo-mesotrophic nutrient levels. However, its north shore receives the inputs of the Grand River, Ontario, which is a significant part of the nutrient loading to the east basin and which drains a largely agricultural catchment. The east basin is therefore not immune to the hypothesized threats from altered non-point loading and is certainly vulnerable to impacts of dreissenid mussels, which have been more abundant in the East Basin than in other parts of Lake Erie or, probably, most other parts of the Great Lakes (Patterson *et al.*, 2005; Burlakova *et al.*, 2014). To date, there has been detection of cyanotoxins in east basin (Ghadouani & Smith, 2005) but phytoplankton blooms have not been problematic. Blooms of *Cladophora* have been. Unlike phytoplankton blooms, *Cladophora* blooms are a problem specific to the nearshore zone, a complicated and challenging object of study.

1.2 Properties and problems of the nearshore zones of great lakes

The nearshore is operationally and variously defined (Yurista *et al.*, 2012b). One generally accepted definition is the peripheral portion of the lake that occurs above the stable seasonal thermocline (Edsall & Charlton, 1997; Yurista *et al.*, 2012b a), which in Lake Erie, is ~20m deep (Mortimer, 1987; Bolsegna and Herdendorf 1993). This was the definition used in this thesis. It may also be delineated by

physical processes, notably shore-parallel circulation that tends to limit exchange between nearshore and offshore waters (Beletsky, Hawley & Rao, 2013; Yurista, Kelly & Scharold, 2016; Valipour *et al.*, 2018); such boundaries are dynamic but often occur at depth contours close to the seasonal thermocline. The nearshore comprises approximately 40% of the area of the East Basin (Haltuch, Berkman & Garton, 2000; Depew, Guildford & Smith, 2006b). This is a large fraction compared to most of the rest of the Great Lakes, although the entire west basin of Lake Erie would qualify as nearshore by this definition. The nearshore substrate in east basin, at least in the north, is dominated by bedrock, boulders and cobble with smaller proportions of the finer-textured sands, silts and muds (Bolsenga and Herdendorf 1993, diver observations). Offshore substrates are, by contrast, heavily dominated by the finer textured materials. The coarser benthic substrates are favourable for attachment by dreissenid mussels and *Cladophora* (Higgins *et al.*, 2008b; Zulkifly *et al.*, 2013), although quagga mussels can colonize finer substrates, like sand and silt (Dermott & Munawar, 1993; Wilson, Howell & Jackson, 2006).

Nutrient and Chl a concentrations tend to differ between nearshore and offshore zones in Lake Erie and the other Laurentian Great Lakes. The nature of the differences has changed over time in some lakes, including Erie. Before the arrival of dreissenid mussels, concentrations of N, P, and chlorophyll a were higher in the nearshore than the offshore (Depew, Guildford & Smith, 2006a; Dove, 2009), in part because of its proximity to many external sources of nutrients (Pennuto *et al.*, 2014; Yurista *et al.*, 2016). Nutrient and chlorophyll a concentrations decreased in nearshore and offshore zones following P-loading decreases under the GLWQA. In Lake Erie, the concentration of Chl a and phytoplankton in the nearshore zone along the north shore decreased further as dreissenid mussels became established, especially in east basin where mussel biomass was largest (Nicholls & Hopkins, 1993). The coincidental arrival of mussels and subsequent decrease in Chl a was observed in nearshore zones around the Great Lakes except in L. Superior, which never developed significant mussel populations (Nicholls, Hopkins & Standke, 1999). While P concentrations also tended to decrease, the ratio of Chl a to P decreased,

consistent with a suppression of phytoplankton by mussel grazing. By the early 2000's, the historical pattern between nearshore and offshore was reversed in eastern Lake Erie, with higher Chl a and primary production in the offshore than the nearshore (Depew *et al.*, 2006a). A similar change was observed in Saginaw Bay of Lake Huron, where the more eutrophic inner bay experienced a differential decrease of nutrient concentrations, Chl a, and primary production as mussels became established (Fahnenstiel *et al.*, 1995a b).

The nearshore shunt hypothesis (Hecky *et al.*, 2004) proposes that mussels have more impact on the relatively shallow and well mixed nearshore water than the deeper, often thermally stratified, offshore waters. This could allow them to mediate the decreased levels of phytoplankton and primary production, and increased water clarity, that has accompanied their appearance in the nearshore in many Great Lakes locations (Fahnenstiel *et al.*, 1995a b; Hall *et al.*, 2008). In some other parts of the Great Lakes, notably Lake Michigan, mussel impacts on offshore phytoplankton have apparently been greater than on nearshore, due largely to an abundance of sand (not a good mussel substrate) in much of the nearshore (Fahnenstiel *et al.*, 2010; Kerfoot *et al.*, 2010). Effects of mussels must be considered in the context of coincident changes in nutrient loading and climate (Warner *et al.*, 2015) but there is abundant evidence for their effects on nutrients, phytoplankton, and water quality wherever they attain a high biomass (Higgins *et al.*, 2011). Where that high biomass is in the relatively shallow waters of the nearshore it can be expected to exert especially significant effects.

The nearshore zone is nonetheless a highly non-uniform area and the role of mussels in it is likely to vary considerably over small to moderate spatial scales. External inputs are likewise distributed in a highly non-uniform way. The east basin of Lake Erie provides a good example. As in other nearshore zones like Lake Ontario (Howell, Chomicki & Kaltenecker, 2012) and Lake Huron (Howell *et al.*, 2014), currents tend to flow parallel to the shore and cross-shore flow is much weaker than shore-parallel flow (Valipour *et al.*, 2018). The Grand River water entering Lake Erie (higher in nutrients and turbidity than the lake) tends to remain coherent for some time (thus forming a so-called plume) and is entrained in the shore-parallel flow (Chomicki *et al.*, 2016). The flow is most often to the east, driven by the prevailing

winds. The plume coherence generates sharp gradients in water quality variables, including nutrient concentrations, over short scales (hundreds of meters) in the cross-shore direction (Chomicki *et al.*, 2016; Depew, Koehler & Hiriart-Baer, 2018). Extremely localized gradients with tightly shore-bound distributions have been observed in other nearshore locations in association with external inputs from smaller tributaries (e.g. Howell *et al.*, 2012; Howell *et al.*, 2014). Reversals of shore-parallel flow do occur, however, and have been observed in east basin. They cause a more diffuse effect of incoming river water that can extend to the west and south of the river mouth (He *et al.*, 2006; Chomicki *et al.*, 2016; Demchenko *et al.*, 2017), and help to drive mixing of river and lake water. The plume coherence varies among seasons, being stronger in spring when temperature differences between river and lake are large, but the fraction of river water present in nearshore water samples was usually <20% at distances of 15-35 km from the river mouth in one study (Depew *et al.*, 2018).

Nearshore zones are generally expected to be more fully mixed in the vertical than offshore zones, since they are by definition too shallow for seasonal thermoclines to persist. However it is well known that river plumes (including the Grand River in east basin) are often coherent in the vertical as well as horizontal, due to differences in density between river and lake water (He *et al.*, 2006; Demchenko *et al.*, 2017). This may result in meaningful differences in nutrients between near-surface and near-bottom locations (Chomicki *et al.*, 2016) and is particularly relevant in connection with the benthic alga *Cladophora*. Nearshore zones can also display ephemeral (hours to days duration) thermal stratification during warm and calm weather episodes, as has been well-documented in the relatively shallow west basin of Lake Erie (Ackerman, Loewen & Hamblin, 2001; Loewen, Ackerman & Hamblin, 2007). Meaningful vertical heterogeneity is thus likely to occur at many times and places in the nearshore, even if it is not the usual state. To add to the potential variability, coastal upwelling events (particularly in Lake Ontario but also in Erie and other Great Lakes) can displace any developing thermal structure in the nearshore with (usually) colder water coming from the deeper offshore (Rao, Milne & Marvin, 2012; Valipour *et al.*, 2016, 2018). Major upwelling episodes in Lake Ontario happen several times during

most summer stratification seasons, with each episode affecting nearshore environmental conditions for approximately a few days to a week.

The strong spatial and temporal variability of environmental conditions in the nearshore is a challenge to any efforts to characterize and predict its properties. It is a particular challenge when addressing one of the most prominent environmental problems affecting many nearshore locations in the Great Lakes: Nuisance growth of *Cladophora.* Not only is *Cladophora* confined to the nearshore, it can thrive only in certain parts of the nearshore and may have important connections to other organisms, notably dreissenid mussels, which are also non-uniformly distributed.

1.3 The twin problems of *Cladophora* and *Dreissena*

Cladophora growth dynamics also change over the course of the growing season, and may be relatively more or less of a sink for P. Early in the growing season, when river discharge and loading are high, *Cladophora* also tends to be growing rapidly, and taking up P at maximal rates of uptake (Higgins *et al.*, 2005b, 2008b; Malkin, Guildford & Hecky, 2008; Auer *et al.*, 2010). This may have the overall effect of making nutrients, and SRP in particular, in the water column environment around it appear to be at a lower concentration than expected. Individual fronds are small, so there is adequate water movement around them, assisting in diffusion and nutrient uptake at a high rate(Escartin & Aubrey, 1995; Dodds & Biggs, 2002; Venier *et al.*, 2012; Zulkifly *et al.*, 2013). Later in the season, however, *Cladophora* fronds tend to form thick mats, and it is believed that this results both in self-shading and increased diffusive boundary thickness that inhibit effective uptake of nutrients. Both of these things contribute to reduced *Cladophora* nutrient, but especially P, uptake. Because there is less nutrient uptake from the environment, there may be relatively greater measured concentrations of nutrients, compared to the early part of the season. *Cladophora* may also become light limited, and will not grow below a certain light intensity. This can include sites that are below the euphotic depth, ~10m deep in this portion of the nearshore of the East Basin, or in particularly turbid areas (Higgins *et al.*, 2005b; Malkin *et al.*, 2008), including areas directly receiving the river plume or areas with a high rate of resuspended bottom

sediments. *Cladophora* growing at adequate light intensities may be capable of drawing SRP down to low levels while *Cladophora* growing near its light limitation limits may be less able to effectively draw down SRP. Abundance and biomass distributions of *Cladophora* in the East Basin support the idea that light is a limiting factor to growth. Further, certain sites may have more roughness elements that enhance mixing (Lorke & MacIntyre, 2009), which may also enhance regeneration of SRP from mixing of water column SRP, mussel excretion SRP, or solubilization of SRP from resuspended particulate matter previously settled at the bottom.

Mussels are thought to be voracious filter feeders that can exert such a large impact on the water column, that water column Chl a concentrations may noticeably decrease (Nicholls & Hopkins, 1993; Yu & Culver, 1999). Long term datasets have indicated that there were changes to water column nutrients and phytoplankton in Lake Erie (Nicholls *et al.*, 1999; Depew *et al.*, 2006a; Winter *et al.*, 2015). Changes to nutrients and Chl a concentrations have also been observed in the Lakes Michigan and Huron (Carrick *et al.*, 2001; Hall *et al.*, 2003; Depew *et al.*, 2006). However, there are actually limits to their filtering abilities in nature, and these limits are often in the form of stratification and boundary layers, which restrict how much of the water column they can access (Ackerman *et al.*, 2001; Edwards *et al.*, 2005; Boegman *et al.*, 2008b). The nearshore phosphorus shunt hypothesis (Hecky *et al.*, 2004) posits that the observed decrease in water column Chl a and increased benthic *Cladophora* is mediated through dreissenid mussel water column feeding of particulate phosphorus, predominantly in the form of phytoplankton and subsequent excretion of soluble P as a byproduct of metabolism, which is in a form readily available for *Cladophora* uptake to support growth. Meta-analysis of data from the great lakes (Higgins & VanderZanden, 2010) point to resultant changes in the food web toward a benthic-based food web, and away from one based in the pelagic. A benthic-based food web may also have an effect on mussel feeding and body condition, which may be enhanced by intercepting some portion of the river plume, which can be high quality food source (sensu Vanderploeg *et al.*, 2017) as SRP in the river becomes incorporated into lower-river phytoplankton biomass (Depew *et al.*, 2018). Experiments have demonstrated a link between higher Chl a concentration with higher Chl a and particulate P assimilation

and P flux by mussels (Vanderploeg *et al.*, 2017). Because of their hypothesized effects on the P cycle, mussels that are able to access the water column may enhance benthic SRP concentrations and greatly decrease suspended phytoplankton Chl a near the lake bed. Density stratification can serve to magnify differences in nutrients and Chl a between the surface layer and the bottom layer.

Mussel excretion is thought to be one of the mechanisms facilitating nuisance *Cladophora* growth in the nearshore. However, the P-richness of mussel excretion is tied to food quality and quantity (Vanderploeg *et al.*, 2017), and on its metabolic needs, including growth and reproduction cycles (Stoeckmann & Garton, 1997; Stoeckmann, 2003; Stoeckmann, Garton & Stoeckmann, 2011). Generally, ingested food is variably allocated toward three energy pathways depending on life cycle and time of the growing season: respiration, growth, and reproduction (Stoeckmann *et al.*, 2011). Depending on their metabolic requirements, mussels will excrete whatever nutrient that is not limiting to them, either N or P. Food quality changes over the course of the growing season as well, as a result of phytoplankton succession and some seston is of higher food quality than others. Mussels that were fed a high-quality diet tended to excrete more P and N than did those feeding on a lower quality diet (Vanderploeg *et al.*, 2017). Later parts of the season tend to be associated with water column stability (i.e. density stratification), which may inhibit how much of the water column mussels can access (Ackerman *et al.*, 2001; Edwards *et al.*, 2005; Loewen *et al.*, 2007; Boegman *et al.*, 2008b). Mussels may re-filter the same water repeatedly, resulting in a drawdown of phytoplankton and reduced mussel feeding, which may have negative implications for body conditions (Casper & Johnson, 2010). Increased water temperatures in the later part of the sampling season promote increased respiration and may become stressed, resulting in decreased nutrient assimilation by mussels, and in relatively more excretion of N and P. While there are quite a number of laboratory or mesocosm studies assessing ingestion, assimilation, egestion, and excretion by mussels (e.g. Ozersky *et al.*, 2009 and references therein), there are fewer published *in situ* measurements (Roditi *et al.*, 1997; Ozersky *et al.*, 2009; Ozersky, Evans & Ginn, 2015). There does not seems to be a very strong knowledge base regarding particle and nutrient fluxes that mussels may mediate in natural systems, and how variable these fluxes may be. There is a large knowledge gap specifically

related to mussel biodeposits (feces, pseudofeces), and their fate, that cannot be tackled in this thesis. This thesis does attempt to approach the problem by assessing how much particulate matter mussels are processing, which would potentially put an upper on biodeposit production and associated P cycling This thesis also attempts to present the first truly *in situ* measurments of soluble P release from mussel-dominated benthic communities.

1.4 Benthic-pelagic coupling in the nearshore

The interactions of *Cladophora* and *Dreissena* with the water column, and their effects on the properties of the water column, are examples of benthic-pelagic coupling. The coupling depends very much on physical conditions near the lake bed. Bottom currents are ultimately generated from surface forcing, from high-frequency internal waves, or from basin-scale internal waves (Lorke & MacIntyre, 2009). In general, water in the top (surface boundary layer – SBL) and bottom (benthic boundary layer - BBL) of lakes moves faster than the water in the middle (interior) of the lake (Wüest & Lorke, 2003). Interaction of surface and internal waves with a sloping bottom may also enhance benthic turbulence. Wave propagation in the water column is stopped in its current path, and instead deflects up- and downslope, resulting in turbulence near the bed, which eventually flattens out into jets (Ivey, Winters & Silva, De, 2000; Lorke, 2007). The motion of the thermocline tilting (i.e. seiches, one of the types of basin-scale internal waves) may either enhance turbulence on its upslope motion and enhance stability on its downslope motion (Chowdhury, Wells & Howell, 2016). Tilting of the thermocline may allow food in deep Chl a maxima (i.e. metalimnetic maxima) to become available to nearshore mussels, promoting improved growth and survival (Malkin *et al.*, 2012). Associated turbulence may also alleviate mass transport limitation of mussel feeding.

The interplay between buoyancy stability and shear (e.g. as described by the Richardson number) dictates whether the water column mixes, dissolved nutrient gradients are formed or are abolished, or

whether there is resuspension of matter accumulated at the bottom (i.e. “sediments”, including settled seston, other less labile particles, and mussel pseudofeces). It can allow for the formation of stratification within the BBL. A stratified BBL may result in layers of water that are vertically mixed within themselves, but are distinct from adjacent layers (Imberger, 1998). When the BBL is stratified, the height of mixing is denoted as Hmix (Lorke & MacIntyre, 2009). Hmix can influence the time scales on which mussel feeding and water column diffusive mixing affect properties of the water column (Boegman *et al.*, 2008a; Schwalb *et al.*, 2013). Hmix helps determine whether mass transport limitation of mussel feeding and near-bottom depletion gradients of Chl a are detectable, potential for elevated near-bottom nutrient concentrations, particularly of SRP and NH_4. Mixing height and stratification in the BBL also reflect physical processes and features of the bottom itself. Bottom roughness, in the form of gravel, cobbles, and rocks, and even dreissenid mussels and *Cladophora*, can influence bottom mixing, introduce form drag, and enhance bottom turbulent mixing (Lorke & MacIntyre, 2009), which may homogenize near-bottom water masses, and obscure benthic gradients (sensu Escartin & Aubrey, 1995). Mussel shells and *Cladophora* biomass may serve as roughness elements that could obscure any obvious detectable gradients that would have otherwise formed. Work has been done to suggest that low-biomass benthic algae (as in the early part of the season) may enhance bottom turbulence in a marine estuary, but high-biomass algae (as in the late part of the season) may enhance stability, as water would flow around the mat (Escartin & Aubrey, 1995; Lawson, McGlathery & Wiberg, 2012). High-biomass algae might also serve to inhibit mussel feeding and excretion by limiting turbulence penetration to the bed, resulting in depletion of food and oxygen for the mussels beneath them (Escartin & Aubrey, 1995; Lawson *et al.*, 2012).

The BBL is comprised of three layers: the momentum boundary layer (MBL), which is on the order of metres thick, the viscous sublayer (VSL, centimetres thick), and the diffusive sublayer (DSL, millimeters thick) (Wüest & Lorke, 2003). Flow in the BBL of lakes is not isotropic (unidirectional), which introduces noise, and may make it difficult to use the log-law of the wall, which is commonly used to describe dissipation in channel flow, to describe energy dissipation in the nearshore. However,

techniques from meteorology have been adapted to exploit this noise in order to estimate dissipation of total kinetic energy in turbulent systems with anisotropic flow (Wiles *et al.*, 2006; Jabbari, Rouhi & Boegman, 2016). Apparent dissipation, diffusivity, and flux into and out of the nearshore lake bottom can be impacted by the interplay of buoyancy and shear, and by benthic concentration gradients. Diffusivity is expected to be greater if water velocity and dissipation is greater, or if buoyancy frequency is smaller (i.e. $Kz = \varepsilon/N^2$). Dissipation divided by the buoyancy frequency give an estimate of diffusivity, which in this thesis has been parameterized for turbulence intensity in stratified flows (Bouffard & Boegman, 2013). The product of diffusivity and the concentration gradient as described using Fick's First Law of diffusivity gives an estimate of flux.

Gradients of Chl a depletion, and SRP and NH_4 enrichment, with proximity to the bottom, are expected to form under quiescent conditions, that is, when buoyancy is relatively greater than shear near-bottom. Conversely, when shear is greater than buoyancy or there are other local sources of bioturbation near-bed (i.e. water movement from mussels' inhalant and exhalent siphons), gradients are expected to be abolished, and resuspension of settled materials at the bed may be possible given their size and weight (sensu Cyr, McCabe & Nürnberg, 2009). There may be a diffusivity threshold between $1x10^{-4}$ and $1x10^{-5}$ m^2/s where near-bottom flow switches from turbulent to laminar (Rao *et al.* 2012; Boegman 2014).

Near-bottom quiescence is necessary for the formation and detection of near-bottom gradients, but near-bottom turbulence may be energetic enough to suspend settled particles ("sediments") off the bottom, depending on their weight and size. Resuspension of bottom sediments and/or the nephleoid layer of loosely suspended sediments (Lorke & MacIntyre, 2009) may enhance solubilisation of near-labile particulate P to dissolved P, which would be readily utilizable for *Cladophora* use (Cyr *et al.*, 2009). Benthic biota may also contribute to bottom bioturbation, which may also serve to stir up sediments up into the overlying water. Dreissenid mussels are well-known to have strong filtration capabilities based on their ability to decrease water column Chl a in a well-mixed water column (Yu & Culver, 1999), and to sometimes locally form Chl a depletion gradients under periods of stratification in other lakes (Schwalb *et al.*, 2013). The jets from their exhalent siphons may be enough to promote

turbulence directly above mussel beds (O'Riordan, Monismith & Koseff, 1993, 1995; Nishizaki & Ackerman, 2017), potentially obscuring formation of nutrient gradients and presence of Chl a depletion gradients very near-bottom.

Fine-scale sampling near the bed allows investigation of nutrient conditions in direct proximity to both mussels and *Cladophora*, which may enhance understanding of the origin of SRP for nuisance *Cladophora* growth. Bulk water column sampling is limited by its coarse-scale resolution. Modified Hesslein samplers, semi-permeable passive membrane samples used *in situ* that use diffusion into the sampling chambers to estimate *in situ* nutrient concentrations (i.e. "peepers") have been used to probe fine-scale nutrient gradients in porewater (Hesslein, 1973; Lewandowski *et al.*, 2015), and Dayton *et al.* (2014) were some of the first to use peepers to assess near-bottom gradients of SRP in two nearshore sites in Lake Michigan. Dayton *et al.* (2014) further modelled formation and abolishment of near-bottom SRP gradients under varying diffusion coefficient rates (i.e. proxies for degree of turbulent mixing); they found that there could be quite significant gradients near bottom under quiescent conditions (low diffusion coefficient), but that the gradient disappeared under increasing diffusion coefficient values. Importantly, however, they noted that while the near-bed gradient disappeared, the water column ~0-0.5m above the bed experienced broad almost-homogenous SRP elevation relative to the base condition. Direct measurement of the SRP gradient near-bottom and measurement of near-bottom velocity (estimated as diffusivity in this thesis) make it possible to estimate the flux of SRP up from the bed using Fick's first law of diffusive flux. This permits assessment and potential validation of mussel-related P fluxes as modelled in Dayton *et al.* (2014) and extrapolated from lab studies, with values measured for natural communities *in situ*.

Fine-scale (e.g. centimetre) gradients may not be detectable in energetic environments like the nearshore of the East Basin, but coarser scale (e.g. metre) gradients might exist, and near-bottom values may be different from surface measurements of the same parameter (Martin, 2010). Thus, there is value in measuring at both coarse and fine vertical scales. Under quiescent conditions there may be little evidence of enrichment at scales greater than tens of centimeters above the bottom, but fine scale

gradients are likely to be present and measurable. Conversely, under more energetic conditions, a layer of enriched near-bottom water may be detectable, but a fine scale gradient may not. This thesis considers both these vertical scales to further understand the proximate controls that may drive nuisance *Cladophora* growth. A greater understanding of the relative impacts of various sources of nutrients enriching nearshore *Cladophora* can help water quality managers determine the best approach to take in understanding, and ideally controlling, nuisance *Cladophora* growth in nearshore areas.

1.5 Objectives and thesis novelty

This thesis attempts to understand the proximate nutrient and physical controls and interactions that may be fueling nuisance *Cladophora* growth in the nearshore of the East Basin, Lake Erie. The objectives in this thesis meant to address this include: (1) advancing a predictive understanding of how the environmental conditions in the (shallow) portion of the nearshore where *Cladophora* grows may differ from other parts of the nearshore, (2) determining whether the flux of phytoplankton and phosphorus into the dreissenid-dominated benthos can be estimated under in situ conditions, and what those fluxes imply for our understanding of dreissenid energetics in nature, (3) determining whether fluxes of available P and N out of dreissenid-dominated benthos can be estimated and how they might compare to our ideas about mussel excretion and the needs of consumers such as *Cladophora*, and (4) providing a new basis on which to assess the role of dreissenids in nutrient cycling and nutrient-dependent problems in the nearshore.

Objective 1 is addressed in chapter 2 using samples collected systematically from shallow and deep nearshore areas over three years of observation. Objective 2 is the subject of chapter 3, where high resolution profiling of Chl a is combined with measurements of near-bed dissipation, thermal structure, and water velocities to enable estimates of fluxes in and out of bottom. Objective 3, the subject of chapter 4, uses additional near-bed measurements of dissolved nutrient profiles to test for, and quantify where possible, fluxes into or out of the bottom. Measurements of *Cladophora* and *Dreissena* biomass in the study area contribute to addressing objective 4, which uses the results of chapters 3 and 4 to assess how

the measured fluxes might figure in schemes for nutrient management, i.e. whether the potential amplification of external loads due to mussels requires adjustments to external inputs. Objective 4 will be the subject of the Conclusions and Implications chapter (chapter 5).

This thesis is novel because it assesses the nearshore benthos and *Cladophora* at progressively finer scales and explicitly considers the modifying effects of near-bottom water motion on the formation and abolishment of P gradients required for *Cladophora* growth. Relatively fewer measurements have been made in the nearshore compared to the offshore; fewer still have further subdivided the nearshore and assessed whether the shallower portions differ compared to the deeper portions. There have been reports on chlorophyll a and nutrients for the nearshore, and measurements of near-bottom water motion, but this thesis is one of the relatively few to attempt to reconcile these two things.

Chapter 2: Spatio-temporal dynamics of nutrients in shallow and deep nearshore zones of eastern Lake Erie: Tributary impacts and implications of SRP methodology variations

Surveys were conducted from May to October, 2013 and 2014, in the northern nearshore ($z < 20$ m) of eastern Lake Erie to determine how the shallow nearshore (<10 m depth, and site of most nuisance *Cladophora* growth) may differ from the deeper (10-20 m) nearshore, identify processes contributing to such differences, and test the vulnerability of standard survey approaches to biases introduced by methodological variations. The 38 km study reach bracketed a major tributary (Grand River, Ontario), which was expected to exert important influence on nutrient concentrations. There were higher SRP, Chl a and PP (but not NH_4) concentrations in the shallow nearshore than deep nearshore, associated with presence of high conductivity river water. The differential enrichment of the shallow nearshore was nonetheless not statistically significant, due to variability within zones. Evidence of direct river influence on nutrient concentrations was weaker in near-bottom (1 mab) than near-surface samples, and was not significant at distance (13-25 km) from the river mouth. Upwelling is an important process in the study area but was not detectable in our observations. Dreissenid mussels were abundant in the reach but spatial patterns of dissolved vs. particulate nutrients did not reveal impacts of mussel excretion and grazing. Measurements of the key variable SRP differed significantly depending whether samples were filtered on-board with minimal delay using a syringe filter or hours later at the shore lab using tower filtration. Despite some large differences between methods and a tendency to higher concentrations with the syringe method, the spatial patterns inferred were similar and both methods indicated a high frequency of SRP concentrations large enough to effectively saturate P uptake by P-limited *Cladophora* (i.e. 2µg/l or more). The results highlighted the challenges in quantifying spatial dynamics within the nearshore zone using ship-based surveys, but did show a pervasive and problematic enrichment of P in the study area, despite efforts to control loadings to Lake Erie.

2.1 Introduction

The nearshore zones of great lakes differ in important ways from the offshore zones and are the site of some of the most pressing environmental problems. While phytoplankton blooms can be a problem in both nearshore and offshore zones, the nuisance growth of the benthic alga *Cladophora* is an important problem that is unique to the nearshore and which continues in many parts of Lakes Erie, Ontario and

Michigan (Higgins *et al.*, 2008b; Auer *et al.*, 2010; Depew *et al.*, 2011; Howell, 2018). The offshore East Basin of Lake Erie is considered oligomesotrophic and SRP concentrations ranged from <1µg/L to >7µg/L from 2003-2013 (Dove & Chapra, 2015); the nearshore is likely to have a similar and potentially higher, range of SRP concentrations. *Cladophora* is a problem specific to the shallower portion of the nearshore zone where sufficient light is available at the bottom (Higgins *et al.*, 2005b; Malkin *et al.*, 2008). It is ubiquitous in the northern nearshore of the East Basin (Higgins *et al.*, 2008b; Depew *et al.*, 2011; Chomicki *et al.*, 2016; Howell, 2017). In this area, *Cladophora* tends to start growing and is at low biomass in the spring (April/May), achieves maximum biomass in June/July. By fall (October), biomass is again low (Higgins *et al.*, 2005b). Many structures for municipal and industrial water intake and wastewater disposal are in the shallower portion of the nearshore zone, which is also the most immediate interface with human activity and terrestrial runoff. While our knowledge of the nearshore zone and its differences from the offshore has certainly grown (e.g. Howell *et al*., 2012, Winter *et al.*, 2015) there is a need to better characterize the shallow nearshore environment and to quantify the processes that determine its environmental properties, especially nutrient concentrations (Makarewicz & Howell, 2012).

The nearshore zone is commonly defined as the peripheral area of the lake that has depths shallower than the seasonal summer thermocline (e.g. Edsall & Charlton, 1997; Yurista *et al.*, 2012), which in Lake Erie would be approximately ≤20m (Boyce 1974, Mortimer 1987). It may also be delineated by physical processes, notably shore-parallel circulation that tends to limit exchange between nearshore and offshore waters (Beletsky *et al.*, 2013; Yurista *et al.*, 2016; Valipour *et al.*, 2018); such boundaries are dynamic but often occur at depth contours close to the seasonal thermocline. Compared to the offshore, the nearshore warms faster in spring and early summer, has a shallower mixing depth and potentially greater light availability, and experiences more direct influence from external inputs (Hecky *et al*., 2004; Rao & Schwab, 2007). External inputs can be from both surface and groundwater flows, including small and ephemeral water courses (Crowe & Shikaze, 2004; Robinson, 2015). As a result, the nearshore often displays higher nutrient concentrations and sometimes higher plankton production than the offshore

(Dove, 2009; Allan *et al.*, 2012; Dove & Chapra, 2015), but variability is also high (Howell *et al.*, 2012; Yurista *et al*., 2016).

Where survey resolution permits, it is generally apparent that conditions vary considerably within the nearshore zone. The mixing zones of external inputs tend to have shore-parallel distributions, reflecting the predominance of shore-parallel circulation, and external inputs are often associated with differential elevation of properties such as specific conductivity, suspended solids, nitrate, and chlorophyll in shallower and more proximate areas relative to deeper and more distant areas within the nearshore zone (Howell *et al.*, 2012a, b; Chomicki *et al*., 2016). This can result in enrichment of the shallow nearshore in P and N even where the nearshore zone as a whole is quite oligotrophic (Makarewicz *et al.*, 2012; Howell *et al*., 2014). The spatiotemporal dynamics within the nearshore zone related to external inputs and their redistribution by mixing, and other processes, are strong (e.g. Chomicki *et al.*, 2016). They pose a challenge to our ability to quantify the properties of the nearshore, especially the shallow nearshore, and relate them to factors susceptible to management action.

Biological factors notably include the invasive dreissenid mussels (*Dreissena polymorpha* and *D. bugensis*), which dominate the benthic biomass in the East Basin of Lake Erie (Burlakova *et al.*, 2014), and have been implicated in a number of changes in the Great Lakes. The changes include increased water clarity (Barbiero & Tuchman, 2004; Auer *et al.*, 2010; Binding *et al.*, 2015), increased availability of hard substrate (Auer *et al.*, 2010), increased benthic regeneration of P (Ruginis *et al.*, 2014), enrichment of the benthos with P relative to N (Arnott and Vanni 1996, Conroy and Culver 2005, Ruginis et al. 2014), altered N and P cycles (Conroy et al. 2005) and diminished phytoplankton abundance and production (Fahnenestiel *et al.*, 2005, Depew *et al.*, 2006). The nearshore shunt hypothesis (Hecky *et al.*, 2004) postulates that effects of dreissenids will be greater in the nearshore, where mussels have better access to the shallower and better-mixed water column, than in the offshore. In parts of East Basin Lake Erie, a reversal of the historical plankton production pattern was observed consequent to colonization by dreissenid mussels, with lower chlorophyll concentrations and primary production in nearshore than offshore (Depew *et al.*, 2006). That reversal was consistent with the nearshore shunt hypothesis (Hecky

et al., 2004) and similar evidence of mussel-mediated changes to nearshore-offshore zonation have been observed elsewhere (e.g. Saginaw Bay, Fahnenstiel *et al.*, 1995). Mussels may also, depending on their spatial distribution and the lake circulation patterns, serve to diminish offshore phytoplankton production as well as, or even more than, nearshore production (e.g. Lakes Huron and Michigan; Cha *et al.*, 2011; Vanderploeg et al. 2010). In the northern east basin of Lake Erie, the object of this study, mussels have been abundant (though patchy) for many years in the nearshore (Patterson, Ciborowski & Barton, 2005; Chomicki *et al.*, 2016) and can potentially exert strong impacts in shallower areas.

It is widely accepted that dreissenids have helped provide the water clarity necessary for prolific *Cladophora* growth while adding to internal loading of P that may further promote its abundance (Auer *et al.*, 2010). *Cladophora* is by contrast a sink for dissolved P, especially in the early part of the growing season, due to high growth rates and associated P-uptake rates (Higgins *et al.*, 2008b). The spatial and temporal signals of dreissenid-mediated internal loading may for this (and other) reasons be largely obscured where *Cladophora* is abundant. NH_4, also excreted by mussels, is thought to be a less limiting nutrient and its spatial distribution may be more reflective of internal loading processes including mussel metabolism. If mussel activity is sufficient to affect water column nutrient concentrations, it might be predicted that NH_4 and perhaps SRP would be elevated, but particulate P and Chl a diminished, where mussel effects were stronger (e.g. in shallower nearshore areas with high mussel biomass).

The portion of Lake Erie of interest in this study exemplifies nearshore reaches that receive inputs from lands with both agricultural and urban effects. The major external load to the East Basin as a whole comes from the Central Basin (León *et al.*, 2005) through advection and exchange of water masses between the basins. The variability in nearshore nutrient dynamics occurs with loading from the Central Basin occurring in the background, making this a complex system to work in. The other large external nutrient source to the nearshore of the East Basin specifically is the Grand River, which experiences strong anthropogenic impact and enters the lake near the middle of the study reach (Depew *et al.*, 2011). Nutrient concentrations in the river near its point of discharge are generally high compared to the lake (Kuntz, 2008; Chomicki *et al.*, 2016; Depew *et al.*, 2018) although there is seasonal variation, with

concentrations of SRP in particular being lower in summer low-flow conditions. The Grand River also has a higher specific conductivity than the lake, which facilitates tracing of river water influence in the area (Chomicki *et al.*, 2016; Depew *et al.*, 2018). Recent studies have shown that the river has a strong but spatially restricted and temporally variable effect on nutrients and chlorophyll in the study reach (Chomicki *et al.*, 2016; Depew *et al.*, 2018). In addition to the Grand River, there are external inputs from much smaller tributaries and drains, and also potential inputs of groundwater (Kornelsen & Coulibaly, 2014; Robinson, 2015; Roy *et al.*, 2017). Such sources can contribute to enrichment of the shallow nearshore but may be a smaller source compared to the Grand River. Groundwater is estimated to contribute a sizable amount of P to the Grand River itself (Maavara *et al.*, 2017), but direct input into the lake has not been well-quantified. Despite the clear evidence for river influence, we still lack a quantitative knowledge of how enriched the shallow nearshore *Cladophora* habitat is compared to deeper nearshore or offshore areas, and how much of the enrichment can be assigned to direct river influence.

The entering river water tends to be warmer than the lake during the spring and early summer seasons of maximal *Cladophora* growth (Chomicki *et al.*, 2016; Demchenko *et al.*, 2017). It is thus buoyant and likely to remain at the surface before cooling and mixing disperse the plume (He *et al.*, 2006). In summer and early fall, temperature and buoyancy differences between river and lake are smaller. Discharge of the Grand River has a spring maximum (often in April), followed by much lower discharge in summer and early fall, although there are some shorter and usually smaller high discharge events associated with summer and fall storms (Howell *et al.*, 2012; Chomicki *et al.*, 2016; Depew *et al.*, 2018). In general, the river's influence would likely be maximal earlier in the spring-summer period. The summer seasonal thermocline in east basin generally forms in June, and may for a time affect the deeper nearshore before thermocline deepening proceeds to its typical later summer depth of approximately 20 m (Boyce 1974; Valipour *et al.*, 2018). Transitory stratification can often occur in spring and summer, even in quite shallow areas (e.g. a dreissenid-colonized reef 7m deep in the West Basin; (Ackerman *et al.*, 2001). Temporal variations of river discharge, plume behaviour and stratification can all affect just how the incoming river water may manifest in the properties of the shallow and deep nearshore zones,

particularly near the lake bed where *Cladophora* lives. Stratification and seasonal temperature changes also affect the feeding, metabolism, and impact of mussels on water column nutrients and plankton (Zhang, Culver & Boegman, 2008; Bocaniov *et al.*, 2014). We may therefore expect that the spatial structure of nutrients in the nearshore zone, and the underlying processes, will change through the spring to early fall season favourable to *Cladophora* growth.

With adequate light and temperature, *Cladophora* growth can be limited by bioavailable phosphorus, typically measured as soluble reactive phosphorus (SRP). Modeling of *Cladophora's* response to light, temperature and phosphorus indicates that, in Great Lakes environments, its growth should be strongly limited by SRP concentrations <1µg/L (Auer *et al.*, 2010), while a concentration of just 2µg/L will effectively saturate growth (Tomlinson *et al.*, 2010), although this value was made based on modelling studies, but has not been demonstrated in real systems. These are low concentrations compared to typical analytical detection limits for SRP (usually 0.5 µg/L or higher) so methodology for sampling and analysis becomes very important when asking about P controls on this nuisance alga. For SRP, it is believed best to filter samples without delay rather than storing them and filtering later (e.g. Jarvie, Withers & Neal, 2002). This is frequently feasible on larger sampling vessels but the smaller vessels often used for nearshore surveys do not make it easy to process samples on the water; more often samples will be filtered many hours later in a shore lab. While several studies have demonstrated that filtration methodology can affect the resulting SRP concentration estimates, we do not currently know whether such methodological variation would have a serious impact on the perceived spatiotemporal patterns in an actual survey, or would affect inferences about processes operating in the study area.

The current study was part of the Great Lakes Nutrient Initiative program of Environment and Climate Change Canada (ECCC), which seeks the knowledge necessary to design P management and loading targets that will protect water quality in Lake Erie, with special consideration to the continuing problem of nuisance *Cladophora* (Depew *et al.*, 2018). It provides a case study of an open, energetic, coastal reach that includes a large tributary (the Grand River) and interacts with oligotrophic offshore waters. Our main objectives were to (1) determine whether the shallow nearshore zone is quantifiably

enriched in nutrients (especially P) relative to the deep nearshore, using a balanced grid survey with multiple sampling expeditions, (2) test, using correlations with specific conductivity and spatial proximity to the river mouth, how much of any enrichment occurring could be attributed to direct riverine influence, (3) determine whether such enrichment was equally apparent at depths close to the bottom-dwelling *Cladophora* as at shallower sampling depths more commonly used in spatial surveys, (4) examine water temperatures and dissolved vs particulate nutrient patterns to test for effects of upwelling and/or internal loading associated with dreissenid mussels, and (5) to determine whether sample handling, specifically promptness of filtration, affects the estimated SRP concentrations and apparent spatio-temporal patterns in the study area.

2.2 Methods

2.2.1 Study area and sampling design

Four transects, each with four stations at depths of 3-5m, 7-10m, 12-15m, and 16-18m (Figure 2.1,

Table 2.1) were established in the nearshore study reach along the north shore of the east basin of Lake Erie. Stations <10m deep comprised the shallow nearshore group, while those >10m deep were in the deep nearshore group. The Grand River enters the lake near station 1274, and the associated transect was termed "mouth" to denote its proximity. The "far west" and "far east" transect were approximately 13 and 25 km distant, respectively, from the mouth transect. The "near-mouth" transect was close to the mouth and in an area often affected by the river plume (Chomicki et al. 2016, Depew et al. 2018). Most sampling was conducted in May, June, August, and September 2013, and June, August, September, and October 2014. Additional sampling was conducted in May 2015. In total, 16 stations were sampled over three years, and corresponded to 61 separate visits to collect nutrients and chla (Table 2.2).

It was not the purpose here to attempt an analysis of *Cladophora* or *Dreissena* abundance or their relationships to measured water column properties, but it is relevant to note some features of their distributions. In the years of this study and immediately preceding, *Cladophora* biomass was maximal in what we define as the shallow nearshore and particularly at depths ≤6 m, commonly attaining values of 50 gDW/m^2 or more along the study reach (Alice Dove, Environment and Climate Change Canada personal communication, Chomicki *et al.*, 2016, Depew *et al.*, 2018). There was very little biomass in the deep nearshore. Dreissenid mussels were present across the study reach, in both shallow and deep areas (Alice Dove, Environment and Climate Change Canada personal communication, Chomicki *et al.*, 2016, Depew *et al.*, 2018). The highest biomass (20-40 g/m^2 shell free dry weight) was in the deep nearshore rather than the shallow. Further comment on distributions of dreissenids and *Cladophora* will follow in the discussion.

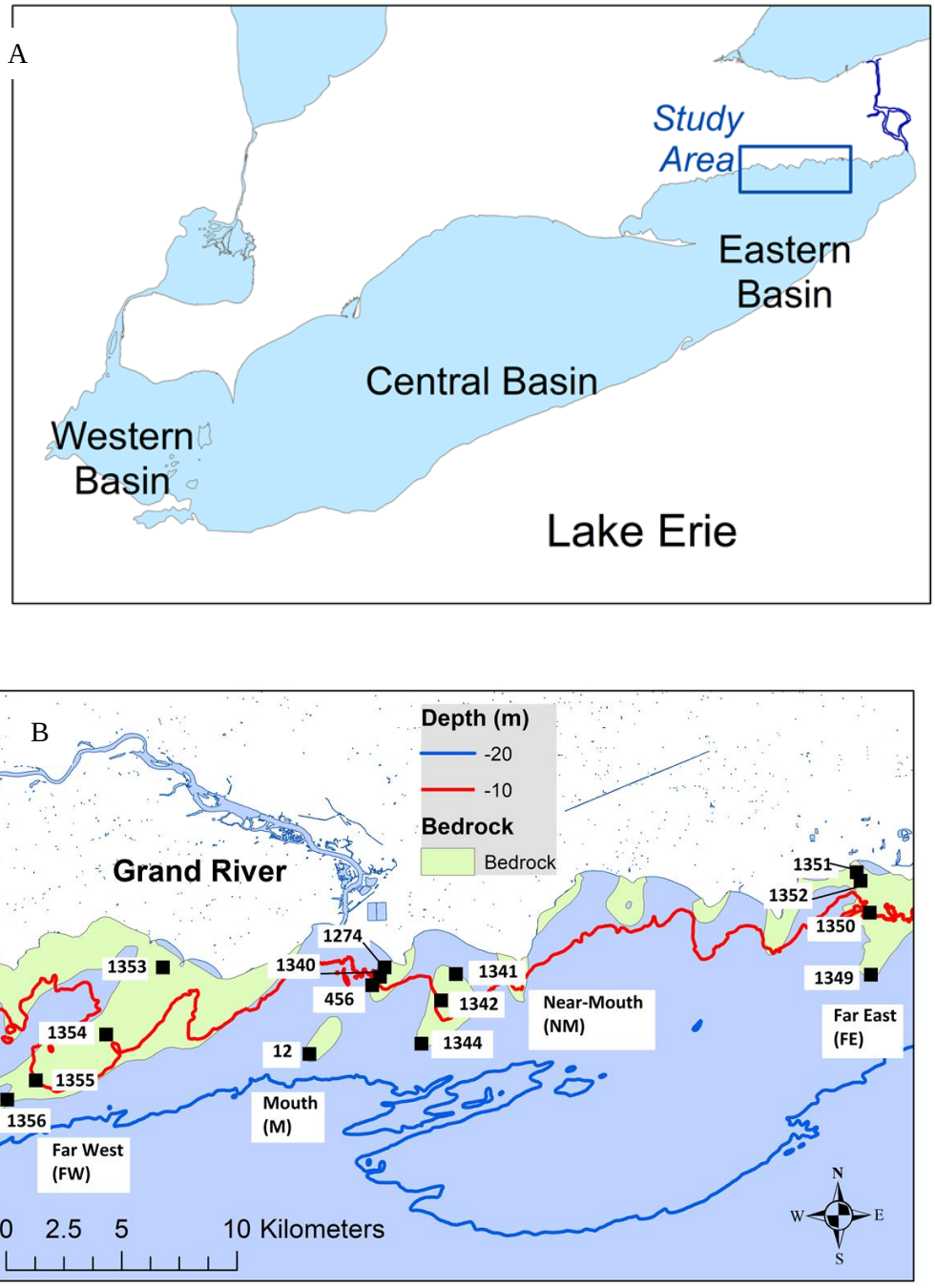

Figure 2.1: The nearshore study area (a) in context of the rest of Lake Erie, and (b) showing shoreline, the Grand River, sampling transects, and the 10m and 20m depth contours.

Table 2.1. Transects and associated stations

Transect	Station Number	Nominal Average Depth (m)	Coordinates (decimal degrees)	
			Lat	Long
Far-West (FW)	1353	3-4	42.840	-79.673
(Tecumseh Shoal)	1354	5-6	42.816	-79.704
(Transect 1)	1355	10-11	42.799	-79.738
	1356	17-20	42.790	-79.756
Mouth (M)	1274	3-4	42.839	-79.553
(Rock Point)	1340	5-6	42.837	-79.556
(Transect 2)	456	10-11	42.834	-79.559
	12	17-20	42.807	-79.595
Near-Mouth (NM)	1341	3-4	42.837	-79.518
(Lighthouse)	1342	5-6	42.828	-79.525
(Transect 3)	1343	10-11	42.822	-79.526
	1344	17-20	42.809	-79.535
Far-East (FE)	1351	3-4	42.874	-79.303
(Port Colborne)	1352	5-6	42.870	-79.301
(Transect 5)	1350	10-11	42.859	-79.295
	1349	17-20	42.824	-79.291

Table 2.2. Sampling summary, showing number of stations visited at any given transect, season, and year. Stations that were not sampled are denoted with "na".

		Early (May/June)				Late (Aug/Oct)			
Depth Group									
	Year	**FW**	**M**	**NM**	**FE**	**FW**	**M**	**NM**	**FE**
Shallow	2013	2	4	3	2	3	4	na	3
	2014	2	2	1	2	1	2	1	1
	2015	na	na	na	na	na	na	na	na
	TOTAL	**4**	**6**	**4**	**4**	**4**	**6**	**1**	**4**
Deep	2013	2	2	1	2	3	3	na	3
	2014	2	1	na	2	1	2	na	na
	2015	1	2	na	1	na	na	na	na
	TOTAL	**5**	**5**	**1**	**5**	**4**	**5**	**0**	**3**
Total stations	**61**								

2.2.2 Sampling and analytical methods

The water column was profiled with a YSI 6600 sonde or an equivalent instrument (June 2013) at a rate of ~0.1m/s, measuring specific conductivity and chla fluorescence as a proxy for phytoplankton biomass in the water column. Only the temperature and conductivity data are presented in the current study. Two profiles were collected at each station, one prior to water sample collection and one after. Specific conductivity data corresponding to the range 0.5m on either side of 1m or B-1 for each given station was averaged to determine the average specific conductivity corresponding to the bulk water samples collected at 1m and B-1.

Duplicate water samples were collected between the hours of 1000 and 1700 using a 10L horizontal VanDorn bottle at 1m below surface (1m) and at 1m above the bottom (B-1). Samples for SRP ("syringe method") were filtered within 30 minutes of collection using a 0.2µm pore nylon syringe filter

(Fisher Scientific). Water for the remaining analyses was stored in a cooler until processing in the shore lab that evening (generally from 1800 to 2300 h). SRP ("tower method") and NH_4 samples were filtered through a 0.2μm polycarbonate filter (AMD) into dedicated sampling containers, and stored in the dark at ~4°C until analysis as soon as possible after field sampling at U. Waterloo, typically 1-5 days. Seston was collected on GF/F filters (AMD) and frozen at -20°C until analysis for chla determination and on acidified (~2-3h) and millipore water-washed GF/F (Whatman) filters, and also frozen at -20°C until analysis for PP determination.

Filters for Chl a were passively extracted overnight (18-24 hours) in 90% acetone in a dark freezer (-20°C) and Chl a determined fluorometrically (Turner Designs, 10-AU, Sunnyvale, CA, USA) with acidification to correct for phaeophytin interference (Holm-Hansen et al. 1965). PP filters were persulfate digested at 100°C for 1h and analysed on an Ultrospec 3100 pro spectrophotometer using the molybdate blue method (Stainton 1980). SRP was also analysed on an Ultrospec 3100 pro spectrophotometer using the molybdate blue method. NH_4 was analysed fluorometrically using the methods detailed in Holmes et al. (1999).

2.2.3 Data analysis and statistics

Data analysis was conducted to find spatiotemporal patterns in nutrients and chla, specifically as it related to proximity to the Grand River, time of sampling, and depth of station. For purposes of formal parametric statistical analysis, data were grouped into "shallow" (<10m deep) vs "deep" (≥10m deep) depth categories, and "early" (May/ June) vs "late" (Aug/Oct) seasonal categories, using 2013 and 2014 data only. This yielded a data set that was reasonably balanced across spatial and temporal categories and amenable to ANOVA in designs that are described in the Results. Tukey HSD post-hoc tests were used to test for differences among transects. All analyses, including the linear regression analysis used in testing methodological influences on SRP estimates, were performed using the statistical toolbox in MatLab (MATLAB version 2016b).

Expected categorical values for two-way contingency tables of season and proximity to the mouth of the river were estimated using the probability of the whole sample set meeting any number of paired scenarios (Table 2.3) for syringe and tower samples. Independence of the two factors: (1) season (early or late) and (2) proximity (proximate – M and NM/distal – FW and FE) of observed samples was assumed, as the sampling sites did not covary with time.

Table 2.3. 2x2 factorial table assessing the combined effects of instances of early or late season and proximate or distal location and its relationship to either syringe or tower SRP filtration, and specifically for samples ≥2µg/l.

Proximity		Season	
		Early	Late
	Proximate	P(Early AND Proximately)	P(late AND proximate)
	Distal	P(early AND distal)	P(late AND distal)

The Independence Rule then allows that the probability of two factors is the product of the individual probabilities (i.e. P(A AND C) = P(A) x P(C) in Table 2.3) (Gotelli and Ellison, 2004; Whitlock and Schluster, 2007). The expected count is then the probability of factor 1 (i.e., proximity) and factor 2 (i.e., season) multiplied by the total sample size described by the equation (Gotelli and Ellison 2004):

$$\hat{Y}_{i,j} = \frac{row\ total\ x\ column\ total}{sample\ size} = \frac{G\ x\ E}{I} = \frac{\sum_{j=1}^{m} Y_{i,j}\ x\ \sum_{i=1}^{n} Y_{i,j}}{N}$$

		Factor 1		
		C	D	
Factor 2	A	P(AC) = P(A)·P(C) = (G · E)/I Expected = ((G·E)/I) ·I	P(AD) = P(A) · P(D) = (G·F)/I Expected = ((G·F)/I) ·I	G
	B	P(BC) = P(B) · P(C) = (H · E)/I Expected = ((H·E)/I) · I	P(BD) = P(B) ·P(D) = (H·F)/I Expected = ((H·F)/I) ·I	H
		E	F	I

2.3 Results

2.3.1 Spatio-temporal patterns in surface and near-bottom samples

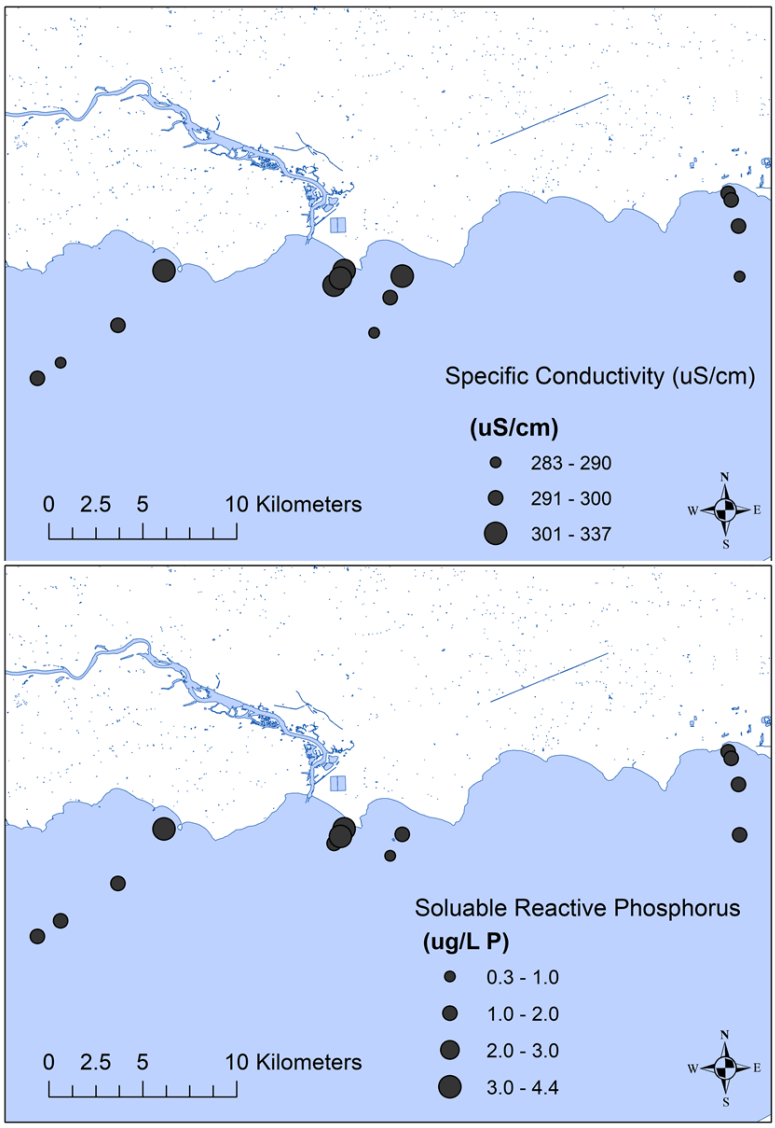

Figure 2.2. The average (2013-2015) spatial distribution of early season (May-June) surface (1m) values for (a) specific conductivity and (b) SRP (syringe method) concentrations.

Specific conductivity in the early season was highest at sites in the shallow nearshore, closest to shore (Figure 2.2). The two central transects (M and NM, Table 1, Fig. 1) closest to the mouth of the

Grand river had among the highest conductivity values but the early season average was highest at a shallow nearshore site to the west on transect FW. The trend to higher conductivity with proximity to shore was not apparent on the eastern (FE) transect, where values were uniformly low. SRP (syringe measurements) showed a pattern similar to conductivity (Fig. 2), with highest values in the shallow nearshore, close to shore. The eastern transect showed relatively low and uniform values for SRP, as for conductivity. The highest SRP values were at shallow nearshore sites on the M and NM transects, close to the Grand River, and not on the FW transect where conductivity showed its maximum value. The elevation of conductivity and SRP in the shallow nearshore on three transects was consistent with influence of water with higher conductivity and nutrient concentrations originating from the Grand River. To better quantify that and other influences, further analysis focused on just the FW, M and FE transects in the years 2013 and 2014. This afforded a relatively balanced sampling design (Table 2.2) and permitted tests of patterns not only near the surface but also near the bottom, and in late as well as early season.

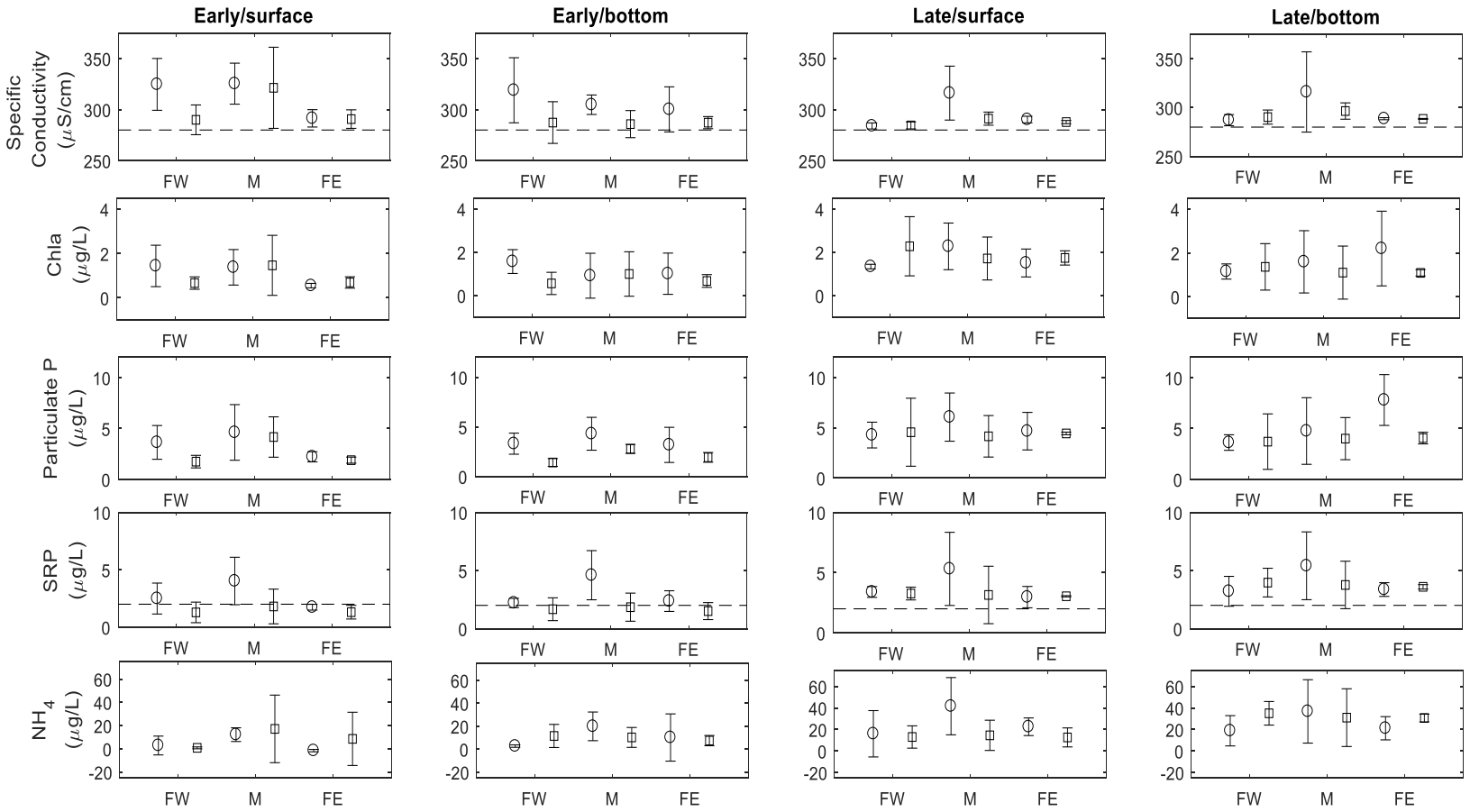

Figure 2.3.Average (2013-2014) values with 95% CI of measured variables in early vs late sampling season, and in surface vs near-bottom samples, at the FW, M and FE transects (cf. Fig. 1), with two pairs of symbols for each transect. Left symbols (circles) are for shallow and right (squares) for deep sites. Dashed lines in conductivity panels represent a typical offshore value, while the lines in SRP panels represent the 2μg/L value.

Average values for conductivity and SRP in surface samples during early season in the balanced data set (Figure 2.3) reflected patterns evident in Figure 2.2. Average conductivity on the M and FW transects was higher at shallow nearshore sites than deeper, but was relatively low and similar between shallow and deep sites at the FE transect. A similar pattern obtained for SRP, with the highest average value at shallow sites on transect M (Figure 2.3). Chl a and PP concentrations showed patterns similar to conductivity and SRP across transects and site depths. Patterns appeared different for NH_4. It showed no tendency to higher concentrations at shallower than deeper sites and, while highest concentrations were on transect M, there were also high concentrations on transect FE far from the river mouth.

In the late season, average surface sample values for conductivity, PP and SRP were still highest overall on transect M (Figure 2.3). Shallow sites still showed higher values than deeper for conductivity, Chla, PP, and SRP on transect M but not on either of the other transects. NH_4 was again different. In contrast to its early season pattern, it tended to higher average values for shallow than deep sites on all three transects, but it did again show high average values on the FE transect (Figure 2.3).

Observations in near-bottom (bottom for short) samples presented both similarities and differences to those in surface samples (Figure 2.3). Bottom samples generally showed higher averages for conductivity, PP and SRP at shallow than deep sites wherever surface samples did (e.g. transect M in early and late seasons). The direction of difference in average NH_4 values between shallow and deep sites was often different for bottom than surface samples, e.g. at the FW and FE transects. The most consistent difference was that bottom samples did not suggest as strong an elevation of conductivity, Chla, PP and SRP values at transect M, relative to other transects, as did surface samples.

Figure 2.3 showed frequent differences of average values between shallow and deep nearshore sites for early and late seasons but ANOVA detected a significant ($p < 0.05$) effect of site depth only for temperature and PP in bottom samples, and no significant effect for any variable in surface sample (Table 2.4). The binning of all sites <10 m deep into the shallow nearshore category may have concealed some of the very nearshore variation (evident in Figure 2) while increasing the variability of values within the shallow site category. Differences between transects (Figure 2.3), were significant for all variables except

temperature in surface samples (Table 2.4). Pairwise comparisons (Tukey HSD post-hoc tests, Table 4) showed that surface values on transect M were significantly ($p < 0.05$) greater than on FE for all variables but temperature and NH_4, and were greater than on FW for conductivity and SRP. Surface values did not differ significantly between FW and FE transects. The differences between transects were weaker in bottom samples. Only SRP showed a significant transect effect in bottom samples (Table 2.3), with significantly higher values at transect M than at FE or FW (Table 4). NH_4 showed a borderline ($p = 0.09$) tendency to higher values at M than at FE (Table 2.4, Table 2.5).

The effect of sampling period was often significant (Table 2.3; Table A2 shows means by period). All variables in surface samples, and all but conductivity and Chl a in bottom samples, differed significantly between early and late period (Table 2.4). Specific conductivity tended to decrease between early and late season samples, except in deep bottom samples in FW and FE. Specific conductivity also decreased in surface M samples, but not bottom. Chl a and PP were higher in late than early season at both sampling depths and across the different transects, with two exceptions (Chla on the FW transect and PP in surface samples from deep sites on transect M). SRP and NH_4 were higher in late than early sampling season in all transects, and in surface and bottom samples.

With values so variable across the sampling period, it might be that effects of riverine inputs and thus differences among site depths or transects could depend on sampling period. If so, significant interactions between factors might be anticipated. In surface samples, NH_4 had a significant interaction between period and site depth, and Figure 3 indeed suggested that there was a more consistent elevation at shallow than deep sites in the late season than the early season. There were no other significant interactions involving surface values. In deep samples, SRP and NH_4 had significant interactions between transect and site depth, reflecting the tendency for differences between transect M and the other transects to be larger for shallow than deep sites (Figure 2.3). The small number of interactions, relative to those possible in such 3-way ANOVA designs, suggested that the main effects did capture most of the variation in the data as aggregated for the analysis.

Table 2.4. F and probability values for main effects in three-way ANOVA to measure effects of transect, sampling period, and site depth category. Separate ANOVA was conducted for samples from the surface (1 m) and bottom (1 m above bottom).

	Sampling depth	**Conductivity**		**Chla**		**PP**		**SRP**		**NH_4**	
		F	**p**	**F**	**p**	**F**	**p**	**F**	**p**	**F**	**p**
Transect	Surface	**15.0**	**$2.13x10^{-5}$**	**3.96**	**0.0276**	**4.88**	**0.0130**	**6.88**	**0.00282**	**4.26**	**0.0215**
	Bottom	2.27	0.119	0.021	0.980	1.93	0.159	**7.36**	**0.00199**	2.48	0.0976
Sampling Period (Season)	Surface	**13.3**	**0.000881**	**9.01**	**0.00479**	**5.85**	**0.0205**	**4.47**	**0.0411**	**4.13**	**0.0493**
	Bottom	0.834	0.367	3.17	0.0836	**9.58**	**0.00368**	**4.18**	**0.0479**	**10.1**	**0.00288**
Site depth category	Surface	3.45	0.0720	0.110	0.742	1.16	0.288	2.54	0.119	0.0800	0.779
	Bottom	2.70	0.109	2.14	0.153	**6.12**	**0.0180**	0.719	0.402	1.40	0.2440

Table 2.5. Adjusted p-values from Tukey HSD post-hoc tests for significant differences between transects in surface and near-bottom samples.

Water quality parameter	Sampling depth	With Group		
		FW-FE	**M-FE**	**FW-M**
Conductivity	surface	0.4396426	**0.0000253**	**0.0013756**
Chla	surface	0.3310499	**0.0207285**	0.4084460
PP	surface	0.8806675	**0.0180632**	0.0606271
SRP	surface	0.7940660	**0.0246814**	**0.0040570**
SRP	bottom	0.8753945	**0.0035837**	**0.0145479**
NH_4	surface	0.7532965	0.1249082	**0.0227050**

As another approach to estimating the role of Grand River water in nutrient variability in the study area, tests for correlation with specific conductivity (higher in river than lake water) may reveal the nature of river water influence. Sites located along the M transect, closest to the river, showed the greatest incidence of significant positive correlations between conductivity and nutrients (Table A6). Correlations for PP and SRP were significant ($p < 0.05$) or borderline significant ($0.05 < p < 0.11$) for both surface and bottom samples and in both early and late periods. Except for surface samples in late season, NH_4 did not show significant correlations with conductivity on transect M. Chl a was significantly and positively correlated with conductivity only in early season surface samples. The correlations suggest a stronger influence of river inputs for particulate and dissolved P than for NH_4 or Chl a at transect M.

Table 2.6. Pearson correlation coefficients of Specific Conductivity with other water quality variables. Bolded values are significant at $p \leq 0.05$.

Transect	Period	Sampling Depth	Chla		PP		SRP		NH_4	
			r	p	r	p	r	p	r	p
FW	Early	surface	**0.817**	**0.007**	**0.906**	**0.001**	**0.748**	**0.021**	0.552	0.123
FW	Early	bottom	0.464	0.208	0.530	0.142	0.588	0.096	0.164	0.673
FW	Late	surface	-0.418	0.350	-0.448	0.313	0.619	0.139	-0.707	0.076
FW	Late	bottom	-0.638	0.089	**-0.753**	**0.031**	-0.147	0.729	0.454	0.258
M	Early	surface	**0.871**	**0.000**	**0.749**	**0.005**	0.511	0.089	0.425	0.168
M	Early	bottom	0.349	0.243	**0.562**	**0.036**	**0.696**	**0.006**	0.423	0.132
M	Late	surface	-0.165	0.696	**0.784**	**0.012**	**0.830**	**0.006**	**0.933**	**0.000**
M	Late	bottom	0.174	0.680	0.612	0.060	0.538	0.109	0.431	0.213
FE	Early	surface	-0.087	0.810	-0.084	0.818	-0.188	0.602	-0.421	0.226
FE	Early	bottom	**0.865**	**0.000**	**0.871**	**0.000**	**0.747**	**0.005**	-0.051	0.875
FE	Late	surface	-0.666	0.102	-0.526	0.225	-0.692	0.085	**0.842**	**0.017**
FE	Late	bottom	-0.322	0.534	0.483	0.332	0.282	0.589	0.381	0.457

Correlation analysis supported the suggestion from Figure 2 that river water could be important to variability at transect FW in early season, with surface Chla, PP and SRP (but not NH_4) showing significant and positive correlations with conductivity (Table A6). In late season, or in bottom samples, correlations were much weaker. No clearly significant positive correlations were observed, and PP actually had a significant negative correlation with conductivity for bottom samples in late season. There was clearly a greater uncoupling between nutrients and conductivity at FW than at M, consistent with weaker river influence and/or greater influence from confounding factors. At FE, Chla, PP and SRP showed no significant correlations with conductivity in surface samples (Table A6). They did show significant positive correlations with conductivity in bottom samples, but only in early season. NH_4 was not correlated with conductivity except in late season surface samples, when it was positively correlated.

2.3.2 Spatio-temporal patterns of SRP and relationships to methodology

Syringe and tower method estimates for SRP were positively correlated, but the relationship was not very tight (Figure 2.4), was not 1:1, and did appear to differ by season. Linear regression analysis for early season returned a slope of 0.448 and intercept of 1.49 ($r = 0.77$, $p<0.0001$) while for late season the slope was 0.541 and the intercept was -0.0243 ($r=0.74$, $p<0.0001$). The slope in both early and late season was <1, showing that syringe values increased relative to tower values as concentrations increased. In the higher concentration range, with samples deriving mainly from transect M, syringe SRP was commonly double the tower value. In the lower range of SRP concentrations, i.e. values of <2 deriving largely from transect FE, tower SRP could exceed syringe, but this was observed almost entirely in early season. Only two samples had a tower value greater than syringe in late season.

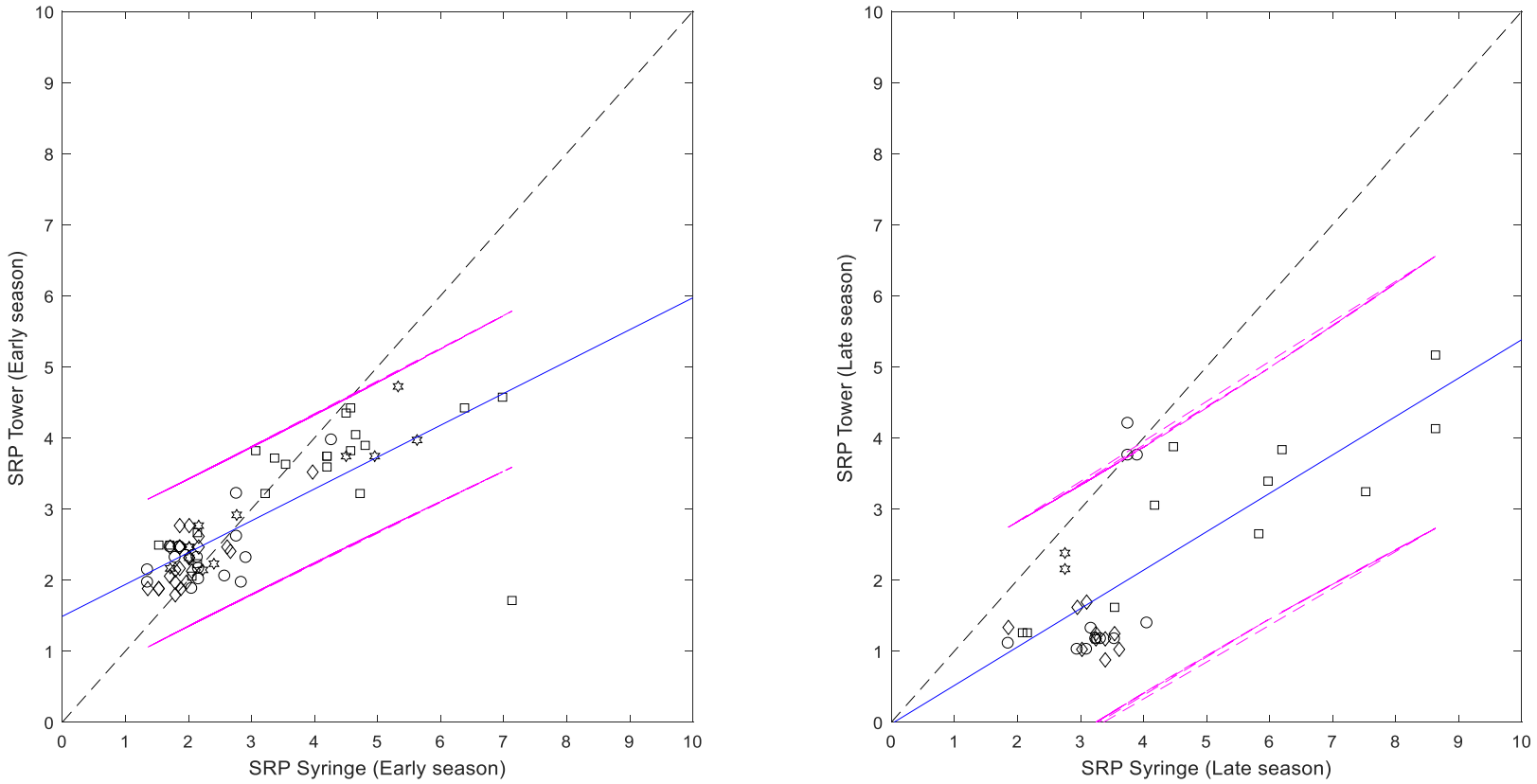

Figure 2.4. Comparison of SRP concentrations by syringe vs tower filtration methods in the (a) early and (b) late sampling seasons. SRP concentrations are in µg/L, the dashed grey line is the 1:1 line, the blue line is the linear fit of SRP syringe and SRP tower data, and the magenta lines indicate the 95% confidence interval of the fit.

There were many similarities in spatial and temporal patterns shown by the two methods (Figure 2.4, Table A6). For example, when syringe results suggested higher SRP at shallow than deep stations, tower results generally did as well (Figure 2.5). Transect M had generally elevated SRP compared to other transects, regardless of the method. ANOVA on results by both methods showed that transect and season were significant influences on SRP in both surface and bottom samples (Table A6). Station depth was not a significant factor for SRP by either method. Despite these similarities, Figure 2.5 did suggest some differences. For example, the elevation of SRP at transect M seemed larger by syringe than tower method, especially in late season. Late season SRP by tower appeared systematically lower than by syringe, with more values below the 2 μg/L value (an approximate threshold for P sufficiency of *Cladophora*.)

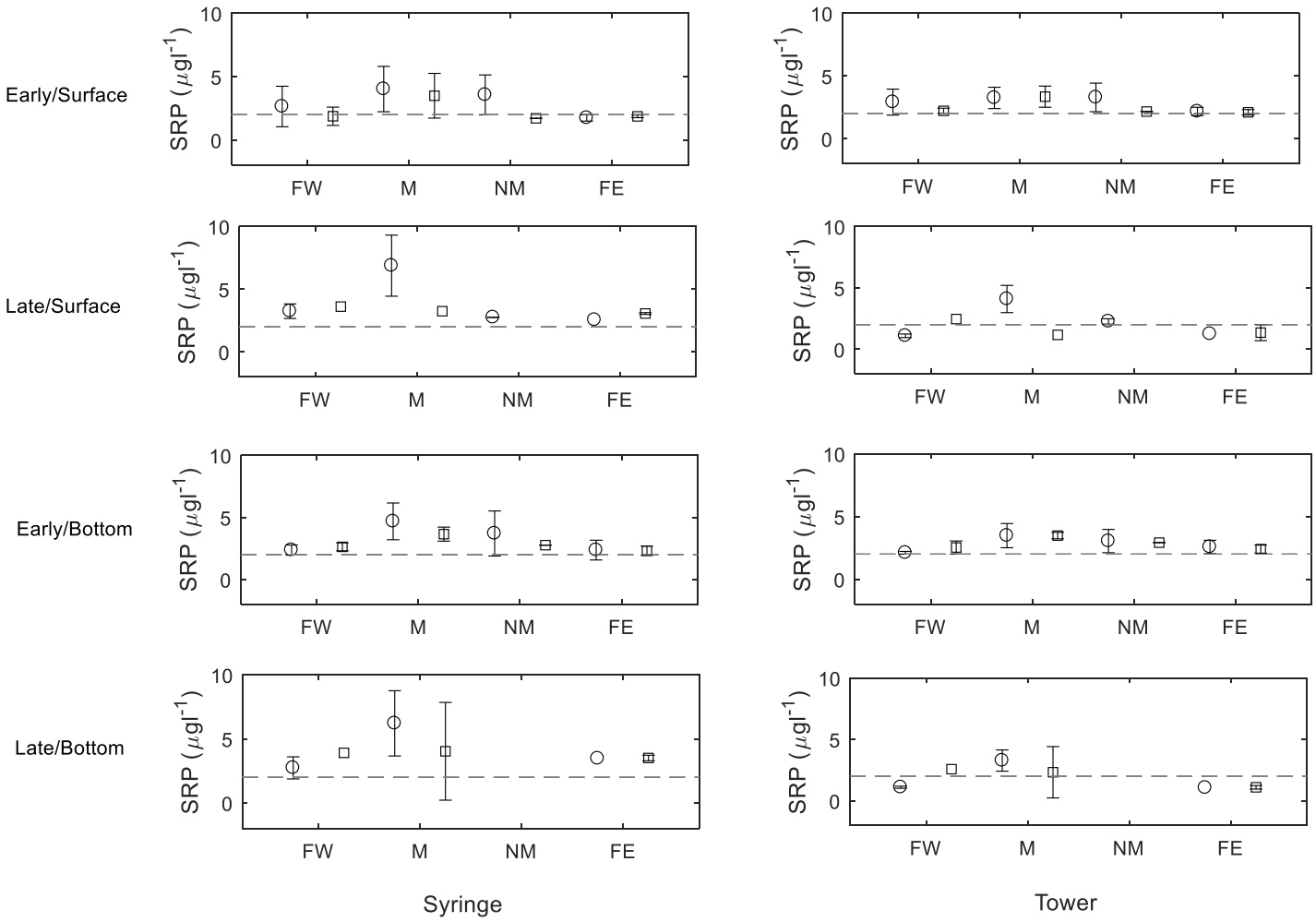

Figure 2.5. Average values for SRP in surface and bottom samples by syringe- and tower filtration methods on three sampling transects in 2013 and 2014. Circles denote shallow sites, squares deep sites, and error bars are 95% confidence intervals. Grey dashed lines indicate 2µg/l.

Neither method suggested a strong or consistent difference between surface and bottom samples (Figure 2.5, Table A6) but there was some evidence that bottom samples could be higher in concentration than surface sample for the syringe results. With station depth a non-significant factor (Table A6), data were pooled across station depths to allow an ANOVA with transect, season and sampling depth as factors (Table 2.7). The analysis confirmed the significant effects of transect and season. The effect of sampling depth approached a significant probability for syringe but not tower. There were no significant interactions with sampling depth. The results thus supported pooling across station and sampling depths for further analysis of spatial and temporal patterns. In subsequent analyses, these are categorized as "proximate" (M and NM stations) and "distal" (FW and FE stations) sample groupings on the assumption that proximity to the Grand River is the main factor that differs among transects. The "early" and "late" season categories were maintained.

Table 2.7. ANOVA results with proximity to the Grand River, season of sampling, and sampling depth as factors. Data were pooled across station depths (shallow and deep).

Sample	factors	F	p	Significant Interactions		
				Interaction	F	p
Syringe	proximity	15.01	0.00			
	season	9.28	0.00			
	sampling depth	1.64	0.20			
Tower	proximity	16.37	0.00	season/prox	3.54	0.00
	season	8.19	0.00			
	sampling depth	0.08	0.92			

Aggregated by season, proximity and method, SRP concentrations (mean and median) were higher for syringe than tower samples, except for the proximate early category, where tower concentrations were higher. The data did not meet assumptions for normality in a Kolmogarov-Smirnov

test even with log-transformation. The means were skewed by some very high measured concentrations, with medians in some cases considerably lower than means (Table 2.8).

A Kruskal-Wallis test (the non-parametric equivalent to a t-test, which was used because of unequal sample sizes) revealed that medians of SRP syringe- and tower-filtered sample distributions differently significantly (χ^2=39.35, p = 1.67x10^{-6}). Post-hoc comparisons showed there were significant differences between syringe and tower medians for both proximate and distal sites in the late season. Medians did not differ significantly between methods in early season.

The frequency of samples >2μg/L appeared to vary between seasons, methods and proximity (Table 2.8). The frequency of above-threshold occurrence of SRP was apparently higher for proximate (i.e. both shallow and deep stations and surface and bottom samples at M and NM transects) than distal sites (shallow and deep stations and surface and bottom samples at FW and FE transects) by both methods, but especially syringe. Notably, both proximate and distal Tower samples showed more instances of above-threshold SRP in the early season, more so than Syringe samples for the same season. This somewhat surprising result reflected the occurrence of some very high SRP values in some distal samples in Figure 2.5 and was also apparent in the relatively large difference between mean and median concentrations for distal sites, at least by syringe method (Table 2.8). The incidence of samples > 2μg/L among seasons, transects (proximity) and SRP method was significantly different ($p<0.05$) from random according to a $\chi 2$ test of a 2x2x2 contingency table ($\chi 2 = 41.3$, df = 9, $\chi 2_{crit} = 16.9190$, p =4.42 x10^{-6}). The effect of season and proximity on the frequency of samples with concentrations >2μg/L was significant ($p<0.05$) by each method (syringe- filtered $\chi 2 = 14.0$, df = 3, $\chi 2_{crit} = 7.8147$, p = 0.00289; tower-filtered $\chi 2 = 27.3$, df =3, $\chi 2_{crit} = 7.8147$, p = 5.13 x10^{-6}).

Table 2.8. Summary statistics for SRP determined by two methods in two periods of observation and two classes of distance from the Grand River.

	Syringe					Tower			
	n (for each of syringe and tower samples)	Mean concentration	Median concentration	95% CI interval from mean	freq>2	Mean concentration	Median concentration	95% CI interval from mean	freq>2
Distal early	42	2.48	2.05	0.355	0.548	2.65	2.46	0.238	0.806
Distal late	20	3.40	3.39	0.369	0.519	1.93	1.32	0.443	0.148
Proximate early	31	3.07	2.16	0.480	0.762	2.83	2.46	0.270	0.881
Proximate late	27	4.25	3.32	0.881	0.950	2.19	1.65	0.564	0.450

2.4 Discussion

It was anticipated that the shallow nearshore, the site of most nuisance *Cladophora* growth, would be enriched in bioavailable P and N compared to the deeper nearshore, with much of the enrichment attributable to the major tributary in the study area and further enhanced in near-bottom samples due in part to internal loading from dreissenid mussels. Some of those patterns were observed but the most striking result was the pervasive abundance of available P (SRP) relative to estimated *Cladophora* needs throughout the study area in both surface and near-bottom samples, and by two variants of standard SRP methodology. Variations in methodology for SRP did influence the perceived patterns of spatiotemporal variations, highlighting one challenge of properly characterizing the complicated and dynamic nearshore zone with traditional surface vessel survey methods.

2.4.1 Nutrient conditions and contributing factors in shallow vs deep nearshore with consideration for surface and near-bottom water samples

The nearshore zone in eastern Lake Erie has been observed to have higher nutrients compared to the offshore (e.g. Dove, 2009) but also lower Chl a (Depew *et al.*, 2006a; Smith *et al.*, 2007; North *et al.*, 2012) in years following the lake's colonization by dreissenid mussels. It is still not entirely clear whether the nearshore should be further subdivided based on gradients of nutrients and Chl a in order to better understand the conditions associated with nuisance *Cladophora* growth, which occurs in the shallower (<10 m) subsection of the nearshore. We sought to clarify whether the shallow nearshore (<10m deep) was enriched compared to the deep nearshore (≥10m deep). We believed there to be two possible sources of this enrichment. One was by terrestrial influences, largely the Grand River (e.g. Chomicki *et al.*, 2016), but also non-point sources such as runoff on the margins directly into the lake and direct groundwater inputs (e.g. Barton, Howell & Fietsch, 2013; Kornelsen & Coulibaly, 2014; Knights *et al.*, 2017; Orihel *et al.*, 2017) that are not as well characterized, but are nonetheless thought to

be potentially important contributors of nutrients to the nearshore. Internal sources of nutrients, including dreissenid mussel excretion and hypolimnetic upwelling, may also be important in nearshore enrichment. If terrestrial sources were the major source of variation between the shallow and the deep nearshore, we expected to see elevation of both particulates (chla and PP) and soluble nutrients (SRP, NH_4) co-occurring with elevated specific conductivity in proximity to the shore (i.e. the shallow nearshore) compared to farther away (the deep nearshore). If dreissenid mussels were a larger driver of the variability in the nearshore, we would expect to see similar or smaller concentrations of particulates but higher concentrations of soluble nutrients in the shallow nearshore than the deeper nearshore. Upwelling of cold hypolimnetic water can be detected by dramatic and sharp decreases in water column temperature toward the lake bottom that is transient in nature (Valipour *et al.*, 2018). Upwelling was unlikely to be an important contributor of nutrient enrichment near bottom in our system, as these dramatic temperature drops were not observed.

The spatial distribution of specific conductivity, chla, PP, and SRP in early season appeared to show an influence of river input, and potentially other external surface loading, with these variables elevated in proximity to the river and closer to shore. Average values were typically higher for shallow than deep nearshore. However, ANOVA did not reveal significant differences for any of the measured variables. Binning stations into the two depth categories, and averaging over time, likely failed to fully capture the spatial and temporal dynamics, which introduce considerable variability within each depth category. Studies elsewhere have found that distinctive patterns of water chemistry in the shallow nearshore are often very tightly coast-bound and dynamic, making them hard to quantify in most survey designs (e.g. Howell *et al.*, 2012). Spatially and temporally restricted episodes of enrichment can still be seen in the present results, however (e.g. Figure 2) and can be of great significance to *Cladophora*, which is capable of luxury uptake and storage of P (Auer *et al.*, 2010).

The pattern of concurrent elevation in NH_4 and SRP and slight depletion of Chl a and PP in bottom samples relative to surface sample patterns (Table A2) provided evidence of dreissenid mussel (internal loading) impacts on the nearshore. Mussels have the highest biomass at depths <10m, would be

expected to have a relatively greater impact on the shallow nearshore compared to the deep, including elevation of dissolved nutrients in the nearshore. The nearshore shunt hypothesis and subsequent experiments investigating it demonstrate that mussels may deplete near-bottom seston (e.g. Schwalb *et al.*, 2013) and enrich the nearshore benthos with soluble nutrients, particularly P and N (e.g. Ozersky *et al.*, 2009). While dreissenid mussels may not be direct sources of P, they are an important pathway for externally loaded P to be introduced in bioavailable form in the benthos. P is more limiting to *Cladophora* growth than N and will be taken up preferentially, especially early in the season when *Cladophora* is at its maximal growth rate (e.g. Higgins *et al*. 2005, 2008), leaving N in the water column. Elevated NH_4 may be a proxy tracer of mussel activity, and elevated NH_4 in concert with decreased Chl a and PP may provide evidence of mussel effects. The directional difference in terms of Chl a and PP showed a decrease at the bottom relative to surface, and SRP and NH_4 showed an increase in the bottom relative to the surface (e.g., Figure 2.3), but these differences were not statistically different, so shunt effects, while suggested, were not obvious.

Tributary inputs from the Grand River may also impact the nearshore, but may not impact all portions of the nearshore in a uniform manner. Specific conductivity has been used as a tracer to probe for the influence of the Grand River on the nearshore in a previous study (Chomicki *et al.*, 2016), and correlations between specific conductivity and SRP, PP, and Chl a at mouth stations lend support for the river acting as source of nutrients and Chl a to the nearshore. Importantly, specific conductivity did not significantly correlate with NH_4, suggesting that there might be another source of this nutrient; dreissenid mussel excretion and other internal loading processes are likely important. Generally, nutrients and Chl a at farther transects (Far West and Far East) did not show elevated specific conductivity (relative to M stations), nutrients, or chla, suggesting that the river's influence is localized to sites within its near vicinity. The far west transect is located closer to the mouth of the Grand River than the far east transect, and observations of elevated specific conductivity and SRP at shallow far-west stations may be consistent with observed reversals in the shore-parallel flow that can occur (He *et al.*, 2006; Chomicki *et al.*, 2016). The positive correlation of SRP with specific conductivity in bottom samples at far-east stations is harder

to explain, as it is generally believed that the river plume is effectively mixed away at this distance. However, models simulating the behaviour of the Grand River plume suggested that in the late spring, the plume mixes with lake water, and is transported at whatever depth it is neutrally buoyant (He *et al.*, 2006). The river tends to be warmer than the lake, and may be buoyant enough as a result that it skirts along the surface quite a distance, before cooling and sinking (Chomicki *et al.*, 2016; Demchenko *et al.*, 2017), and may be transported relatively intact with the shore-parallel flow some distance before gradually becoming mixed away.

Specific conductivity, chla, PP, SRP, and NH_4 in surface samples showed a strong significant effect with proximity to the river, suggesting that the higher conductivity and these measured variables near the mouth was likely a result of river influence. Chomicki *et al*. (2016) noted that the specific conductivity of the Grand River was closer to 800µS/cm while the lake was ≤290µS/cm, and stations closest to the mouth of the river were 300-400µS/cm. This suggests strong mixing with lake water, which should serve to dilute the incoming river plume nutrient and Chl a load. However, despite the drop in specific conductivity, SRP and NH_4 still showed a proximity effect in a three-way ANOVA in surface samples, and in bottom samples for SRP, which may be related to sediment loading and nutrient release from these sediments. This could suggest that the river has some role in elevating SRP and NH_4 concentrations, but not directly via river inputs, mediated through release from river-borne particles that settled out and decomposed at the lake bottom, proximate to the river. As the Grand River represents the largest tributary load to this portion of Lake Erie, sediment suspended in the plume may interact with bottom turbulence, resulting in release of soluble P (Cyr *et al.*, 2009), thus contributing to an increase in soluble P and N, that may either remain near-bottom, or become mixed into the water column. Mussels may also play a role in solubilizing nutrients contained in particles entering from the river, and may do especially well if the particles are of a high quality, such as phytoplankton. In mesocosm experiments, zebra mussels tended to excrete more SRP with higher amounts of PP ingested (Vanderploeg *et al.*, 2017), and it is possible that quagga mussels in our study at mouth and near-mouth stations would do especially well supplemented by river seston. Chl a and PP were significantly and relatively well-

correlated with specific conductivity at shallow mouth sites, and may help to explain the elevated SRP and NH_4 in proximity to the river mouth. These results point to the need for other forms of nearshore water quality monitoring, with a special focus on material going into and out of the lake bottom.

Cladophora biomass was extremely high at shallow stations in the FE transect based on concurrent sampling done by Environment Canada (Table C2), despite lack of evidence of a strong river enrichment effect in this area (i.e. specific conductivity was ~300µS/cm) (Figure 2.3, Table 2.6). A combination of mussel effects (increased water clarity and near-bottom nutrients) and non-point terrestrial sources in this area would help to explain this phenomenon. Upwelling is thought to bring nutrient-rich hypolimnetic water into contact with this portion of the nearshore (MacIntyre & Jellison, 2001; Valipour *et al.*, 2018). However, upwelling did not appear to be occurring at our sites at the time of sampling at any given station, as no part of the water column was significantly colder than other stations on the same transect measured earlier in the day. This drop in water column temperature associated with upwelling (MacIntyre & Melack, 1995) was not seen in our stations; that is not to say that upwelling did not occur or is important to near-bottom nutrient enrichment. At the time of sampling, which captures a "snapshot" of nutrient conditions, upwelling may not have been an important part of near-bottom enrichment or strong turbulence may have muted the cold water temperatures associated with upwelling.

Sampling period (early vs late season) showed a significant effect for chla, PP, SRP, and NH_4 in surface and bottom samples. However, these nutrients were generally higher in the late period, while specific conductivity was concurrently lower. This suggests that the relative increases in Chl a and nutrients was due to factors other than the river, and may be a result of a shift in nutrient supply and demand processes. This may be related to both *Cladophora* P uptake and mussel P excretion. *Cladophora* in the early part of the growing season (e.g. May-June) is expected to have a higher internal P concentration (Higgins *et al.*, 2008b), which combined with increasing photoperiod, could be sufficient to support rapid growth and biomass production. Rapid growth would result in decreased internal P concentration, resulting in maximum rates of P uptake from the environment to support growth. Conversely, in the late part of the season (August/October), self-shading results in light, not phosphorus,

limiting growth; *Cladophora* might not be expected to take up as much P from the environment in these scenarios. A relative decrease in P uptake by *Cladophora* might result in SRP elevation in the late part of the season in surface and bottom samples, which was seen in Figure 2.3. Because of their abundance, it is possible that dreissenid mussels may have variable effect on the nutrient environment at the bottom where *Cladophora* are located. Early in the season, much of their ingested nutrients might be directed more toward growth and reproduction, resulting in less P excretion (Arnott & Vanni, 1996; Stoeckmann, 2003; Stoeckmann *et al.*, 2011). In the later part of the season, a higher Chl a concentration and increased water temperature may result in greater feeding, respiration, and nutrient excretion. This too, might result in water column SRP appearing to be slightly higher in the late season compared to the early season. The combination of a high demand/lower overall supply in the early part of the season, and a reduced demand/higher overall supply in the later part of the season may help to explain the enrichment of Chl a and nutrients in the late part of the season that is not strongly related to specific conductivity. While horizontal and temporal patterns of nutrient and chla are important in understanding what may be driving nuisance *Cladophora* biomass in the nearshore, nutrients and chla located near bottom have a more direct effect on the mussel feeding and excretion, and on *Cladophora* growth than at the surface.

Cladophora growing at the lake bottom may experience different nutrient conditions relative to the surface, but surface samples commonly collected in routine water quality monitoring may not adequately capture nutrient conditions and dynamics near-bottom. The Grand River and dreissenid mussels were expected to variably impact surface and bottom samples in different proportions; dreissenid mussels were expected to show a larger effect in bottom samples consistent with the nearshore shunt hypothesis (i.e. significantly elevated SRP and NH_4, and significantly decreased chla). However, based on three-way ANOVA, sample depth (i.e. surface vs bottom, Table 2.4) did not have a significant effect explaining distribution of water quality parameters, suggesting that these sources have a relatively weak impact relative to other sources of variation.

Surface and bottom samples showed similar spatiotemporal patterns in nutrients and Chl a relative to the Grand River, suggesting that the river is a source of nutrients and Chl a to this portion of

the East Basin nearshore. Apparent PP concentrations tended to increase with time, and may have reflected resuspension events that tended to occur more often during late season sampling in our study site. Increased tributary loading did not appear to be the reason for enhanced PP concentration in the nearshore, as M station PP did not increase in the late season relative to the early season. Specific conductivity was almost to offshore background levels in the late season at FW and FE stations, which suggests that enhanced PP concentrations at these stations was not due to tributary loading of sediment. Shallow FW stations in the early part of the season also show elevation, and this was likely due to current reversals, which are common (He *et al.*, 2006; Chomicki *et al.*, 2016). Slight, non-significant elevations in SRP and NH_4 and decreased Chl a in bottom samples relative to their surface counterparts may point to dreissenid mussel activity as a further source of nutrients that need to be considered. Plume effects appeared to be extremely localized and largely mixed thought the water column at further sites, since specific conductivity at farther sites was not elevated. Martin (2010) found slight enrichment within 0.5m of the bottom, but they were often not significantly different from surface measurements. The East Basin nearshore is relatively energetic, and near-bottom mixing relatively strong, which would serve to limit near-bottom nutrient gradients, but would enhance overall bulk concentrations (sensu Dayton *et al.* 2014). SRP occurred above limiting concentrations in the nearshore in both surface and bottom samples, suggesting a relatively enriched sampling area that may be favourable for nuisance *Cladophora* growth over the entire sampling area.

Proximity and time of season were important for both surface and bottom samples, and may need to be explicitly considered in future work to understand the causal factors controlling nuisance *Cladophora* biomass, but sample depth may not be as important a consideration. Surface and bottom means and nutrient distributions showed slight, but not statistical differences, suggesting that surface samples may be indicative of the near-bottom nutrient environment in the northern nearshore of Lake Erie's East Basin, though they should be interpreted with caution. It is nonetheless recommended that near-bottom samples be collected if *Cladophora* and the benthic environment are the target considerations.

2.4.2 SRP methodology and spatiotemporal patterns inferred from sampling surveys

Spatiotemporal nutrient pattern determinations in lakes still tend to be based on data collected from small surface vessel surveys. Variation in SRP filtration methodology, including filtration pressure, time between sample collection and filtration, type of filter, and volume of sample filtered, may affect estimated SRP concentrations, and may further influence perceptions of spatiotemporal patterns of SRP in sampled lakes. Where SRP spatiotemporal patterns of SRP are important for informing management decisions, knowing how sampling methodology may or may not affect interpretations is vital.

It was not possible with the current data to diagnose which of the possible mechanisms were contributing to the methodological differences observed. However, perceived patterns of spatiotemporal variations of SRP may influence interpretations of underlying nutrient cycling processes in the study area. The frequency of SRP>2µg/L, for example, was similar between methods in early season, but was higher by syringe method in late season (Table 8). Syringe filtered samples also showed a greater incidence of SRP above threshold near bottom compared to 1 m below surface than did tower filtered samples, and at sites not believed to be directly impacted by the Grand River plume (e.g. far-west and far-east deep (distal) stations).

The method and timing of sample filtration may have important impacts on the resultant SRP concentration, as a result of methodological differences that could skew sample concentration. The apparent difference in results (i.e., a lack of 1:1 relationship) between the two methods was sensitive to season of sampling, but did not appear to be related to sample holding time. These spatiotemporal variations suggest that variations in the nature of the sample material may be related to the disparities between methods. The syringe filtration and tower filtration methods differed in their sample handling (sample transfer methods, filter types and pressures) and the interval between sample collection and filtration. Filtration is ideally done as soon as possible (Jarvie *et al.*, 2002; Worsfold *et al.*, 2005; Worsford *et al.*, 2016) but operational constraints (e.g. sample boat size and capacity) may necessitate sample holding instead of immediate filtration. Syringe filtration can be done immediately, but contamination may have a larger effect on a smaller water sample (30mL). Tower samples, by contrast,

use larger volumes of water, but whole water must be held for longer, are transferred multiple times. Both methods may be sensitive to inadequate apparatus rinsing between samples. In all cases, filtration must be done under relatively low pressure to avoid cell lysis or filter breakage, which would contaminate the sample. The act of filtration can break apart algae, including flagellated, ciliated, or microfibril-containing algae (Bloesch & Gavrieli, 1984; Taylor & Lean 1991; Fisher & Lean 1992; Leppard *et al*., 1977; Taylor, 2010), resulting in artificially higher measured concentrations in dissolved P (Taylor, 2010). P bound to small particles (e.g. cell fragments or viruses) can pass through 0.2μm pore filters under vacuum, but might not otherwise passively go through (Taylor, 2010) and may react with the molybdenum blue reagent, resulting in slight over-estimation of SRP in the sample (Stainton 1980, Taylor 2010). The pressure during syringe filtration is dictated by the force with which the sample collector pushes on the syringe plunger, which may impact the resultant filtrate. During sampling, care was taken to exert sub-maximal force, only as was necessary to move sample water through the filter. Further, highly productive waters might clog the filter, impacting the resultant filtrate.

The slightly surprising trend of slightly lower SRP concentration in the early part of the season in syringe samples may be related to P-cycling processes occurring in relation to whole-water storage vs almost immediate sample processing. In the early part of the season, there is likely to be a large demand for SRP from both suspended phytoplankton (i.e. the spring bloom) and benthic algae, including *Cladophora*, which tends to rapidly grow once temperature and photoperiod are no longer inhibiting to growth (Higgins *et al.*, 2005b, 2008b, 2012; Auer *et al.*, 2010). Despite relatively large concentrations of TP entering the lake, SRP might be in relatively short supply relative to sinks. Similarly, distal sites are less likely than proximate sites to be directly impacted by the river plume, and also have a more favourable benthic light climate that may promote luxury uptake by phytoplankton(Litchman & Nguyen, 2008) and heterotrophic bacteria (Khoshmanesh *et al.*, 2002; Orihel *et al.*, 2017) in the sample. Conversely, sample water with a low SRP concentration as a result of uptake processes by benthic algae and phytoplankton may experience relief of P uptake demand, recycling processes remain the same, resulting in a net change in tower filtered SRP compared to syringe filtered SRP. Samples taken from

distal sites tended to have a lower phytoplankton biomass (based on Chl a as a proxy) than samples from closer to the river mouth, in part because the Grand River inputs phytoplankton. Proximate samples in the late season were similar between syringe and tower filtration methods. The similarity between syringe and tower filtration methods in the late season may have been related to the reduced number of samplings due to summer storm-related operational constraints. Fewer sites were visited on these days, and sampling holding time between collection and tower filtration was often hours shorter than some samples collected in the early part of the season. Differences in filtration methodology may affect how absolute concentrations of SRP are perceived, but in terms of magnitude and direction of spatial patterns of SRP, at least points in the same direction.

This paper's key findings demonstrate that tributary influence is clear but spatially restricted near the mouth of the Grand River. Mussels may have an impact on nearshore nutrient enrichment in the shallow nearshore, but the current methodology is not sufficient to fully capture their impacts near bottom, and other methods are needed. The method of filtering for SRP does not change the main nutrient distribution patterns, but does alter the apparent frequencies of occurrence between the early and late sampling season. Filtering as early as possible, in line with published literature, is the best approach. SRP is quite elevated in the nearshore, and is likely more than enough to support nuisance *Cladophora* growth in this area. This elevation in nearshore SRP appears to be from a number of sources, including the river, mussels, non-point sources, loading from the Central basin, and other physical processes that serve to liberate or introduce SRP.

Chapter 3: Vertical structure and benthic-pelagic coupling in the rocky and energetic nearshore of a dreissenid-colonized Great Lake

Dreissenid mussel feeding may be an important mechanism in benthic-pelagic coupling, and the impacts of water column stratification and near-bottom water motion may impact the flux of chla into mussel beds. Stations ranging from 3-18m deep located in the northern nearshore of East Basin Lake Erie were profiled for temperature and chla using a YSI sonde and near-bottom water velocity was measured with an acoustic Doppler current profiler (ADCP), from which diffusivity was estimated. Mussels were collected from quadrats at each of the sites over the course of two years. Stratification was found to be common, even at shallow 3m sites, and most often occurred in June. While there was evidence of coarse vertical differences in Chl a and nutrients between surface and near-bottom, there did not appear to be many instances of these coarse vertical differences associated with the presence or absence of stratification. Upwelling was not a source of near-bottom nutrient enrichment. Within the near-bottom water column, Chl a depletion gradients were predicted and observed, although they were not predicted at a frequency greater than a random guess. Near-bottom diffusivity ranged between 10^{-3}-$10^{-4}$$m^2$/s on average. Assimilation flux (the product of estimated mussel assimilation/feeding rate and mussle biomass) and turbulent diffusive flux (the product of the near-bottom concentration gradient of Chl a and diffusivity) of Chl a had a very weak negative correlation, while assimilation flux correlated moderately with mussel biomass. Dreissenid mussels can have large impacts on shallow systems, but stratification and near-bottom water motion impacts their ability to siphon in and assimilate their food. These limitations could directly impact their nutrient excretion, particularly of soluble phosphorus, which is a nutrient of great interest in understanding and controlling nuisance Cladophora in the nearshore.

3.1 Introduction

The reappearance of nuisance Cladophora blooms in the East Basin of Lake Erie following colonization by non-native dreissenid mussels and without known increases in phosphorus loading to the lake suggests that mussel feeding and excretion (benthic-pelagic coupling) (Hecky *et al.* 2004) may be an important mechanism providing phosphorus to Cladophora. Dreissenid mussel biomass is high in the East Basin nearshore (Burlakova *et al.*, 2014) and its maintenance requires a high flux of seston, particularly phytoplankton, into the benthos. Phosphorus in the seston will be partially retained in new mussel biomass but will also be released in feces, pseudofeces, and as excreted (dissolved) phosphorus.

Dissolved (SRP) phosphorus excretion (Martin 2010; Dayton *et al.* 2014; Chomicky *et al.* 2016; Depew *et al.* 2018) has received more attention than particulate release. Mussel excretion (and faecal production) will be limited by food quality as well as the feeding rate. Based on mesocosm experiments, dreissenid mussels excrete less soluble P when their food quantity and quality is low (Vanderploeg *et al.,* 2017). The flux of P emanating from mussels is thus hard to predict but a knowledge of their rates of feeding and P intake in natural settings can at least establish an upper bound. Knowledge of feeding rates under fully natural conditions is still limited, however.

The interplay between turbulence and stability in the near-bottom water column affects mussel feeding through mass transport limitation (Ackerman *et al.*, 2001; Boegman *et al.*, 2008b; Schwalb *et al.,* 2013). When mass transport limitation occurs, feeding rates will be less than expected from lab studies under more ideal conditions and depletion of phytoplankton (as indexed by Chl a) near the bottom may be expected. Where there are gradients of diminishing Chl a towards bottom, it may be possible to estimate the flux of Chl a into mussel beds under fully natural conditions as a diffusive flux process. Such estimates have never been made for dreissenid mussels. There has been evidence of overall chla depletion through the water column following dreissenid mussel introduction (Fahnenstiel *et al.*, 1995a; Yu & Culver, 1999) in well-mixed water columns. Early estimates of their impacts on the West Basin of Lake Erie suggested that mussels may be capable of filtering the 7m high water column between 3.5-18.8 times a day but it was soon realized that physical constraints on their access to seston would often make their effective filtering rates much lower (MacIssac *et al.,* 1992; Boegman *et al.,* 2008). Mass transport limitation can be expected to vary with strength of stratification and near-bottom turbulence (Schwalb *et al.*, 2013). The intensity of depletion of Chl a near-bottom should also vary with mussel biomass and the corresponding rate of seston filtration. However, the jets from the exhalent siphons of the mussels can cause turbulence, enhancing near bottom mixing, and obscuring near bottom gradients (O'Riordan *et al.*, 1993, 1995; Nishizaki & Ackerman, 2017). The incidence of near-bottom Chl a depletion and its relationship to turbulence, stratification and mussel biomass is not currently well defined for systems dominated by dreissenid mussels.

Stability, in the form of stratification, serves to impede turbulence and turbulent delivery of seston to mussels. Stratification can form from incident solar irradiation heating the water surface, while bottom waters remain relatively cool. This temperature separation may lead to density stratification (Kalff 2002), which may serve to isolate bottom waters from surface waters. Extremely warm calm conditions (Loewen *et al.*, 2007) can also be drivers of stratification in the nearshore. The magnitude of temperature or density difference necessary to hinder mixing processes is relatively small. A relatively small density difference of ~$1x10^{-3}$ kg/m^3 was found to be enough to isolate a mixing layer of some meters height above lake bottom from overlying waters in the Central Basin (Valipour *et al.* 2015). Similar small density differences may occur in the nearshore near-bottom. A temperature change corresponding to $\Delta 0.1°C/m$ was found to be enough to effectively form stratification, and restrict mixing in Lake Erie (Boegman *et al.* 2008). Others have used the density equivalent of a 2°C change at a 25°C reference temperature over the height of the water column to indicate enough stability in the water column to prevent vertical exchange (T. Howell, personal communication). Presence or absence of stratification may be an important factor in mussel effects in the nearshore through mass transport limitation of their feeding activities.

Stratification serves to cut off a portion of the water column that dreissenid mussels can access, so they are more likely to filter the same water repeatedly, which may result in a very strong near-bottom depletion gradient. Stratification in the nearshore or in shallow systems like the West Basin (Ackerman *et al.*, 2001) and Lake Simcoe (Schwalb *et al.*, 2013) has been previously documented, and may impede mussel filtration effects. Schwalb *et al.* (2013) noted that there were instances of near-bottom chla depletion that corresponded to areas of Lake Simcoe where mussel biomass was high and stratification was present, but depletion was not seen at sites where stratification did not occur. The same is likely experienced in the East Basin nearshore, but has not yet been extensively documented. In no lake has the prevailing level of near-bottom turbulence been measured and related to the incidence of near bottom Chl a depletion.

Whether mussels are food limited under periods of stratification and near-bottom stability should depend on the time it takes for their feeding to reduce the seston concentration compared to the time it takes for mixing to replenish the seston (Koseff *et al.*, 1993; Ackerman *et al*., 2001; Boegman *et al.*, 2008; Schwalb *et al.*, 2013). The grazing (TG) and mixing (TD) timescales may be important descriptors for when and where depletion may occur near-bottom. When grazing takes less time than mixing (TG<TD), near-bottom depletion gradients are expected to occur. Conversely, when grazing time is as long as or longer than mixing time (TG≥TD), near-bottom depletion gradients (and mass transport limitation) are not expected to occur (Koseff *et al.*, 1993; Boegman *et al.*, 2008; Schwalb *et al.*, 2013). Comparing predicted vs. observed near-bottom presence or absence of near-bottom gradients could indicate whether using TG and TD is a useful, quick tool in determining where near-bottom depletion may be occurring.

This chapter uses measurements of mussel biomass, density stratification, water column turbulence and vertical profiles of Chl a in the dreissenid dominated nearshore of eastern Lake Erie to address three objectives: (1) to test the hypothesis that the strength of stratification, level of turbulence, and mussel biomass will determine the incidence and strength of near-bottom Chl a depletion and thus the degree of mass transport limitation of mussel feeding rates. (2) to determine whether the time scales for mussel grazing and vertical mixing indicate that mass transport limitation is common and whether predictions from time scales are consistent with measured Chl a profiles. (3) to use a diffusive flux approach, based on measured Chl a gradients, diffusivity, and Fick's first law of diffusion, to quantify the flux of Chl a into the dreissenid-dominated benthos and thus to estimate mussel feeding rates under entirely natural *in situ* conditions.

3.2 Methods

Mussel feeding may decrease water column Chl a concentrations, enhancing light at the bottom, and on near-bottom SRP concentrations, enhancing nutrients at the bottom, both of which are important for stimulating *Cladophora* growth and biomass. Stratification can limit the extent of mussel feeding impacts

on the water column, constraining mussel impacts to the benthic boundary layer. Knowing when and where stratification occurs is important for knowing when mussels may exert a relatively greater impact on the benthic boundary layer through filtration on near-bottom Chl a (this chapter) and excretion of SRP (Ch 4). The timescale on which they feed and cause a layer of depletion vs the timescale on which mixing will abolish evidence of near-bottom depletion could be useful in predicting near-bottom Chl a depletion. With this in mind, the water column was profiled to determine presence or absence of stratification, stratification's relationship with Chl a and nutrient differences between surface and bottom waters, stratification and mixing heights, and estimatesof Chl a gradients and flux into mussel beds. Flux of Chl a downward was estimated two independent ways, from mussel feeding (assimilative) flux and turbulent diffusive flux; these estimates were compared against each other to determine if assimilative flux reasonably fell within the range of diffusive flux.

3.2.1 Study area and data collection

Work was conducted along three transects in the northern nearshore of East Basin Lake Erie in the time period between May or June and October in 2013 and 2014, and in May in 2015 (Figure 3.1). These transects were located west of the Grand River mouth, just outside of the Grand River mouth, and in the East, near Port Colborne. Stations were located on bedrock, and varied in nominal depth from 3-5m, 5-7m, 10-12m, and 16-18m deep.

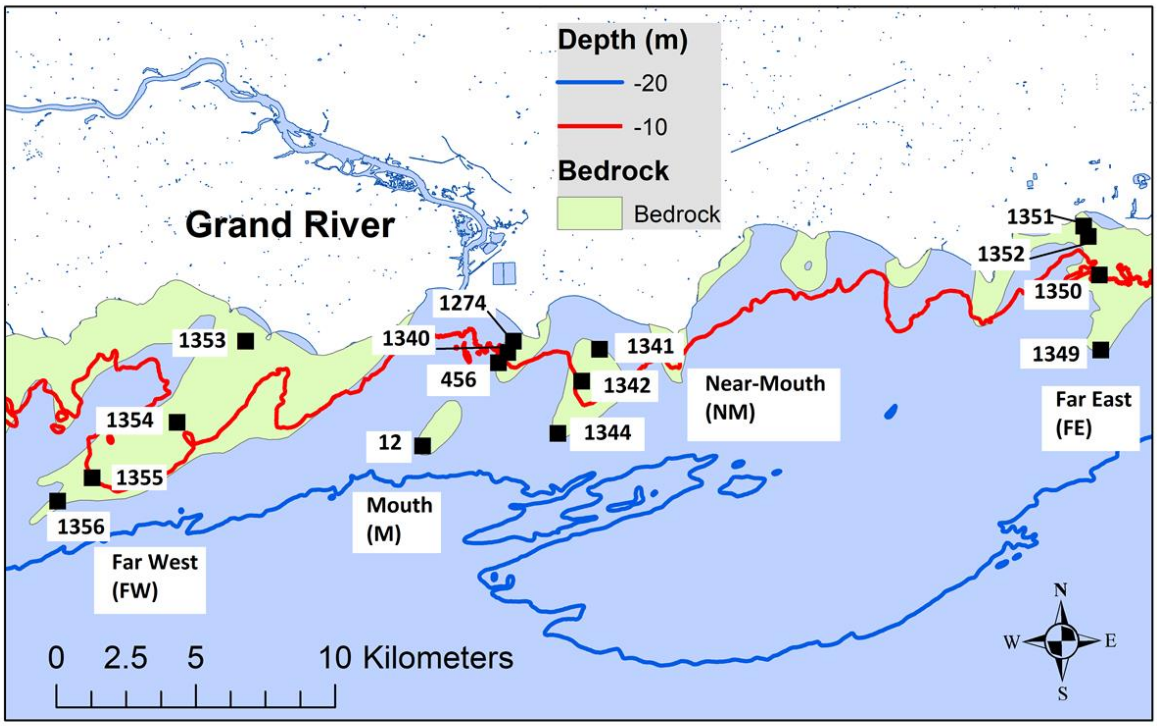

Figure 3.1. Map of the northern nearshore of the East Basin, Lake Erie, centred on the Grand River indicating stations (squares), and the four named sampling transects as they are discussed in the paper.

Bulk water samples were collected for nutrients (SRP, NH_4, PP), and Chl a, and a YSI 6600V2 sonde was used to measure water column specific conductivity, temperature, and optical Chl a. The YSI specific conductivity probe had an accuracy of ±0.5% of the reading +0.001mS/cm and a resolution of 0.001-0.01mS/cm. The temperature probe was accurate to ±0.15° C, with a resolution of 0.01°C. The Chl a probe had a resolution to 0.1µg/L or 0.1% of relative fluorescence units (RFU); accuracy was determined by serial dilution of rhodamine and its linear relationship to RFU (R^2>0.9999). In the cases where YSI profiles were missing or unusable, Fluoroprobe profiles were used; these also had a resolution of 0.1µg/L. Optical Chl a concentrations were corrected against extracted Chl a for the same stations, comparing Chl a at 1m below surface and 1m above bottom with averaged optical Chl a taken at the same height ±0.5m at each station. The ratio of optical Chl a to extracted Chl a was multiplied against all

the optical Chl a estimates to correct them. Chl a near-bottom gradients that had been corrected against extracted Chl a were determined using YSI or Fluoroprobe profiles.

Differences between 1m and near-bottom (1m above the bottom) Chl a, specific conductivity, and temperature were categorized using limits that were ~10x higher than the respective detection limits, to prevent spurious results, but not so high that all differences between surface and bottom were discounted. The temperature threshold between surface and bottom was 1°C, which was much greater than the Δ0.1°C/m associated with water column stability, and the accuracy limits of the YSI 6600V2 sonde. The specific conductivity threshold was 10μS/cm, and in line with observations by Chomicki *et al.* (2016) and our own observations between a station heavily impacted by the Grand River (station 1274, located right outside the mouth), and a station that was as close as possible to being similar to the offshore (station 1349), based on previous published measurements of offshore specific conductivity (e.g. Depew et al. 2006). The Chl a threshold was set at 1μg/L, higher than the optical detection limit on the YSI sonde, and also biologically relevant.

Physical measurements of near-bottom water velocity and temperature were made using a down-looking acoustic Doppler current profiler (ADCP, Nortek 2 MHz HR Aquadopp) and RBR temperature probes (TR-1060) that were deployed near the lake bottom. The ADCP was mounted 2m off the bottom and measured horizontal water velocity in 256 measurements collected at a frequency of 1Hz per sampling burst. Each sampling burst occurred every 12 or 15 minutes, depending on the sampling date. Measurements were collected from the bottom to a height of almost 2m above bottom at 3cm height intervals. The ADCP's horizontal velocity accuracy was ±1% of the measured value. RBR temperature loggers were mounted at 10cm height intervals from 10-80cm above bottom (10-40cm above bottom in May 2013), continuously measuring at a frequency of 1Hz. Its initial accuracy was ±0.002°C, with a resolution of ~0.00005°C. The RBR temperatures were averaged over the ~4 minute ADCP measurement bursts to estimate buoyancy frequency.

The height of the water column was determined from the YSI depth recording, and maximum depth was set to a height of 0m. The optical sensors on the YSI and Fluoroprobe are not mounted right at

the bottom of the sondes, but were located ~5cm (YSI) and 20cm (Fluoroprobe) above the bottom of the sondes. For this reason, the YSI was largely used for estimates of diffusive flux of Chl a near-bottom, and the Fluoroprobe was used to supplement water column temperature data to assess instances of stratification. Chl a data was minimally modified to remove repeating values, as when the sondes touched bottom. This was done for all available Chl a profiles.

Mussels were collected by divers at three 0.15m^2 quadrats within ~10m radius of the station GPS coordinates on dates within 1-2 weeks before or after water column sampling. Divers placed quadrats to represent the range of apparent mussel abundance at the site. All mussels within the quadrats were removed from the substrate and placed in watertight collection bags. Harvested mussels were kept on ice during sampling at other stations. Upon return to lab, the mussels were brushed to remove debris, sorted for size abundance, and soft tissue was removed from the shells. The soft tissue was freeze dried and weighed to determine shell-free dry weight (SFDW). Mussel biomass and abundance collected during the growing season in each of the sampling years was averaged to one value on the assumption that mussel abundance and biomass would not change greatly over the course of the six months, and to account for heterogeneous distributions and potentially diver bias in selecting where to place quadrats.

3.2.2 Determining height of stratification and the grazing and mixing timescales

Determining where in the benthic boundary layer above-bottom there was stability that corresponded to the mixing height (Hmix) or height of stratification (Hstrat) was important in determining how much of the water column mussels would have access to, and potentially on the presence of Chl a gradients. Bottom mixing height is important, as it is a critical component of estimates of the grazing timescale (TG) and the turbulent mixing timescale (TD). Hmix was determined as the height above bottom that corresponded to a change in density of 10^{-3} kg/m^3 (Valipour, Bouffard & Boegman, 2015) and Hstrat was the height above bottom that corresponded Δ0.15°C/m, similar to the parameter in Schwalb *et al.*(2013). In most instances, Hmix was used as the height term in TG and TD (Figure 3.2), but when Hmix was

<10cm (and in reality, closer to 1-2cm), Hstrat was used (Figure. 3.2) because such small heights were difficult to measure accurately.

The pressure sensor used to determine depth on the YSI is only accurate to ~2cm. Furthermore, the pressure sensor is not located right at the bottom of the sonde, which means that there is further uncertainty in the smaller Hmix estimates. When stratification was absent, the height of the water column was used in calculating TG and TD (Figure 3.2).

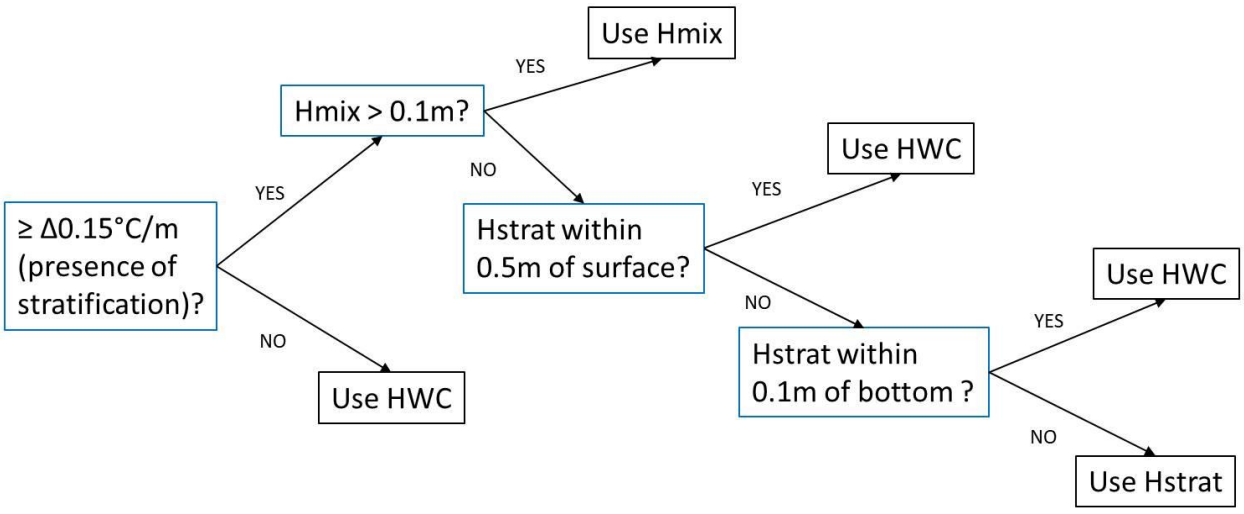

Figure 3.2. Decision tree for determining which height to use to calculate TG or TD. Hmix is the height of mixing in a stratified benthic boundary layer, corresponding to a density change of 10^{-3}kg/m^3, Hstrat is the height of stratification, corresponding to a temperature change of 0.15°C, and HWC is the height of the water column.

In the equations for TG (Equation 3.1) and TD (Equation 3.2), H is the height of mixing (Hmix), height of stratification (Hstrat) or depth of water column. In equation 3.1, α is the areal clearance rate of the mussels (Koseff *et al.* 1993; Boegman *et al.*, 2008b; Schwalb *et al.*, 2013). It was estimated as the product of published estimates for specific mussel clearance rates of 90mL/mussel/h for zebra mussels (Ackerman *et al.*, 2001) and the measurements of areal abundance (mussels/m^2) of mussels, and units

corrected to be expressed in days. The clearance rate estimate of 90mL/mussel/h was used because both Ackerman *et al.* 2001, and Boegman *et al.* 2008b used them. Boegman *et al.* (2008b) additionally explored ± 50% in a sensitivity analysis. For this work, only 90mL/mussel/h were used to draw comparisons between the TG estimates in this paper and previous literature.

Equation 3.1

$$TG = \frac{H}{\alpha}$$

Where:

- H is height above the bed (m)
- α is the areal clearance rate ($m^3\ m^{-2}\ s^{-1}$)

Equation 3.2

$$TD = H^2/Kz$$

Where:

- H is height above the bed (m)
- Kz is diffusivity, determined using the Reb parameterization method of Bouffard and Boegman, 2013 (m^2/s).

Kz was directly estimated from the ratio of dissipation (Equation 3.3) and buoyancy frequency (Equation 3.4). Dissipation was calculated using the structure function method (Wiles *et al.*, 2006) with parameterized C (Jabbari *et al.*, 2016) from near-bed water velocity data. Buoyancy frequency was estimated from temperature as measured by RBR loggers.

Equation 3.3

$$\varepsilon = \left[\frac{G(z,r)}{Cr^{2/3}}\right]^{3/2}$$

Where:

- ε is dissipation (m^2/s^2)
- G(z,r) is the mean squre difference in the velocity fluctuation (z) between two points that are r distance apart from Wiles *et al.* (2006)
- C is a parameterised constant fromJabbari *et al.* (2016)

Equation 3.4

$$N^2 = -\frac{g}{\rho}\frac{\partial \rho}{\partial z}$$

Where:

- N^2 is the buoyancy frequency (s^{-1})
- g is acceleration (~9.81 m^2/s)
- ρ is density estimated from temperature (kg/m^3)
- z is depth

Equation 3.5

$$Kz_{(Reb)} = \begin{cases} D, & if\ Reb < 10^{2/3} * Pr^{-1/2} \\ 0.5D * Reb^{3/2}, & if\ Reb \geq 10^{2/3} * Pr^{-0.5} \& Reb \leq (3\log(\sqrt{Pr}))^2 \\ 0.2Dv * Reb, & if\ Reb \leq \left(3\log(\sqrt{Pr})\right)^2 \& Reb \leq 100 \\ 2v * Reb^{0.5}, & if\ Reb > 100 \end{cases}$$

Where:

- $Kz_{(Reb)}$ is diffusivity calculated using the Reb parameterization
- D is the diffusivity of phosphate ($3.6X10^{-6}$ cm^2/s)
- Pr is Prandtl's number
- Reb is the turbulence intensity parameter (Reb = ε/(νN^2).

Depletion of near-bottom Chl a, and mass transport limitation of mussel feeding, is predicted to develop when TG:TD<1. TG:TD as a predictor of near-bottom depletion depends on assumed feeding

rates for mussels and does not by itself predict the magnitude of depletion. It was therefore considered useful to make comparisons between TG:TD and observed near-bottom Chl a profiles.

3.2.3 Estimating Chl a flux into the bottom

Chl a flux downward into the mussel bed was estimated two independent ways. The first was to calculate assimilation flux as a product of observed mussel biomass and a Chl a assimilation rate predicted from published work on mussels elsewhere (Vanderploeg *et al.* 2017). The relationships between Chl a concentration and assimilation rate (Equation 3.6) from Vanderploeg *et al.* (2017) were used to estimate the mussel assimilation rate in this study. The estimates used the product of near-bottom (2-5 cm above bottom) Chl a measurements and the measured areal mussel biomass to determine the areal flux of Chl a. These estimates are termed assimilation fluxes because they depend on the published relationship for mussel Chl a assimilation.

Equation 3.6

$$AChla = 0.0054[Chl\ a] - 0.002$$

Where:

- AChl a is the assimilation of Chl a in (µg/mgSFDW/h)
- [Chl a] is the concentration of Chl a

The second method for estimated the downward flux of Chl a used measurements of Chl a and diffusivity with no assumed values for mussel feeding rates (Equation 3.7). These estimates are termed diffusive fluxes because they depend on the measured diffusivities and can only be made where mass transport limitation allows development of Chl a gradients near the bottom. Fluxes were estimated for stations where near-bottom Chl a profiles showed evidence of a significant ($p \leq 0.05$) gradient of decrease between 0.025- 0.5m above bottom. This particular function was used in order to be able to capture all

forms of near-bottom gradients that may exist, and as a quick way to sort through numerous profiles from multiple sampling dates, stations, and replicates.

Diffusive Chl a flux was estimated using Fick's First Law (Equation 3.7), implying the presence of a constant source and sink.

Equation 3.7

$$J_{chla} = -\frac{\partial Chla}{\partial H} \cdot Kz_{(Reb)}$$

Where:

- $J_{Chl\ a}$ is the diffusive flux of Chl a downward
- ∂Chl a/∂H is the Chl a concentration gradient
- Kz is the diffusivity using the Reb parameterization

Each estimate of diffusive Chl a flux was done corresponding to individual profiles and measurements from a single ADCP burst. In total, this corresponds to a diffusive flux estimate based on measurements occurring over five minutes. As such, an assumption of constant source and sink is reasonable. Because a constant source and sink were assumed, near-bottom (i.e. 0.025-0.35m) Chl a profiles were assumed to have a linear gradient 2-5cm above bottom, but not necessarily above this portion of the near-bottom profile. Similarly, diffusivity estimated for each burst was relatively invariant in most cases, and the fitted linear slope of diffusivity to height did not differ significantly from the fitted linear slope of zero for the mean diffusivity over height. As a result, the slope of a linear fit line was the gradient used in diffusive flux calculations. ADCP burst measurements corresponding closely in time to sonde deployment and water column measurement were used for flux estimates. Diffusivity values did not have any significant trend with height above bottom of the range of relevance so a single average value of diffusivity was assumed to apply across the measured Chl a gradient. The resulting diffusive flux estimates (in $g/m^2/d$) were accordingly constant with height above bottom.

3.3 Results

3.3.1 Thermal stratification and near bottom conditions

Cladophora and mussel peak biomass distributions were not spatially co-occuring, at least in terms of water depth (Figure 3.3**Error! Reference source not found.**). On average, Cladophora peak biomass occurred ≤3m deep, whereas mussel peak biomass occurred between 5-7m deep. Average Cladophora mass additionally was greatest as shallow sites that were located away from the mouth at FW and FE stations (Table B5), suggesting that increased light availability was also important for nuisance biomass.

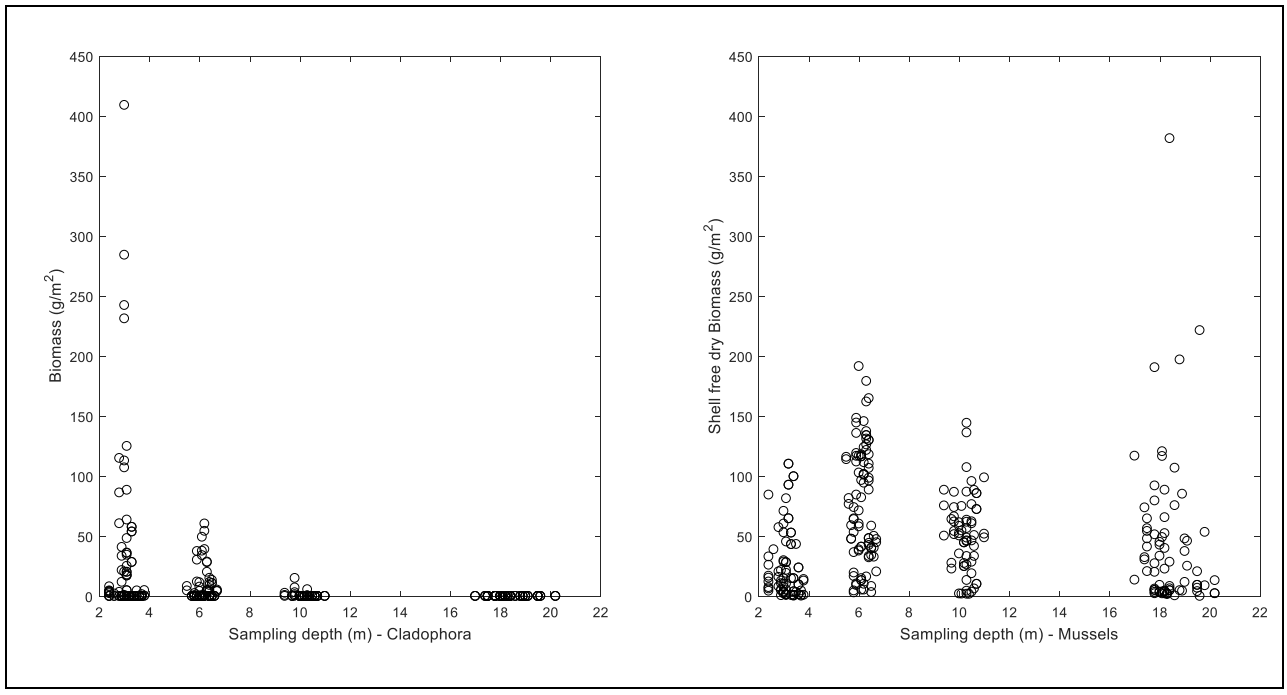

Figure 3.3. Cladophora and mussel biomass distributions in at nearshore sites

Stratification was a common occurrence in the northern nearshore East Basin in both shallow and deep portions of the nearshore and in the early and late parts of the sampling season. Of the 64 samples taken over the course of the growing season (approximately May-October) in 2013-2015, 42 sites were stratified, 12 sites were not stratified, and 10 did not have a reliable water column profile to judge stratification. Intensive sampling in 2015 specifically resulted in approximately 16 profiles (six profiles per each of the four stations sampled), and of these profiles taken at 10m stations, most were stratified.

There was approximately similar sampling frequency between shallow (<10m) and deep (≥10m) stations on FW, M, and FE transects, which were sampled the most frequently. There were more samples collected in the early (May/June) part of the season relative to the late (August/October) part of the season (Table **3.1**).

Stratification tended to occur more often early in the season and tended to occur slightly more often at deep sites than shallow sites (Table 3.1). Incidence of stratification was nevertheless similar for shallow and deep sites on the same transect. All stations, with the exception of shallow mouth stations, were stratified in the early part of the sampling season. Most samples collected in the late part of the sampling season were stratified, but there was a relatively greater incidence of non-stratification. The shallow M and NM stations did not exhibit stratification in the late part of the sampling season, but other shallow and deep sites in the FW and FE transects experienced greater incidence of stratification than non-stratification in the late part of the season.

Table 3.1. Summary table of the incidence, location, and time of season, where there appeared to be either temperature stratification or no stratification in 2013-2015

			Stratified		Not Stratified		No profile	
Transect	Depth group	number of profiles taken	Early	Late	Early	Late	Early	Late
	shallow	8	2	3	0	1	2	0
Far West	deep	10	4	3	0	1	2	0
	shallow	12	3	0	2	4	1	2
Mouth	deep	12	7	2	0	1	0	2
	shallow	5	4	0	0	1	0	0
Near Mouth	deep	1	1	0	0	NA	0	0
	shallow	7	4	2	0	1	0	0
Far East	deep	9	5	2	0	1	1	0
Total count		64	30	12	2	10	6	4

The incidence of above-threshold difference between surface taken 1m below surface (“surface”) and those taken 1m above bottom (“bottom”) without specifically also considering presence or absence of stratification revealed some potentially unexpected patterns (Table 3.2). Most of the samples did not

have coarse vertical differences between surface and bottom above the absolute threshold (e.g. for specific conductivity, that was either >10μS/cm, indicating surface was greater than bottom, or <10μS/cm, indicating that bottom was greater than surface). More than 50% of the samples collected for specific conductivity, temperature, chla, and SRP were not above the absolute threshold criteria previous set. Where specific conductivity, temperature, and Chl a that did occur above absolute threshold, surface samples had a greater value than bottom samples, indicating that specific conductivity at the bottom was at least 10μS/cm less than the surface, temperature at the bottom was at least 1°C less than the surface, and that Chl a at the bottom was less than 1μg/L at the surface. Of the SRP and NH_4 samples with above-threshold concentrations, the majority of these samples had greater concentrations at the bottom than at the surface that were above-threshold. NH_4 was the only parameter where occurrence of sub-threshold differences was less than above-threshold differences.

Table 3.2. Incidence of samples where the difference between surface and bottom chla, specific conductivity, and temperature were above-threshold (listed below in table) in 2013-2015 regardless of incidence of stratification.

			Surface greater than bottom		Bottom greater than surface		Samples not greater than absolute threshold	
	Absolute Difference Threshold (surface minus bottom)	Total number of samples	Number of samples above threshold	frequency	Number of samples above threshold	frequency	Number of samples	frequency
Chla	≥1µg/L	61	9	0.148	2	0.033	50	0.820
SC	≥10µS/cm	51	8	0.157	2	0.039	41	0.804
T	≥1°C	52	28	0.538	0	0	24	0.462
SRP	≥0.5µg/L	64	2	0.0313	20	0.313	42	0.656
NH_4	≥5µg/L	64	12	0.188	30	0.479	22	0.344

Note: Specific conductivity, temperature, and Chl a have fewer than 64 total samples because some profiles used to measure specific conductivity were unusable, other profiles used to measure temperature and specific conductivity have measurement gaps in the profile, and a few samples of extracted Chl a were obviously degraded and not included.

There were a few instances of presence of a different water mass, possibly part of the metalimnion, operationally defined as a >2°C drop in temperature near-bottom and toward the bottom relative to a relatively uniform profile above it (Figure 3.4). With the exception of one NM shallow station (1341), all the other stations which appeared to experience the presence of different water masses were deep stations, three of which were the deepest FW station (1356). Differences between near surface and near-bottom specific conductivity, where data existed, showed that specific conductivity near bottom was greater than at surface at these stations, but did not fall about the set threshold for meaningful

difference (i.e. >|10µS/cm|). Upwelling did not appear to be a common occurrence in relation to SRP and NH_4 vertical patterns in these samples.

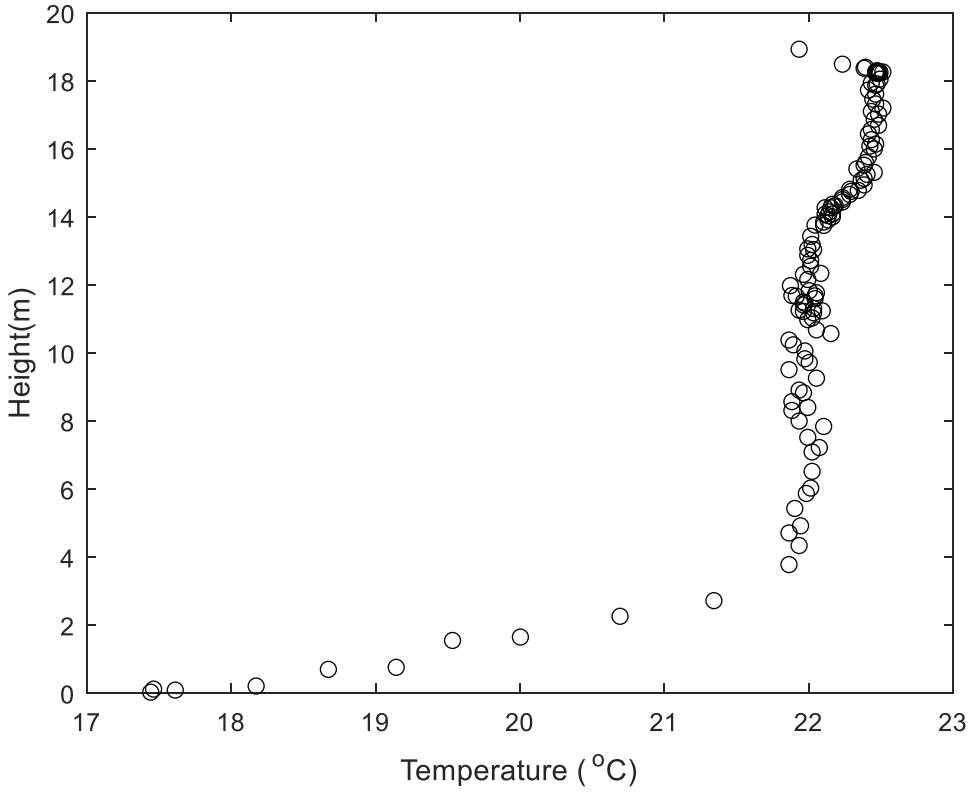

Figure 3.4. Example plot showing a different water mass at the bottom (e.g. cooler water from the metalimnion and/or hypolimnion) seen in a sudden drop >2°C in the temperature profile toward the bottom (Station 1356, October 2014)

There were only very few instances of above-threshold differences between surface and bottom chla, specific conductivity, and temperature when specifically considered in relation to the presence or absence of stratification (Table 3.3). There were very few instances where Chl a or specific conductivity occurred above threshold difference between the surface and bottom under periods of stratification, and fewer still under periods of no stratification. Temperature unsurprisingly showed above-threshold differences between surface and bottom in relation to presence of stratification, and two instances of above-threshold temperature differences under absence of stratification. Elevations in temperature,

specific conductivity, and Chl a at the surface under unstratified conditions largely occurred at M stations. SRP and especially NH_4 elevations under stratified conditions further point to mussel effects in near-bottom waters under stratification, even though Chl a data did not also show such a clear pattern. Only mouth stations showed a combined temperature and specific conductivity elevation above threshold (Table 3.3); this is unsurprising, as these stations are located <1km from the river mouth. One far west station experienced elevated surface temperature relative to the bottom and elevated specific conductivity at the bottom relative to the surface. There were several FW, M, and FE stations that experienced elevated surface temperature and a concurrent sub-threshold elevation in specific conductivity.

Table 3.3. Summary table of transects where stations displayed a temperature difference between surface and bottom ≥2°C and the corresponding specific conductivity difference between surface and bottom, either above-threshold (ΔSC≥|10µS/cm|) or where there was a sub-threshold difference (ΔSC<|10µS/cm|).

Transect	Total samples where ΔT>2°C	Δ SC >10µS/cm surface greater	Δ SC <-10µS/cm bottom greater	Δ SC<|10µS/cm| sub-threshold difference
FW	6	0	1	5
M	8	6	0	2
NM	0	0	0	0
FE	5	0	0	5

3.3.2 Evidence for near bottom Chl a depletion and mass transport limitation of mussel grazing

There was sometimes evidence in water column profiles of chl a depletion at stratified sites, but it also occurred at non-stratified sites. Likewise, there were also cases lacking in apparent chl a depletion at both stratified and unstratified sites (Figure 3.5). Some stations showed evidence of stratification in the temperature profile and a corresponding near-bottom Chl a depletion profile (Figure 3.4a). Other profiles seemed to indicate a near-uniform water column temperature profile that would not indicate stratification, but showed a near-bottom Chl a depletion profile (Figure 3.4b). Finally, the other observed profiles were ones that indicated stratification in the temperature profile, but there did not appear to be evidence of a

near-bottom Chl a depletion profile. Incidence of Chl a depletion may reflect the interplay of varying mussel grazing pressure and vertical mixing strength.

A

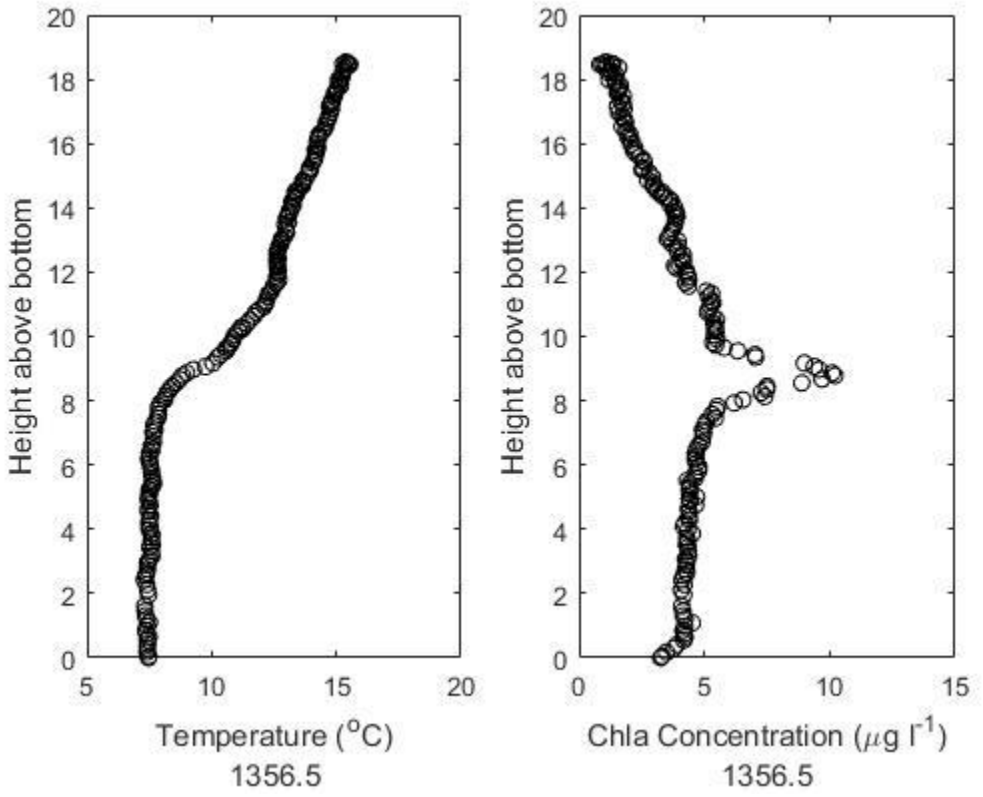

B

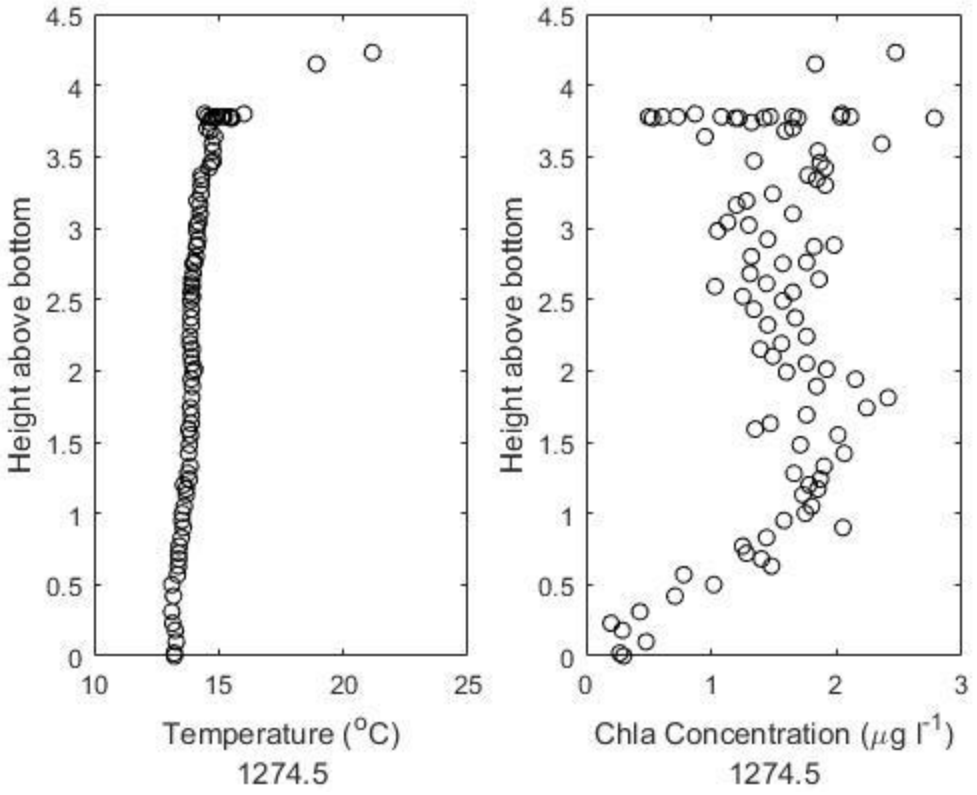
Height above bottom
Temperature (°C)
1274.5
Height above bottom
Chla Concentration (μg l-1)
1274.5

C

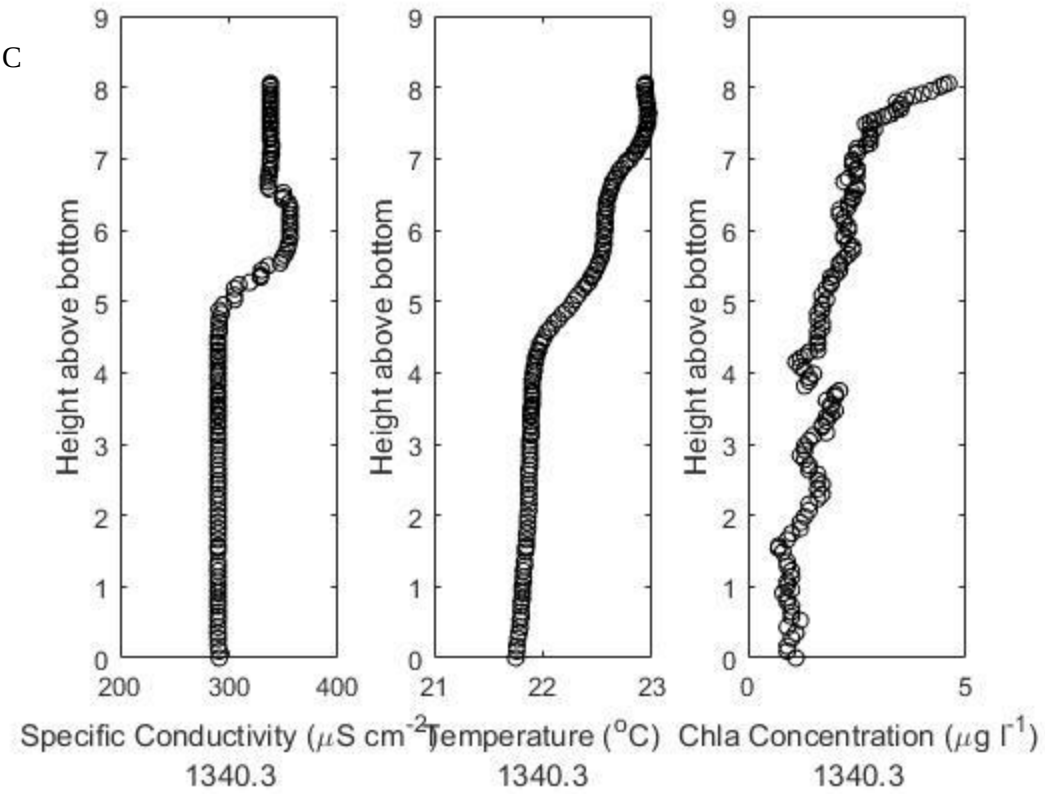

Figure 3.5. Example figure of near-bottom Chl a depletion under stratified and unstratified conditions. Example profiles include (a) presence of stratification and presence of near-bottom Chl a depletion (Station 1356, June 2014), (b) no stratification and presence of near-bottom Chl a depletion (Station 1274, June 2014), and (c) presence of stratification and no evidence of near-bottom Chl a depletion depletion (Station 1340, August 2013). Water column temperature and specific conductivity profiles for the same example stations are included for context.

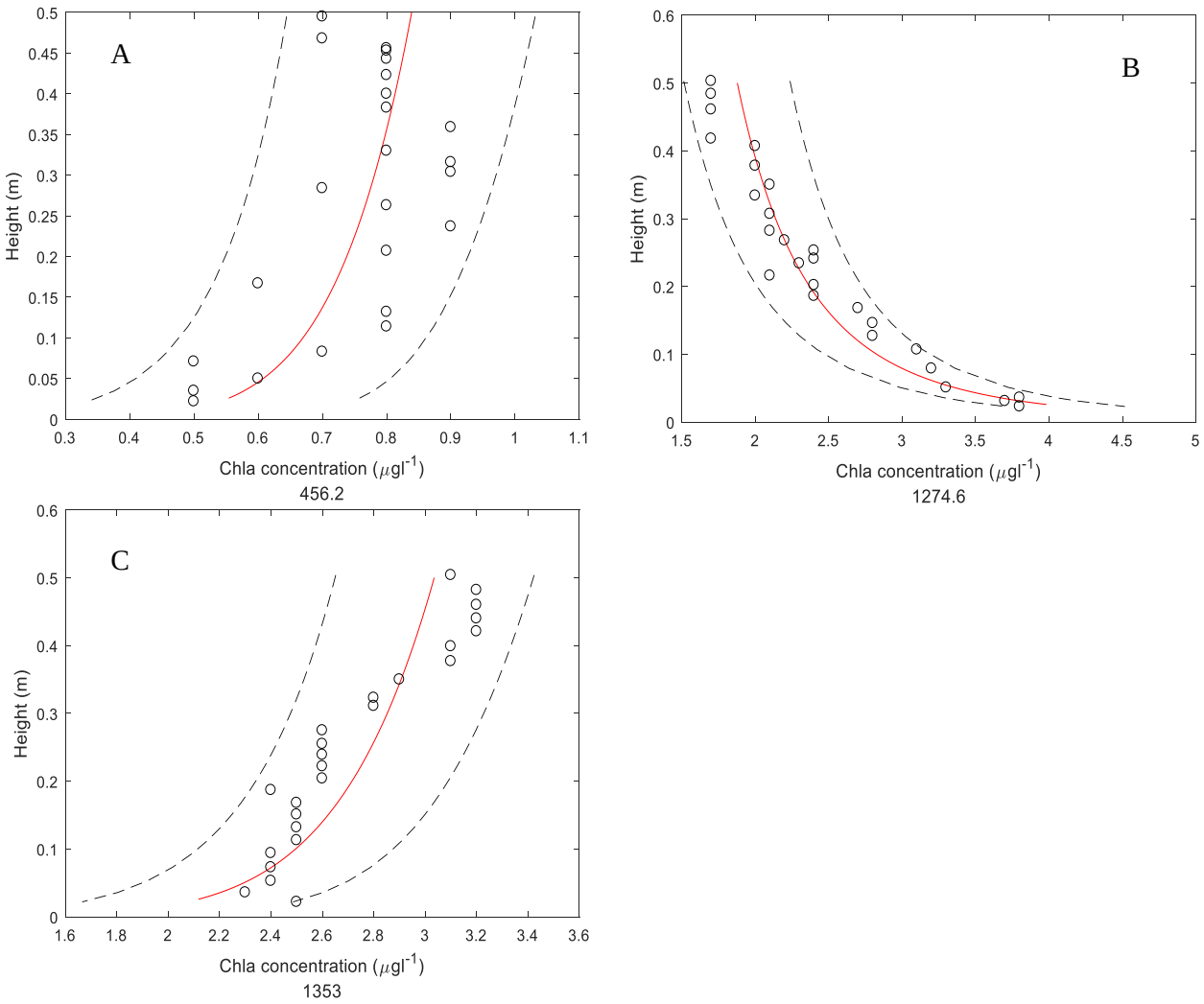

Figure 3.6. Example near bottom (0-1mab) profiles showing a (a and c) significant ($p \leq 0.05$) decreasing trend, and (b) a significant increasing trend. Solid line is the power fit (form $b \cdot x^m$) line, and dashed lines are the fit's predicted 95% confidence intervals.

Significant near-bottom Chl a depletion gradients were sometimes observed in the nearshore (Figure 3.6 a and c). There were also other types of near-bottom patterns of Chl a, including patterns that were not a significant decrease (Table B5) and patterns of apparent increase (Figure 3.6b). Of 71 near-bottom Chl a profiles measured in 2013-2015, only 33 showed observable significant near-bottom gradients (Table B5); of the 38 profiles that did not show significant near-bottom depletion, three showed a pattern of increasing Chl a toward the bottom, 20 did not show evidence of any gradient, 11 did not show an observable depletion gradient toward bottom despite prediction of such a gradient, and four showed an observable depletion gradient that was also predicted. Predicted near-bottom depletion using the relationship between TG:TD could also be used, and compared against observed near-bottom Chl a gradients.

The ratio of grazing timescales (TG) and diffusive mixing timescales (TD) was expected to be significantly different under periods of stratification and non-stratification. The relationship between TG:TD under stratified conditions was TD = 1.77*TG + 0.5882 (R_{adj}^2 = 0.4481, $p>0.05$) and the relationship of TG:TD under unstratified conditions was TD = 1.902*TG + 0.8777 (R_{adj}^2 = 0.6778, $p>0.05$). However, the distribution of TG:TD under stratified conditions compared to the distribution of TG:TD under unstratified conditions was not significantly different in a Mann-Whitney U-test/Wilcox Rank Sum test (U= 998, p = 0.6021) (Figure 3.7). The distribution of TG:TD under both stratified and unstratified conditions deviated significantly from the hypothesized log:log line (stratified: U= 1394, p = 0.0129; unstratified: U= 178, p = 0.005283). More of the points lay above or on the log:log line (31 of 49 points), suggesting that the ratio of TG:TD<1, and depletion of Chl a near bottom should be a relatively common occurrence in the nearshore. Data falling above the line (i.e. TD>TG) suggest that grazing timescales were orders of magnitude shorter than diffusive mixing timescales and that dreissenid mussels may be able to draw down water column chla, potentially resulting in an observable gradient of Chl a depletion toward the bottom. Data falling below the line (i.e. TD<TG) suggest that diffusive mixing timescales were shorter than dreissenid mussel grazing rate timescales, and that near-bottom gradients

may not be detectable. Predictions of depletion near-bottom are most useful if they correspond to observations of near-bottom (e.g. 0-0.5m above bottom) Chl a depletion gradients.

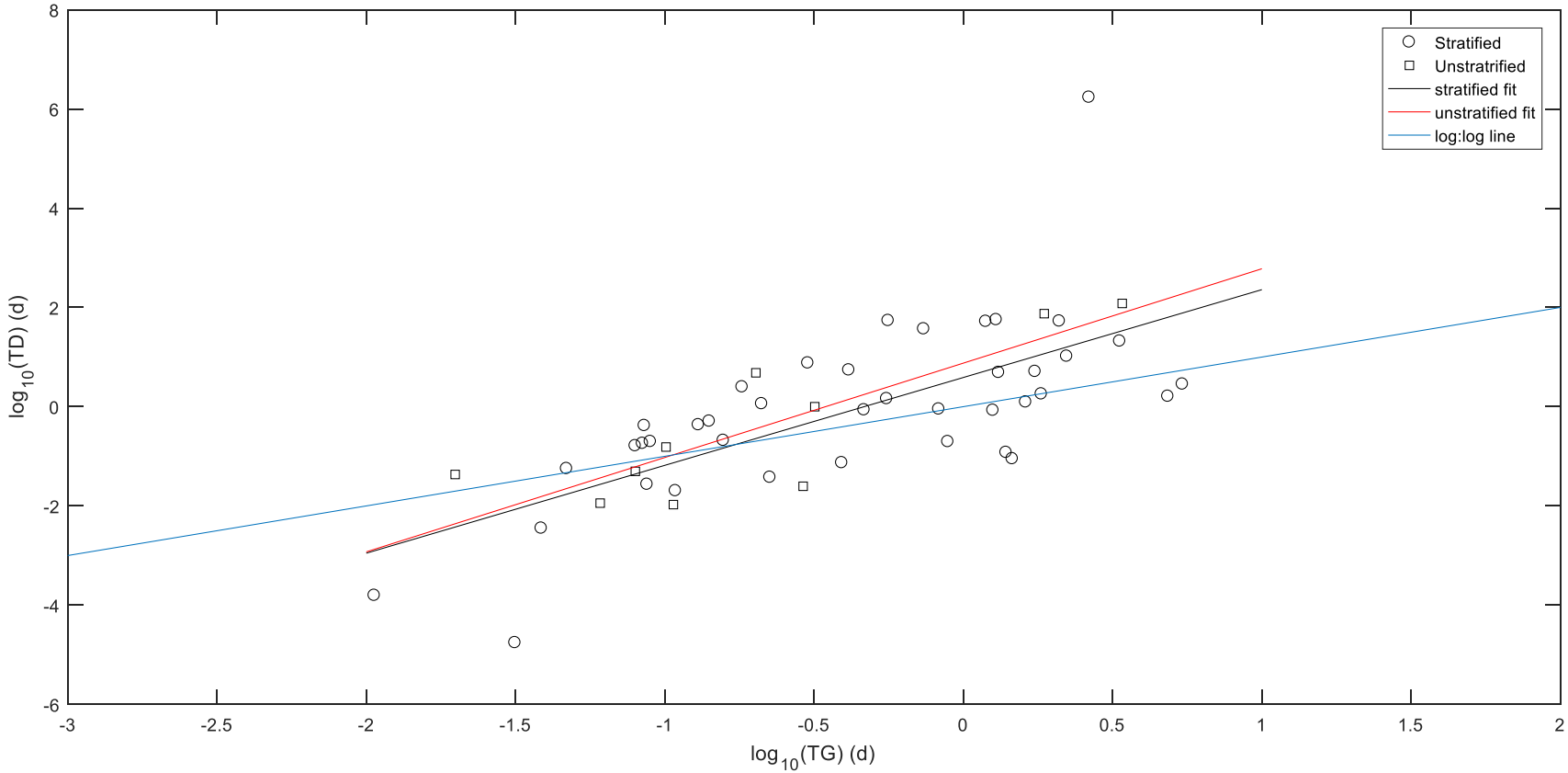

Figure 3.7. Relationship between grazing time (TG) to diffusive mixing time (TD) under stratified and unstratified conditions. Points that fall about the log:log line experience a longer mixing timescale relative to the grazing timescale, predicting near-bottom depletion of chla. Points that fall below the log:log line experience a shorter mixing timescale relative to the grazing timescale, predicting lack of a near-bottom depletion of chla

The relationship between the grazing and mixing timescales had a weak, but non-significant relationship with average mussel biomass (Figure 3.8). Presence or absence of stratification either resulted in a positive semi-log relationship, as in the case of TG:TD under stratified conditions, or a negative semi-log relationship, as in unstratified conditions. The negative relationship between TG:TD and mussels under stratified conditions suggested that the grazing time was shorter than the mixing time with increasing mussel biomass. The positive relationship between TG:TD and mussels under unstratified conditions suggested that grazing time was longer than mixing with increasing mussel biomass, in line with work by Boegman *et al.* (2008) and Schwalb *et al.* (2013).

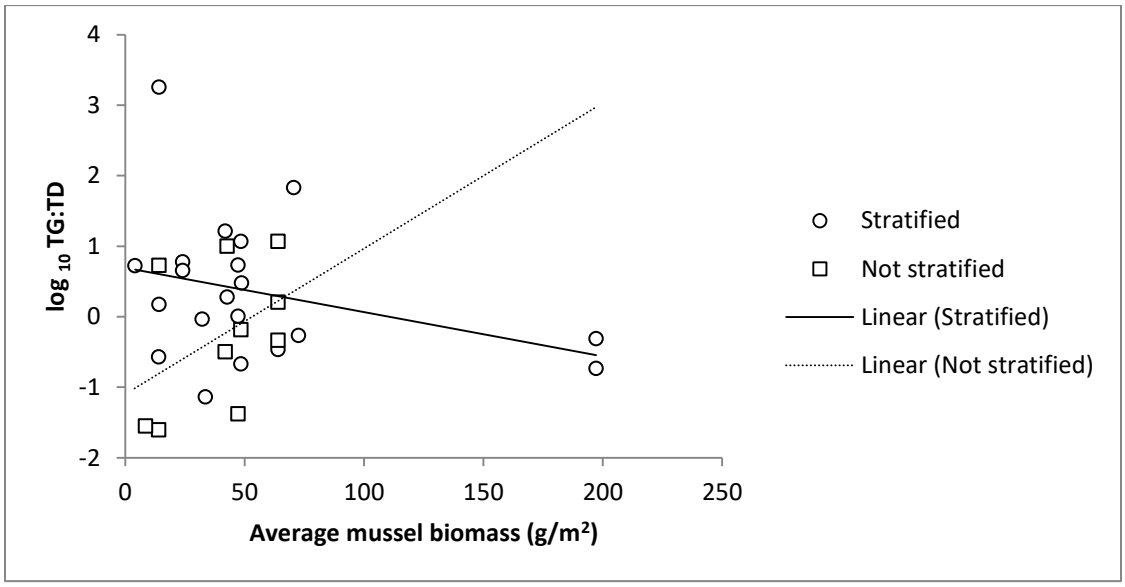

Figure 3.8. All available TG plotted against averaged mussel biomass (gSFDW/m^2) for all sampling dates in 2013-2015. Mussel biomass was averaged per station from three quadrat samples and per year.

TG:TD did not predict near-bottom depletion at frequencies greater than what might be predicted by a random guess ($\chi^2 = 0.032$, df =1, $\chi^2_{crit} = 3.841$), as evidenced by $\chi^2 < \chi^2_{crit}$ (Table 3.4). Predicted and observed significant depletion ($p \leq 0.05$ in a power fit of near-bottom Chl a profiles (Table B5) was the most frequent outcome in a 2x2 factorial test (Table 3.4, Table 3.5) and predicted depletion but observed no-depletion (Table 3.4, Table 3.6) next most frequent outcome. Predicted no-depletion was less

common (Table 3.4, Table B3, Table B4), but there were more instances of a mismatch in prediction and observation when no depletion near-bottom was predicted.

Table 3.4. 2x2 factorial table of predicted and observed depletion or no depletion (i.e. increasing profile near bottom or a straight profile).

	Predicted depletion	Predicted no depletion
Observed significant depletion	25	8
Observed no significant depletion	11	4

Stations where there was a match between predicted (TG:TD<1) and observed significant near-bottom Chl a depletion did not appear to be related to any specific station depth (shallow or deep), but did appear to occur most frequently in the earl part of the sampling season in May and June (Table 3.5)of these stations where there was a correspondence between predicted and observed depletion were not stratified. Most of the stations that TG:TD predicted would not experience near-bottom depletion (TG:TD≥1), but nevertheless experienced significant near-bottom depletion, were shallow 3m stations, and one 18m station (Table 3.6). Like stations with observed and predicted Chl a depletion, there did not appear to be a pattern of depletion with depth or month of sampling.

Table 3.5. Stations displaying correspondence between TG:TD prediction of near-bottom Chl a depletion and significant ($p \leq 0.05$) observed near-bottom (0-0.5mab) Chl a depletion. Stations that did not have observable significant near-bottom Chl a depletion were not included. Where there are two stations on the same sampling date, both replicate profiles showed significant decreases.

Sampling date	Stations	Nominal Station depth (m)(transect)	Stratification (Y or N)	TG:TD	R^2 ($p \leq 0.05$)
Jun-14	1274	3m (M)	N	0.38	0.557
Jun-14	1353	3m (FW)	N	0.27	0.547
Jun-14	1354	5m (FW)	N	0.02	0.984
Jun-14	1354	5m (FW)	N	0.02	0.871
Jun-14	1355	10m (FW)	N	0.04	0.717
Jun-14	1355	10m (FW)	N	0.04	0.707
Jun-14	1356	18m (FW)	Y	0.75	0.889
Jun-14	1350	10m (FE)	N	0.02	0.377
Jun-14	1349	18 (FE)	N	0.01	0.944
Aug-14	456	10m (M)	N	0.00	0.538
Aug-13	1353	3m (FW)	N	0.93	0.904
Oct-13	1274	3m (M)	NA	0.46	0.607
Oct-13	1274	3m (M)	NA	0.46	0.752
Jun-14	1353	3m (FW)	N	0.27	0.500
Jun-14	1274	3m (M)	N	0.38	0.225
Jun-14	1274	3m (M)	N	0.38	0.341
Jun-14	1354	5m (FW)	N	0.02	0.337
Jun-14	1355	10 (FW)	N	0.04	0.473
Jun-14	1356	18m (FW)	Y	0.75	0.544
Jun-14	1352	5m (FE)	N	0.16	0.349
Jun-14	1349	18m (FE)	N	0.01	0.141

Aug-14	1274	3m (M)	N	0.04	0.296
May-15	456	10m (M)	Y	0.14	0.228
May-15	456	10m (M)	Y	0.08	0.215
May-15	456	10m (M)	Y	0.28	0.569

Table 3.6. Stations displaying incongruence between TG:TD prediction of lack of near-bottom Chl a depletion and significant (p≤0.05) observed near-bottom (0-0.5mab) Chl a depletion. Stations that did not have observable significant near-bottom Chl a depletion were not included.

Sampling date	Stations	Nominal Station depth (m)(transect)	Stratification (Y or N)	TG:TD	R^2 (p≤0.05)
Jun-14	1353	3m (FW)	N	1.27	0.393
Oct-14	1274	3m (M)	Y	10.88	0.154
Aug-13	1356	18m (FW)	NA	1.91	0.712
Aug-13	1356	18m (FW)	NA	2.91	0.897
Oct-14	1356	18m (FW)	N	10.05	0.526
Jun-14	1351	3m (FE)	Y	5.29	0.433
Jun-14	1355	10m (FW)	N	1.04	0.146
Jun-14	1353	3m (FW)	N	1.27	0.540

Of the stations that showed significant observed near-bottom chla depletion, there did not appear to be any systematic relationship between depletion and station depth (Table 3.5, Table 3.6). Many of the stations where observed significant depletion corresponded with prediction were shallow (nominally 3m) stations (e.g. 1274, 1353), but there were others that corresponded to nominally 10 and 18m deep stations. Most of the stations where near-bottom Chl a depletion was observed occurred in the early part of the growing season, and specifically in June 2014. Surprisingly, most of these stations did not appear to have gross water column stratification, at least according to the thresholds used in this paper.

3.3.3 Diffusive fluxes of Chl a and mussel filtration activity

Estimates of diffusive Chl a flux and mussel filtration activity could indicate how much of an impact mussels may have on the nearshore water column. Only stations where there was evidence of a significant decreasing trend in Chl a toward bottom were considered for further diffusive flux estimations (Figure 3.9). Diffusivity was small at the time of Chl a profiling, ranging from 1.92×10^{-7} to 1.01×10^{-4} m^2/s (Table 3.7).

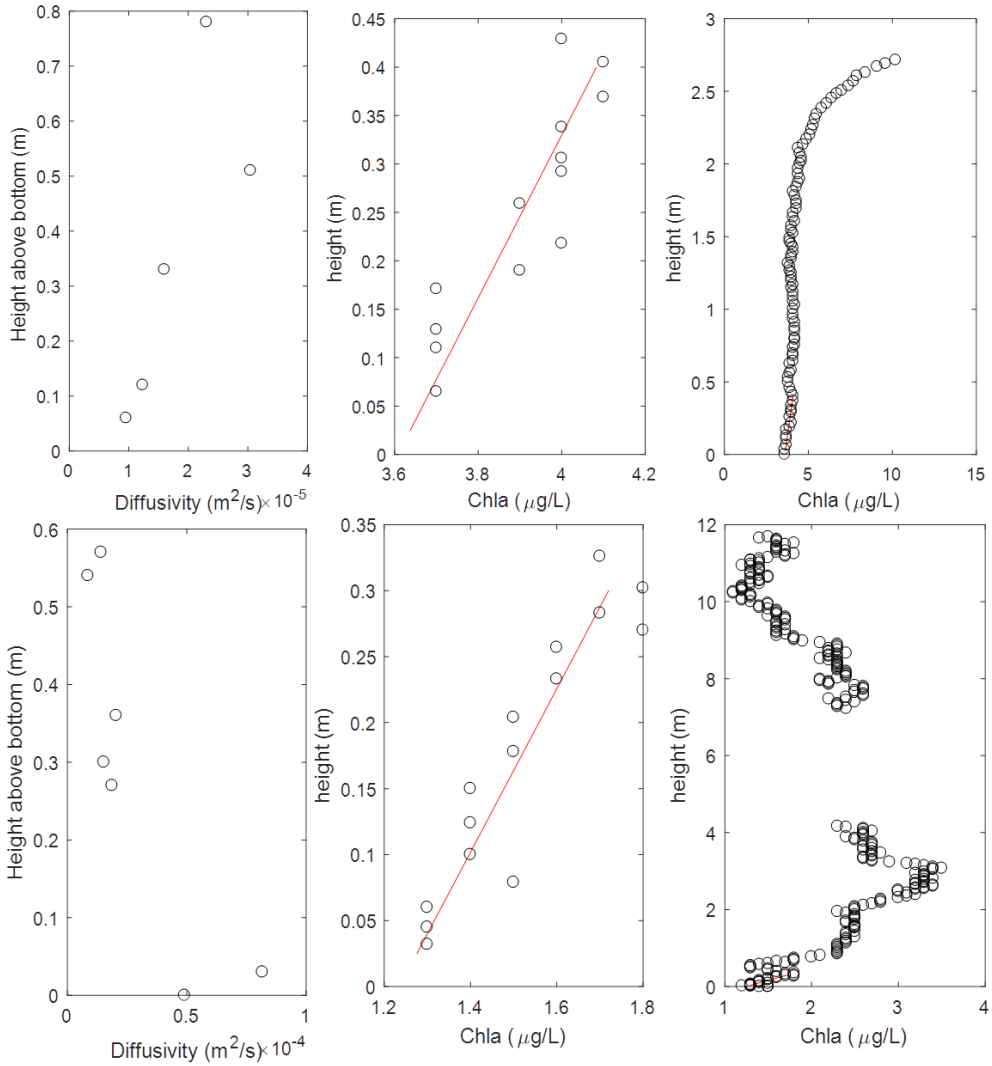

Figure 3.9. Example plots of near-bottom diffusivity, Chl a gradients and linear fits used to estimate diffusive flux of Chl a toward the bottom both at 0-0.5mab (left panels) and in context of the whole water column (right panels) at a (a) shallow station 1274, October 2013, and a (b) deep station 1355, June 2014.

Estimated assimilation flux corresponded within approximately one order of magnitude of estimated diffusive flux for individual stations and dates (Table 3.7, Table B5). There did not appear to be a relationship between station depth and depletion, although there appeared to be a greater number of instances of depletion gradients at stations in the far-west and far-east transects, regardless of depth. Estimated assimilative flux of Chl a was relatively high in the nearshore, and appeared to be greatest at

stations that were ≥5m deep (Table 3.7). There was no clear trend that certain station depths were more likely than others to show depletion gradients (i.e. it was not overwhelmingly deep stations). Many of the stations with depletion gradients appeared to be those that fell on the FW and FE transects, and station 1274, 456, and 1341 on the M and NM transects. At these stations, the range of diffusive flux fell within an order of magnitude of estimated assimilation flux, but was often lower than estimated assimilation flux. Like assimilation flux, there did not appear to be a spatial pattern of elevated or suppressed diffusive flux.

Table 3.7. Summary table of depth and deployment-averaged diffusivity, diffusive flux downward, and assimilation flux for all individual profiles that showed significant near-bottom (0-0.5mab) Chl a depletion in samples taken in 2013-2015.

Station	Nominal station depth (m) (transect)	Sampling date	Diffusivity (m^2/s)	Diffusive flux ($g/m^2/d$)	Mussel biomass (g/m^2)	Chla concentration near bottom (µg/L)	Assimilation flux ($g/m^2/d$)
1353	3m (FW)	Aug-13	1.01E-04	4.08E-03	32.22	2.5	1.20E-02
1353	3m (FW)	Aug-13	1.01E-04	1.64E-02	32.22	1.7	8.65E-03
1274	3m (M)	Oct-13	1.92E-07	1.97E-05	64.04	3.6	3.30E-02
1274	3m (M)	Oct-13	1.26E-05	1.38E-03	64.04	2.8	2.63E-02
1355	10m (FW)	Jun-14	4.87E-05	1.21E-02	36.76	0.9	3.72E-02
1355	10m (FW)	Jun-14	2.54E-05	3.54E-03	36.76	1.3	3.28E-02
1356	18m (FW)	Jun-14	4.25E-05	4.41E-03	102.05	2.7	2.47E-02
1356	18m (FW)	Jun-14	1.79E-05	6.71E-04	102.05	3.1	1.20E-02
1274	3m (M)	Jun-14	4.1E-05	1.66E-03	26.62	1.6	6.80E-03
1274	3m (M)	Jun-14	4.86E-05	1.73E-03	26.62	1.5	6.45E-03
1353	3m (FW)	Jun-14	4.54E-05	7.82E-03	13.98	2.5	5.20E-03
1353	3m (FW)	Jun-14	4.4E-05	1.60E-02	13.98	2.1	4.48E-03
456	10m (M)	May-15	9.17E-05	8.53E-03	197.17	0.5	3.32E-02

Average Mussel biomass had a modest positive correlation with average assimilative chla flux, although there was more variation at higher mussel biomass (Figure 3.10). At mussel biomass ranging from 0-100g/m^2, there appeared to be a steeper slope between biomass and assimilation flux, compared to the relationship between mussel biomass >100g/m^2 and assimilative flux.

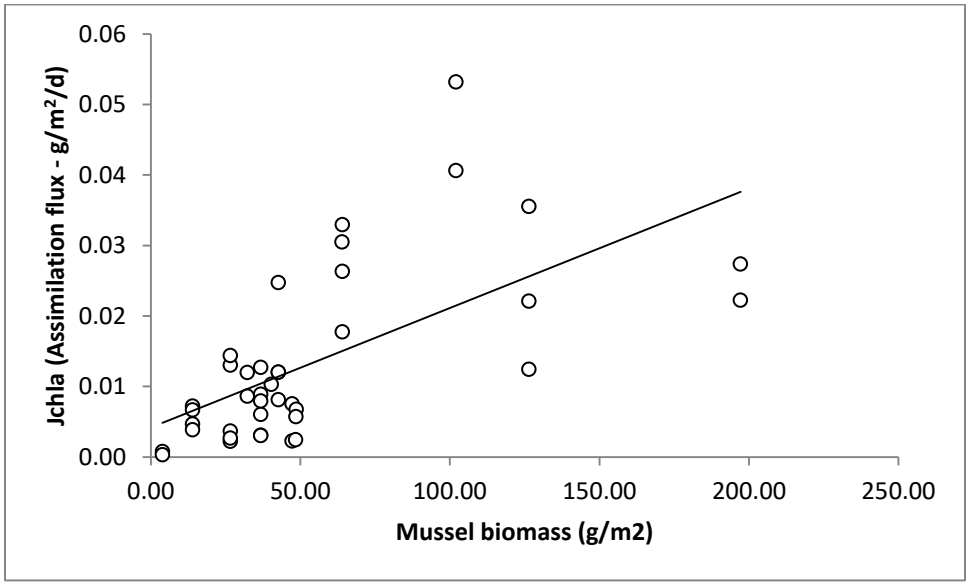

Figure 3.10. Average mussel biomass and average chla assimilative flux

There did not appear to be a strong systematic relationship between diffusive flux and assimilation flux, though there may have been a very weak negative relationship between the two (Figure 3.11). Increasing diffusive flux, which implies a stronger diffusivity or a stronger near-bottom Chl a gradient, was associated with a lower assimilation flux, and vice versa. At least in these instances, stronger mixing was not correlated with a greater assimilation flux, suggesting that strong mixing may have been slightly inhibitory. However, there are only a handful of points for comparison.

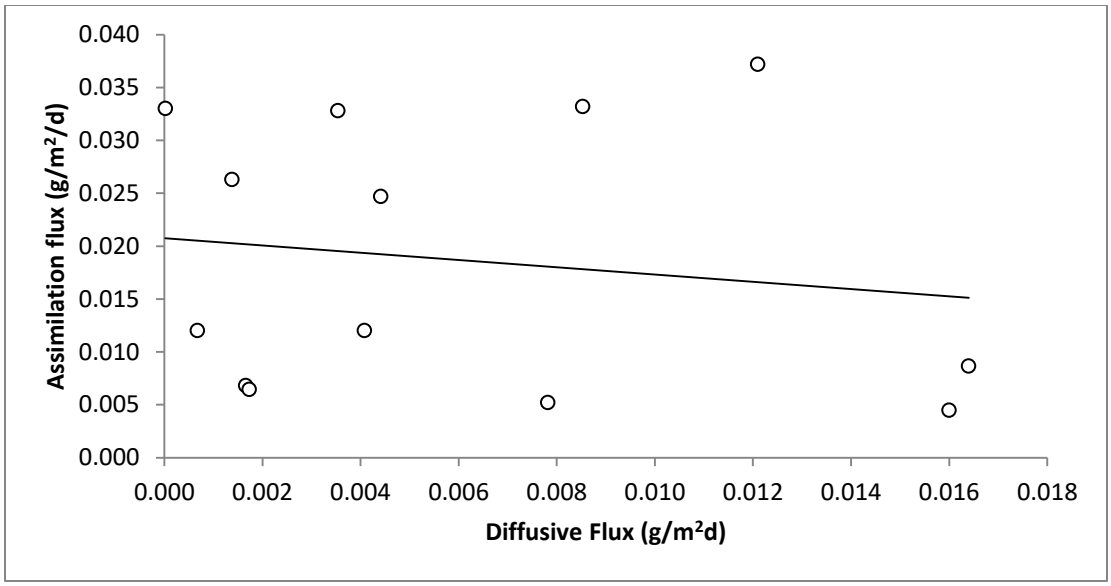

Figure 3.11. Chl a diffusive flux vs Chl a assimilation flux. Points correspond to the diffusive and assimilation flux data presented in Table 3.7.

3.4 Discussion

Shallow nearshore environments are thought to be vertically well-mixed, but the current study suggests that there are more instances than would be expected for stratification to occur. Nearshore stratification may impact benthic-pelagic coupling, particularly in the way mussels access food in the water column, and in Chl a patterns in the near-bottom water column, especially in the nearshore of the East Basin, which has a very large mussel presence. Near-bottom supply and control of near-bottom fluxes of Chl a and other nutrients appears to be controlled by processes more complex than just simple stratification. Limitation to mussel filtration through mass transport limitations was observed, but not typical in this study. Where mussel fitration effects were observed, it was possible to estimate mussel filtration and lends support to the idea that mussels may play a large role in the flux of particles, and particularly chla, into the nearshore bed.

3.4.1 Thermal stratification and differences between near-bottom and near-surface conditions

Thermal stratification was common in the East Basin nearshore, based on the Δ0.15°C/m criteria used in this paper, and this is the limit of accuracy of the YSI 6600 V2 sonde. This criterion is in line with previously published works, which suggest that temperature change of even Δ0.1°C/m may be enough to promote stability. Boegman *et al.* (2008) noted that a site in the Western Basin of nearshore resisted water column mixing when the temperature change was ~0.1°C/m. Similarly, Valipour *et al.* (2015) noted that a change in density of $1x10^{-3}kg/m^3$ was enough to promote stratification in the benthic boundary layer, denoting the mixing height, Hmix. Thermal stratification and at least temporary water column stability appears to be possible even in the shallow nearshore, which is thought to always be well-mixed.

Stratification may have appeared to occur more frequently in FW and FE transects because those water columns tend to be clearer than M and NM stations, allowing for greater penetration of solar energy to set up stratification. The observation that stratification occurred more frequently in the early part of the season could have been caused by a sampling bias in the sense that there were more samples taken in the early part of the season. This was in part because late season summer and fall storms prevented sampling, and because there were three sites that had repeat sampling in the early portion of May 2015.

Relative measurements between surface and bottom samples could give indication of the relative effects of the Grand River, dreissenid mussels, and other bottom enrichment processes that could drive coarse horizontal variation. The Grand River is both warmer and has higher specific conductivity than receiving lake waters, so a combination of both elevated temperature and specific conductivity in the surface relative to the bottom beyond threshold could indicate where the river had the greatest impacts. M stations were the only sites sampled that met this criterion, and this is in line with the findings of other workers (Chomicki *et al.*, 2016; Depew *et al.*, 2018), suggesting that the Grand River would enrich the surface relative to the bottom in a very localized area. Elevated specific conductivity at the surface was

not found at FW and FE sites, suggesting that the Grand River only had localized effects on surface waters. Bottom waters at a few FW and FE sites were both elevated in specific conductivity in bottom samples, but had temperature above threshold at the surface. The source of this elevated specific conductivity could have been a relatively intact river plume that had cooled and sunk, and whose signal was detected at these farther stations.

Dreissenid mussels may have also been responsible for areas of near-bottom depletion of Chl a and elevation of SRP and NH_4, which may have been overlaid by the river's temperature and specific conductivity signal. Both depletion of water column Chl a near bottom (Malkin *et al.*, 2012; Schwalb *et al.*, 2013) and elevation of near bottom soluble nutrients (Dayton, Auer & Atkinson, 2014) support the supposition that dreissenid mussels may have had an effect. Evidence of Chl a depletion and nutrient elevation near-bottom was subtle, and this may have been due in part to bottom turbulence, which can result in a relatively well-mixed benthic boundary layer, even in the presence of stratification (Wüest & Lorke, 2003). Local roughness elements may cause localized turbulence (Lorke & MacIntyre, 2009), which may also serve to obscure bottom depletion gradients that might have otherwise been more pronounced. Of all the possible sources of nutrient elevation and Chl a depletion near-bottom, that correspond to patterns of temperature and specific conductivity, dreissenid mussel feeding and excretion appears to be the most likely driver, and which may interact with other processes, leading to a less obvious near-bottom Chl a depletion gradient.

Because most stations met the criteria for stratification, internal wave motions, including seiches and decomposition of Kelvin-Helmholz waves, could introduce different water masses to the nearshore benthos, but may have obscured clear temperature gradients. Offshore hypolimnetic water may be a source of nutrients to the nearshore during upwelling events, and may be responsible for up to 30% of nutrient transport of currents perpendicular to shore (Valipour *et al.*, 2018). Hypolimnetic water has been observed between 4-8°C in Lake Erie (Schertzer *et al.*, 1987), so intrusion of the hypolimnion in the nearshore would have been expected to appear as a front of cold water and recorded on profiling sondes

as a sudden drop in temperature to values close to hypolimnion temperature. There was no evidence of this very cold water in bottom water temperature profiles, even at deep stations, suggesting that upwelling was not an important mechanism of near-bottom variability in this study. This is in line with other researchers working in the same study area concurrent with this study also did not find evidence of upwelling from offshore buoy data in 2014 (Depew *et al.*, 2018). The near-mouth stations that experienced this phenomenon in the early part of the sampling season in 2013 and 2014 may have experienced this largely disparate water column temperature due to cooler receiving waters and a warm intruding river plume. Conversely, only one deep far-west station showed this pattern in the later part of the season in 2013 and 2014, and this might be upward movement of deeper water. Further, the tilting of the thermocline may have interacted with a sloped bottom may serve to enhance mixing at the surface-water interface (Ivey *et al.*, 2000; Chowdhury *et al.*, 2016). This may at least partially explain why temperatures near-bottom at these particular limited number of stations were lower than the rest of the water column, but much warmer than the hypolimnion. The upward motion of thermocline tilting has been demonstrated to enhance mixing and promote buoyancy instability (Chowdhury *et al.*, 2016). Specific conductivity was not elevated, but in line with published offshore values of specific conductivity (~280-290µS/cm) (Chomicki *et al.*, 2016), at these deeper sites suggesting that these cooler temperatures were likely not hypolimnetic lake water intrusion (i.e. upwelling) and likely had a terrestrial source. Nevertheless, stratification may still be important in limiting mass transport, and may have important impacts on mussel filtration and mussel impacts on near-bottom chla.

3.4.2 Potential for mass transport limitation of mussel filtration and potential influences on estimates

Water column stratification may still have been important in limiting supply of seston to mussels, even if strong differences on a very coarse scale are not often observed. Stratification may still be important to mussel feeding, and may limit food supply to mussels, resulting in localized depletion

gradients. One way of estimating the potential for mass transport limitation is to compare grazing (TG) and mixing (TD) time scales. TG:TD predicted that depletion would be a common occurrence in the nearshore, supporting the mechanism of mussel-mediated benthic pelagic coupling, and mussel impacts on water column chla. This is an especially important point, because many observations and measurements on mussel feeding have been made under non-stratified conditions; mussels may actually have access to less food under typical conditions than these other measurements might suggest.

Differences between predicted and observed near-bottom Chl a depletion may have been related to assumptions in calculating TG and TD, and in the way in which observations were collected. Stratification height above bottom (H) is an important factor used in calculating both TG and TD, and the inaccuracies in this estimate can result in an inaccurate TG or TD. Consequently, predicted depletion estimates could also be inaccurate. Hmix, which tended to be a similar height to the height of near-bottom stratification, was used most of the time (Table B6), except in cases when Hmix was only around 1cm high. Mussel grazing rate and the grazing timescale makes an assumption of mussel areal pumping rate, using the values estimated in Ackerman, Loewen & Hamblin (2001). If actual mussel pumping rates in this portion of the nearshore is not similar to estimates from the West Basin, grazing time would be greater than predicted. Further, TG was also calculated from average mussel abundance in this study. Mussel distribution is patchy in this portion of the nearshore (Patterson *et al*., 2005, Burlakova *et al*., 2018), and it is possible that profile observations were conducted over a smaller patch than average.The onset and breakdown of stratification in the nearshore happens over many hours; profiles for most stations were collected only twice per station per hour and may have missed a detectable gradient when the sondes were cast.

Interaction of near-bottom currents with bottom roughness elements may have obscured formation or maintenance of near-bottom Chl a depletion gradients, as discussed in the previous section, resulting in a disparity between predicted and observed near-bottom Chl a depletion. Flow in the benthic boundary of most lakes tends to be turbulent (Wüest & Lorke, 2003), but not always. This could have important

implications for the likelihood or not of formation of benthic gradients under circumstances other than very quiescent conditions. Sampling was conducted under calm conditions (surface wind speed <10knots, ~5m/s), which should be related to benthic quiescence. Surface wind speeds of 6m/s may be the threshold between bottom quiescence and turbulence (Boegman *et al.*, 2008b; Dayton *et al.*, 2014), and a diffusivity between $1x10^{-4}$ and $1x10^{-5}$ m^2/s may correspondingly be a threshold between quiescence and turbulence (Edwards *et al.*, 2005).

Various sources of bottom turbulence including form drag and dreissenid mussel jets from exhalent siphons may have made obscured near-bottom Chl a gradients. Roughness elements including bottom cobble and rocks, mussel shells, and *Cladophora* biomass may have introduced form drag that enhanced turbulent mixing near-bottom that obscured observable gradients from forming (Lorke & MacIntyre, 2009). Form drag may have served to homogenize gradients of temperature, specific conductivity, and Chl a concentration. The greater the number of roughness elements, the more likely that a near-bottom velocity profile will be in the turbulent range (Lorke & MacIntyre, 2009). The size of *Cladophora* filaments may also impact near-bottom turbulence and mixing. Water tends to flow over large benthic mats, and shear is greatest over the mat (Escartin & Aubrey, 1995), but the mat itself reinforces a type of quiescence below it (Lawson *et al.*, 2012). Further, large *Cladophora* mats may serve to inhibit mussel feeding by essentially smothering them, leading to decreased feeding, and non-formation of a near-bottom Chl a depletion gradient. Conversely, short benthic vegetation filaments tend to enhance sediment resuspension and nutrient flux from these sediments (Lawson *et al.*, 2012). In the nearshore of the East Basin, this may be analogous to the early part of the season, where both mussel pseudofeces and settled particles (including phytoplankton) may become resuspended. In the early part of the season, near-bottom measured Chl a may have contained at least some resuspended phytoplankton, obscuring a depletion gradient that might have formed from mussel feeding. While mussel feeding is expected to create a near-bottom depletion gradient, their exhalent siphons may create localized pockets of very near-bed turbulence (on the order of centimeters) that may serve to disrupt the viscous sublayer (O'Riordan *et*

al., 1993, 1995; Nishizaki & Ackerman, 2017), and which may obscure depletions gradients very close to the bed, perhaps within 10cm of the bed.

. The potential limitations in calculating TG may have been related largely to estimations of mussel abundance (m^{-2}) and areal pumping rates (ml/mussel/h), the product of which is the estimate for mussel grazing rates ($ml/m^2/h$). The areal pumping rate value of 90 ml/mussel/h used in this study was taken from a previously published papers (Ackerman *et al.*, 2001) for zebra mussels an average of 16.9mm long, collected from the West Basin, and determined experimentally in a flume. Quagga mussel pumping behaviour and pumping rate may be impacted by a variety of environmental conditions as found in the East Basin nearshore, including variable temperature (Tyner *et al.* 2015) and oxygen (Stoeckmann, 2003), food availability and quality (Vanderploeg *et al.* 2017), and internal physiological state (Stoeckmann & Garton, 1997), including respiration rate (Tyner, Bootsma & Lafrancois, 2015) as it exists in the nearshore of the East Basin. Feeding and pumping rate, is related to food quality (Johengen, Vanderploeg & Leibeig, 2014, Vanderploeg *et al.*, 2017), and so pumping rate in mussels located proximate to external sources of nutrients like a tributary may also be different from mussels located further away from such a source. The estimated pumping rate determined in situ may be an oversimplification of mussel pumping behaviour in the nearshore, which may directly impact the grazing timescale (TG), and may in part explain the relatively low agreement between prediction and observation of near-bed Chl a depletion gradients in the nearshore. Some sites, including those directly impacted by the Grand River plume, may also have such high background water column Chl a that depletion gradients may not be evident, even if the mussels in that area or filtering at their maximum capacities. There may be a number of abiotic and physiological influences that resulted in some uncertainty in estimating the grazing time scale.

Similarly, calculating TD may be impacted by the mixing height chosen and the model used to calculate dissipation, and ultimately diffusivity. Determining mixing height is largely subjective, based on the phenomenon being investigated. Changes in density were determined from profiling sonde

temperature profiles, which only captured "snapshots" of water column structure. For almost all stations, only two profiles were taken over the course of an hour, approximately 30-45 minutes apart. These short intervals may have missed actual formation of stratification, or only captured the onset or breakdown of stratification. Stratification in the nearshore tends to be weak and transient anyway, so these small number of water column profiles may have failed to adequately capture this. If this is the case, mixing height may also be incorrectly estimated. ADCP measurements of near-bottom water velocity were captured in four-minute measuring bursts every 12 or 15 minutes, and from which dissipation and diffusivity were calculated and averaged. The temporal mismatch between a snapshot temperature profile to determine mixing height and a heavily averaged diffusivity estimate may have further influenced estimation of TD.

Because the nearshore does not stably stratify in the same way that the offshore does, quantifying what the mixing height near-bottom is may be difficult, and as yet there is no one single definition or description of it in a highly energetic and variable system such as this. For this reason, this paper used multiple criteria to define height of mixing. Profile measurements of temperature and Chl a may have also terminated above where mussels would be expected to have the most obvious effect on near-bed gradients. Optical Chl a probes are mounted a 5-10 centimeters above the bottom of the sonde, meaning that they may not adequately capture very near-bottom Chl a concentrations. If estimated Hmix is very small (i.e. <10cm high), it becomes very difficult to tell if there would be appreciable mixing below this, or if the relevant water column height is actually the height of stratification or the height of the water column. For this reason, Hmix calculated <10cm high was disregarded, and the Hstrat (height of stratification) was used instead. Obviously, a different height will impact both estimates of grazing time (TG) and also of diffusive mixing time (TD). Previous work in the Central Basin found Hmix to be meters high (Valipour *et al.*, 2015), and that evidence of near-bottom Chl a depletion was detectable 1-2m above the bottom (Edwards *et al.*, 2005; Schwalb *et al.*, 2013), which lends support to using the stratification height when Hmix <10cm. This approach is slightly different from the approach taken by

Schwalb *et al.* (2013), which assessed the near-bottom ln (chla)-ln(depth) relationship. They did not estimate near-bottom Chl a flux into the bed, however.

3.4.3 Fluxes of Chl a and relationship to mussel filtration

The flux of Chl a into the benthos and its relationship to mussel filtration is an important component of benthic-pelagic coupling. Diffusive flux of Chl a into the benthos has not been widely estimated using the methods put forward in this paper, which makes some of the first estimates in a heavily mussel-impacted area. There may be limitations to these diffusive flux estimates based on the steady-state model assumptions used, particularly the assumption of a linear Chl a gradient near-bottom, and a uniform diffusivity over the same height range. Comparison against a physiologically-based estimate of assimilative (feeding rate) flux may clarify the utility and significance of estimating diffusive flux this way, and the implications for a nearshore environment.

A steady-state model was used to estimate diffusive flux downward into the bed and despite some limitations of the assumptions, including the assumption that Chl a diffused in the same way a dissolved molecule wouldit seems reasonable to estimate flux of Chl a downward. Diffusive flux was not expected to vary with height above bottom, at least at heights near-bottom. Chl a flux near-bottom was assumed constant, and so calculations assumed constant source of phytoplankton Chl a and constant sink of Chl a (dreissenid mussels), and a constant turbulent diffusivity over the height of the near-bottom water column between 0-1mab. Because of these assumptions, it was possible to create a linear fit in near-bottom Chl a data, which usually extended no higher than 0.5mab. Using a steady-state model does not account for sedimentation of Chl a out of the water column into the benthos. Settling and sedimentation would lead to an accrual of seston and a gradient of increase at the bottom, not a net depletion gradient toward bottom, so it is reasonable to assume that there could be some sort of sink in the benthos. Dreissenid mussels are the dominant zoobenthic organism both in abundance and biomass in the East Basin (Burlakova *et al.*, 2018), so it is reasonable that they are the Chl a sink in this area. As such, it is a

reasonable assumption that diffusive flux of Chl a into the bed is almost entirely as a result of mussel filtering activities. This steady-state estimation of downward Chl a is probably an oversimplification of near-bottom Chl a behaviour, but it is a reasonable first step in approximating downward Chl a flux. This approach is also one of the first to use a water column profiler that is part of the typical water quality monitoring arsenal to measure Chl a for the purposes of estimating near-bottom Chl a flux. Its use may be a valuable proof-of-concept for others who may want to get more out of their Chl a profile data.

Estimated assimilation and diffusive flux values were similar, and most estimates were within one order of magnitude, but assimilation flux estimates tended to be greater than the diffusive flux estimates. This might have been due to the fact that the assimilation rates calculated by Vanderploeg *et al.*, (2017) were done in mesocosms, and exchange with the wider environment did not occur, nor was there explicit consideration of the effects of water motion, or depletion of Chl a directly above mussel beds. The only source of turbulent mixing in such closed systems would come from mussel siphon activity, which can act directly above the bed, but not much farther above it (O'Riordan *et al.*, 1995; Nishizaki & Ackerman, 2017). This may have resulted in artificially higher values, relative to in-lake estimates, where the intensity of mixing processes might serve to modify their feeding behaviour. Dreissenid mussel feeding is enhanced by turbulent mixing, up to a certain point, but beyond this point, mixing forces serve to hinder feeding instead of enhancing it (Ackerman, 1999).

This simplified flux model is reasonable in the context of comparing against assimilation flux and grazing timescales. Assimilation flux is estimated from mussel biomass and assimilation rate; assimilation rate is itself estimated from Chl a concentrations based on mussel feeding in a closed laboratory system (Vanderploeg *et al.* 2017), so also does not have fine spatiotemporal resolution. The grazing timescale is estimated from the height of mixing and an assumed grazing rate of 90 mL/mussel1/h (Koseff *et al.*, 1993; Boegman *et al.*, 2008b), which is the product of mussel abundance and areal pumping rate. The pumping rate was determined for zebra mussels (Ackerman *et al.*, 2001), which have slightly different physiological energetics compared to quagga mussels (Stoeckmann, 2003), and is likely

not be the most accurate pumping rate for quagga mussels. This highlights the importance of the pumping rate and assimilation rate estimates in estimating both TG and assimilation flux, and how important it is to keep these potential sources of variation in mind. Different laboratory and experimental setups can yield different estimates, which will directly impact estimates of assimilation flux and/or estimates of TG. However, it is useful for estimating what range of grazing timescales may be expected in the nearshore of Lake Erie. Vanderploeg *et al.* (2017) used mussels from a different lake for their experiments, and the phytoplankton concentration in these lakes may be different than what is found in the nearshore of the East Basin. They found a positive, moderately correlated relationship between Chl a concentration and Chl a assimilation rate. With this in mind, it is possible that the estimated diffusive flux is actually closer to assimilation flux in Lake Erie. Further, while field sampling was conducted on calm days with surface wind speed no greater than 10knots, there were instances where the preceding days experienced strong storm events, and that momentum may have served to obscure gradients that would have otherwise formed at the bottom. With the exception of very shallow (nominally 3m deep) stations in June 2013, the stations that demonstrated near-bed depletion of Chl a tended to have very small near-bottom diffusivity. This could insinuate two things: the first is that formation of near-bed gradients may be more ubiquitous in this part of Lake Erie, but strong near-bed mixing processes serve to obscure these obvious gradients. The fetch of the lake is oriented in the same direction as the prevailing wind direction (Bolsegna and Herdendorf 1993). Shore parallel flow is stronger than cross-flow (He *et al.*, 2006; Chomicki *et al.*, 2016). Because surface wind input is ultimately the source of energy input transmitted to the lake bed, being oriented along the prevailing wind direction means that Lake Erie can quickly switch between quiescent and energetic. The second is that formation of near-bed gradients may only occur under very quiescent conditions, and that there is a threshold between 10^{-5} and $10^{-4} m^2/s$ where the near-bottom environment switches from quiescent to energetic (Edwards *et al.*, 2005; Bouffard & Boegman, 2013).

In general, a large proportion of the flux of Chl a downward to the lake bed is likely to be intercepted and used as food by the mussels, as they are the dominant taxa in the East Basin (Burlakova *et al.*, 2014). Incoming food energy can be used to meet metabolic demands (i.e. respiration, staying alive), for growth, or for reproduction (Stoeckmann & Garton, 1997, 2001). Food quality may vary spatially and some parts of the nearshore like those located near the mouth of the Grand River may have higher food quality than others (i.e. a higher proportion of high-quality phytoplankton compared to a higher proportion of inedible silts and sediments). This may account for some stations that appeared to experience depletion gradients frequently, including stations of all station depths in the far-west and far-east transects, although they were not the most frequently sampled. The most frequently sampled stations were on the mouth transect (stations 1274, 1340, 456), and with few exceptions, these stations experienced a depletion gradient in the early summer months; that is, early in the growing season. Part of this may be related to occurrence of the spring bloom, warmer water and reduced low-temperature stress on mussels, and relatively easy access to a well-mixed water column. Lake Erie is a temperate dimictic lake, and the spring bloom in these lakes tends to be diatoms, based on typical phytoplankton succession (Kalff, 2002) and aided by a fully mixed water column (i.e. spring mixis). As long as the diffusive mixing is at least as long as the grazing time, this mixing could be beneficial for mussel feeding.

Stratification in the nearshore appears to be a common phenomenon, but obvious differences in specific conductivity, nutrients and Chl a are not easily seen in coarse water collection such as the surface bottom bulk water sampling typically done in routine water quality samplings. However, there does appear to be some effect of stratification on how much of the water column dreissenid mussels are able to access, and careful profiles of the water column, and especially near-bottom may be useful in assessing how much of an impact mussels have on phytoplankton in the nearshore.

Chapter 4: Diffusive flux estimates of *in situ* dreissenid mussel contributions to near-bottom available P confirm the importance of mussels in nearshore P cycling

Mussels have been implicated in benthification of phosphorus through their filtration and excretion activities in the nearshore of the Laurentian Great Lakes, particularly East Basin Lake Erie, where resurgence of nuisance *Cladophora* suggests non-limiting concentrations of bioavailable phosphorus at the lake bed. Near-bottom water motion may play a key role in structuring the near-bed environment. Diffusive fluxes of particulate phosphorus (PP) downward were calculated using Fick's Law and measurements of near-bottom Chl a gradients, PP:chla ratios, and the vertical eddy diffusivity. Diffusive fluxes of SRP upward were similarly calculated from measured vertical gradients of SRP and the measured vertical eddy diffusivity. SRP fluxes were also estimated using literature relationships and measured mussel biomass and PP concentrations. *Cladophora* uptake was estimated using the *Cladophora* Growth Model and measured Cladophora biomass. The range of diffusivity in the nearshore was relatively consistent between stations, regardless of depth , and tended to be in the range of 10^{-5} - 10^{-3} m^2/s. There was evidence of PP flux down into the beds. Peeper data suggested that there was an SRP concentration gradient ≤20cm above bottom. Diffusive SRP flux estimates were between $4.20x10^{-4}$ - $5.18x10^{-2}$ $g/m^2/d$. Diffusive flux estimates were in a range similar to indirect assimilation and excretion flux estimates, which were based on extrapolated relationships between mussel feeding and excretion rates and mussel biomass from previously published literature values. Areal SRP flux estimates and areal *Cladophora* uptake estimates suggest that mussels are producing more SRP than *Cladophora* is able to take up over the area as a whole. Horizontal advection may be important in moving nutrient rich water from deeper portions of the nearshore where mussels are abundant but *Cladophora* is light limited, to shallower portions of the nearshore where *Cladophora* is not light limited, but where mussel biomass is at intermediate levels. Mussels appear capable of providing enough SRP to sustain *Cladophora* growth in the euphotic zone, but there may be a spatial separation between where SRP is produced and where it is taken up. More work may need to be done to fully understand the interaction between mussel excretion, bulk water motion, and *Cladophora*.

4.1 Introduction

Cladophora resurgence to nuisance levels is a problem in many nearshore environments. Light tends to be a limiting factor, and limits the depth to which *Cladophora* can grow. There is evidence that mussels have improved light penetration to the benthos (Stewart, Miner & Lowe, 1998; Barbiero & Tuchman, 2004) and have increased benthic habitat for *Cladophora* growth (Stewart *et al.*, 1998; Wilson *et al.*, 2006; Stewart & Lowe, 2008) However, in areas where light is not limiting, including many portions of the nearshore, P-limitation tends to be the factor limiting *Cladophora* growth (Higgins *et al.*, 2005b, 2008b; Malkin *et al.*, 2008). External loading may provide P to support *Cladophora* biomass, but the flux of P from mussels may be similarly important. However, there is much less information currently available regarding flux of P from mussels in natural settings, including how water motion may impact this flux. The *in situ* study done by Ozersky *et al.* (2009) is one of the closest to a natural system, but because they placed rocks and mussels in closed containers, they were not able to simulate diffusivity accurately. However, near-bottom water motion is an important consideration in the formation or abolishment of near-bottom nutrient gradients.

Mussel feeding of water column particulate phosphorus (PP) and benthic soluble phosphorus (SRP) excretion (the nearshore phosphorus shunt) (Hecky *et al.*, 2004) may play a role in formation of near-bottom nutrient gradients, and may be an important mechanism which could support nuisance *Cladophora* growth. Dreissenid mussels have been observed to impact water column chl a concentrations under a mixing water column (Mellina, Rasmussen & Mills, 1995; Mills *et al.*, 1996; Yu & Culver, 1999; Edwards *et al.*, 2005) and may form depletion gradients near-bottom under instances of stratification (Schwalb *et al.*, 2013, 2014). Chlorophyll a and PP have a relationship (Smith *et al.*, 2005), and it may be possible to estimate a PP gradient and PP flux downward from near-bottom Chl a profiles (Ch 3) and site-specific chla:PP relationships. Trying to assess how much of an impact dreissenid mussel excretion in the nearshore is a priority, as a result.

Previous reports have suggested that mussels can produce enough SRP to support *Cladophora* growth in the nearshore of Lake Ontario (Ozersky *et al.*, 2009). Reappearance of nuisance *Cladophora* growth shortly after zebra mussel introduction to the Great Lakes would suggest this as well. Mussels as a source of nutrients may have management implications, especially as other potential nutrient sources, such as tributaries or upwelling, may also be important in providing nutrients for nuisance *Cladophora* growth in the spring (Chomicki *et al.*, 2016). However, direct tributary impacts may be highly localized (Ch2; He *et al.*, 2006; Chomicki *et al.*, 2016; Depew, Koehler & Hiriart-Baer, 2018) and mussels may interact with, and process, tributary inputs of SRP found near-bottom and in proximity to *Cladophora* (Depew *et al.*, 2018), reinforcing the importance of considering mussel excretion in the context of nuisance *Cladophora* growth. Tributaries may be a good source of food for dreissenids, and may act synergistically to enhance dreissenid feeding and excretion (Boegman *et al.*, 2008a). The relative P assimilation and richness of mussel excretia is thought to relate back to its food richness, and there are positive relationships between Chl a concentration and PP assimilation rate, and between PP concentration and P excretion rate (Vanderploeg *et al.*, 2017). Mussels in general excrete N:P inversely to their somatic needs, and will excrete more P when it is in excess to their needs (Morehouse, Dzialowski & Jeyasingh, 2013). SRP coming from deeper portions of the lake, including the hypolimnion and the deeper nearshore, may also be important in supplementing nutrients for *Cladophora* growth. Horizontal advection may also be an important mechanism for bringing nutrient rich water from deeper areas into the nearshore, especially in May and June (Valipour *et al.*, 2018). Valipour *et al.* (2018) were looking specifically at upwelling of the hypolimnion, but it is possible that this may be a mechanism to bring water from deeper sections to shallower sections of the nearshore.

Accurate and precise sampling of near-bottom nutrient gradients in the vicinity of *Cladophora* can present an operational challenge, but detection of these gradients could be informative in understanding how mussels may be mediating nuisance *Cladophora* growth. While bulk water sampling may capture elevated SRP as close as 0.5m above bottom (Martin, 2010) in some instances, this type of

sampling may not capture what is happening within centimeters of bottom, where elevated soluble nutrients would be most important. Near-bottom gradients are likely not to form instantaneously and passive samplers such as Modified Hesslein samplers ("peepers") (Hesslein, 1973) may be a useful way to capture this gradient without disturbing the near-bottom water column in the process. Peepers work on the principle of a equilibration of SRP concentration between the inside and outside of the sampling membranes, which takes ~6h based on dye studies in quiescent water (Dayton *et al.*, 2014). Dayton, Auer, and Atkinson (2014) Measured near-bottom SRP gradients in Lake Michigan, and attempted to model these gradients based on mussel biomass and assumed values of biomass-specific excretion rates, in order to predict the nature and incidence of near-bottom gradients across the growing season in their study area. Being able to measure gradients is important because a lack of a gradient could suggest that SRP formed by mussels is being mixed away into the water column, and therefore not available for *Cladophora* uptake. Nitrogen is thought to be less limiting to algae growth than phosphorus in freshwater systems (Schindler, 1971, 1977), although it may become limiting in the water column in the offshore (Guildford *et al.* 2005; North *et al.* 2007). If *Cladophora* takes up phosphorus almost as quickly as it is being made available, an NH_4 gradient may be more likely than SRP to form near-bottom. Near-bottom ammonium profiles may provide additional evidence of mussel impacts that are not obscured by nutrient cycling in the same way that phosphorus is, especially in a dynamic benthic boundary layer.

There may be many reasons why near-bottom concentration gradients of soluble nutrients may or may not be readily detected. Calm conditions and stratification are thought to promote the formation of near-bottom gradients. Nearshore stratification, though weaker and of shorter duration than offshore stratification, may create conditions that lead to bulk separation of the water column (Ackerman *et al.*, 2001; Edwards *et al.*, 2005; Loewen *et al.*, 2007; Boegman *et al.*, 2008b). This water column separation may prevent mixing between the surface and near-bed, and which may enhance the detection of near-bottom gradients. Studies in Lake Simcoe have noted that there was evidence mussels located at mid-to-deep nearshore depths experienced a lack of food under instances of near-seasonal stratification (Schwalb

et al., 2013). Previous work has found that an air-surface wind speed of ~6m/s (~11knots) can be enough to promote bottom mixing (Boegman *et al.*, 2008b; Dayton *et al.*, 2014); below this, there might not be enough inputted energy to promote turbulent mixing at the bottom. Similarly, there have been observations that diffusivity between 10^{-4} and 10^{-5} m^2/s near-bottom may be the threshold at which a quiescent benthic layer switches to an energetic one (Edwards *et al.*, 2005; Bouffard, Ackerman & Boegman, 2013), which may be the difference between formation and abolishment of near-bed gradients. In these instances, an obvious SRP gradient near bottom may not be detectable, but a diffuse layer of relatively enriched water may remain that can be detectable in bulk water samples, especially if presence of stratification limits total water column mixing. This may explain why other workers have observed elevated SRP at heights 0.5-1m above bottom (Martin, 2010) in a portion of the Lake Ontario nearshore, and why there was slight, non-significant near-bottom SRP elevation observed in Ch2 and Ch3. Homogenization of near-bottom water masses may be the result of interaction of water flowing over a rough bottom. Mussels, *Cladophora*, and bottom substrate may also act as roughness elements that enhance near bottom turbulence and mixing. This roughness element enhanced turbulence may further obscure near bottom nutrient gradients, even at a lower diffusivity that should promote the formation of gradients. *Cladophora* at low biomass enhances turbulence, but large mats of *Cladophora* may inhibit turbulence at the core of the mat, leading to decreased nutrient uptake (Lawson *et al.*, 2012) and increased self-shading (Higgins, Hecky & Guildford, 2008a) that leads to senescence and sloughing.

Direct measurements of near-bottom gradients and estimates of diffusive flux of PP into and SRP out of the bed have not been widely done. The timing of the original mussel introduction and subsequent resurgence of nuisance *Cladophora* during the growing season may be coincidental. The relationship between mussel feeding and excretion, and *Cladophora* dominance during the growing season is worth exploring further, however. The objectives of this paper include (1) determining how often near-bottom nutrient gradient can be detected, and whether they are common, rare, or absent, (2) where near-bottom gradients exist, what are the flux of SRP inferred to be knowing mussel biomass and current knowledge

of mussel excretion, (3) comparing the downward flux of PP, the upward flux of SRP, and *Cladophora* SRP uptake rates, and whether predicted fluxes could support *Cladophora* biomass as it occurs in the nearhsore, and (4) determining whether mussel flux is larger than *Cladophora* nutrient needs, when considering all available evidence in the preceding objectives.

4.2 Methods

Dreissenid mussels are hypothesized to enhance near-bottom soluble phosphorus (SRP) through their water column feeding of particulate phosphorus (PP) and near-bottom excretion. This feeding and excretion is thought to be an important mechanism in the resurgence of nuisance Cladophora growth in the nearshore of the East Basin. Estimating the flux of SRP from the benthos to overlying water where Cladophora is, and comparing how much is coming up from the bottom with how much Cladophora is taking up may provide evidence of mussel effects in the nearshore. Efforts were made to detect gradients of particulate P (PP) and SRP in proximity to mussel beds. Diffusive flux of soluble reactive phosphorus (SRP) out of the nearshore lakebed was estimated using measured water velocity, temperature, and gradients of SRP. At select sites, estimates of NH_4 out of the bottom were concurrently estimated. Mussel excretion flux was also estimated using estimates of Chl a concentration from corrected water column profiles using two similar methods and mussel biomass data. *Cladophora* SRP uptake estimates were estimated using the *Cladophora* Growth Model (CGM) using previous published estimates of internal phosphorus concentration for this part of Lake Erie (Higgins, Hecky & Guildford, 2005a).

4.2.1 Sampling site and data collection

Field work was conducted in the rocky nearshore of the East Basin at stations of different depths and proximities to the land-lake margin along four transects, centered on the mouth of the Grand River (Figure 4.1). Five stations were specifically chosen for deployment of modified Hesslein samplers ("peepers"), semi-permeable passive dissolved nutrient samplers, in June 2014 (1353 and 1351) and May 2015 (456, 1350, and 1355) and for estimates of diffusive flux using the SRP gradient captured in the

peepers. Water column Chl a profiles collected at all sites showed in Figure 1 in 2013 and 2014 were used to estimate flux of PP downward that mussels may be filtering, flux of SRP out of the bed, and *Cladophora* areal uptake rates.

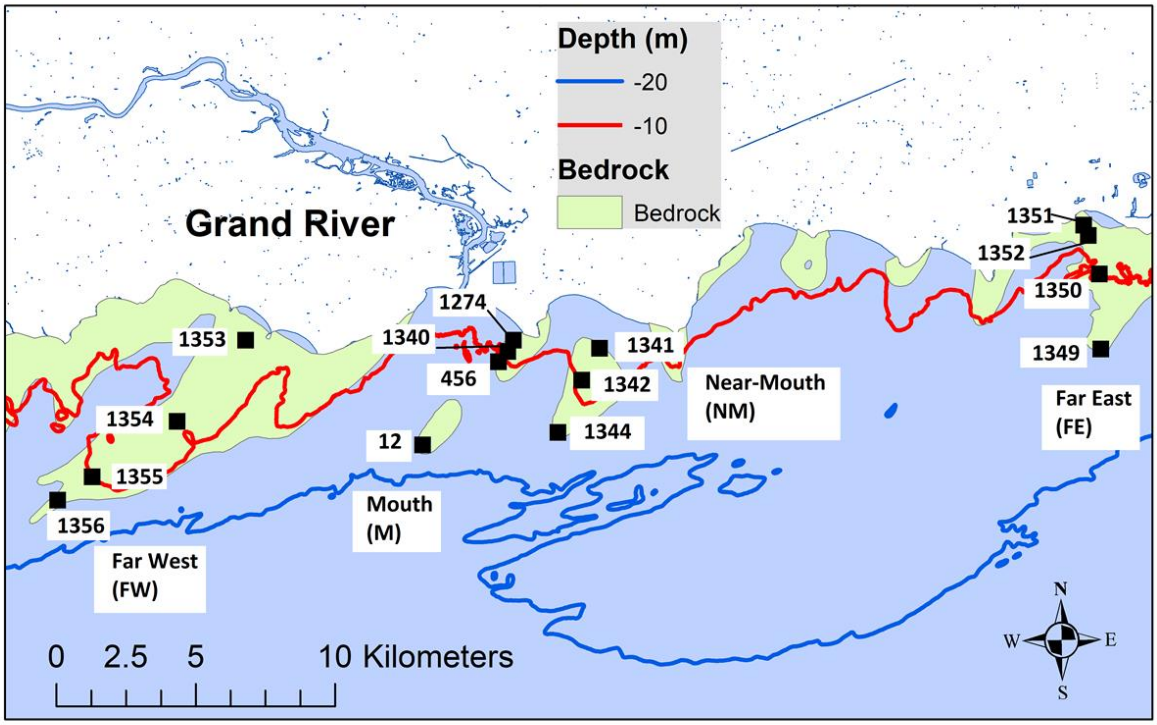

Figure 4.1. Map of the northern nearshore of the East Basin, Lake Erie, centred on the Grand River indicating stations (squares), and the four named sampling transects as they are discussed in the paper.

4.2.2 Data collection and analysis, and estimation of diffusivity

A variety of recording instruments were deployed in order to measure near-bed water velocity, temperature, and chlorophyll a fluorescence. An acoustic Doppler current profiler (ADCP) (Nortek) mounted on a tripod in down-looking mode 2m above the bed measured at a rate of 1Hz every 12 (May 2015) or 15 (June 2014) minutes at 3cm height intervals. Concurrently, eight RBR temperature profilers

(Ruskin) mounted at 10cm intervals above bottom recorded temperature every 10 seconds. In 2014, deployments were ~1h long and at the 3m depth contour, while deployments in 2015 were ~6-8h long at the 10m depth contour. The water column was also profiled using a YSI 6600V2 sonde, collecting temperature, specific conductivity, and Chl a profiles. In 2014, the water column was profiled twice per site, approximately 45min apart. In 2015, the water column was profiled approximately 5-6 times per site, approximately hourly.

Modified Hesslein samplers ("peepers") were used to passively sample for near-bed gradients of SRP, and in the case of 10m station deployments, NH_4 at 2.5cm height intervals above bottom. Peeper frames were acid washed and great care was taken to minimize P contamination, including wearing new clean nitrile gloves and laying the frames on sheets of aluminum foil, when 0.45μm pore size polycarbonate membrane sheets (Sterlitech Corp.) were secured to the frames, and when the peepers were assembled. Assembled peepers were filled with MilliQ ultrapure water and transported in an acid washed transport container in a MilliQ water bath until deployment in the field. Peepers were deployed for 6-8h, and sampled immediately upon retrieval into acid-washed falcon tubes and stored in a cooler in the field, and at 4°C until analysis using the Molybdate blue method (Stainton, 1970). Chl a profiles were corrected against extracted Chl a from bulk water samples taken within an hour of profile collection from the same site, using the same methodology as Ch3. Temperature profiles were used to note the presence or absence of stratification that may impact the formation of near-bottom nutrient gradients, again, using the same methodology as Ch 3. Specific conductivity profiles were collected as a way to track the influence of the river on the site where peepers were deployed.

Particulate P (PP) was estimated from Chl a YSI profiles that had been corrected against extracted Chl a (Table 4.1). Near-bottom Chl a profiles were converted to PP using the sampling date-specific PP:chla ratio of extracted Chl a and digested PP from bulk water samples.

Table 4.1. Coefficients used to determine [PP] from [Chl a] (determined from the relationship [PP]=a*[Chl a]+b).

Sampling date	May-13	Jun-13	Aug-13	Oct-13	Jun-14	Aug-14	Oct-14	May-15
Slope (a)	1.2318	1.8495	0.97112	0.95463	0.18487	1.4761	-0.32923	0.98742
Intercept (b)	2.4415	1.6676	3.5839	3.3446	2.4611	1.9039	1.8537	1.4913

Mussels and Cladophora were harvested by collaborators at the same stations within a week or two of our field sampling. Mussels were collected manually by divers at three $0.15m^2$ quadrats per station, carefully removing mussels intact from all substrate, including cobble. Their sampling was also conducted when weather conditions permitted. Mussels were kept cool and sent to the lab as quickly as possible where they were counted for abundance (expressed as number of mussels/m^2), their soft body parts were dissected from the shells, dried, and weighed for shell-free dry weight (SFDW) and biomass (expressed as g/m^2). Cladophora was collected in a similar manner to the mussels for biomass in dry weight (gDW/m^2).

Diffusivity was calculated from estimated dissipation (ε) and buoyancy frequency (N^2). Dissipation (ε) was calculated from the ADCP velocity, amplitude, and correlation files using the structure function method (SFM) (Wiles *et al.*, 2006) (Equation 4.1), including the parameterization of constant C based on shear velocity (Jabbari *et al.*, 2016). This method was chosen over Log Law of the Wall (LLOW) because of its applicability to the nearshore system. LLOW assumes steady state (i.e. isotropic unidirectional flow), whereas SFM takes advantage of the noise generated in the system to calculate dissipation (Wiles *et al.*, 2006). Temperature data recorded from the RBR thermistors was used to calculate the buoyancy frequency (N^2) (Equation 4.2). Because temperature and density have a known relationship in freshwater (Kalff, 2002), temperature was suitable to use for estimating the buoyancy frequency. Salinity was negligible in this system, and was not explicitly used in the estimation of density. Thus, density was related only to temperature of the water column.

Dissipation using the structure function method

Equation 4.1

$$\varepsilon = \left[\frac{G(z,r)}{Cr^{2/3}}\right]^{3/2}$$

Where:

- ε is dissipation (m^2/s^2)
- G(z,r) is the mean squre difference in the velocity fluctuation (z) between two points that are r distance apart from Wiles *et al.* (2006)
- C is a parameterised constant fromJabbari *et al.* (2016)

Equation 4.2

$$N^2 = -\frac{g}{\rho}\frac{\partial \rho}{\partial z}$$

Where:

- N^2 is the buoyancy frequency (s^{-1})
- g is acceleration (~9.81 m^2/s)
- ρ is density estimated from temperature (kg/m^3)
- z is depth

Diffusivity was calculated from dissipation (Equation 4.1) and buoyancy frequency (Equation 4.2), and using the refined parameterizations of Kz based on Prandtl's number (Pr) and the turbulence intensity parameter Reb (Bouffard and Boegman 2013)($Kz_{(Reb)}$). Diffusivity under this parameterization collapses back to Osborn diffusivity under certain conditions (Bouffard & Boegman, 2013). D is the molecular diffusivity of P; the value used was determined by Krom and Berner (1980) to be $3.3x10^{-6}$ cm^2/s.

Diffusivity using the TAP parameterization method

$$Kz_{(Reb)} = \begin{cases} D, & if\ Reb < 10^{2/3} * Pr^{-1/2} \\ 0.5D * Reb^{3/2}, & if\ Reb \geq 10^{2/3} * Pr^{-0.5} \& Reb \leq (3\log(\sqrt{Pr}))^2 \\ 0.2Dv * Reb, & if\ Reb \leq \left(3\log(\sqrt{Pr})\right)^2 \& Reb \leq 100 \\ 2v * Reb^{0.5}, & if\ Reb > 100 \end{cases}$$

Equation 4.3

Where:

- $Kz_{(Reb)}$ is diffusivity calculated using the Reb parameterization
- D is the diffusivity of phosphate ($3.6X10^{-6}$ cm^2/s)
- Pr is Prandtl's number
- Reb is the turbulence intensity parameter ($Reb = \varepsilon/(vN^2)$).

Dissipation, buoyancy frequency, and diffusivity were interpolated in MATLAB (function interp1) to a 2.5cm interval (the interval of peeper heights) from heights of 10cm to 35cm above bottom for sites that included peeper measurements for flux estimates; 2.5cm is the interval of the peeper cell heights. For all other stations, dissipation, buoyancy frequency, and diffusivity were interpolated to a 3cm interval over a common range of 15-78cm; this is because the smallest measurement interval was 3cm bins for the ADCP, the height range for the RBR temperature sensors was 10-80cm, and the lowest recorded ADCP velocity reading was ~15cm high.

4.2.3 Estimation of PP, SRP, and NH_4 flux from mussels

Flux of PP and SRP that mussels may be filtering was estimated two ways, using relationship and equations found in Vanderploeg *et al.* (2017) and Dayton *et al.* (2014), and mussel biomass from samples taking in 2013-2015 (2013 and 2014 data from A. Dove, Environment Canada). Particulate P was estimated from the lowest reliably optically measured Chl a from the YSI sonde and using the chla:PP relationship (Table 4.1) determined from bulk water samples. A downward flux of PP was then estimated using the measured Chl a, mussel biomass, and the chla:APP relationship found in Vanderploeg (Equation 4.4) and also using the estimated PP, measured mussel biomass and the relationship for PP flux found in Dayton et al. 2014 (Equation 4.6). P excretion rate (Pex) was estimated by using the

relationship between PP concentration and P excretion as published in Vanderploeg *et al*. 2017 (Equation 4.5) together with measured mussel biomass. APP and Pex were multiplied by the measured mussel biomass to generate areal flux estimates in units of μgP/m^2/h, and converted to units of g/m^2/d. SRP flux was also estimated from the equations Dayton *et al* (2014), using the same coefficients they used (Equation 4.7). These estimates of SRP flux were then converted to units of g/m^2/d.

Chla-APP in Vanderploeg *et al.* 2017

$$APP = 0.0192[Chl\ a] - 0.001$$ **Equation 4.4**

Where:

- APP is the particulate P assimilation rate (μgPP/mgSFDW/h)
- [Chl a] is the Chl a concentration (μg/L) from Chl a profiles

PP-Pex in Vanderploeg *et al.* 2017

$$Pex = 0.004[PP] + 0.0035$$ **Equation 4.5**

Where:

- Pex is the mussel P excretion rate (μg/mgSFDW/h)
- [PP] is the particulate P concentration (μg/L) estimated from Chl a profiles

JPP in Dayton *et al.* 2014

$$J_{PP} = F \cdot B \cdot P_{PP}$$ **Equation 4.6**

Where:

- J_{PP} is the flux of particulate phosphorus down into the mussel beds (mg/m^2/d and corrected to units of g/m^2/d)
- F = 3.89 × 10−4 m^3/mgAFDW/d (estimated from mean mussel filtration rate, in aquarium studies in Fanslow *et al.* 1995)
- B = station-specific mussel biomass (mgAFDW/m^2), determined from mussels sampled for this paper
- P_{pp} = particulate P concentration (μg/L or mg/m^3), determined from field measurements

JSRP in Dayton *et al.* 2014

$$J_{SRP} = f \cdot J_{PP} \qquad \textbf{Equation 4.7}$$

Where:

- J_{SRP} is the flux of SRP coming out of mussel beds (mg/m^2/d, corrected to units of g/m^2/d)
- f =0.64, theconversion efficiency from PP to SRP, determined in a mesocosm study in James *et al.* 2000
- J_{PP} is the flux of P downward, determined in Equation 4.6

SRP diffusive flux (Equation 4.8) from the bottom was also estimated using the concentration gradient of SRP from peeper data and mean Kz calculated using the TAP parameterization method. The gradient of SRP near-bottom where there appeared to be a linear gradient was multiplied against the depth- and deployement-averaged diffusivity to yield an estimate of SRP flux for the three stations where peepers were deployed in 2015.

Flux of SRP upward using Fick's first law.

$$J = K_z \frac{\partial PO_4}{\partial z} \qquad \textbf{Equation 4.8}$$

Where:

- J is the diffusive flux of SRP upward from the bottom (mg/m^2/s corrected to units of g/m/d)
- Kz is the diffusivity estimated in Equation 4.3 in m^2/s
- $\partial PO_4/\partial dz$ is the near-bottom SRP gradient (µg/L/m or mg/m^3/m)

4.2.4 Estimates of *Cladophora* P uptake

Cladophora uptake was estimated using the product of estimated P uptake rate (%P/d) using the Cladophora Growth Model (Higgins *et al.*, 2005a)(Equation 4.9), and mussel biomass (g/m^2). The P uptake rate was converted from units of %P/d to units of gP/gDW/d. *Cladophora* biomass data was

provided by Alice Dove (ECCC). To simplify estimates, some of the coefficients were assumed including, τ was 0.88, Q was 0.1, and SRP concentration was 2µg/L. τ was determined from average ambient water temperature (Equation 4.10). SRP was assumed to be 2µg/L, as this is the concentration threshold above which *cladpohra* is expected to grow to nuisance biomass (Auer *et al.*, 2010; Ch2).

Cladophora Growth Model (amended by Higgins et al. 2005)

$$p = pMAX * \tau * \frac{SRP}{(Km + SRP)} * \frac{Kq}{(Kq + Q - Q_0)}$$ **Equation 4.9**

Where:

- P is P uptake (%P/d)
- pMAX is maximum specific P uptake (d^{-1})
- τ is the temperature dependant coefficient for P uptake (unitless)
- SRP is the SRP concentration (µg/L)
- Km is the half-saturation constant for uptake of external SRP (µg/L)
- Kq is the half-saturation constant for uptake as a function of internal P (%P)
- Q is the internal P concentration (%P of dry weight,)
- Q_o is the minimum internal P concentration (0.05%P of dry weight, Canale & Auer, 1982)

Determining τ (from Painter and Jackson 1989)

Equation 4.10

$$\tau = \begin{cases} e^{\frac{(t-18)}{39}}, & t < 18°C \\ e^{\frac{(18-t)}{18.75}}, & t \geq 18°C \end{cases}$$

4.3 Results

4.3.1 Changes in the water column over the course of on-station sampling

The water column showed evidence stratification and changes in water column specific conductivity and Chl a over the course of the day from intensive profiling in 2015 (Figure 4.2). Near bottom profiles also reflected some changes over the course of the day, but the changes were not as

dramatic as they were in the water column. Temperature differences between the surface and bottom of the water column increased from ~1.5°C in the morning, to ~2°C mid-day, to ~8°C in the late afternoon. The bottom 3 or 4m however remained ~ 8°C for the duration of the day. Similarly, specific conductivity in the bottom 3 or 4m remained relatively consistent, just above 270μS/cm. Like water column temperature, water column specific conductivity changed over the course of the day, and in the surface particularly. At mid-day (panel B), surface specific conductivity increased slightly from 280μS/cm to 295μS/cm, and may have been influenced from an incoming river plume. In the late afternoon (panel C), the specific conductivity comes back to ~ 275-285μS/cm, and especially in the surface, which may have been indicative of lake water moving into the measurement site. Water column Chl a was variable, but was otherwise fairly consistent over the height of the water column. Near-bottom (0-1.5mab) Chl a patterns appeared to change over the course of the day, although the difference between 0 and 1mab was between 0 .5-0.8μg/L. In the morning (panel A) and afternoon (panel C), near-bottom Chl a appeared to increase toward the bottom, but at mid-day (panel B), near-bottom Chl a appeared to decrease toward bottom. Near-bottom dissipation ranged from approximately $10^{-8} – 10^{-7}$ m^2/s^3 in the morning and late afternoon (panels A and C), and between approximately $5x10^{-9} – 5x10^{-8}$ m^2/s^3 in mid-day, which corresponding to the time when near-bottom Chl a showed a pattern of decrease toward the bottom. Diffusivity remained around 10^{-4} m^2/s over the course of the day, and showed a less variable profile compared to dissipation.

Stations 1353 (Figure 4.3) and 1351 (Figure 4.4) showed evidence of stability in the water column, near-bottom water column structuring of dissipation and diffusivity, and Chl a structure. There were sampling gaps over a portion of the height of the water column in some of the profiles, but near-bottom conditions can still be seen. Unlike Station 456 presented above, these two stations were each sampled for an hour toward the end of the sampling day, so stratification, if it were to form, would be most likely to be observed.

(a)

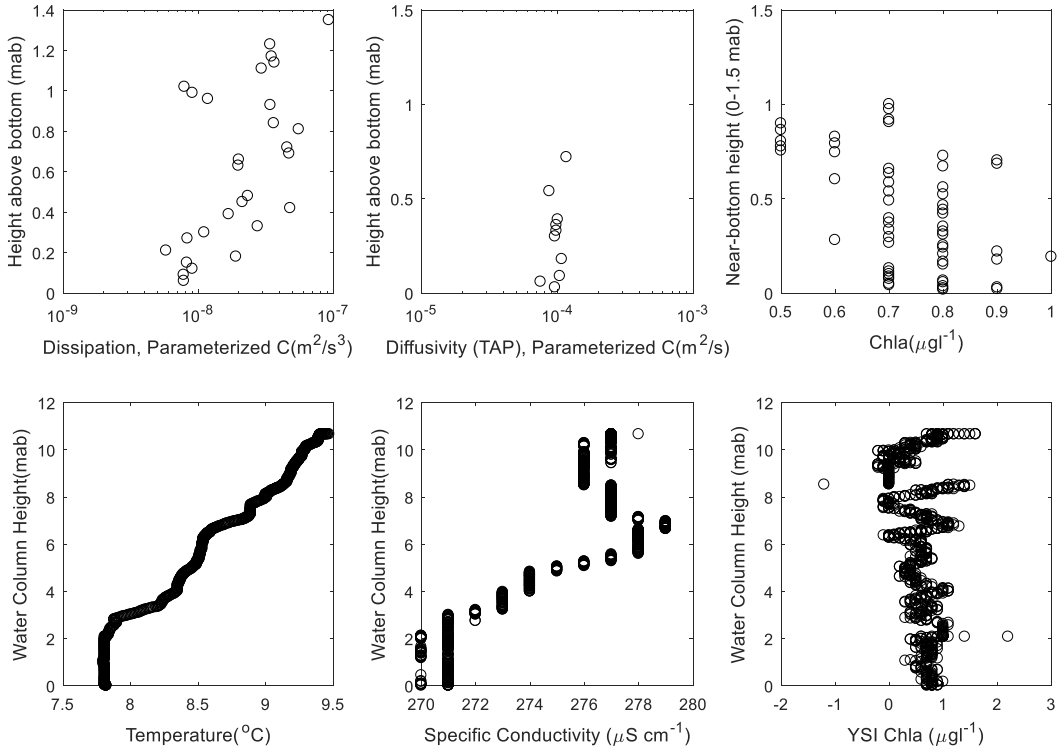
Height above bottom (mab)
Dissipation, Parameterized C(m2/s3)
Height above bottom (mab)
Diffusivity (TAP), Parameterized C(m2/s)
Near-bottom height (0-1.5 mab)
Chla(μgl-1)
Water Column Height(mab)
Temperature(°C)
Water Column Height(mab)
Specific Conductivity (μS cm-1)
Water Column Height (mab)
YSI Chla (μgl-1)

(b)

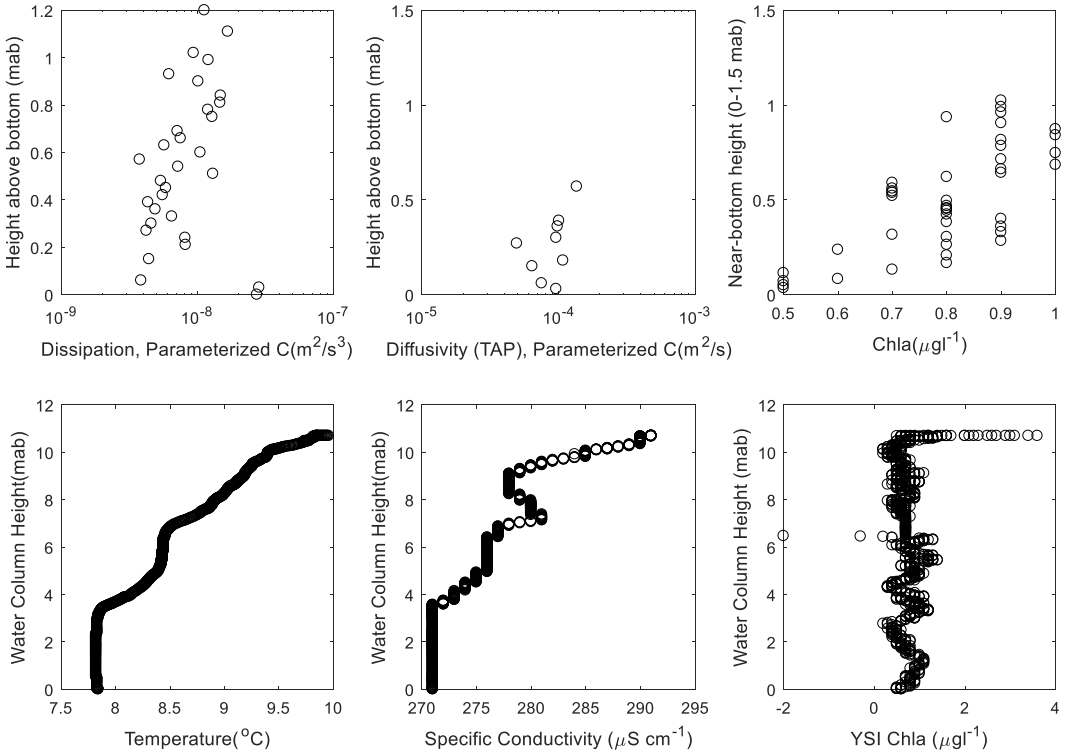
Height above bottom (mab)
Dissipation, Parameterized C(m2/s3)
Diffusivity (TAP), Parameterized C(m2/s)
Near-bottom height (0-1.5 mab)
Chla(μgl-1)
Water Column Height(mab)
Temperature(°C)
Specific Conductivity (μS cm-1)
Water Column Height (mab)
YSI Chla (μgl-1)

(c)

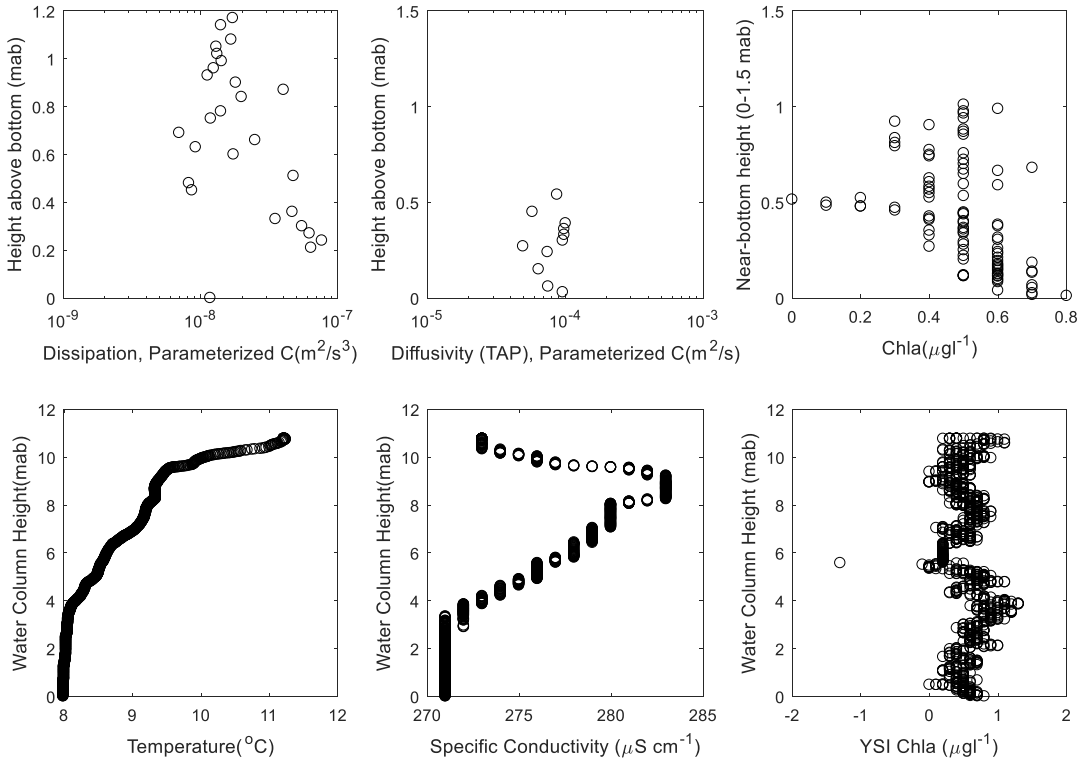

Figure 4.2. Near-bottom dissipation, diffusivity, and near-bottom chla, and water column temperature, water column specific conductivity, and water column Chl a from an intensely sampled station (Station 456, M transect, nominally 10m deep) in (a) the morning, (b) mid-day, and (c) afternoon)

(a)

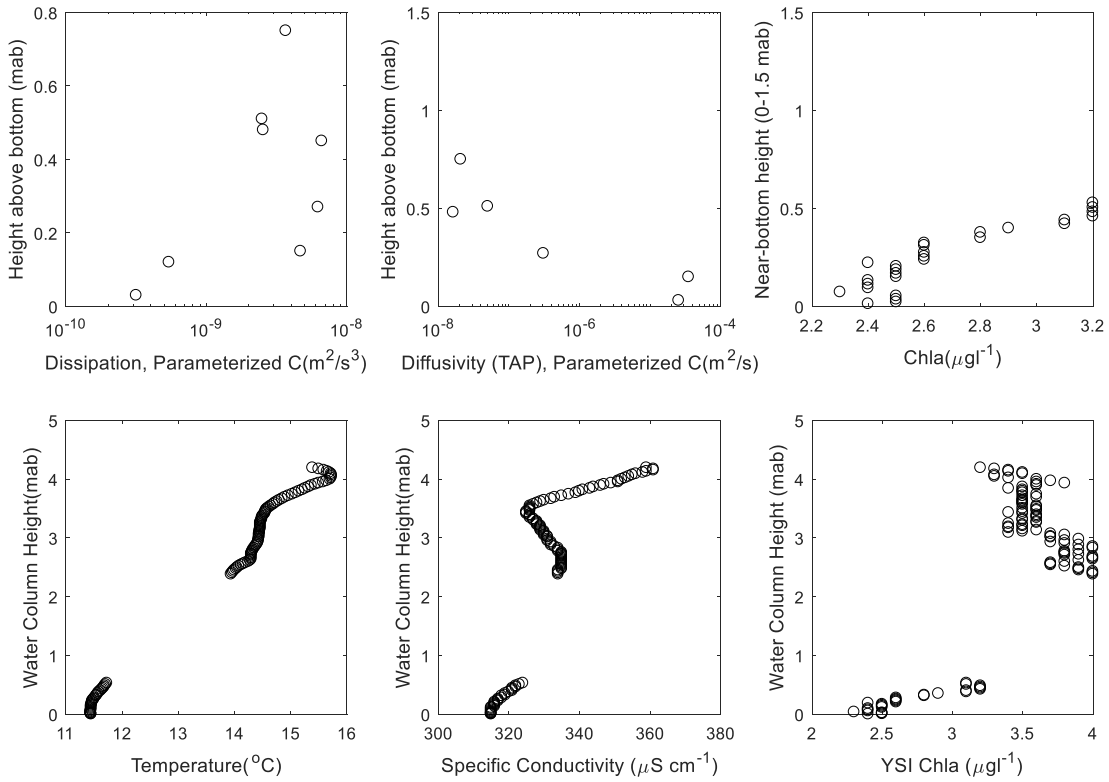
Height above bottom (mab)
Dissipation, Parameterized C(m2/s3)
Diffusivity (TAP), Parameterized C(m2/s)
Near-bottom height (0-1.5 mab)
Chla(μgl-1)
Water Column Height(mab)
Temperature(°C)
Specific Conductivity (μS cm-1)
Water Column Height (mab)
YSI Chla (μgl-1)

(b)

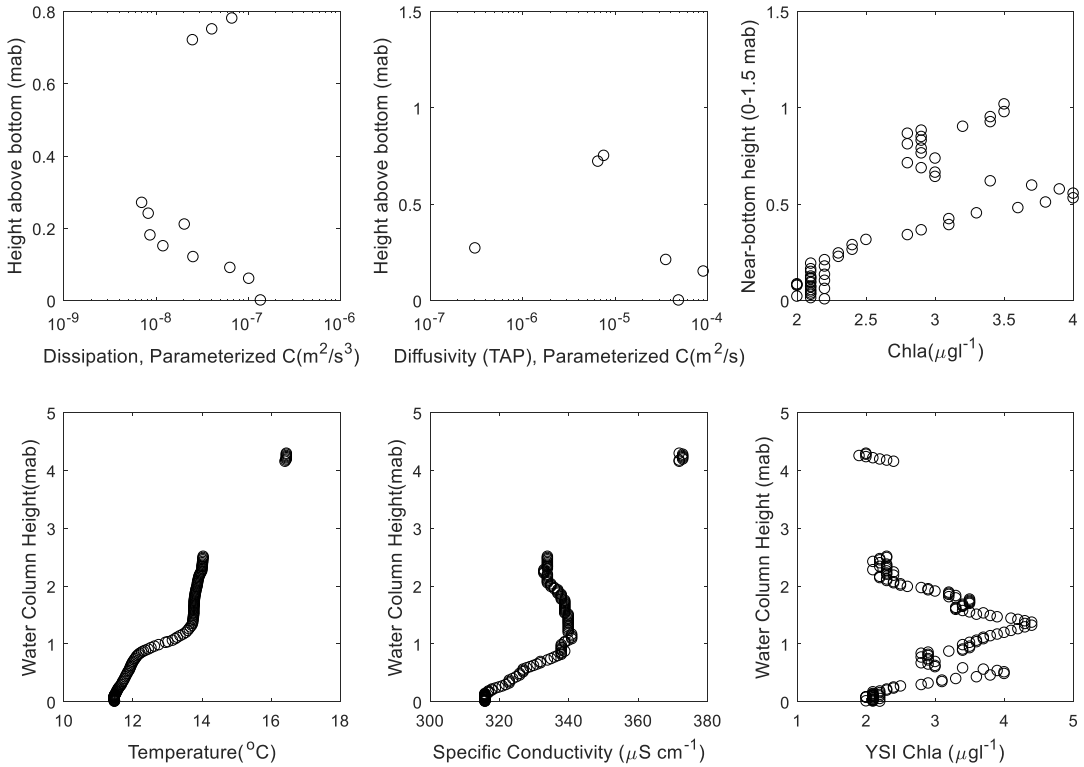

Figure 4.3. Near-bottom dissipation, diffusivity, and near-bottom chla, and water column temperature, water column specific conductivity, and water column Chl a from the (a) beginning and (b) end of a one-hour sampling at station 1353.

(a)

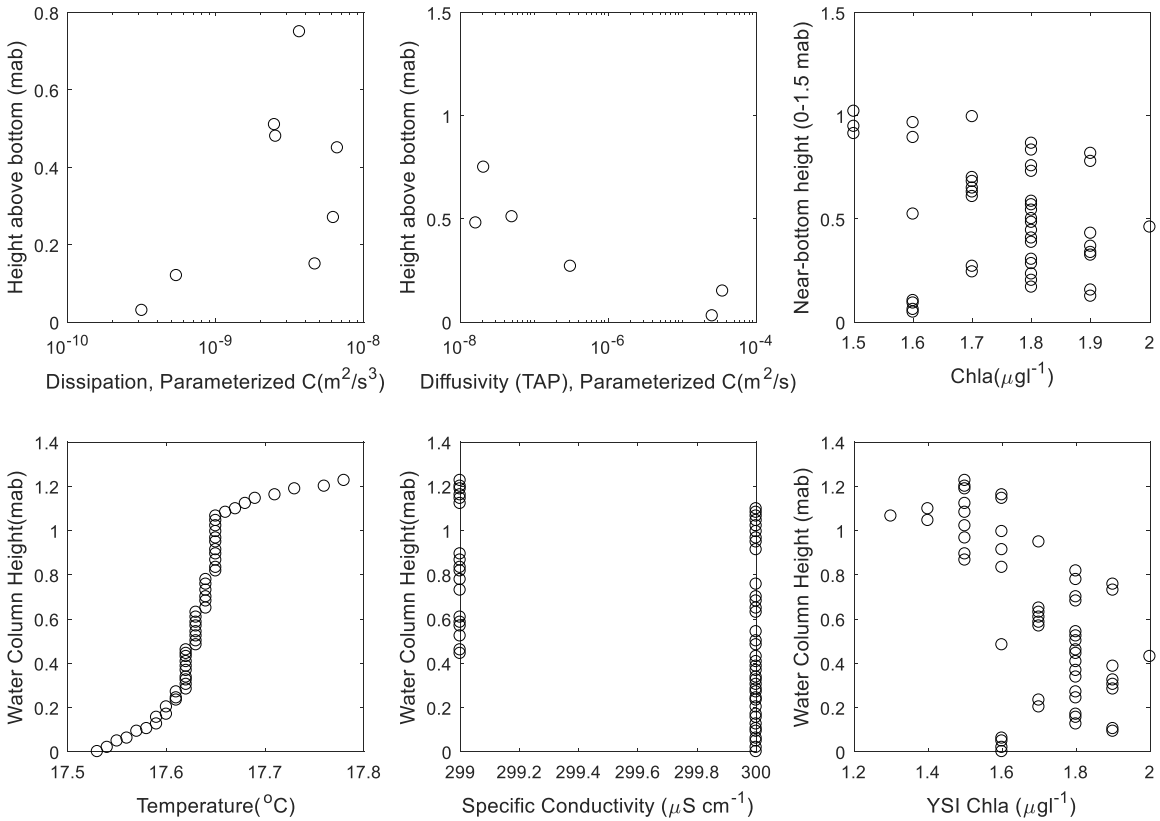
Height above bottom (mab)
Dissipation, Parameterized C(m2/s3)
Diffusivity (TAP), Parameterized C(m2/s)
Near-bottom height (0-1.5 mab)
Chla(μgl-1)
Water Column Height(mab)
Temperature(oC)
Specific Conductivity (μS cm-1)
Water Column Height (mab)
YSI Chla (μgl-1)

(b)

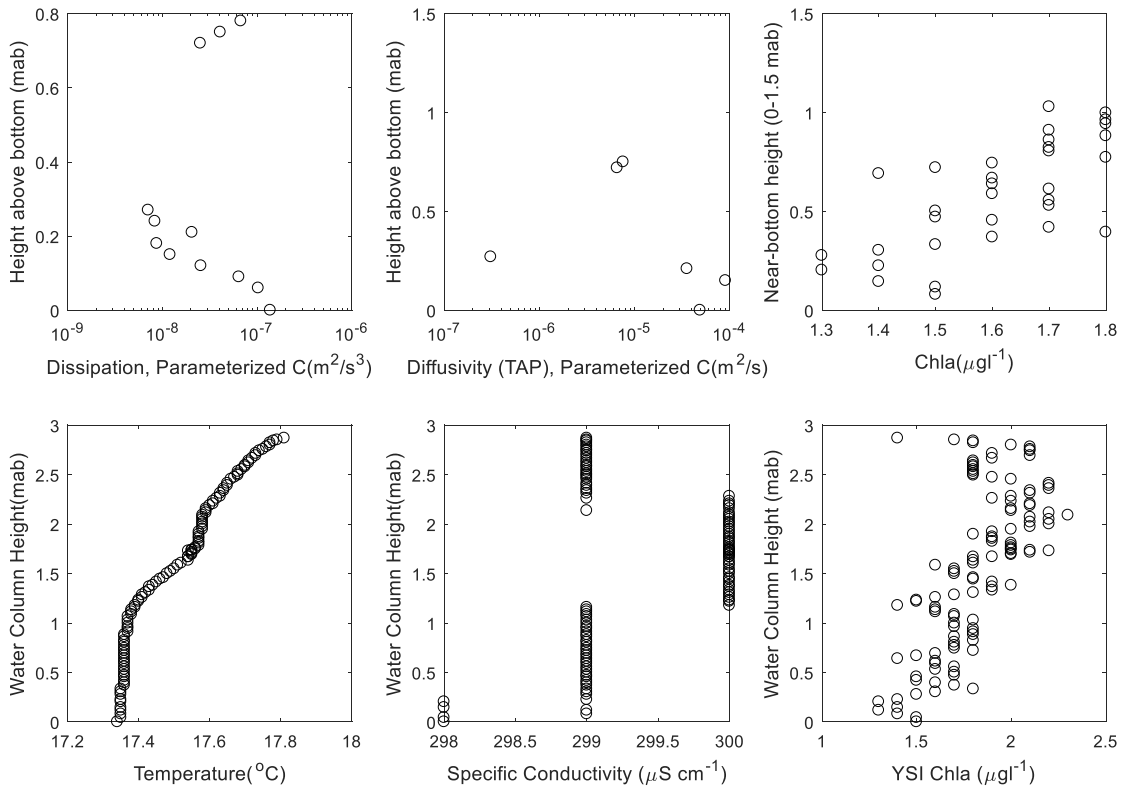

Figure 4.4. Near-bottom dissipation, diffusivity, and near-bottom chla, and water column temperature, water column specific conductivity, and water column Chl a from the (a) beginning and (b) end of a one-hour sampling at station 1351.

4.3.2 Near-bottom diffusivity and nutrient patterns and gradients

Near-bottom particulate P, SRP, and NH_4 patterns are expected to vary in relation to near-bottom diffusivity. Height-averaged near-bottom diffusivity was relatively consistent over the different stations, sampling seasons, and years, and tended to fall between 10^{-4} and 10^{-5} m^2/s, although June 2013 was particularly energetic (most diffusivities in the range of 10^{-3} m^2/s), and station 456 sampled in August 2014 was particularly quiescent. The June 2013 and August 2013 height-averaged diffusivities in the energetic range were observed even at deeper stations (e.g. 1355, 1356, 1350, 1349), where a lower diffusivity might have been expected. There was no relationship with depth on any of the sampling dates either.

Table 4.2. Deployment and height-averaged near-bottom diffusivity at different sampling sites and dates.

Station	May 2013	June 2013	August 2013	October 2013	June 2014	August 2014	October 2014	May 2015
1353	NA	2.55E-04	2.49E-04	NA	2.30E-05	3.02E-06	NA	NA
1354	NA	3.02E-04	1.12E-04	1.80E-05	7.71E-06	NA	NA	NA
1355	NA	3.82E-03	NA	7.25E-06	2.39E-05	NA	NA	NA
1356	NA	2.57E-03	1.45E-04	1.09E-05	3.33E-05	NA	NA	NA
1274	8.73E-05	2.88E-03	1.64E-04	7.78E-06	2.00E-05	1.13E-06	3.95E-05	NA
1340	7.31E-05	3.30E-04	1.62E-04	1.57E-05	2.06E-05	NA	NA	NA
456	8.73E-05	2.77E-04	1.61E-04	1.26E-06	5.34E-06	7.99E-10	5.51E-05	1.06E-04
12	NA	NA	1.06E-04	NA	NA	NA	NA	NA
1341	9.30E-05	2.77E-04	NA	NA	3.13E-05	1.42E-06	NA	NA
1342	NA	2.66E-04	NA	NA	NA	NA	NA	NA
1344	NA	1.34E-03	NA	NA	NA	NA	NA	NA
1351	NA	3.24E-03	1.05E-04	1.85E-05	2.82E-05	NA	NA	NA
1352	NA	3.62E-03	NA	1.53E-05	2.02E-05	NA	NA	NA
1350	NA	3.65E-03	1.07E-04	1.49E-05	4.74E-06	NA	NA	NA
1349	NA	1.82E-03	1.31E-04	NA	1.32E-05	NA	NA	NA

Mean near- bottom diffusivity, particulate P, SRP (Figure 4.5, Figure 4.6, Figure 4.7), and in some instances, NH_4 (Figure 4.7) showed some evidence of near-bottom gradients, but often variability in samples was so great that these gradients may not have been statistically significant. In some cases, the near-bottom PP profile appeared to decrease near-bottom, but other times exhibited a more complex profile. All the SRP and NH_4 profiles exhibited large variation from the mean (Table 4.3), but on average, there appeared to be evidence of increasing near-bottom SRP and NH_4 concentration in both replicates (456.1 and 456.2) at station 456. Contrary to expectations, stations 1355 and 1350 showed the highest SRP concentration at the top of the peepers, but mean NH_4 through the bottom water column was relatively invariant; this may have been in part due to the large variation between sample replicates. NH_4

samples were not collected for stations 1353 and 1351 (n = 2, pseudo-replicates from two sides of the same peeper), and SRP profiles did not appear to show an increase toward bottom, expect within 10-15cm of the bottom. But these points did not fall outside the 95% confidence interval, and were not significantly different from the rest of the near-bottom SRP samples.

Mean PP bottom profiles were expected to decrease toward the bottom, and some of them decreased as expected. Mean PP at 456.1 displayed a decrease toward the bottom, as did Chl a at 1351 and 1353. Unlike 456.1, which appeared to decrease all the way to the bed, PP at 1351 and 1353 appeared to decrease to a point above the bed, and then were constant from that point to the bed. Mean PP at 1355 appeared to increase toward bottom, while mean PP at 1350 and 456.2 did not appear to vary above bottom, with the exception of a few points that were a much lower concentration about 20cm above bottom (1350), or much higher just above bottom (456.2).

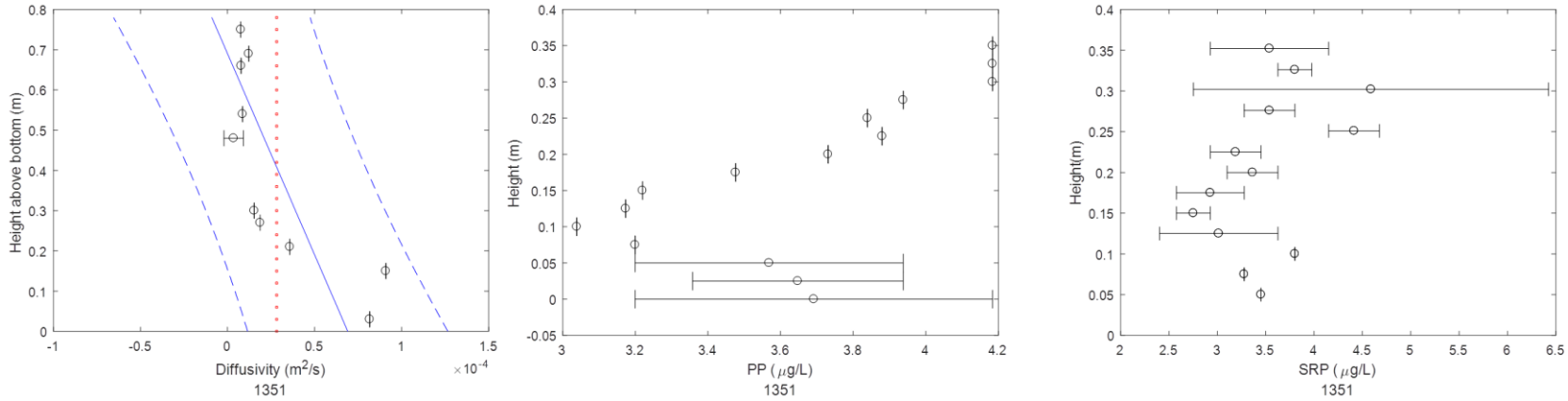

Figure 4.5. Near-bottom burst-averaged diffusivity, particulate P, SRP and (0-1mab) at station 1351. The PP profile shown is estimated from the Chl a profile for this site. Conversion units are found in Table **4.1**.

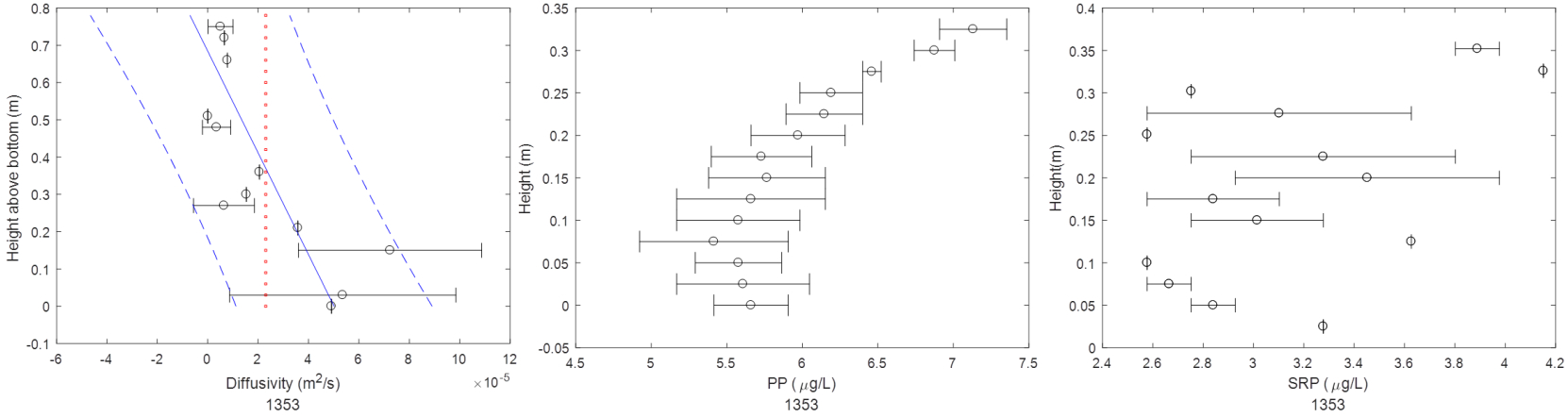

Figure 4.6. Near-bottom burst-averaged diffusivity, particulate P, SRP and (0-1mab) at station 1353. The PP profile shown is estimated from the Chl a profile for this site. Conversion units are found in Table **4.1**.

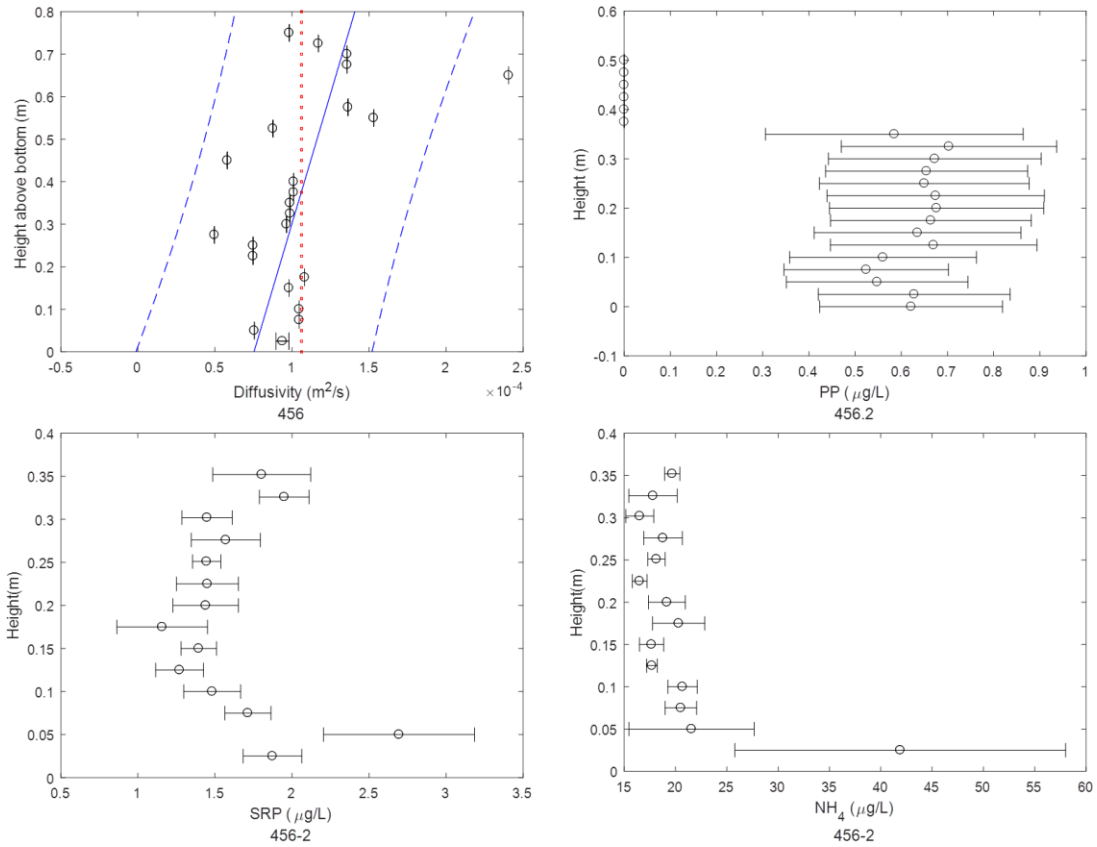

Figure 4.7. Near-bottom burst diffusivity, particulate P, SRP and NH_4 profiles (0-1mab) at stations 456. The PP profile shown is estimated from the Chl a profile for this site. Conversion units are found in Table **4.1**. Station 1350, 1355, and 456 (sampling 1) are in the appendix/supplementary.

Table 4.3. Average gradients (slopes) of SRP or NH_4 with height, standard error, and R^2, at 0.025 - 0.2mab. Significant relationships ($p \leq 0.05$ were not found).

Station				
SRP	**Sampling date**	**Gradient**	**Gradient SE**	**R^2**
456	May 2015	-3.92	-0.36	0.54
1355	May 2015	-3.02	0.90	0.06
1350	May 2015	-2.45	-0.86	0.45
456	May 2015	-5.66	-0.46	0.51
1351	June 2014	-2.87	-3.50	0.19
1353	June 2014	1.58	2.75	0.065

NH_4		**Gradient**	**Slope SE**	**R^2**
456	May 2015	-56.7	-17.7	0.45
1355	May 2015	-27.7	-9.4	0.40
1350	May 2015	-4.94	2.6	0.014
456	May 2015	-84.3	-57.1	0.42

4.3.3 Estimates of particulate P flux downward to and SRP up from the bed

4.3.3.1 Estimates of PP flux into the bed

Near-bottom PP flux is a measure of how much food, in units of P, mussels might be filtering (Table 4.4), and was estimated three ways (calculation details in methods), and compared, at stations where a significant bottom Chl a gradient was observed in Ch3. In these samples, diffusive flux estimates were more similar to the PP flux estimates using determined product of Pex (in Vanderploeg *et al.*) and mussel biomass . PP flux estimates using the equations to estimate PP flux in Dayton *et al.* tended to be about an order of magnitude greater than either PP flux estimates from Vanderploeg or from diffusive flux estimates. Far West and Mouth transects were most represented in these samples, but both shallow and deep stations on these transects showed evidence of near-bottom PP depletion. There was also no seasonal pattern when a significant downward PP gradient was observed, as depletion was

observed both in the late summer and the early summer. The August 2013 depletion were a little surprising to observe, as the near-bottom depth averaged diffusivity was slightly greater than at other times when depletion was observed, but was not as great as June 2013.

Table 4.4. Particulate flux downward taken from individual profiles estimated at stations and sampling dates where a significant ($p \leq 0.05$) near-bottom Chl a gradient was detected. Significant near-bottom Chl a gradients (used to estimate PP gradients in this chapter) were determined in Ch3.

Station	Sampling date	Station depth (Transect)	Chl a (µg/L)	PP (µg/L	Mussel biomass (g/m^2)	Vanderploeg PP flux ($g/m^2/d$)	Dayton PP flux ($g/m^2/d$)	Diffusive PP flux ($g/m^2/d$)
1353	Aug-13	3m (FW)	2.5	9.0	32.2	0.0430	0.1123	0.0146
1353	Aug-13	3m (FW)	1.7	6.1	32.2	0.0310	0.0764	0.0588
1274	Oct-13	3m (M)	3.6	12.0	64.0	0.1102	0.2999	0.0001
1274	Oct-13	3m (M)	2.8	9.4	64.0	0.0880	0.2333	0.0046
1355	Jun-14	10m (FW)	0.9	2.2	36.8	0.0149	0.0317	0.0299
1355	Jun-14	10m (FW)	1.3	3.2	36.8	0.0196	0.0458	0.0087
1356	Oct-13	18m (FW)	1.8	6.0	42.7	0.0402	0.1000	0.0024
1356	Jun-14	18m (FW)	2.7	6.6	102.0	0.0999	0.2638	0.0109
1356	Jun-14	18m (FW)	3.1	7.6	102.0	0.1130	0.3029	0.0017
1274	Jun-14	3m (M)	1.6	3.9	26.6	0.0167	0.0408	0.0041
1274	Jun-14	3m (M)	1.5	3.7	26.6	0.0159	0.0382	0.0043
1353	Jun-14	3m (FW)	2.5	6.2	14.0	0.0128	0.0335	0.0192
1353	Jun-14	3m (FW)	2.1	5.2	14.0	0.0110	0.0281	0.0394
456	May -15 (rep. 2)	10 (M)	0.5	0.7	197.2	0.0332	0.0572	0.0127

There were many more near-bottom Chl a profiles, and estimates of PP flux downward and SRP upward were estimated to get a sense of an upper bound in terms of what mussels can consume and release, even if no near-bottom depletion gradients were evident. These conditions may differ in the early and late parts of the growing season that may be relevant to nuisance *Cladophora* growth. The estimates

of average flux of PP downward and SRP upward, using the relationships in Vanderploeg and the estimates in Dayton showed some differences between the early (May and June data from 2013-2015) (Figure 4.8a, Table C3) and late (August and October data from 2013-2014) (Figure 4.8b, Table C4) season. Estimates of PP and SRP flux using the calculation methods in Dayton were larger than the estimates of flux calculate from the PP:Pex relationship in Vanderploeg, as evidenced by slopes steeper than the 1:1 line. The relationship between estimates of PP flux and SRP flux using Dayton's estimates compared to Vanderploeg's estimates varied between the early sampling season and late season. In the early part of the season, the Dayton PP flux estimates were approximately 2 times (a slope of ~2), and the SRP flux estimates were about 6.5 times that of Vanderploeg estimates. In the late season, the Dayton PP flux estimates were ~1.6 times greater and the SRP flux ~11 times greater than the Vanderploeg estimates.

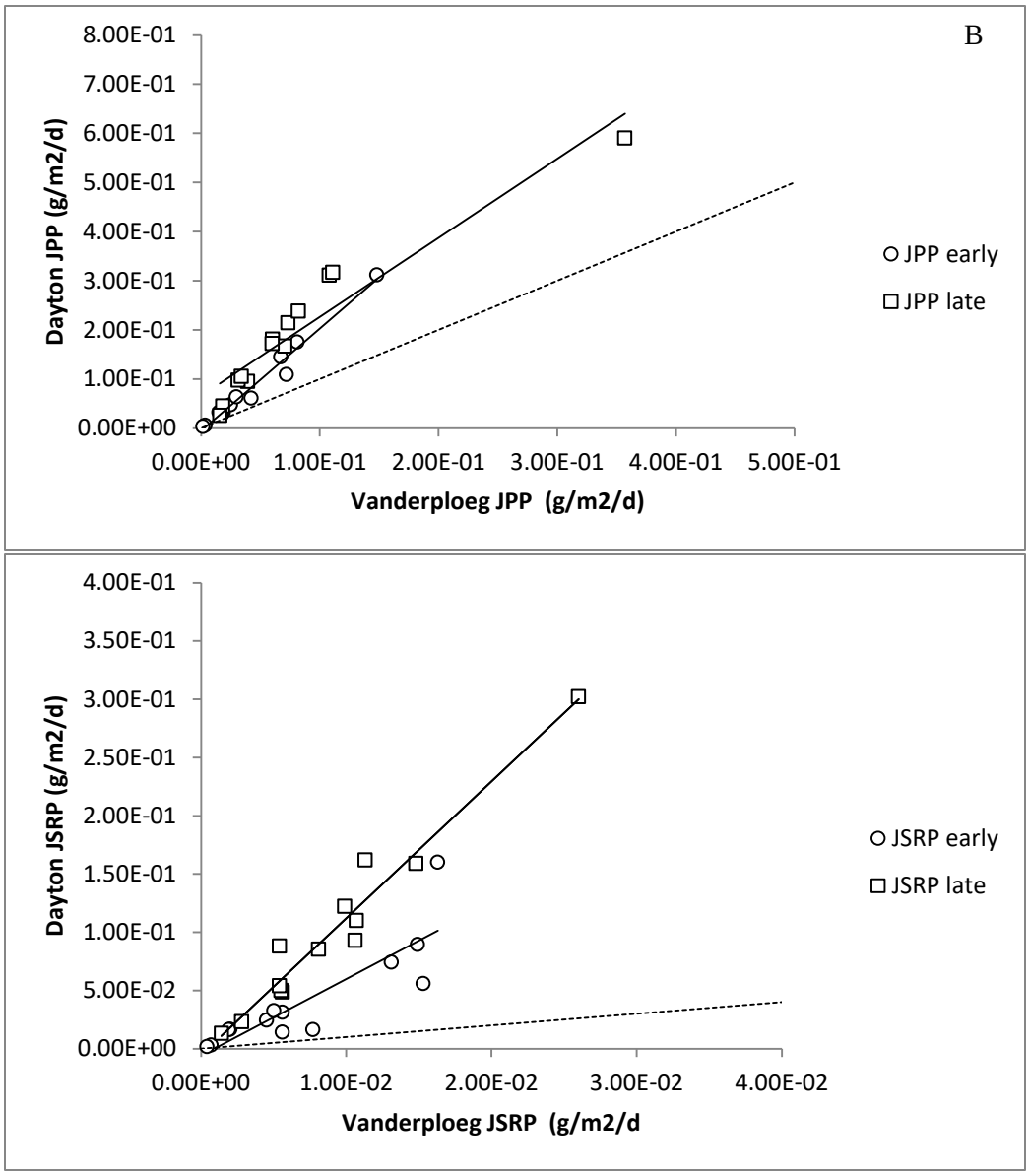

Figure 4.8. Comparison of average Vanderploeg and Dayton (a) PP and (b) SRP excretion fluxes in the early part (black circles) and in the late part of the sampling season (grey squares). The dashed line indicates the 1:1 line.

Estimated SRP flux from both methods also increased with increasing mussel biomass for both the Vanderploeg and Dayton estimates (Figure 4.9). Estimates from Vanderploeg tended to be consistent

over both the early and later parts of the sampling season. Conversely, Dayton estimates were greater than the Vanderploeg estimates. Late season estimates were also greater than the early season estimates.

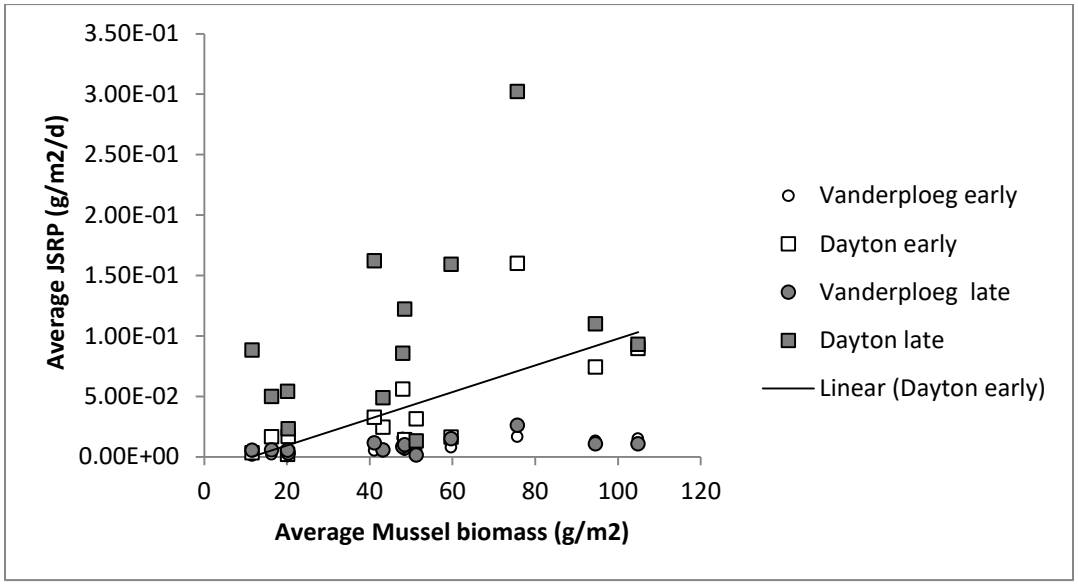

Figure 4.9. Comparison of average mussel biomass against average Vanderploeg (circles) and Dayton (squares) P excretion flux estimates in the early (black symbols) and late (grey symbols) parts of the sampling season.

4.3.3.2 Estimates of diffusive SRP flux out of the bed

Estimates of average diffusive SRP flux was greater at 10m sites (456, 1350, 1355) than at 3m sites (Table 4.5) from peeper-measured SRP gradients. There was large variability in near-bottom gradients of SRP (Figure 4.5, Figure 4.6, Figure 4.7), so estimates lack precision. However, these are some of the first diffusive flux estimates for SRP in this portion of the nearshore. In line with Figure 4.5 and Figure 4.6, there was a very small SRP gradient. This may be a result of a relatively small excretion rate, or that the source of SRP at stations 1351 and 1353 was smaller than a potential sink. There was a spatial mismatch between *Cladophora* and mussel biomass as well. At 3m stations, there was a fairly large *Cladophora* biomass relative to mussel biomass, but at 10m stations, there was quite a bit of mussel

biomass, but almost no *Cladophora* biomass. In fact, it appeared that there was no real flux of SRP per-day at 1351 (standard error was greater than the mean estimate), and a very small areal flux of P per-day at 1353. Per-mussel P production was relatively similar between the three 10m stations, although the second sampling of 456 suggested a greater gradient and flux of SRP than in the first sampling. Comparing between diffusive SRP flux and estimated excretion flux from the Vanderploeg and Dayton equations showed that mussel produced P flux estimates within one order of magnitude of each other. The estimates using Dayton were almost the same as the diffusive flux estimates at the 10m stations, but overestimated P flux at the 3m stations. The Vanderploeg estimates tended to estimate a P flux ~ one order of magnitude less than the diffusive flux estimates, but were closer to diffusive flux estimates at the 3m stations. Estimates of average diffusive NH_4 flux was greater than SRP flux at all stations where both were measured. NH_4 flux was greatest at station 456, followed by 1350, and 1355, and echoes the pattern of greater SRP flux at 456, which may be in part because of its location close to the mouth of the Grand River.

Table 4.5. Estimated mean areal SRP-flux and NH_4-flux for peeper stations and estimated per-mussel P production. Standard errors in brackets. Stations 456.1, 1350, and 1355 (denoted by *) did not have ADCP data, so flux was estimated using the depth and burst-averaged diffusivity for 456.2 (Kz = 1.06×10^{-4} m^2/s).

Station	Daily P flux ($gP/m^2/d$)	Daily N flux ($gN/m^2/d$)	Mussel tissue biomass ($gSFDW/m^2$)	Cladopohra biomass (gDW/m2)	Daily P flux per gDW (gP/gSFDW/d)	Daily N flux per gDW (gN/gSFDW/d)	Daily P flux per gDW (Vanderploeg estimates) (gP/gSFDW/d)	Daily P flux per gDW (Dayton estimates) (gP/gSFDW/d)	Presence (+) or absence (-) of stratification
456.1 *	0.03591	0.5196	48.02	0	1.72	24.95	0.116	1.09	+
	(0.00715)	(0.1299)	(5.53)	(0)	(0.0395)	(0.718)	(0.0109)	(0.0741)	
1350 *	0.02765	0.2993	48.48	0.096	1.34	14.51	0.451	2.32	+
	(0.01716)	(0.1273)	(4.36)	(0.071)	(0.0748)	(0.555)	(0.0166)	(0.0924)	
1355 *	0.01888	0.1232	59.72	1.67	1.13	7.36	0.308	2.32	+
	(0.00774)	(0.2521)	(9.56)	(0.79)	(0.0740)	(2.41)	(0.0108)	(0.1071)	
456.2	0.05183	0.7718	48.02	0	2.49	37.06	0.116	1.09	+
	(0.02461)	(0.6445)	(5.53)	(0)	(0.136)	(3.56)	(0.0109)	(0.0741)	
1351	-0.0097		11.61	50.10	-0.113		0.0287	0.238	+
	(0.01319)		(2.04)	(24.53)	(0.0269)		(0.0012)	(0.0105)	
1353	0.00042		20.4	37.89	0.00857		0.112	1.02	+
	(0.00036)		(4.22)	(11.84)	(0.00152)		(0.0021)	(0.0443)	

4.3.4 Estimated *Cladophora* uptake rates and comparison with estimated mussel excretion

Total estimated mussel P production was greater than estimated *Cladophora* uptake at almost all stations and by both excretion flux estimates (Figure 4.10, Table 4.6). In sum of all the average P excretion estimates over the whole nearshore sampling stations, Vanderploeg estimates were 0.1 $g/m^2/d$ and Dayton estimates 0.87 $g/m^2/d$. The sum of all the average P uptake by *Cladophora*, conversely, was only 0.02 $g/m^2/d$. By both estimates, excretion was greater than uptake over all the stations, resulting in ~ 0.08 – 0.85 $g/m^2/d$ excess P. At individual stations, however, there might be greater uptake than excretion.

Three 3m stations (1351, 1341, and 1353) all experienced greater P uptake than P production where SRP flux was estimated using Vanderploeg's PP:Pex relationship, but only one station (1341) experienced greater P uptake than P production using Dayton's estimates of SRP flux; these stations also correspondingly had the highest *Cladophora* biomass of all the stations. The greatest mussel biomass and estimated excretion was at 5m stations, but the greatest mean *Cladophora* biomass and uptake was at 3m stations (Ch3, Figure 3.1). Mussel excretion estimates were lowest at the 3m stations, and tended to peak at the 5m and 18m stations. Caution does need to be taken in interpreting these results, as these estimates assumed that mussel biomass, and therefore excretion, is the same over the entire sampling season, which is an oversimplification of their feeding and excretion activities.

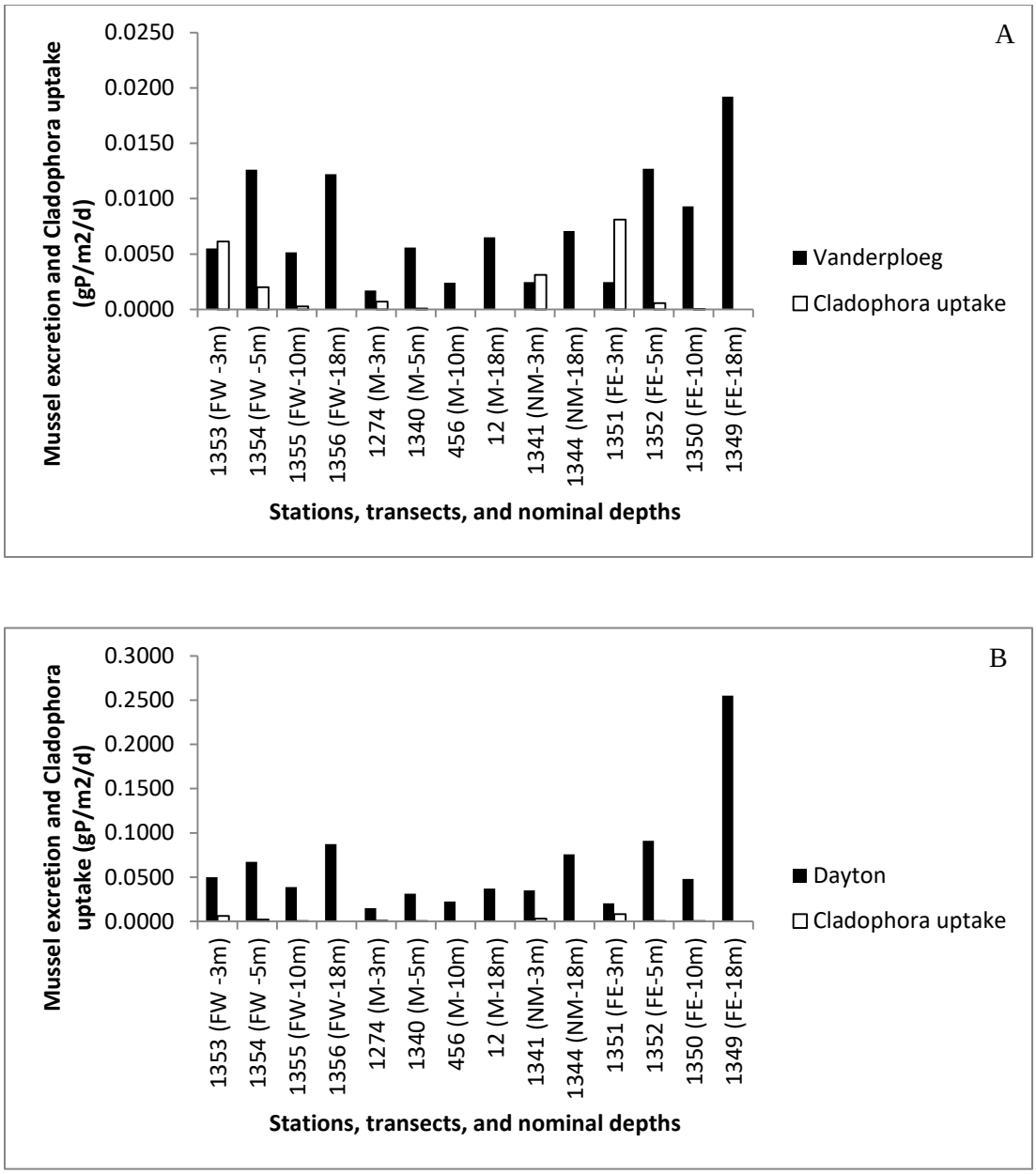

Figure 4.10. Season-averaged estimated mussel excretion (black bars) or Cladophora uptake at sampled stations between 2013-2015, comparing estimates of P excretion from (a) Vanderploeg and (b) Dayton.

Table 4.6. Estimated mean areal SRP flux from mussel beds and areal *Cladophora* uptake rate. Data presented is the average from all available samples. *Cladophora* estimated uptake rate was 1.62×10^{-2} %P/d (coefficients: $\tau = 0.88$, $Q = 0.1$, and [SRP]=2μg/L). The daily P production was greater than daily P uptake at all stations except 1351, 1341, and 1353.

		Cladophora biomass (g/m^2)		Mussel Biomass (g/m^2)		Mussel excretion flux ($gP/m^2/d$)				*Cladophora* uptake flux ($gP/m^2/d$)	
						Vanderploeg		Dayton			
Station (Transect)	Depth (m)	Average	SE	Average	SE	Average	SE	Average	SE	Average	SE
1353 (FW)	3	37.89	11.84	20.37	4.22	5.49×10^{-3}	5.06×10^{-4}	4.99×10^{-2}	1.05×10^{-2}	6.13×10^{-3}	1.91×10^{-3}
1354 (FW)	5	12.29	4.13	104.87	8.34	1.26×10^{-2}	2.04×10^{-3}	6.72×10^{-2}	1.17×10^{-2}	1.99×10^{-3}	6.67×10^{-4}
1355 (FW)	10	1.67	0.79	59.72	9.56	5.16×10^{-3}	1.13×10^{-3}	3.89×10^{-2}	1.12×10^{-2}	2.70×10^{-4}	1.28×10^{-4}
1356 (FW)	18	0	0	75.66	22.49	1.22×10^{-2}	1.73×10^{-3}	8.75×10^{-2}	1.97×10^{-2}	0	0
1274 (M)	3	4.34	2.17	43.25	7.77	1.71×10^{-3}	3.65×10^{-4}	1.50×10^{-2}	2.93×10^{-3}	7.02×10^{-4}	3.50×10^{-4}
1340 (M)	5	0.44	0.29	94.58	10.72	5.59×10^{-3}	NA	3.12×10^{-2}	NA	7.06×10^{-5}	4.61×10^{-5}
456 (M)	10	0	0	48.02	5.53	2.42×10^{-3}	1.97×10^{-3}	2.26×10^{-2}	1.34×10^{-2}	0	0
12 (M)	18	0	0	22.77	5.11	6.51×10^{-3}	2.13×10^{-3}	3.72×10^{-2}	1.56×10^{-2}	0	0
1341 (NM)	3	19.24	5.92	16.33	3.08	2.45×10^{-3}	2.21×10^{-3}	3.50×10^{-2}	2.64×10^{-2}	3.11×10^{-3}	9.57×10^{-4}
1344 (NM)	18	0	0	51.28	6.15	7.08×10^{-3}	2.34×10^{-3}	7.58×10^{-2}	2.74×10^{-2}	0	0
1351 (FE)	3	50.10	24.53	11.61	2.04	2.47×10^{-3}	5.69×10^{-4}	2.05×10^{-2}	5.13×10^{-3}	8.10×10^{-3}	3.97×10^{-3}
1352 (FE)	5	3.51	1.06	41.10	2.68	1.27×10^{-2}	1.51×10^{-3}	9.11×10^{-2}	1.43×10^{-2}	5.67×10^{-4}	1.71×10^{-4}
1350 (FE)	10	0.096	0.071	48.48	4.36	9.30×10^{-3}	3.80×10^{-3}	4.79×10^{-2}	2.12×10^{-2}	1.55×10^{-5}	1.15×10^{-5}
1349 (FE)	18	0	0	20.21	9.43	1.92E-02	6.35×10^{-3}	2.55×10^{-1}	1.01×10^{-1}	0	0

4.4 Discussion

Because of their relevance to nuisance *Cladophora* growth, near-bottom nutrient gradients and their relation to physical and biological conditions in the nearshore are of great interest. Physical forcing may be the difference between formation and abolishment of near-bottom soluble nutrient gradients; this may be related to both water column variability and magnitude of near-bottom dissipation and diffusivity. How much of a source of bioavailable phosphorus dreissenid mussels are estimated to be and how much of a sink *Cladophora* may be, may help elucidate whether mussels alone could support nuisance *Cladophora* biomass in the East Basin nearshore of Lake Erie, or whether other sources of P may also be important.

4.4.1 Physical impacts on near-bottom particulate P and dissolved P in the nearshore

Changes in water column structure and transmission of energy through the water column and near-bottom over the course of the day may influence formation or abolishment of near-bottom SRP gradients. Stratification in the nearshore tends to be weaker and more transient than offshore stratification but may still be significant in shaping water column specific conductivity, temperature and density, and Chl a and nutrient distributions when it does occur (Edwards *et al.*, 2005; Loewen *et al.*, 2007; Boegman *et al.*, 2008b; Dayton *et al.*, 2014). Stratification in the nearshore forms in response to solar heating of surface water resulting in density differences between heated and unheated water. The transient thermocline deepens over the course of the day, ultimately breaking down again with cessation of solar heat input or strong forcing that overcomes buoyancy. Chl a profiles, which were used to estimate PP profiles, changed over the course of the day as stratification deepened, suggesting that there were physical processes shaping the Chl a distribution in the water column, and which could have had implications for mussel feeding (as discussed in Ch3) and excretion.

An important potential effect of stratification may be a separation of water masses resulting in different nutrient concentrations and gradients near-bottom relative to the surface. Incoming river water is often warmer than receiving lake waters, and the Grand River in particular has a higher specific conductivity and nutrients than even the lake near the mouth of the river (PWMN data; (Chomicki *et al.*, 2016). There is evidence that the river is at least partially responsible for inputting SRP into the nearshore (Chomicki *et al.*, 2016), and that it appeared to co-vary with specific conductivity (Ch2). Water column specific conductivity near-bottom tended to be approximately the same as offshore lake specific conduticity, suggesting that the river did not have a large impact on the benthos and on SRP found there. Temperature profiles did not support evidence of offshore hypolimnetic upwelling, suggesting that elevated SRP did not come from nutrient-rich hypolimnetic water, but may have come from the local benthos. Work conducted in the same area and time also did not find evidence of upwelling (Depew *et al.*, 2018). Chl a profiles did not show strong gradients of depletion near-bottom, but that may have been a reflection of bottom mixing, or a disconnect between mussel feeding and excretion. Previous studies have noted that SRP concentrations within 0.5m of the bottom in bulk-water samples that were elevated relative to measurements taken near the surface (Martin, 2010). Other studies have observed and modelled near-bottom SRP gradients (Dayton *et al.*, 2014). However, using it should be noted that peepers were originally intended for sediment sampling (Hesslein 1976), where external forcing was less of a factor in capturing gradients, and that a peeper will not capture dynamic SRP gradients. Instead, it is likely to capture an average gradient over the course of the whole day.

There might be a diffusivity threshold between 10^{-4} and 10^{-5} m^2/s (Edwards *et al.*, 2005) that marks the difference between quiescence and turbulence in the benthic boundary layer that dictates whether near-bottom gradients may form or not. Diffusivity ranged between 10^{-3} and 10^{-10} m^2/s in the study area, and at stations where a detectable near-bottom Chl a depletion gradient was observed, the diffusivity tended to fall between 10^{-6} and $10^{-4} m^2/s$. Sampling was conducted under quiescent surface conditions (e.g. surface winds <10 knots), so any bottom water motion was largely a result of internal forcing. If the

previous days were also relatively quiescent or there was strong stability in the water column, both dissipation and diffusivity might be smaller than expected. Early in the season, water column temperature tends to be relatively uniform, but later in the growing season, diel stratification may impact water stability, and inhibit mixing. Diel stratification might impact deeper stations more than shallower stations, since the transient thermocline may deepen all the way to the bottom at shallow stations (Wüest & Lorke, 2003), and not actually serve to limit water column exchange. Near-bottom stability is expected to enhance formation of phosphorus gradients, while near-bottom turbulence is expected to abolish gradients (Dayton *et al.*, 2014). Modelling studies using peeper phosphorus data and changing forcing suggested that greater forcing resulted in a smaller gradient located closer to the bottom, but with a slightly elevated near-bottom SRP concentration that extended to a greater height above bottom (Dayton *et al.*, 2014). Our sampling was conducted under conditions where low forcing is expected, and capture of near-bottom phosphorus gradients would be more likely to occur.

Estimates of diffusive flux fell within the range of other excretion flux estimates and other published data by Ozersky *et al.* (2009). This suggests that peeper sampling and measured water velocity to estimate diffusivity may be a useful tool in directly estimating near-bottom SRP gradients and diffusive flux. This is one of the first studies to directly measure both near-bottom SRP concentration and near-bottom water velocity, and paves the way for further studies of the same kind in the nearshore of Lake Erie and other lakes. The surprising pattern of negative near-bottom SRP gradients at 3m might be a reflection of both uptake demand and enhanced mixing, both from near-bottom turbulence and surface waves. *Cladophora* has high metabolic demand for SRP early in the growing season, when it is growing most rapidly, which case in June 2014, when the 3m stations were sampled. June is an interesting time to sample, because depending on spring conditions, *Cladophora* may be getting relatively large. In these cases, *Cladophora* at this stage of growth may additionally act to smother mussels, damping near-bottom mixing directly over the mussels, thereby limiting how much the mussels can feed and excrete (Higgins *et al.*, 2008b; Howell, 2017). It is not clear from this work that *Cladophora* biomass in June is great enough

to inhibit mussel feeding but not so great as to promote self-shading and limit nutrient and gas exchange itself, resulting in senescence at the holdfast (sensu Higgins *et al*. 2008).

There was also evidence of diel stratification in the 10m station on the date of sampling, suggesting that there may have been some damping in water column exchange, which may have inhibited feeding activity through the boundary layer, and subsequently excretion. Mussels located at 10m may experience slightly more environmental stress than those at 3m, may retain more nutrients to cope with slightly less-ideal environmental conditions in terms of temperature and food limitation due to different water masses (e.g. Malkin *et al.*, 2012), and may subsequently excrete less P per mussel. However, in samples, there were more mussels on average at the 10m station than there were at 3m station, which may have also skewed the per-mussel excretion rate lower. Mussels located at deeper stations are less likely to be sloughed off by ice in the winter and other physical disturbances compared to mussels at shallower stations, and this may explain the differences in mussel biomass at the 3m and 10m sites.

Peepers indiscriminately capture SRP near-bottom, and the source of this SRP could be from both mussels and anything else contributing to internal loading, including decomposition processes and other benthic organisms' excretia. Dreissenid mussels have been associated with an increase in worms and Oligochaete and Turbillarid worms, and some chironomids (Higgins & Vander Zanden, 2010; Burlakova *et al.*, 2018). These benthic animals may also be a source of benthic SRP that cannot be separated from dreissenid SRP using peeper sampling. Settled matter (phytoplankton and other seston) may also accumulate between mussel shells. When these flocs break down from interacting with near-bottom currents (Cyr *et al.*, 2009), they might be considered a previously unrealized source of soluble P to the nearshore, and also cannot be distinguished from mussel SRP using peeper sampling. Biofilms that occur on the hard surfaces have been estimated to contribute approximately 0.45μgP/h in *in situ* enclosures (Ozersky *et al.*, 2009). Dreissenid mussels account for the vast majority (≥90%) of zoobenthic abundance and biomass in the East Basin (Burlakova *et al.*, 2018), that it is likely that much of the SRP measured near-bottom are from them. Detectable gradients of ammonium may point to mussel effects on near-

bottom nutrients in the near-bottom environment, even in the absence of a coincident SRP gradient. Detection of nutrient gradients near-bottom may also relate to the relative sources (dreissenid mussels) and sinks (*Cladophora*) present. Mussel tissue N:P reflects its food's N:P ratio (Naddafi, Eklöv & Pettersson, 2009; Vanderploeg *et al.*, 2017), and ranged from ~11:1 under high food quality (enriched) conditions to ~40:1 under low food quality conditions in laboratory experiments (Vanderploeg *et al.*, 2017). An N:P >32 to indicate *Cladophora* P-limitation at nearshore sites in Lake Ontario (Kahlert, 1998; Malkin, 2007), so N:P≤ 32 might be a reasonable estimate of *Cladophora* N:P ratio in the nearshore of the East Basin. Only the 10m stations were sampled for a NH_4 gradient concurrently with SRP, and at this station, and most of the replicates showed a near-bottom increase in this nutrient. This may point to another way in which to probe for SRP release from the bed, by using a proxy that is less in-demand than SRP.

The interaction of near-bottom turbulence with mussel uptake and excretion may have obscured some of the fine-scale gradients of N and P, which were found only rarely in the current work. While convincing gradients of SRP and NH_4 elevation, and Chl a depletion, were not observed, near-bottom bulk water samples from 1m above the bottom, and within ~40cm of the bottom were elevated relative to 1m below surface samples. The diffusivity at these stations tended to be greater than $1x10^{-4}$ - $1x10^{-5}$ m^2/s, which has been proposed as the threshold between quiescence and turbulence near-bottom (Edwards *et al.*, 2005; Boegman *et al.*, 2008b). Simulations of a benthic gradient by Dayton *et al.* (2014) demonstrated that low diffusivities (e.g. $2.5x10^{-4}cm^2/s$) were associated with a strong near-bottom concentration gradient that was closer to the bottom, and at higher diffusivities ($7.5x10^{-3}cm^2/s$) with a weaker near-bottom concentration gradient that extended higher into the water column. This is not surprising, as molecular diffusion is very slow, so in the absence of turbulence, most of concentration gradient would stay near the source. Mussel jets themselves may introduce localized turbulence that extends centimeters above their exhalent siphons (O'Riordan *et al.*, 1995; Nishizaki & Ackerman, 2017) that could disrupt a continuous near-bottom gradient of increasing nutrients. Stratification in the water

column and within the benthic boundary layer may form distinct regions of the water column that do not mix and have nutrient and Chl a concentrations dissimilar to each other. The combination of discrete water masses and above-threshold near-bottom mixing may have resulted in the observed pattern of elevated NH_4 and SRP near-bottom relative to below-surface. Martin (2010) noted a similar pattern in the nearshore of Lake Ontario.

Different time scales used to detect putative presence of nutrient gradients (integrations over the whole day) and Chl a gradients (instantaneous profiles), may have also influenced the lack of detectable gradients near-bottom and the non-concordance between increasing nutrient and decreasing Chl a gradients near-bottom. Peepers work on the principle of concentration equilibration as the result of molecular diffusion between the inside and outside of individual sampling cells, but diffusion is slow and only works over very small distances. Hesslein samplers were originally developed to sample gradients in sediments (Hesslein, 1973), which experience far less turbulent mixing than the water environment above it. Peepers require a long equilibration time, approximately 6-8h estimated by Dayton *et al.* (2014); near-bottom gradients in the nearshore of Lake Erie may not be fully captured, especially as Lake Erie in general tends to be very dynamic (*sensu* Bolsegna & Herdendorf, 1993). Care was taken to deploy peepers under calm conditions to maximize the likelihood of capturing near-bottom gradients. However, currents in the benthic boundary layer are derived from surface forcing and internal waves, and may have a significant time delay between the initial forcing at the surface or thermocline, and the effects near-bottom (Wüest & Lorke, 2003; Lorke & MacIntyre, 2009). This is not to say that the data is not useful, but does serve as a reminder to interpret data with caution. There is a further temporal disconnect between peeper sampling for near-bottom nutrient gradients and Chl a gradients from sonde profiles. Where peepers provided an integrated sample of near-bottom nutrient conditions, profiles provided an instantaneous "snapshot" of the water column that could change subject to internal forcing and mussel feeding behaviour.

Different methodologies and assumptions in estimating mussel SRP flux may at least partially explain why estimates made here were loosely comparable with other estimates. The passive sampling method used here, and in Dayton *et al.* (2014),suggested that there could be a relatively large gradient of SRP near-bottom and should be detectable. However, because P is a limiting nutrient in freshwater systems (Schindler, 1977), and particularly to *Cladophora*, this assumption may not hold. Part of the rationale for sampling in May was to limit the potential effect of a strong P sink (i.e. large *Cladophora* biomass) in proximity to mussels that might skew measured SRP gradients near bottom. Water motion near-bottom can be highly variable, which may disrupt transiently formed gradients before equilibration can occur with the inside of peeper cells. Ozersky *et al.* (2009) estimated mussel P-flux in closed containers, which effectively ignores the impact of water motion on the formation of near-bottom gradients, and for a shorter time than the measurements in this paper. Measuring in closed containers has the same effect as measuring under extremely quiescent conditions that allow formation instead of abolishment of gradients. Diffusive flux estimates fell within the same range as estimated assimilation flux by two methods and with Ozersky's estimated fluxes. P excretion rate was calculated from the PP concentration in a different lake than Lake Erie (Vanderploeg *et al.*, 2017), which may have minutely different abiotic conditions that affect mussel feeding and assimilation rate, and excretion rate. Estimates of SRP flux are highly influenced by both the estimated SRP excretion rate and mussel biomass estimates. Vanderploeg *et al.* (2017)'s PP:Pex relationship had a low R^2 value, suggesting that while there might have been a relationship between PP and Pex, it is not particularly strong, even if it is significant. These results' similarities to calculated diffusive flux suggest that this approach is reasonable to estimate bottom SRP using an estimate of PP, which itself can be estimated from Chl a profile data. Estimates of SRP flux using the approach found in Dayton *et al.* (2014), were also determined from estimates of PP flux downward, and PP concentration was also estimated from Chl a profile data. These estimates used the same values published in Dayton *et al.* (2014), which were used to determine SRP flux in the nearshore of Lake Michigan at a depth of 8m, and may not be the most realistic values for a 3m and a 10m site in

nearshore East Basin, Lake Erie. However, this is still a reasonable approach, because it sets a general range of expected SRP flux from the bottom. SRP fluxes calculated in this system were in line with previously published work by Vanderploeg *et al.* (2017) and Ozersky *et al.* (2009), but not with Dayton *et al.* (2014), and this may be related to modelling assumptions, but also to mussel feeding, food quality, and the relative source-sink relationship between mussels and *Cladophora* in different systems.

4.4.2 Interaction between mussel excretion and *Cladophora* uptake in the nearshore

Dreissenid mussels are likely an important source of phosphate to *Cladophora*, in part because of their close spatial proximity to each other. Mussel excretion and *Cladophora* demand are likely to change over the course of the growing season and with depth. This interaction, and the assumptions inherent in the model estimates for mussel excretion and *Cladophora* uptake may be the difference between whether or not mussels producing enough SRP to support *Cladophora* biomass.

Model assumptions and their impact on interpretation of mussel excretion and Cladophora uptake need to be kept in mind, as there are only a few pieces of data in this work from which conclusions have been drawn. Environmental and physiological conditions of the mussels used in the Vanderploeg et al. (2017) and Dayton et al. (2014) studies were assumed to be would be equally applicable for estimating PP flux down and SRP flux up from quagga mussel beds in the nearshore of the East Basin. It is important to note that the study system in this work is dissimilar to theirs. Vanderploeg et al. (2017) harvested mussels from a different lake and conducted seston richness experiments in mesocosms, which did not account for near-bed water motion. Dayton et al. (2014) used coefficients determined for zebra mussels in Lake Huron and lakes in Wisconsin. Both these approaches used corrected Chl a YSI profile data to estimate PP; SRP was estimated from PP. While an approach like this would be valuable for ease of data collection, each conversion step from Chl a to PP to SRP introduces error into the estimates. Mussel biomass is also a key component of PP and SRP flux estimations, and error could be introduced from the collection methodology. The divers who collect the mussels must make judgements regarding

representative low, medium, and high biomass patches of mussels at any given station, and they may experience selection bias.

Estimates of Cladophora uptake could have also been similarly affected by model assumptions used in this work. Biomass estimates of Cladophora may have similarly been biased by diver selection. Collecting biomass following a storm in the late part of the season, when large mats can slough away, may also impact biomass estimates. Assumed growth rate was maximal (0.6d-1), which seems reasonable in the early part of the growing season, with increased photoperiod and light penetration, increased P from point and non-point sources, and very little self-shading as the filaments are still small. The internal P content (Qp) was assumed to be related to depth as described by Malkin et al. (2008). Their study site was the nearshore of Lake Ontario, and it was assumed that the nearshore of the East Basin would be similar enough. Qp for this work was estimated for each nominal station depth from the previously published relationship on Cladophora collected in 2006 (Malkin, Guildford & Hecky, 2008).

On average, estimated rates of *Cladophora* P uptake did not exceed that of mussel excretion flux over the entire nearshore area, suggesting that flux out of the benthos may be able to support *Cladophora* growth and biomass. However, *Cladophora* P uptake rates did exceed excretion flux rates at some of the shallowest sites that did not have a turbid water column. However, it is important to note that there is fairly significant spatial heterogeneity in coarse distribution of both mussels and *Cladophora*. That is, stations with the greatest *Cladophora* biomass did not necessarily correspond to the greatest mussel biomass, and that at the deepest stations there are mussels but no *Cladophora*. *Cladophora* is spatially limited by light, however, and was growing at its greatest average biomass at 3m and likely at shallower. These estimates are consistent with SRP flux estimates calculated from the peepers; that is, that stations 1351 and 1353 appeared to have a negative average SRP flux (a decreasing gradient toward the bottom) and 456 had a positive average SRP flux (increasing gradient toward the bottom) (Table 4.5). Stations 1351 and 1353 were sampled in June, still early in the season when *Cladophora* might be growing most rapidly, and intercepting SRP at a rate faster than the time needed for the peepers to equilibrate with its

surroundings. Station 456 was sampled in May, under similar conditions as 1351 and 1353, but because it is a 10m deep station, may have had relatively more mussel P being released than there was a sink for it. During periods of high *Cladophora* growth (early in the season, and potentially also after a storm sloughing event) in shallow stations, mussel excretion may not be enough to account for all the biomass, and nutrient enrichment from other sources, including and especially the Grand River, may be necessary to support all the biomass. As such, it may still be important to control or decrease Grand River SRP inputs to decrease direct effects on *Cladophora* growth, and on seston inputs to decrease the indirect effects of mussel feeding and excretion. Mussels in this portion of Lake Erie have been suggested to have more effect from their excretion activities than their phytoplankton filtering abilities (Zhang, Culver & Boegman, 2011), so limiting how much and the nutrient richness of their food may also decreasing their SRP inputs (sensu Vanderploeg *et al.*, 2017).

The estimates presented in this paper suggest that dreissenid mussel excretion alone can, on average over the whole study area, support *Cladophora* biomass in this portion of the northern nearshore of the East Basin, consistent with the findings of Ozersky *et al* (2009), which found that dreissenid excretion was enough to support *Cladophora* biomass in the nearshore of Lake Ontario. The high *Cladophora* biomass might still be explained if sources not in their direct vicinity (i.e. the mussels growing below them) are considered. Deep stations (i.e. ≥10m) are light limiting to *Cladophora* growth, but mussels could still feed and excrete soluble P, and this nutrient-rich water may be advected shoreward, providing SRP to *Cladophora* in shallower portions of the nearshore where they are not light limited. The Grand River likely provides a non-trivial amount of SRP to the nearshore, and was responsible for elevated SRP in close proximity to the river mouth (Chomicky *et al.* 2016). Other studies have noted that following the GLWQA, tributary total phosphorus has been decreasing, but SRP appears to have either held steady or increased (Dove & Chapra, 2015). The Grand River and mussels may be working synergistically, in the sense that the Grand River is a source of nutrient-rich particulate matter and phytoplankton that is a good food source for dreissenids, which in turn excrete more SRP (Zhang *et*

al., 2011). Groundwater has been implicated in enhancing P to the Grand river (Maavara *et al.*, 2017), and may do the same at the lake margins. This may be particularly true if the lake level is below the groundwater table, and groundwater flows into the lake (Robinson, 2015), and conversely, lake water will infiltrate groundwater when the lake level is higher than the groundwater table. Direct surface runoff at the margins may also be an important source of P to the nearshore (Joosse & Baker, 2011). While estimates of mussel excretion flux and SRP flux out of the bottom and *Cladophora* uptake rates were relatively simplified in this paper, they provide a reasonable first step in estimating how much mussels are contributing to near-bottom nutrient flux and how it may be related to nuisance *Cladophora* biomass.

Cladophora may sometimes have a greater demand for SRP than what mussels produce locally at stations where there is high *Cladophora* biomass and relatively low mussel biomass. Mussel-derived P may be enough to support the majority of *Cladophora* biomass but may not be the only thing contributing SRP. Mussels' range extends far deeper than *Cladophora*, as *Cladophora* becomes light limited at ~10m deep, and the majority of nuisance biomass occurs ≤5m deep. Potential supplementary sources may include SRP from deeper portions of the lake and supplementation from the Grand River and other non-point sources. Horizontal advection and wholescale water mass movement as a result of seiching could potentially introduce nutrient-rich water from deeper sites where mussels have fed or decomposition processes of settled seston have liberated SRP, to shallower sites where *Cladophora* can take up SRP. The Grand River is known to carry a relatively high SRP load (PWQMN) and the area of the lake in close proximity experiences elevated SRP concentrations relative to the offshore (Chomicki *et al.*, 2016). However, two of our shallow and deep sites (1351 and 1350) were located at a far east transect by the city of Port Colborne which is not believed to be heavily influenced by the grand river plume, and still experienced some of the highest *Cladophora* biomass during the growing season. Direct non-point source inputs from groundwater and septic systems may have contributed to nuisance growth in that area, but these were not directly measured in this work.

Calculated excretion flux was often greater than *Cladophora* uptake rate in this paper, but it is unlikely that all of the excreted SRP will be taken up by *Cladophora*. PP flux was also greater than SRP flux, suggesting that there may also be particulate detritus that will eventually break down and release P as well. PP flux was approximately 1.5 times greater than SRP flux, so this pool of decaying detritus may be important in benthic P cycling, and for P available for *Cladophora* uptake. Diffusive flux estimates cannot distinguish between SRP flux from mussel excretion and from P-liberation from particulate waste. As such, estimates of SRP diffusive fluxes are likely to be slightly larger than mussel excretion flux when both are compared on a biomass-specific basis on specific sampling dates and sites. Nevertheless, even if diffusive flux over-estimates how much mussels are capable of producing, this could represent an upper bound to mussel influence on soluble P release in the nearshore.

The lack of strong near-bottom nutrient gradients may have been related to other factors in the nearshore other than mussels, that served to obscure these gradients. Relatively high background nutrients from terrestrial and lake sources and relatively strong mixing may have obscured strong gradients on a finer scale near-bottom, contrary to what was expected. A near-bottom gradient may not be much greater above background, giving the appearance of no gradient, especially if there is only a relatively small sink (e.g. in the early part of the season, when *Cladophora* is still small). High diffusivities have been demonstrated to reduce appearance of near-bottom gradients (Dayton *et al.*, 2014), and if stratification serves to isolate the bottom of the water column from the top, what may be detectable is only an entire region or band of the water column that is enriched near bottom relative to the surface (Wüest & Lorke, 2003). Bottom roughness, including bottom substrate, mussels and *Cladophora* serve as roughness elements that create form drag that enhances turbulence and mixing (Wüest & Lorke, 2003; Lorke & MacIntyre, 2009). *Cladophora* may also not be the only sink for P in the nearshore; other benthic algae or bacteria may be taking up this nutrient as well.

This paper estimates SRP flux up from the bottom using three calculation methods, one of which is novel in the sense that SRP gradients and water velocity were directly measured, and used to estimate

diffusive flux. Diffusive flux estimates were in line with flux estimates from mussel excretion and biomass, and were in line with published values in other systems. Because mussels are the dominant zoobenthic organism in the nearshore of the East Basin, they contribute the majority of internal biological internal loading. The balance between estimated mussel excretion and *Cladophora* uptake suggests that there is slightly more excretion than uptake, which may partially explain why measured SRP in the nearshore, even at the surface is much higher than the offshore.

Chapter 5: Thesis conclusions

5.1 Summary and Synthesis

Nuisance Cladophora in the nearshore is indicative of nearshore nutrient enrichment and eutrophication, and its presence points to concerns on a larger scale that impact food webs, industry, and economies. Cladophora resurgence in the nearshore, largely at depths ≤10m deep, was driven by the complex interaction of light and nutrient availability, the time of year, and physical processes in the water column and near bottom. Mussel biomass was the dominant benthic invertebrate in the nearshore, although its distribution was patchy at smaller scales; its peak biomass was between 5-10m deep. Tributary input and mussels also work to impact the availability of light and nutrients but appear to have very limited spatial impacts on their own; water motion in the nearshore on both a coarse and fine scale modify tributary and mussel effects.

Light and nutrients availability that drive Cladophora biomass and distribution in the nearshore appeared to be impacted by both the tributary and the presence of mussels. The Grand River appeared to have very localized impacts based on specific conductivity measured at various points in the nearshore. SRP was elevated at stations near the mouth of the river, which should enhance Cladophora growth. However, stations located close to the mouth also experienced light limitation from the turbid river plume, so Cladophora was not at high biomass in these areas. Cladophora located at stations in the far-west and far-east transects had greater biomass, despite the lack of apparent river nutrient input. Mussel feeding may be the reason for greater Cladophora biomass at the far-west and far-east shallow stations, both for their feeding activities on seston (and particularly phytoplankton), which would enhance water clarity, but also through their excretion activities. The nearshore shunt hypothesis posits that mussel water column particulate phosphorus feeding and soluble phosphorus benthic deposition is one of the mechanisms by which nuisance Cladophora has become a reestablished problem.

How and when sampling was conducted could impact interpretation of nutrient dynamics and patterns. For this reason, sampling data in this thesis was split between early (May and June) and late (August and October) sampling season, the nearshore split into the shallow (<10m) and deep (≥10m) portions, and soluble reactive phosphorus (SRP) was filtered using two different methods. . Syringe filtration immediately on-station and tower filtration at the end of the field day showed that the difference in filtering methodology, possibly including the delay between sample collection and filtration, did affect absolute concentrations of SRP, but the general patterns were the same. Season was found to be a major factor driving horizontal nutrient patterns in the nearshore, and particularly in chla and SRP. This seasonal effect may be important, as early in the season Cladophora is at low biomass, but growing rapidly from combined favourable temperature, nutrients, and light. Most of the observed stratification occurred in the early part of the sampling season, which could be important for the impact of the river plume on near bottom waters, water column exchange, and near-bottom impacts of mussels.

The nearshore of large lakes behaves differently than the offshore, in the sense that they are dynamic, and are commonly thought to be well-mixed. The impact of a tributary and mussels in this portion of the nearshore may interact with large scale water motion and near-bottom turbulence that is advantageous to Cladophora. Shore parallel currents often moved the river plume in an eastward direction, and mixing appeared strong enough that river nutrient and seston inputs had a relatively spatially limited direct effect. However, there may be synergy between seston richness and mussel feeding and excretion richness, and the river may create conditions that enhance Cladophora biomass in an indirect way. This thesis found that stratification formed frequently, even at stations as shallow as 3m deep, but was often weak and transient. Stratification could impede water column exchange and mixing between surface and bottom waters, and could be an important mechanism to investigate in terms of mussel feeding and excretion, and on Cladophora growth. This thesis found that there were instances of near-bottom gradients in chla, SRP, and NH_4, suggesting that mussels can experience feeding limitations. Similarly, near-bottom gradients of SRP suggest that the near-bottom environment can be quiescent

enough at times for an appreciable pool of SRP to form in the vicinity of Cladophora, and may be an important part in explaining nuisance Cladophora's resurgence in the nearshore following dreissenid mussel introduction. Diffusivity in the near-bottom water column at all stations, including the deepest 20m stations, fell within a range typically considered to be turbulent, or on the boundary between quiescence and turbulence. The near-bottom energetic regime may be the reason why very clearly obvious gradients were not always seen, but were predicted.

The northern nearshore of East Basin Lake Erie originally experience nuisance Cladophora growth (>50gDW/m^2) in the 1950's and 1960's as a result of tributary phosphorus loading. Cladophora biomass subsequently declined following loading controls under the Great Lakes Water Quality Agreement. The current nuisance biomass does not appear to be a direct result of tributary loading, suggesting that even if tributary loading of both total and soluble phosphorus was decreased, Cladophora biomass may not come back down to <50gDW/m^2, and this might be the resulting system, an alternate stable state. Even if external loading is reduced, the idea of an alternate stable state means that the nearshore of the East Basin may be permanently shifted to a benthic-based system. Cladophora may persist at high biomass at the expense of water column phytoplankton, impacting a food web with phytoplankton at its base. This thesis is novel for considering both external and internal sources of phosphorus, and the role of water movement and physical processes in driving contemporary nuisance Cladophora growth and shaping its distribution in the nearshore.

5.2 Contributions, advancements, and limitations of work

This thesis has helped advance our understanding of benthic-pelagic coupling and the role of tributary loading and mussel impacts on nuisance *Cladophora* growth in the rocky nearshore of the East Basin, Lake Erie. This work made some of the first direct SRP and NH_4 flux estimates with *in situ* mussel communities and the most representative estimates of ambient nutrient concentrations in the East Basin nearshore benthos, and was one of the first to explicitly consider vertical patterns of nutrient and

Chl a variation in relation to mussels, in addition to horizontal patterns of variation in relation to a major tributary. This thesis was also one of the first to provide a direct estimate of diffusive SRP flux up from the benthos, and the use of profiler Chl a to estimate Chl a and particulate P flux into mussel beds. This methodology may be a useful tool for water quality managers to use to get a quick approximation of mussel impacts on Chl a and nutrient fluxes near bottom, in the absence of more sophisticated water profilers. However, there are still some limitations to the work that were discovered in the process of doing the sample collection for this work. The biggest limitation of this work is the lack of long-term (i.e. ≥8h) ADCP deployments and long-term sampling; deployments were short overall, and did not capture water motion patterns that occur on longer timescales. Longer deployments and water column profiles over the course of the day would have been especially useful in understanding how stratification forms and decays over the course of the day. Longer deployments may have also captured evidence of upwelling and seiching. Finally, the horizontal scale of measurement may not have been fine enough to really elucidate the relationship between the land and lake at the margins at depths shallower than 3m deep. The land-lake margin could be an important aspect of non-point source loading, and the sampling design in this thesis did not allow adequate investigation of this. Nevertheless, this thesis makes some important contributions to the field of limnology.

5.3 Future work

This thesis has answered some questions relating to benthic-pelagic coupling and the role of tributaries, mussels, and near-bottom water motion, but has also uncovered new avenues for investigation. In particular, to really tease apart the relative impact of tributary loading and mussel activities, similar sampling could be done in an area with (a) minimal tributary inputs, but high mussel biomass, and (b) an area with relatively enriched tributary inputs and no mussels in receiving waters. Similarly, modeling exercises could be conducted, perhaps in ELCOM-CAEDYM, varying physical forcing, mussel and benthic algae biomass, and/or phosphorus variables. Conducting a similar set of experiments with longer

(e.g. ≥24h) ADCP and other instrument deployments to capture more of the physical processes that occur in the rocky nearshore. Deploy surface wave AWAC to measure surface wave effects on mixing, especially at shallow stations. Similarly, sampling at stations very close to shore to further understand the interaction of the lake-land margin, and non-point source surface and groundwater loading on the very-shallow nearshore. Finally, the big unknown in mussel-mediated nutrient cycling in the nearshore is what contribution feces and pseudofeces play, and particularly how resuspension impacts solubilization of semi-labile phosphorus.

Chapter 6: References

Ackerman J.D. (1999) Effect of velocity on the filter feeding of dreissenid mussels (Dreissena polymorpha and Dreissena bugensis): implications for trophic. *Canadian Journal of Fisheries and Aquatic Sciences* **56**, 1551–1561.

Ackerman J.D., Loewen M.R. & Hamblin P.F. (2001) Benthic-Pelagic Coupling over a Zebra Mussel Reef in Western Lake Erie. *Limnology and Oceanography* **46**, 892–904.

Allan J.D., Mcintyre P.B., Smith S.D.P., Halpern B.S., Boyer G.L., Prusevich A., *et al.* (2012) Joint analysis of stressors and ecosystem services to enhance restoration effectiveness. *PNAS* **110**, 372–377.

Arnott D.L. & Vanni M.J. (1996) Nitrogen and phosphorus recycling by the zebra mussel (Dreissena polymorpha) in the western basin of Lake Erie. *Canadian Journal of Fisheries and Aquatic Sciences* **53**, 646–659.

Auer M.T., Tomlinson L.M., Higgins S.N., Malkin S.Y., Howell E.T. & Bootsma H.A. (2010) Great Lakes Cladophora in the 21st century: Same algae-different ecosystem. *Journal of Great Lakes Research* **36**, 248–255.

Baker D.B., Confesor R., Ewing D.E., Johnson L.T., Kramer J.W. & Merry B.J. (2014) Phosphorus loading to Lake Erie from the Maumee , Sandusky and Cuyahoga rivers : The importance of bioavailability. *Journal of Great Lakes Research* **40**, 502–517.

Barbiero R.P. & Tuchman M.L. (2004) Long-term Dreissenid Impacts on Water Clarity in Lake Erie. *Journal of Great Lakes Research* **30**, 557–565.

Barton D.R., Howell E.T. & Fietsch C.-L. (2013) Ecosystem changes and nuisance benthic algae on the southeast shores of Lake Huron. *Journal of Great Lakes Research* **39**, 602–611.

Beletsky D., Hawley N. & Rao Y.R. (2013) Modeling summer circulation and thermal structure of Lake Erie. *Journal of Geophysical Research: Oceans* **118**, 6238–6252.

Binding C.E., Greenberg T.A., Watson S.B., Rastin S. & Gould J. (2015) Long term water clarity changes in North America's Great Lakes from multi-sensor satellite observations. *Limnology and Oceanography* **60**, 1976–1995.

Bocaniov S.A., Smith R.E.H., Spillman C.M., Hipsey M.R. & Leon L.F. (2014) The nearshore shunt and the decline of the phytoplankton spring bloom in the Laurentian Great Lakes: Insights from a three-dimensional lake model. *Hydrobiologia* **731**, 151–172.

Boegman L., Loewen M.R., Culver D. a., Hamblin P.F. & Charlton M.N. (2008a) Spatial-Dynamic Modeling of Algal Biomass in Lake Erie: Relative Impacts of Dreissenid Mussels and Nutrient Loads. *Journal of Environmental Engineering* **134**, 456–468.

Boegman L., Loewen M.R., Hamblin P.F. & Culver D.A. (2008b) Vertical mixing and weak stratification over zebra mussel colonies in western Lake Erie. *Limnology and Oceanography* **53**, 1093–1110.

Bouffard D., Ackerman J.D. & Boegman L. (2013) Factors affecting the development and dynamics of hypoxia in a large shallow stratified lake: Hourly to seasonal patterns. *Water Resources Research* **49**, 2380–2394.

Bouffard D. & Boegman L. (2013) A diapycnal diffusivity model for stratified environmental flows. *Dynamics of Atmospheres and Oceans* **61**–**62**, 14–34.

Burlakova L.E., Barbiero R.P., Karatayev A.Y., Daniel S.E., Hinchey E.K. & Warren G.J. (2018) The benthic community of the Laurentian Great Lakes: Analysis of spatial gradients and temporal trends from 1998 to 2014. *Journal of Great Lakes Research*.

Burlakova L.E., Karatayev A.Y., Pennuto C. & Mayer C. (2014) Changes in Lake Erie benthos over the last 50years: Historical perspectives, current status, and main drivers. *Journal of Great Lakes Research* **40**, 560–573.

Casper A.F. & Johnson L.E. (2010) Contrasting shell/tissue characteristics of Dreissena polymorpha and Dreissena bugensis in relation to environmental heterogeneity in the St. Lawrence River. *Journal of Great Lakes Research* **36**, 184–189.

Cha Y., Stow C.A., Nalepa T.F. & Reckhow K.H. (2011) Do invasive mussels restrict offshore phosphorus transport in lake huron? *Environmental Science and Technology* **45**, 7226–7231.

Chapra S.C. & Dolan D.M. (2012) Great Lakes total phosphorus revisited: 2. Mass balance modeling. *Journal of Great Lakes Research* **38**, 741–754.

Chomicki K.M., Howell E.T., Defield E., Dumas A. & Taylor W.D. (2016) Factors influencing the phosphorus distribution near the mouth of the Grand River, Ontario, Lake Erie. *Journal of Great Lakes Research* **42**, 549–564.

Chowdhury M.R., Wells M.G. & Howell T. (2016) Movements of the thermocline lead to high variability in benthic mixing in the nearshore of a large lake. *Water Resources Research* **52**, 3019–3039.

Conroy J.D., Edwards W.J., Pontius R.A., Kane D.D., Zhang H., Shea J.F., *et al.* (2005a) Soluble nitrogen and phosphorus excretion of exotic freshwater mussels (Dreissena spp.): Potential impacts for nutrient remineralisation in western Lake Erie. *Freshwater Biology* **50**, 1146–1162.

Conroy J.D., Kane D.D., Dolan D.M., Edwards W.J., Charlton M.N. & Culver D.A. (2005b) Temporal Trends in Lake Erie Plankton Biomass : Roles of External Phosphorus Loading and Dreissenid Mussels. *Journal of Great Lakes Research* **31**, 89–110.

Crowe A.S. & Shikaze S.G. (2004) Linkages between groundwater and coastal wetlands of the Laurentian Great Lakes. *Aquatic Ecosystem Health & Management* **7**, 199–213.

Cyr H., McCabe S.K. & Nürnberg G.K. (2009) Phosphorus sorption experiments and the potential for internal phosphorus loading in littoral areas of a stratified lake. *Water Research* **43**, 1654–1666.

Dayton A.I., Auer M.T. & Atkinson J.F. (2014) Cladophora, mass transport, and the nearshore phosphorus shunt. *Journal of Great Lakes Research* **40**, 790–799.

Demchenko N., He C., Rao Y.R. & Valipour R. (2017) Surface river plume in a large lake under wind forcing: Observations and laboratory experiments. *Journal of Hydrology* **553**, 1–12.

Depew D.C., Guildford S.J. & Smith R.E.. H. (2006a) Nearshore – offshore comparison of chlorophyll a and phytoplankton production in the dreissenid- colonized eastern basin of Lake Erie. *Canadian Journal of Fisheries and Aquatic Sciences* **63**, 1115–1129.

Depew D.C., Guildford S.J. & Smith R.E.H. (2006b) Nearshore-offshore comparison of chlorophyll a and phytoplankton. *Canadian Journal of Fisheries and Aquatic Sciences* **63**.

Depew D.C., Houben A.J., Guildford S.J. & Hecky R.E. (2011) Distribution of nuisance Cladophora in the lower Great Lakes: Patterns with land use, near shore water quality and dreissenid abundance. *Journal of Great Lakes Research* **37**, 656–671.

Depew D.C., Koehler G. & Hiriart-Baer V. (2018) Phosphorus Dynamics and Availability in the

Nearshore of Eastern Lake Erie: Insights From Oxygen Isotope Ratios of Phosphate. *Frontiers in Marine Science* **5**.

Dermott R. & Munawar M. (1993) Invasion of Lake Erie Offshore Sediments by Dreissena, and Its Ecological Implicatoins. *Canadian Journal of Fisheries and Aquatic Sciences* **50**, 2298–2304.

Dodds W.K. & Biggs B.J.F. (2002) Water velocity attenuation by stream periphyton and macrophytes in relation to growth form and architecture. *Journal of the North American Benthological Society* **21**, 2–15.

Dolan D.M. & Chapra S.C. (2012) Great Lakes total phosphorus revisited: 1. Loading analysis and update (1994-2008). *Journal of Great Lakes Research* **38**, 730–740.

Dolan D.M. & McGunagle K.P. (2005) Lake Erie Total Phosphorus Loading Analysis and Update: 1996–2002. *Journal of Great Lakes Research* **31**, 11–22.

Dove A. (2009) Long-term trends in major ions and nutrients in Lake Ontario. *Aquatic Ecosystem Health & Management* **12**, 281–295.

Dove A. & Chapra S.C. (2015) Long-term trends of nutrients and trophic response variables for the Great Lakes. *Limnology and Oceanography* **60**, 696–721.

Edsall T.A. & Charlton M.N. (1997) *NEARSHORE WATERS OF THE GREAT LAKES*.

Edwards W.J., Rehmann C.R., McDonald E. & Culver D.A. (2005) The impact of a benthic filter feeder: limitations imposed by physical transport of algae to the benthos. *Canadian Journal of Fisheries and Aquatic Sciences* **62**, 205–214.

Escartin J. & Aubrey D.G. (1995) Flow structure and dispersion within algal mats. *Estuarine Coastal and Shelf Science* **40**, 451–472.

Fahnenstiel G., Pothoven S., Vanderploeg H., Klarer D., Nalepa T. & Scavia D. (2010) Recent changes in primary production and phytoplankton in the offshore region of southeastern Lake Michigan ☆. *Journal of Great Lakes Research* **36**, 20–29.

Fahnenstiel G.L., Bridgeman T.B., Lang G.A., McCorkmick M.J. & Nalepa T.F. (1995a) Phytoplankton Productivity in Saginaw Bay, Lake Huron: Effects of Zebra Mussel (Dreissena polymorpha) Colonization. *Journal of Great Lakes Research* **21**, 465–475.

Fahnenstiel G.L., Lang G.A., Nalepa T.F. & Johengen T.H. (1995b) Effects of Zebra Mussel (Dreissena polymorpha) Colonization on Water quality Parameters in Saginaw Bay, Lake Huron. *Journal of Great Lakes Research* **21**, 435–448.

Ghadouani A. & Smith R.E.H. (2005) Phytoplankton Distribution in Lake Erie as Assessed by a New in situ Spectrofluorometric Technique. *Journal of Great Lakes Research* **31**, 154–167.

Hall S.R., Pauliukonis N.K., Mills E.L., Rudstam L.G., Schneider C.P., Lary S.J., *et al.* (2008) A Comparison of Total Phosphorus , Chlorophyll a , and Zooplankton in Embayment , Nearshore , and Offshore Habitats of Lake Ontario. *Journal of Great Lakes Research* **29**, 54–69.

Haltuch M.A., Berkman P.A. & Garton D.W. (2000) Geographic information system (GIS) analysis of ecosystem invasion : Exotic mussels in Lake Erie. *Limnology and Oceanography* **45**, 1778–1787.

He C., Rao Y.R., Skafel M.G. & Howell T. (2006) Numerical modelling of the Grand River plume in Lake Erie during unstratified period. *Water Quality Research Journal of Canada* **41**, 16–23.

Hecky R.E., Smith R.E., Barton D.R., Guildford S.J., Taylor W.D., Charlton M.N., *et al.* (2004) The nearshore phosphorus shunt: a consequence of ecosystem engineering by dreissenids in the

Laurentian Great Lakes. *Canadian Journal of Fisheries and Aquatic Sciences* **61**, 1285–1293.

Hesslein R.H. (1973) An in situ sampler for close interval pore water studies. *Limnology and Oceanography*, 912–914.

Higgins S.N., Hecky R.E. & Guildford S.J. (2005a) Modeling the Growth, Biomass, and Tissue Phosphorus Concentration of Cladophora glomerata in Eastern Lake Erie: Model Description and Field Testing. *Journal of Great Lakes Research* **31**, 439–455.

Higgins S.N., Hecky R.E. & Guildford S.J. (2008a) The collapse of benthic macroalgal blooms in response to self-shading. *Freshwater Biology* **53**, 2557–2572.

Higgins S.N., Malkin S.Y., Todd Howell E., Guildford S.J., Campbell L., Hiriart-Baer V., *et al.* (2008b) An ecological review of Cladophora glomerata (Chlorophyta) in the Laurentian Great Lakes. *Journal of Phycology* **44**, 839–854.

Higgins S.N., Pennuto C.M., Howell E.T., Lewis T.W. & Makarewicz J.C. (2012) Urban influences on Cladophora blooms in Lake Ontario. *Journal of Great Lakes Research* **38**, 116–123.

Higgins S.N., Todd Howell E., Hecky R.E., Guildford S.J., Smith R.E., Howell E.T., *et al.* (2005b) The Wall of Green: The Status of Cladophora glomerata on the Northern Shores of Lake Erie's Eastern Basin, 1995–2002. *J. Great Lakes Res. Internat. Assoc. Great Lakes Res* **31**, 547–563.

Higgins S.N. & Vander Zanden M.J. (2010) What a difference a species makes: a meta–analysis of dreissenid mussel impacts on freshwater ecosystems. *Ecological Monographs* **80**, 179–196.

Higgins S.N., Vander Zanden M.J., Joppa L.N. & Vadeboncoeur Y. (2011) The effect of dreissenid invasions on chlorophyll and the chlorophyll : total phosphorus ratio in north-temperate lakes. *Canadian Journal of Fisheries and Aquatic Sciences* **68**, 319–329.

Howell E.T. (2017) Cladophora (green algae) and dreissenid mussels over a nutrient loading gradient on the north shore of Lake Ontario.

Howell E.T. (2018) Influences on Water Quality and Abundance of Cladophora, a Shore-Fouling Green Algae , over Urban Shoreline in Lake Ontario. *Water* **10**, 1–31.

Howell E.T., Barton D.R., Fietsch C. & Kaltenecker G. (2014) Fine-scale nutrient enrichment and water quality on the rural shores of Southeast Lake Huron. *Journal of Great Lakes Research* **40**, 126–140.

Howell E.T., Chomicki K.M. & Kaltenecker G. (2012) Patterns in water quality on Canadian shores of Lake Ontario: Correspondence with proximity to land and level of urbanization. *Journal of Great Lakes Research* **38**, 32–46.

Imberger J. (1998) Flux paths in a stratified lake : A review. *Physical Processes in lakes and oceans* **54**, 1–17.

Ivey G.N., Winters K.B. & Silva, De I.P.D. (2000) Turbulent mixing in a sloping benthic boundary layer energized by internal waves. *Journal of Fluid Mechanics* **418**, S0022112000008788.

Jabbari A., Rouhi A. & Boegman L. (2016) Evaluation of the structure function method to compute turbulent dissipation within boundary layers using numerical simulations. *Journal of Geophysical Research: Oceans* **121**, 5888–5897.

Jarvie H., Withers P. & Neal C. (2002) Review of robust measurement of phosphorus in river water: sampling, storage, fractionation and sensitivity. *Hydrology and Earth System Sciences* **6**, 113–131.

Joosse P.J. & Baker D.B. (2011) Context for re-evaluating agricultural source phosphorus loadings to the Great Lakes. *Canadian Journal of Soil Science* **91**, 317–327.

Kane D.D., Conroy J.D., Richards R.P., Baker D.B. & Culver D.A. (2014) Re-eutrophication of Lake Erie : Correlations between tributary nutrient loads and phytoplankton biomass. *Journal of Great Lakes Research* **40**, 496–501.

Kerfoot W.C., Yousef F., Green S.A., Budd J.W., Schwab D.J. & Vanderploeg H.A. (2010) Approaching storm : Disappearing winter bloom in Lake Michigan. *Journal of Great Lakes Research* **36**, 30–41.

Knights D., Parks K.C., Sawyer A.H., David C.H., Browning T.N., Danner K.M., *et al.* (2017) Direct groundwater discharge and vulnerability to hidden nutrient loads along the Great Lakes coast of the United States. *Journal of Hydrology* **554**, 331–341.

Kornelsen K.C. & Coulibaly P. (2014) Synthesis review on groundwater discharge to surface water in the Great Lakes Basin. *Journal of Great Lakes Research* **40**, 247–256.

Kuntz T. (2008) *System and plankton metabolism in the lower Grand River , Ontario By*.

Lawson S.E., McGlathery K.J. & Wiberg P.L. (2012) Enhancement of sediment suspension and nutrient flux by benthic macrophytes at low biomass. *Marine Ecology Progress Series* **448**, 259–270.

León L.F., Imberger J., Smith R.E.H., Hecky R.E., Lam D.C.L. & Schertzer W.M. (2005) Modeling as a Tool for Nutrient Management in Lake Erie: a Hydrodynamics Study. *J. Great Lakes Res. Internat. Assoc. Great Lakes Res* **31**, 309–318.

Lewandowski J., Meinikmann K., Nützmann G. & Rosenberry D.O. (2015) Groundwater - the disregarded component in lake water and nutrient budgets. Part 2: effects of groundwater on nutrients. *Hydrological Processes* **29**, 2922–2955.

Litchman E. & Nguyen B.L. V (2008) Alkaline Phosphatase Activity as a Function of Internal Phosphorus Concentration in Freshwater Phytoplankton. *Journal of Phycology* **1383**, 1379–1383.

Loewen M.R., Ackerman J.D. & Hamblin P.F. (2007) Environmental implications of stratification and turbulent mixing in a shallow lake basin. *Canadian Journal of Fisheries and Aquatic Sciences* **64**, 43–57.

Lorke A. (2007) Boundary mixing in the thermocline of a large lake. *Journal of Geophysical Research: Oceans* **112**, 1–10.

Lorke A. & MacIntyre S. (2009) Hydrodynamics and Mixing in Lakes , Reservoirs , Wetlands and Rivers. *River Ecosystem Ecology: A Global Perspective. Encyclopedia of Inland Waters* **1**, 505–514.

Maavara T., Slowinski S., Rezanezhad F., Meter K. Van & Cappellen P. Van (2017) The role of groundwater discharge fluxes on Si:P ratios in a major tributary to Lake Erie. *Science of the Total Environment* **622623**, 814–824.

MacIntyre S. & Jellison R. (2001) Nutrient fluxes from upwelling and enhanced turbulence at the top of the pycnocline in Mono Lake, California. *Hydrobiologia* **466**, 13–29.

MacIntyre S. & Melack J.M. (1995) Vertical and Horizontal Transport in Lakes : Linking Littoral , Benthic , and Pelagic Habitats. *Journal of the North American Benthological Society* **14**, 599–615.

Mackie G.L. (1991) Biology of the exotic zebra mussel, Dreissena polymorpha, in relation to native bivalves and its potential impact in Lake St.Clair. *Hydrobiologia*, 251–268.

Makarewicz J.C. (1993) Phytoplankton Biomass and Species Composition In Lake Erie , 1970 to 1987. *Journal of Great Lakes Research* **19**, 258–274.

Makarewicz J.C., Bertram P., Makarewicz J.C. & Bertram P. (1991) Evidence for the Restoration of the Lake Erie Ecosystem Evidence for the Lake the Erie Restoration of Ecosystem Water quality ,

oxygen levels , and pelagic function appear to be improving. *Bioscience* **41**, 216–223.

Makarewicz J.C. & Howell E.T. (2012) The Lake Ontario Nearshore Study: Introduction and summary. *Journal of Great Lakes Research* **38**, 2–9.

Malkin S.Y., Guildford S.J. & Hecky R.E. (2008) Modeling the growth response of Cladophora in a Laurentian Great Lake to the exotic invader Dreissena and to lake warming. *Limnology and Oceanography* **53**, 1111–1124.

Malkin S.Y., Silsbe G.M., Smith R.E.H. & Todd Howell E. (2012) A deep chlorophyll maximum nourishes benthic filter feeders in the coastal zone of a large clear lake. *Limnology and Oceanography* **57**, 735–748.

Martin G.M. (2010) Nutrient sources for excessive growth of benthic algae in Lake Ontario as inferred by the distribution of SRP.

Mellina E., Rasmussen J.B. & Mills E.L. (1995) Impact of zebra mussel (Dreissena polymorpha) on phosphorus cycling and chlorophyll in lakes. *Canadian journal of fisheries and aquatic sciences* **52**, 2553–2573.

Michalak A.M., Anderson E.J., Beletsky D., Boland S., Bosch N.S., Bridgeman T.B., *et al.* (2013) Record-setting algal bloom in Lake Erie caused by agricultural and meteorological trends consistent with expected future conditions. *PNAS* **110**, 6448–6452.

Mills E.L., Rosenberg G., Spidle A.P., Ludyanskiy M., Pligin Y. & A Y B.M. (1996) A Review of the Biology and Ecology of the Quagga Mussel (Dreissena bugensis), a Second Species of Freshwater Dreissenid Introduced to North America 1. *American Zoologist* **36**, 271–286.

Morehouse R.L., Dzialowski A.R. & Jeyasingh P.D. (2013) Impacts of excessive dietary phosphorus on zebra mussels. *Hydrobiologia* **707**, 73–80.

Mortimer C.H. (1987) Fifty Years of Physical Investigations and Related Limnological Studies on Lake Erie, 1928-1977. *Journal of Great Lakes Research* **13**, 407–435.

Naddafi R., Eklöv P. & Pettersson K. (2009) Stoichiometric Constraints Do Not Limit Successful Invaders: Zebra Mussels in Swedish Lakes. *PLoS ONE* **4**, e5345.

Nalepa T.F., Fanslow D.L. & Lang G.A. (2009) Transformation of the offshore benthic community in Lake Michigan: Recent shift from the native amphipod Diporeia spp. to the invasive mussel Dreissena rostriformis bugensis. *Freshwater Biology* **54**, 466–479.

Nicholls K.H. & Hopkins G.J. (1993) Recent Changes in Lake Erie (North Shore) Phytoplankton: Cumulative Impacts of Phosphorus Loading Reductions and the Zebra Mussel Introduction. *Journal of Great Lakes Research* **19**, 637–647.

Nicholls K.H., Hopkins G.J. & Standke S.J. (1999) Reduced chlorophyll to phosphorus ratios in nearshore Great Lakes waters coincide with the establishment of dreissenid mussels. *Canadian Journal of Fisheries and Aquatic Sciences* **56**, 153–161.

Nishizaki M. & Ackerman J.D. (2017) Mussels blow rings: Jet behavior affects local mixing. *Limnology and Oceanography* **62**, 125–136.

North R.L., Smith R.E.H.H., Hecky R.E., Depew D.C., León L.F., Charlton M.N., *et al.* (2012) Distribution of seston and nutrient concentrations in the eastern basin of Lake Erie pre- and post-dreissenid mussel invasion. *Journal of Great Lakes Research* **38**, 463–476.

O'Riordan C.A., Monismith S.G. & Koseff J.R. (1993) A study of concentration boundary-layer

formation over a bed of model bivalves. *Limnology and Oceanography* **38**, 1712–1729.

O'Riordan C.A., Monismith S.G. & Koseff J.R. (1995) The effect of bivalve excurrent jet dynamics on mass transfer in a benthic boundary layer. *Limnology and Oceanography* **40**, 330–344.

Orihel D.M., Baulch H.M., Casson N.J., North R.L., Parsons C.T., Seckar D.C.M., *et al.* (2017) INVITED REVIEW Internal phosphorus loading in Canadian fresh waters: a critical review and data analysis. *Canadian Journal of Fisheries and Aquatic Sciences* **74**, 2005–2029.

Ozersky T., Evans D.O. & Ginn B.K. (2015) Invasive mussels modify the cycling, storage and distribution of nutrients and carbon in a large lake. *Freshwater Biology* **60**, 827–843.

Ozersky T., Malkin S.Y., Barton D.R. & Hecky R.E. (2009) Dreissenid phosphorus excretion can sustain C. glomerata growth along a portion of Lake Ontario shoreline. *Journal of Great Lakes Research* **35**, 321–328.

Patterson M.W.R., Ciborowski J.J.H. & Barton D.R. (2005) The Distribution and Abundance of Dreissena Species (Dreissenidae) in Lake Erie , 2002. *Journal of Great Lakes Research* **31**, 223–237.

Pennuto C.M., Burlakova L.E., Karatayev A.Y., Kramer J., Fischer A. & Mayer C. (2014) Spatiotemporal characteristics of nitrogen and phosphorus in the benthos of nearshore Lake Erie. *Journal of Great Lakes Research* **40**, 541–549.

Rao Y.R., Milne J.E. & Marvin C.H. (2012) Hydrodynamics and water quality in western Lake Ontario. *Journal of Great Lakes Research* **38**, 91–98.

Ray W.J. & Corkum L.D. (1997) Predation of zebra mussels by round gobies , Neogobius melanostomus. *Environmental bBology of Fishes* **50**, 267–273.

Robinson C. (2015) Review on groundwater as a source of nutrients to the Great Lakes and their tributaries. *Journal of Great Lakes Research* **41**, 941–950.

Roy J.W., Spoelstra J., Robertson W.D., Klemt W. & Schiff S.L. (2017) Contribution of phosphorus to Georgian Bay from groundwater of a coastal beach town with decommissioned septic systems. *Journal of Great Lakes Research* **43**, 1016–1029.

Ruginis T., Bartoli M., Petkuviene J., Zilius M., Lubiene I., Laini A., *et al.* (2014) Benthic respiration and stoichiometry of regenerated nutrients in lake sediments with Dreissena polymorpha. *Aquatic Sciences* **76**, 405–417.

Scavia D., David Allan J., Arend K.K., Bartell S., Beletsky D., Bosch N.S., *et al.* (2014) Assessing and addressing the re-eutrophication of Lake Erie: Central basin hypoxia. *Journal of Great Lakes Research* **40**, 226–246.

Schertzer W.M., Saylor J.H., Boyce F.M., Robertson D.G. & Rosa F. (1987) SEASONAL THERMAL CYCLE OF LAKE ERIE. *Journal of Great Lakes Research* **13**, 468–486.

Schindler D.W. (1971) Carbon, Nitrogen, and Phosphorus and the eutrophication of freshwater lakes. *Journal of Phycology* **7**, 321–329.

Schindler D.W. (1977) Evolution of Phosphorus Limitation in Lakes. *Science* **195**, 260–262.

Schwalb A., Bouffard D., Ozersky T., Boegman L. & Smith R.E.H. (2013) Impacts of hydrodynamics and benthic communities on phytoplankton distributions in a large, dreissenid-colonized lake (Lake Simcoe, Ontario, Canada). *Inland Waters* **3**, 269–284.

Schwalb A.N., Bouffard D., Boegman L., Leon L., Winter J.G., Molot L.A., *et al.* (2014) 3D modelling of

dreissenid mussel impacts on phytoplankton in a large lake supports the nearshore shunt hypothesis and the importance of wind-driven hydrodynamics. *Aquatic Sciences* **77**, 95–114.

Smith R.E.H.H., Hiriart-Baer V.P., Higgins S.N., Guildford S.J. & Charlton M.N. (2005) Planktonic Primary Production in the Offshore Waters of Dreissenid-infested Lake Erie in 1997. *Journal of Great Lakes Research* **31**, 50–62.

Smith R.E.H.H., Parrish H.C., Vid D., Depew C., Hadouani A.G., Parrish C.C., *et al.* (2007) Spatial patterns of seston concentration and biochemical composition between nearshore and offshore waters of a Great Lake. *Freshwater Biology* **52**, 2196–2210.

Steffen M.M., Belisle B.S., Watson S.B., Boyer G.L., Wilhelm S.W. & Erie L. (2014) Status , causes and controls of cyanobacterial blooms in Lake Erie. *Journal of Great Lakes Research* **40**, 215–225.

Stewart T.W. & Lowe R.L. (2008) Benthic Algae of Lake Erie (1865-2006): A Review of Assemblage Composition, Ecology, and Causes and Consequences of Changing Abundance. *The Ohio Journal of Science* **108**, 82–94.

Stewart T.W., Miner J.G. & Lowe R.. (1998) Quantifying mechanisms for zebra mussel effects on benthic macroinvertebrates: organic matter production and shell-generated habitat. *Journal of the North American Benthological Society* **17**, 81–94.

Stoeckmann A. (2003) Physiological energetics of Lake Erie dreissenid mussels: a basis for the displacement of Dreissena polymorpha by Dreissena bugensis. *Canadian Journal of Fisheries and Aquatic …* **60**, 126–134.

Stoeckmann A.M. & Garton D.W. (1997) A seasonal energy budget for zebra mussels (Dreissena polymorpha) in western Lake Erie. *Canadian Journal of Fisheries and Aquatic Sciences* **54**, 2743–2751.

Stoeckmann A.M., Garton D.W. & Stoeckmann a N.N.M. (2011) Flexible Energy Allocation in Zebra Mussels (Dreissena polymorpha) in Response to Different Environmental Conditions Flexible energy allocation in zebra mussels (Dreissena polymorpha) in response to different environmental conditions. *Chicago Journals* **20**, 486–500.

Stumpf R.P., Wynne T.T., Baker D.B. & Fahnenstiel G.L. (2012) Interannual variability of cyanobacterial blooms in Lake Erie. *PLoS ONE* **7**.

Taylor W.D. (2010) Nature of dissolved P regenerated by plankton: Implications for the ssPO4 radiobioassay and for the nature of dissolved P. *Aquatic Sciences* **72**, 13–20.

Tomlinson L.M., Auer M.T., Bootsma H.A. & Owens E.M. (2010) The Great Lakes Cladophora Model : Development , testing , and application to Lake Michigan. *Journal of Great Lakes Research* **36**, 287–297.

Tyner E.H., Bootsma H.A. & Lafrancois B.M. (2015) Dreissenid metabolism and ecosystem-scale effects as revealed by oxygen consumption. *Journal of Great Lakes Research* **41**, 27–37.

Valipour R., Bouffard D. & Boegman L. (2015) Parameterization of bottom mixed layer and logarithmic layer heights in central Lake Erie. *Journal of Great Lakes Research* **41**, 707–718.

Valipour R., León L.F., Depew D., Dove A. & Rao Y.R. (2016) High-resolution modeling for development of nearshore ecosystem objectives in eastern Lake Erie. *Journal of Great Lakes Research* **42**, 1241–1251.

Valipour R., Rao Y.R., León L.F. & Depew D. (2018) Nearshore-offshore exchanges in multi-basin coastal waters: Observations and three-dimensional modeling in Lake Erie. *Journal of Great Lakes*

Research.

Vanderploeg H.A., Sarnelle O., Liebig J.R., Morehead N.R., Robinson S.D., Johengen T.H., *et al.* (2017) Seston quality drives feeding, stoichiometry and excretion of zebra mussels. *Freshwater Biology* **62**, 664–680.

Venier C., Figueiredo da Silva J., McLelland S.J., Duck R.W. & Lanzoni S. (2012) Experimental investigation of the impact of macroalgal mats on flow dynamics and sediment stability in shallow tidal areas. *Estuarine, Coastal and Shelf Science* **112**, 52–60.

Warner D.M., Lesht B.M., Great U., Science L. & Arbor A. (2015) Relative importance of phosphorus , invasive mussels and climate for patterns in chlorophyll a and primary production in Lakes Michigan and Huron. *Freshwater Biology* **60**, 1029–1043.

Wiles P.J., Rippeth T.P., Simpson J.H. & Hendricks P.J. (2006) A novel technique for measuring the rate of turbulent dissipation in the marine environment. *Geophysical Research Letters* **33**, 1–5.

Wilson K.A., Howell E.T. & Jackson D.A. (2006) Replacement of Zebra Mussels by Quagga Mussels in the Canadian Nearshore of Lake Ontario: the Importance of Substrate, Round Goby Abundance, and Upwelling Frequency. *J. Great Lakes Res. Internat. Assoc. Great Lakes Res* **32**, 11–28.

Winter J.G., Palmer M.E., Howell E.T. & Young J.D. (2015) Long term changes in nutrients, chloride, and phytoplankton density in the nearshore waters of Lake Erie. *Journal of Great Lakes Research* **41**, 145–155.

Worsfold P.J., Gimbert L.J., Mankasingh U., Omaka O.N., Hanrahan G., Gardolinski P.C.F.C., *et al.* (2005) Sampling, sample treatment and quality assurance issues for the determination of phosphorus species in natural waters and soils. *Talanta* **66**, 273–293.

Worsford P., McKelvie I., Monbet P., Worsfold P., McKelvie I. & Monbet P. (2016) Determination of phosphorus in natural waters: A historical review. *Analytica Chimica Acta* **918**, 8–20.

Wüest A. & Lorke A. (2003) Small-scale hydrodynamics in lakes. *Annual Review of Fluid Mechanics* **35**, 373–412.

Yu N. & Culver D.A. (1999) Estimating the effective clearance rate and refiltration by zebra mussels, Dreissena polymorpha, in a stratified reservoir. *Freshwater Biology* **41**, 481–492.

Yurista P.M., Kelly J.R., Miller S. & Alstine J. Van (2012a) Lake Ontario: Nearshore conditions and variability in water quality parameters. *Journal of Great Lakes Research* **38**, 133–145.

Yurista P.M., Kelly J.R., Miller S.E. & Van Alstine J.D. (2012b) Water quality and plankton in the united states nearshore waters of Lake Huron. *Environmental Management* **50**, 664–678.

Yurista P.M., Kelly J.R. & Scharold J. V. (2016) Great Lakes nearshore-offshore: Distinct water quality regions. *Journal of Great Lakes Research* **42**, 375–385.

Zhang H., Culver D.A. & Boegman L. (2008) A two-dimensional ecological model of Lake Erie: Application to estimate dreissenid impacts on large lake plankton populations. *Ecological Modelling* **214**, 219–241.

Zhang H., Culver D.A. & Boegman L. (2011) Dreissenids in Lake Erie: An algal filter or a fertilizer? *Aquatic Invasions* **6**, 175–194.

Zulkifly S.B., Graham J.M., Young E.B., Mayer R.J., Piotrowski M.J., Smith I., *et al.* (2013) The Genus Cladophora Kützing (Ulvophyceae) as a Globally Distributed Ecological Engineer. *Journal of Phycology* **49**, 1–17.

Appendix A: Chapter 2 tables and figures

Table A1.Means and standard errors (in brackets) of *Cladophora* biomass, vertical attenuation coefficient (Kd), and SRP concentration at FW, M, and FE stations in 2013 and 2014. *Cladophora* and mussel data from Alice Dove (Environment Canada).

	FW		M		FE	
	Shallow	Deep	Shallow	Deep	Shallow	Deep
Mussel biomass (g/m^2)	833.66 (330.69)	868.18 (139.03)	879.98 (326.88)	565.94 (153.81)	432.15 (165.31)	533.97 (184.32)
Early Season *Cladophora* Biomass (g/m^3)	17.3 (14.3)	0.189 (0.189)	0.00 (0)	0.00 (0)	5.25 (5.25)	0 (0)
Late Season *Cladophora* biomass (g/m^3)	33.9 (14.6)	1.32 (1.32)	5.39 (4.37)	0 (0)	42.7 (37.1)	0.0838 (0.0838)
Kd (m^{-1})	0.41 (0.06)	0.30 (0.02)	0.50 (0.09)	0.30 (0.04)	0.40 (0.05)	0.28 (0.02)
SRP (µg/L)	2.90 (0.22)	2.78 (0.18)	4.80 (0.39)	3.25 (0.30)	2.48 (0.21)	2.53 (0.16)

1

Table A2. Mean and 95% confidence intervals for water quality variables in the surface and near-bottom samples in the (a) FW, (b) M, and (c) FE surface and bottom samples at shallow and deep stations in the early and late parts of the sampling season.

(a) Far-West

	Shallow				Deep			
	surface		Bottom		surface		Bottom	
mean	Early	Late	Early	Late	Early	Late	Early	Late
SC	325	284	319	287	290	285	287	290
CI	299-350	281-287	287-351	281-293	275-305	281-288	267-308	283-297
Temp	15.9	21.9	14.9	21.4	13.2	20.3	9.4	17.9
CI	14.9-17	18.5-25.4	13-16.9	18.7-24.1	8.3-18	17.6-23	4.6-14.2	16.7-19
Chla	1.44	1.34	1.57	1.15	0.67	2.27	0.56	1.36
CI	0.5-2.37	1.23-1.44	1.02-2.12	0.8-1.49	0.39-0.94	0.91-3.64	0.04-1.07	0.3-2.42
PP	3.63	4.27	3.3	3.62	1.74	4.55	1.41	3.71
CI	1.97-5.29	2.98-5.55	2.24-4.37	2.85-4.38	1.13-2.36	1.16-7.93	1.01-1.8	0.98-6.44
SRP	2.49	3.4	2.21	3.21	1.29	3.27	1.67	3.96
CI	1.15-3.84	2.95-3.84	1.81-2.6	1.92-4.49	0.39-2.18	2.74-3.8	0.69-2.65	2.73-5.19
NH_4	2.86	15.98	2.69	18.78	0.84	13	11.52	35
CI	-16.19	-43.04	1.65-3.74	4.71-32.84	0.03-1.66	2.64-23.36	1.45-21.59	24.06-45.94

(b) Mouth

	Shallow				Deep			
	surface		Bottom		surface		Bottom	
mean	Early	Late	Early	Late	Early	Late	Early	Late
SC	325	316	305	316	321	291	286	296
CI	305-345	290-343	295-314	275-357	282-361	285-298	273-299	288-305
Temp	15.5	20.7	13.2	20.4	12	19.7	8.6	20
CI	13.7-17.4	17.8-23.6	10.8-15.7	17.7-23.1	7.5-16.5	16.9-22.4	5.1-12.1	17.5-22.5
Chla	1.38	2.27	0.91	1.59	1.46	1.71	0.99	1.1
CI	0.58-2.18	1.19-3.34	-2.07	0.17-3.01	0.11-2.82	0.72-2.7	-2.05	-2.42
PP	4.61	6.05	4.3	4.75	4.16	4.14	2.78	4
CI	1.88-7.35	3.65-8.45	2.65-5.95	1.48-8.03	2.18-6.15	2.07-6.21	2.32-3.23	1.93-6.08
SRP	4.02	5.31	4.59	5.4	1.81	3.15	1.84	3.76
CI	1.96-6.09	2.28-8.34	2.48-6.71	2.49-8.32	0.29-3.32	0.77-5.53	0.64-3.05	1.71-5.8
NH_4	12.19	41.61	19.88	36.77	17.16	14.54	10.25	30.98
CI	6.3-18.09	15.03-68.19	7.4-32.36	7.33-66.22	-58.11	0.5-28.59	1.59-18.91	4.17-57.8

(c) Far-East

	Shallow				Deep			
	surface		Bottom		surface		Bottom	
mean	Early	Late	Early	Late	Early	Late	Early	Late
SC	291	290	300	289	291	288	287	288
CI	283-300	287-293	278-322	288-290	282-300	286-289	281-293	288-289
Temp	17.7	20.3	17	19.5	14.2	21.3	10.2	20.6
CI	17.2-18.2	17.8-22.8	16.5-17.6	16.9-22.1	10.5-17.8	19-23.6	5.6-14.7	18.3-22.8
Chla	0.55	1.5	1	2.19	0.69	1.73	0.67	1.09
CI	0.45-0.65	0.86-2.14	0.05-1.96	0.49-3.9	0.44-0.95	1.4-2.06	0.38-0.96	0.94-1.23
PP	2.22	4.65	3.18	7.8	1.89	4.43	1.92	4.06
CI	1.72-2.71	2.78-6.52	1.41-4.95	5.3-10.3	1.59-2.18	4.3-4.56	1.44-2.41	3.49-4.63
SRP	1.74	2.97	2.37	3.36	1.31	3.04	1.51	3.59
CI	1.49-1.99	2.08-3.85	1.48-3.26	2.77-3.95	0.71-1.9	2.99-3.09	0.77-2.24	3.4-3.78
NH_4	-1.52	22.51	10.16	21.12	8.57	12.6	7.49	30.65
CI	-3.03	14.32-30.7	-41.12	10.34-31.9	-45.8	3.77-21.42	3.04-11.95	27.05-34.25

Table A3. Means and 95% confidence intervals for syringe and tower samples in shallow and deep stations in the early and late parts of the sampling season at the four sampling transects.

	FW		M		NM		FE	
	Syringe	Tower	Syringe	Tower	Syringe	Tower	Syringe	Tower
Early/Shallow								
mean	2.420	2.571	4.403	3.428	3.452	3.087	2.367	2.018
(CI)	(0.762)	(0.000)	(1.010)	(0.581)	(1.044)	(0.625)	(0.401)	(0.284)
Early/Deep								
(mean)	2.174	2.304	3.424	3.409	2.212	2.614	2.224	1.995
(CI)	(0.343)	(0.229)	(0.771)	(0.364)	(0.598)	(0.451)	(0.202)	(0.175)
Late/Shallow								
(mean)	2.937	1.099	6.493	3.706	2.753	2.267	1.155	3.008
(CI)	(0.564)	(0.065)	(1.359)	(0.613)	(0.000)	(0.220)	NA	NA
Late/Deep								
(mean)	3.659	2.599	3.398	1.738	NA	NA	1.294	3.220
(CI)	NA	NA	NA	NA	NA	NA	(0.200)	(0.233)

Table A4. Observed and expected counts of syringe and tower samples categorized by ≤2µg/L and >2µg/L at from either early or late season and either distal or proximate samples.

	Number of Syringe samples ≤2µg/L		Number of Syringe samples>2µg/L		Number of Tower samples ≤2µg/L		Number of Tower samples>2µg/L	
	Observed	Expected	Observed	Expected	Observed	Expected	Observed	Expected
Early/Distal	32	32	10	10	37	29	5	13
Late/Distal	19	15	1	5	9	14	11	6
Early/Proximate	17	24	14	7	25	22	6	9
Late/Proximate	14	11	1	4	4	10	11	5

Table A5. Observed distribution of binned SRP data by concentration compared to the expected Poisson distribution of syringe and tower sample in either early or late season and at distal or proximate sites to the mouth of the Grand River.

	Syringe/ Early/ Proximate		Syringe/ Early/ Distal		Tower/ Early/ Proximate		Tower/ Early/ Distal		Syringe/ Late/ Proximate		Syringe/ Late/ Distal		Tower/ Late/ Proximate		Tower/ Late/ Distal	
SRP (µg/L)	Obs	Exp	Obs	Exp	Obs	Exp	Obs	Exp	Obs	Exp	Obs	Exp	Obs	Exp	Obs	Exp
0 to 1	0	4	0	3	0	4	0	4	0	1	0	0	1	3	0	3
1 to 2	14	9	10	8	6	8	5	10	1	2	1	2	10	5	11	6
2 to 3	9	8	18	10	16	8	24	11	2	3	4	3	0	4	3	5
3 to 4	4	5	1	9	9	6	7	9	10	3	8	4	3	2	4	3
4 to 5	4	3	8	6	0	3	6	5	1	2	2	4	1	1	1	2
5 to 6	0	1	2	3	0	1	0	2	1	1	1	3	0	0	1	1
6 to 7	0	0	2	1	0	0	0	1	0	1	1	2	0	0	0	0
7 to 8	0	0	1	1	0	0	0	0	0	0	1	1	0	0	0	0
>=9	0	0	0	0	0	0	0	0	0	0	2	0	0	0	0	0

Table A6. ANOVA results for effects of transect (an index of proximity to the Grand River), season of sampling (early/late), and station depth (shallow/deep). Data were pooled across sampling depths (surface and bottom).

Sample	factors	F	p	Significant Interactions		
				Interaction	F	p
Syringe / surface	proximity	4.29	0.00			
	season	6.22	0.02			
	station depth	0.00	NA			
Syringe / bottom	proximity	3.49	0.01			
	season	5.18	0.03			
	station depth	0.00	NA			
Tower / surface	proximity	4.45	0.00	prox/season	2.75	0.04
	season	5.31	0.03			
	station depth	0.00	NA			
Tower / bottom	proximity	3.62	0.01			
	season	8.31	0.01			
	station depth	0.00	NA			

Appendix B: Chapter 3 tables and figures

Table B1. Data for stations showing an absolute specific conductivity difference between surface and near-bottom above threshold (10µS/cm), and corresponding temperature differences.

Date	Station		|SC Diff|≥10	
Surface greater				
			Δ T	Δ SC
May-13	456	M	6.224	56.35
May-13	1340	M	5.095	38.75
Jun-13	456	M	3.286	48
Jun-13	1340	M	2.469	40.27
May-15	456	M	2.373	57.46
Jun-15	456	M	2.391	62.76
Bottom greater				
Jun-14	1355	FW	3.275	-20.94

Table B2. Frequency of above-threshold occurrence between surface and bottom samples of water quality variables, chla, and nutrients under presence or absence of stratification.

		Stratified conditions (differences above threshold)					Unstratified Conditions (differences above threshold)					Total number of stratification/WQ samples
		N stratified	surface greater than bottom relative to the total number of samples		Bottom greater than surface relative to the total number of samples		N un-stratified	surface greater than bottom relative to the total number of samples		Bottom greater than surface relative to the total number of samples		
	Absolute Difference (surface minus bottom) Threshold		n	f	n	f		n	f	n	f	
Chla	≥1µg/L	4	3	0.0588	1	0.0196	3	2	0.0392	1	0.0196	51
SC	≥10µS/cm	6	5	0.1136	1	0.0227	1	1	0.0227	0	0	44
T	≥1°C	21	21	0.4773	0	0	2	2	0.0455	0	0	44
SRP	≥0.5µg/L	6	1	0.0185	5	0.0926	2	0	0	2	0.0370	54
NH_4	≥5µg/L	39	12	0.222	27	0.500	9	4	0.0741	5	0.0926	54

Note: total number of samples reflects sample data that had both water column profiles to be able to make a decision on presence or absence of stratification and also contained data on specific conductivity, temperature, chla, SRP, or NH_4

Table B3. Observed no depletion, predicted no depletion (non-significant, p>0.05)

Date	Sampling date	Stations	TG:TD	R^2	R
2014FP	Jun-14	1351	5.29	0.384	0.620
2014FP	Jun-14	1341	1.31	0.0475	0.218
2014FP	Oct-14	456	3.21	0.0631	0.251
2015 YSI	May-15	1351	5.29		

Table B4. observed no depletion, predicted depletion (non-significant, p>0.05)

Date	Sampling date	Stations	TG:TD	R^2	R
2014FP	Jun-14	1352	0.160	0.190	0.436
2014FP	Jun-14	1340	0.0756	0.0517	0.227
2014FP	Aug-14	1353	0.0249	3.31E-04	0.018
2014FP	Aug-14	1341	0.0283	0.156	0.395
2013 YSI	May-13	1349	0.0727	0.264	0.514
2013 YSI	Jun-13	1355	0.453	0.0211	0.145
2014 YSI	Jun-14	1350	0.0228	0.0656	0.256
2014 YSI	Jun-14	1340	0.0756	0.0829	0.288
2014 YSI	Aug-14	456	1.54E-06	0.199	0.446
2014 YSI	Aug-14	1353	0.0249	0.0221	0.149
2014 YSI	Aug-14	1341	0.0283	0.0934	0.306

Table B5. Supplementary data for Table 3.7, detailing values used to estimate assimilation flux of chla. This includes data on near-bottom Chl a concentrations and their corresponding heights near-bottom, estimated mussel assimilation of Chl a based on the relationship found in Vanderploeg *et al.* (2017), and mussel biomass (2013 and 2014 data from A. Dove, Environment Canada). Data is shown for calculations from both YSI and FluoroProbe profiles.

Station	Date	Height	Chla concentration at this height	Chla assimilation rate	Mussel biomass	Assimilation flux estimates	Evidence of observed significant (p<0.05) depletion (*)
YSI	2013	closest to 2.5cmab (m)	(ug/L)	(ug/mgDW/h)	Mussel biomass (g/m2)	Jchla (g/m2/d)	
1274	August	0	1.1	7.94E-03	64.04	1.22E-02	
1340	August	0.029	1.5	1.01E-02	63.98	1.55E-02	
456	August	0.026	1.5	1.01E-02	47.26	1.15E-02	
456	August	0.021	3.4	2.04E-02	47.26	2.31E-02	
12	August	0.027	2.3	1.44E-02	36.78	1.27E-02	*
12	August	0.02	1.5	1.01E-02	36.78	8.92E-03	*
1353	August	0.046	2.5	1.55E-02	32.22	1.20E-02	*
1353	August	0	1.7	1.12E-02	32.22	8.65E-03	*
1356	August	0.027	1.1	7.94E-03	42.68	8.13E-03	*
1356	August	0.021	1.8	1.17E-02	42.68	1.20E-02	*
1351	August	0.027	1.8	1.17E-02	14.11	3.97E-03	
1351	August	0.024	2.8	1.71E-02	14.11	5.80E-03	
1350	August	0.015	2	1.28E-02	48.40	1.49E-02	
1349	August	0.015	1.7	1.12E-02	33.58	9.01E-03	
1349	August	0.02	2.8	1.71E-02	33.58	1.38E-02	
1354	August	0.026	2	1.28E-02	72.58	2.23E-02	

1354	August	0.023	2	1.28E-02	72.58	2.23E-02	
1274	October	0.036	3.6	2.14E-02	64.04	3.30E-02	*
1274	October	0.024	2.8	1.71E-02	64.04	2.63E-02	*
1354	October	0.037	1.9	1.23E-02	72.58	2.14E-02	
1354	October	0.008	1.5	1.01E-02	72.58	1.76E-02	
1355	October	0.024	3	1.82E-02	85.24	3.72E-02	
1355	October	0.036	2.6	1.60E-02	85.24	3.28E-02	
1356	October	0.022	4.1	2.41E-02	42.68	2.47E-02	*
1356	October	0.048	1.8	1.17E-02	42.68	1.20E-02	*
1351	October	0.016	23.2	1.27E-01	14.11	4.31E-02	
1352	October	0.03	5.944	3.41E-02	41.91	3.43E-02	
1352	October	0.005	5.679	3.27E-02	41.91	3.29E-02	
1350	October	0.018	6.9	3.93E-02	48.40	4.56E-02	
1350	October	0.042	2.3	1.44E-02	48.40	1.67E-02	
1340	October	0.026	2.7	1.66E-02	63.98	2.55E-02	
1340	October	0.024	3.4	2.04E-02	63.98	3.13E-02	
456	October	0.016	9.5	5.33E-02	47.26	6.05E-02	
456	October	0.024	4.3	2.52E-02	47.26	2.86E-02	

YSI	2014	height closest to 2.5cmab	chla	Achla	Mussel biomass (g/m2)	Jchla (g/m2/d)	
1354	June	0.028	2.6	1.60E-02	126.39	4.87E-02	
1354	June	0.021	1.8	1.17E-02	126.39	3.56E-02	*
1355	June	0.029	0.9	6.86E-03	36.76	6.05E-03	*
1355	June	0.022	1.3	9.02E-03	36.76	7.96E-03	*
1356	June	0.025	2.7	1.66E-02	102.05	4.06E-02	*
1356	June	0.037	3.1	1.87E-02	102.05	4.59E-02	
1352	June	0.023	1.6	1.06E-02	40.30	1.03E-02	*
1352	June	0.012	1.7	1.12E-02	40.30	1.08E-02	
1350	June	0.027	1.8	1.17E-02	4.10	1.15E-03	

1350	June	0.023	2	1.28E-02	4.10	1.26E-03	
1349	June	0.027	1.2	8.48E-03	3.87	7.88E-04	*
1349	June	0.026	1.3	9.02E-03	3.87	8.39E-04	
1340	June	0.014	1.2	8.48E-03	125.18	2.55E-02	
1340	June	0.028	2.7	1.66E-02	125.18	4.98E-02	
456	June	0.023	4.8	2.79E-02	48.53	3.25E-02	
456	June	0.027	4.7	2.74E-02	48.53	3.19E-02	
1341	June	0.038	6.8	3.87E-02	8.57	7.97E-03	
1341	June	0.022	6.1	3.49E-02	8.57	7.19E-03	
1353	June	0.022	2.5	1.55E-02	13.98	5.20E-03	
1353	June	0.029	2.1	1.33E-02	13.98	4.48E-03	
1351	June	0.02	1.4	9.56E-03	4.10	9.41E-04	
1351	June	0.015	1.6	1.06E-02	4.10	1.05E-03	
1274	June	0.019	1.6	1.06E-02	26.62	6.80E-03	
1274	June	0.043	1.5	1.01E-02	26.62	6.45E-03	
1274	August	0.021	3.4	2.04E-02	26.62	1.30E-02	*
1274	August	0.023	3.8	2.25E-02	26.62	1.44E-02	*
456	August	0.043	5.8	3.33E-02	48.53	3.88E-02	
456	August	0.023	2.8	1.71E-02	48.53	1.99E-02	
1353	August	0.015	3.6	2.14E-02	13.98	7.20E-03	*
1353	August	0.028	2.2	1.39E-02	13.98	4.66E-03	*
1341	August	0.035	6.4	3.66E-02	8.57	7.52E-03	
1341	August	0.021	1.9	1.23E-02	8.57	2.52E-03	
1356	September	0.021	2.7	1.66E-02	102.05	4.06E-02	
1356	September	0.04	3.4	2.04E-02	102.05	4.99E-02	
1274	October	0.031494	1.386261	9.49E-03	26.62	6.06E-03	
456	October	0.02417	2.284241	1.43E-02	48.53	1.67E-02	

YSI	2015	height closest to 2.5cmab	chla	Achla	Mussel biomass (g/m2)	Jchla (g/m2/d)

456	May	0.022	1.4	9.56E-03	197.17	4.52E-02	
456	May	0.033	1.2	8.48E-03	197.17	4.01E-02	
456	May	0.025	1	7.40E-03	197.17	3.50E-02	
456	May	0.015	0.7	5.78E-03	197.17	2.74E-02	
456	May	0.029	1.9	1.23E-02	197.17	5.80E-02	
1350	May	0.022	1	7.40E-03	87.94	1.56E-02	
1350	May	0.02	1.4	9.56E-03	87.94	2.02E-02	
1350	May	0.023	0.6	5.24E-03	87.94	1.11E-02	
1350	May	0.022	0.2	3.08E-03	87.94	6.50E-03	
1350	May	0.024	0.7	5.78E-03	87.94	1.22E-02	
1355	May	0.026	0.5	4.70E-03	143.60	1.62E-02	
1355	May	0.021	0.5	4.70E-03	143.60	1.62E-02	
1355	May	0.024	0.5	4.70E-03	143.60	1.62E-02	
1355	May	0.023	-0.1	1.46E-03	143.60	5.03E-03	
456	May	0.025	0.8	6.32E-03	197.17	2.99E-02	
456	May	0.022	0.5	4.70E-03	197.17	2.22E-02	*
456	May	0.027	0.8	6.32E-03	197.17	2.99E-02	
456	May	0.021	0.7	5.78E-03	197.17	2.74E-02	*
456	May	0.024	0.6	5.24E-03	197.17	2.48E-02	
456	May	0.025	0.7	5.78E-03	197.17	2.74E-02	

FP	2013	height closest to 2.5cmab (m)	chla (ug/L)	Achla (ug/mgDW/h)	Mussel biomass (g/m2)	Jchla (g/m2/d)	
456	May	0.02	0.86	6.64E-03	47.26	7.54E-03	*
1340	May	0.03	3.31	1.99E-02	63.98	3.05E-02	*
1341	May	0.03	1.19	8.43E-03	24.10	4.87E-03	
1274	May	1.95	1.79	1.17E-02	64.04	1.79E-02	
1341	June	0	2.29	1.44E-02	24.10	8.31E-03	
456	June	0	0	2.00E-03	47.26	2.27E-03	*
1274	June	0.01	1.77	1.16E-02	64.04	1.78E-02	*

1350	June	0.02	0.02	2.11E-03	48.40	2.45E-03	*
1350	June	0.01	0.09	2.49E-03	48.40	2.89E-03	
1351	June	4.57	1.26	8.80E-03	14.11	2.98E-03	
1344	June	2.4	1.93	1.24E-02	48.69	1.45E-02	
FP	2014	height closest to 2.5cmab	chla	Achla	Mussel biomass (g/m2)	Jchla (g/m2/d)	
1274	June	0.02	0.27	3.46E-03	26.62	2.21E-03	*
1274	June	0.03	0.69	5.73E-03	26.62	3.66E-03	*
1353	June	0	3.31	1.99E-02	13.98	6.67E-03	*
1353	June	0.01	1.75	1.15E-02	13.98	3.84E-03	*
1354	June	0.04	0.98	7.29E-03	126.39	2.21E-02	*
1354	June	0.03	0.39	4.11E-03	126.39	1.25E-02	*
1355	June	0.01	0.28	3.51E-03	36.76	3.10E-03	*
1355	June	0.04	0.27	3.46E-03	36.76	3.05E-03	*
1356	June	0.01	3.65	2.17E-02	102.05	5.32E-02	*
1356	June	0.05	3.32	1.99E-02	102.05	4.88E-02	
1351	June	0	1.09	7.89E-03	4.10	7.76E-04	
1351	June	0.02	0.57	5.08E-03	4.10	5.00E-04	
1352	June	0.01	1.86	1.20E-02	40.30	1.16E-02	
1352	June	0.04	1.43	9.72E-03	40.30	9.40E-03	
1350	June	0	0.7	5.78E-03	48.62	6.74E-03	*
1350	June	0.03	1.12	8.05E-03	48.62	9.39E-03	
1349	June	0	0.31	3.67E-03	3.87	3.42E-04	*
1340	June	0	0.23	3.24E-03	125.18	9.74E-03	
1340	June	0	0.24	3.30E-03	125.18	9.90E-03	
456	June	0	1.5	1.01E-02	48.53	1.18E-02	
456	June	0.05	0.35	3.89E-03	48.53	4.53E-03	
1341	June	0.03	1.6	1.06E-02	8.57	2.19E-03	
1341	June	0.01	1.06	7.72E-03	8.57	1.59E-03	

1274	August	0.03	1.52	1.02E-02	26.62	6.52E-03	
1274	August	0	0.88	6.75E-03	26.62	4.31E-03	
456	August	0	0.54	4.92E-03	48.53	5.73E-03	*
456	August	0	1.99	1.27E-02	48.53	1.48E-02	
1353	August	0	1.29	8.97E-03	13.98	3.01E-03	
1353	August	0	0.8	6.32E-03	13.98	2.12E-03	
1341	August	0	1.17	8.32E-03	8.57	1.71E-03	
1341	August	0.03	6.7	3.82E-02	8.57	7.86E-03	
1356	September	0	31.65	1.73E-01	102.05	4.23E-01	
1356	September	0	19.64	1.08E-01	102.05	2.65E-01	
1274	October	0.02	0.41	4.21E-03	26.62	2.69E-03	*
456	October	0.02	0.46	4.48E-03	48.53	5.22E-03	

Table B6. Comparison of height of mixing (Hmix), height of stratification (Hstrat), and height of water column (HWC) used for estimating TG and TD. Highlighted cells indicate the height used, and stations where stratification could not be determined due to instrument malfunction were not included.

Station	Date	Hmix	Hstrat	HWC
456	May-13	0.39	3.84	11.58
1340	May-13	0	5.68	9.11
1341	May-13	0	0.55	3.73
1274	May-13	0.64	0.39	4.26
1341	Jun-13	0	2.17	3.87
456	Jun-13	0	6.56	11.95
1274	Jun-13	0	2.49	4
1350	Jun-13	0	9.02	12.75
1350	Jun-13	0	3.25	12.7
1352	Jun-13	0	5.28	6.7
1351	Jun-13	0.1	1.34	3.6
1351	Jun-13	0.04	1.77	3.88
1344	Jun-13	0	13.51	17.84
1344	Jun-13	0	13.8	17.96
1342	Jun-13	0.01	1.06	7
1342	Jun-13	0.11	4.52	6.97
1353	Aug-13	0	3.31	3.92
1353	Aug-13	0	3.38	4.13
1356	Aug-13	0	7.14	18.53
1356	Aug-13	0	3.01	18.5
1351	Aug-13	0	0	3.64
1351	Aug-13	0	1.95	3.65
1350	Aug-13	0	8.07	12.39
1350	Aug-13	0	11.52	12.41
1349	Aug-13	0	7.49	16.2
1349	Aug-13	0	3.13	16.22
1354	Aug-13	0	1.54	7.12
1354	Aug-13	0	4.23	7.06
1274	Oct-13	0.21	1.8	4.08
1274	Oct-13	0.13	3.56	4
1354	Oct-13	1	2.72	7.17
1354	Oct-13	0.11	2.71	7.13
1355	Oct-13	0.08	9.55	12.59
1355	Oct-13	0.94	12.09	12.56

1356	Oct-13	0.2	18.64	18.73
1356	Oct-13	0	9.66	18.6
1351	Oct-13	0.06	0.95	3.49
1351	Oct-13	0.21	2.31	3.45
1352	Oct-13	1.1	3.34	6.86
1352	Oct-13	1.2	3.67	6.81
1350	Oct-13	0.13	1.64	12.68
1350	Oct-13	0.76	3.44	12.61
1340	Oct-13	0.03	6.52	9.63
1340	Oct-13	0.49	8.56	9.68
456	Oct-13	1.2	8.5	12.4
456	Oct-13	0.25	1.2	12.38

Station	Date	Hmix	Hstrat	HWC
1274	Jun-14	0	3.02	4.24
1274	Jun-14	0.01	0.14	4.3
1353	Jun-14	0	2.91	4.79
1353	Jun-14	0	3.32	4.78
1354	Jun-14	0	4.1	8.04
1354	Jun-14	0.11	3.95	7.75
1355	Jun-14	0	10.13	12.04
1355	Jun-14	0	10.78	11.99
1356	Jun-14	0.89	15.26	18.99
1356	Jun-14	0.66	9.06	18.99
1351	Jun-14	0.18	1.33	3.66
1351	Jun-14	0.67	2.83	3.81
1352	Jun-14	0.01	5.6	6.54
1352	Jun-14	0	6.47	7.12
1350	Jun-14	0	0.39	12.79
1350	Jun-14	0	9.23	13.04
1349	Jun-14	0	7.88	16.19
1340	Jun-14	0	4.02	9.97
1340	Jun-14	0	2.22	9.94
456	Jun-14	0	8.84	12.04
456	Jun-14	0	0.98	11.77
1341	Jun-14	0	2.51	4.35
1341	Jun-14	0	1.15	4.35
1274	Aug-14	0	0.79	4.09
1274	Aug-14	0	0.93	4.07
456	Aug-14	0	11.86	11.89
456	Aug-14	0	9.91	11.9

1353	Aug-14	0	4.47	5.08
1353	Aug-14	0	4.38	5.11
1341	Aug-14	0	4.08	4.58
1341	Aug-14	0	3.62	4.68
1356	Oct-14	0	14.05	18.92
1356	Oct-14	0	0.09	18.83
1274	Oct-14	0.11	3.16	4.48
456	Oct-14	0.36	3.04	11.64

Station	Date	Hmix	Hstrat	HWC
456	May-15	2.161	10.659	10.704
456	May-15	3.238	10.128	10.737
456	May-15	1.987	9.905	10.625
456	May-15	1.221	10.132	10.576
456	May-15	0.719	10.177	10.557
456	May-15	1.291	9.597	10.773

Appendix C: Chapter 4 tables and figures

Table C1. Estimated PP flux downward using the relationship found in Dayton *et al.* (2014) and Vanderploeg *et al.* (2017).

YSI2013	Sampling date	height closest to 2.5cmab (m)	chla (µg/L)	Mussel biomass (g/m2)	PP (µg/L)	Vanderploeg ($g/m^2/d$)	Dayton ($g/m^2/d$)	Diffusive flux ($g/m^2/d$)
1274	Aug-13	0	1.1	64.0	3.9	4.37E-02	9.82E-02	
1340	Aug-13	0.029	1.5	64.0	5.4	5.56E-02	1.34E-01	
456	Aug-13	0.026	1.5	47.3	5.4	4.11E-02	9.88E-02	
456	Aug-13	0.021	3.4	47.3	12.2	8.28E-02	2.24E-01	
12	Aug-13	0.027	2.3	36.8	8.2	4.56E-02	1.18E-01	3.78E-02
12	Aug-13	0.02	1.5	36.8	5.4	3.20E-02	7.69E-02	1.29E-02
1353	Aug-13	0.046	2.5	32.2	9.0	4.30E-02	1.12E-01	-1.46E-02
1353	Aug-13	0	1.7	32.2	6.1	3.10E-02	7.64E-02	-5.88E-02
1356	Aug-13	0.027	1.1	42.7	3.9	2.92E-02	6.55E-02	-3.74E-02
1356	Aug-13	0.021	1.8	42.7	6.5	4.30E-02	1.07E-01	-1.68E-02
1351	Aug-13	0.027	1.8	14.1	6.5	1.42E-02	3.54E-02	
1351	Aug-13	0.024	2.8	14.1	10.0	2.08E-02	5.51E-02	
1350	Aug-13	0.015	2	48.4	7.2	5.33E-02	1.35E-01	
1349	Aug-13	0.015	1.7	33.6	6.1	3.23E-02	7.96E-02	
1349	Aug-13	0.02	2.8	33.6	10.0	4.95E-02	1.31E-01	
1354	Aug-13	0.026	2	72.6	7.2	7.99E-02	2.02E-01	
1354	Aug-13	0.023	2	72.6	7.2	7.99E-02	2.02E-01	
1274	Oct-13	0.036	3.6	64.0	12.0	1.10E-01	3.00E-01	-6.58E-05
1274	Oct-13	0.024	2.8	64.0	9.4	8.80E-02	2.33E-01	-4.63E-03
1354	Oct-13	0.037	1.9	72.6	6.4	7.14E-02	1.79E-01	
1354	Oct-13	0.008	1.5	72.6	5.0	5.88E-02	1.42E-01	

1355	Oct-13	0.024	3	85.2	10.0	1.25E-01	3.33E-01	
1355	Oct-13	0.036	2.6	85.2	8.7	1.10E-01	2.88E-01	
1356	Oct-13	0.022	4.1	42.7	13.7	8.27E-02	2.28E-01	2.09E-02
1356	Oct-13	0.048	1.8	42.7	6.0	4.02E-02	1.00E-01	-2.38E-03
1351	Oct-13	0.016	23.2	14.1	77.6	1.44E-01	4.26E-01	
1352	Oct-13	0.03	5.944	41.9	19.9	1.15E-01	3.24E-01	
1352	Oct-13	0.005	5.679	41.9	19.0	1.10E-01	3.10E-01	
1350	Oct-13	0.018	6.9	48.4	23.1	1.53E-01	4.34E-01	
1350	Oct-13	0.042	2.3	48.4	7.7	5.60E-02	1.45E-01	
1340	Oct-13	0.026	2.7	64.0	9.0	8.52E-02	2.25E-01	
1340	Oct-13	0.024	3.4	64.0	11.4	1.05E-01	2.83E-01	
456	Oct-13	0.016	9.5	47.3	31.8	2.02E-01	5.84E-01	
456	Oct-13	0.024	4.3	47.3	14.4	9.57E-02	2.64E-01	
YSI 2014								
1354	Jun-14	0.028	2.6	126.4	6.4	1.20E-01	3.15E-01	
1354	Jun-14	0.021	1.8	126.4	4.4	8.75E-02	2.18E-01	
1355	Jun-14	0.029	0.9	36.8	2.2	1.49E-02	3.17E-02	-2.99E-02
1355	Jun-14	0.022	1.3	36.8	3.2	1.96E-02	4.58E-02	-8.71E-03
1356	Jun-14	0.025	2.7	102.0	6.6	9.99E-02	2.64E-01	-1.09E-02
1356	Jun-14	0.037	3.1	102.0	7.6	1.13E-01	3.03E-01	-1.65E-03
1352	Jun-14	0.023	1.6	40.3	3.9	2.53E-02	6.17E-02	
1352	Jun-14	0.012	1.7	40.3	4.2	2.66E-02	6.56E-02	
1350	Jun-14	0.027	1.8	4.1	4.4	2.84E-03	7.07E-03	
1350	Jun-14	0.023	2	4.1	4.9	3.10E-03	7.85E-03	
1349	Jun-14	0.027	1.2	3.9	3.0	1.94E-03	4.45E-03	
1349	Jun-14	0.026	1.3	3.9	3.2	2.06E-03	4.82E-03	
1340	Jun-14	0.014	1.2	125.2	3.0	6.27E-02	1.44E-01	
1340	Jun-14	0.028	2.7	125.2	6.6	1.23E-01	3.24E-01	
456	Jun-14	0.023	4.8	48.5	11.8	8.00E-02	2.23E-01	
456	Jun-14	0.027	4.7	48.5	11.6	7.85E-02	2.18E-01	

1341	Jun-14	0.038	6.8	8.6	16.7	1.96E-02	5.58E-02	
1341	Jun-14	0.022	6.1	8.6	15.0	1.77E-02	5.01E-02	
1353	Jun-14	0.022	2.5	14.0	6.2	1.28E-02	3.35E-02	-1.92E-02
1353	Jun-14	0.029	2.1	14.0	5.2	1.10E-02	2.81E-02	-3.94E-02
1351	Jun-14	0.02	1.4	4.1	3.4	2.32E-03	5.50E-03	
1351	Jun-14	0.015	1.6	4.1	3.9	2.58E-03	6.28E-03	
1274	Jun-14	0.019	1.6	26.6	3.9	1.67E-02	4.08E-02	-4.08E-03
1274	Jun-14	0.043	1.5	26.6	3.7	1.59E-02	3.82E-02	-4.27E-03
1274	Aug-14	0.021	3.4	26.6	6.5	2.48E-02	6.70E-02	
1274	Aug-14	0.023	3.8	26.6	7.2	2.74E-02	7.49E-02	
456	Aug-14	0.043	5.8	48.5	11.0	7.39E-02	2.08E-01	
456	Aug-14	0.023	2.8	48.5	5.3	3.80E-02	1.01E-01	
1353	Aug-14	0.015	3.6	14.0	6.9	1.37E-02	3.73E-02	
1353	Aug-14	0.028	2.2	14.0	4.2	8.87E-03	2.28E-02	
1341	Aug-14	0.035	6.4	8.6	12.2	1.43E-02	4.06E-02	
1341	Aug-14	0.021	1.9	8.6	3.6	4.80E-03	1.21E-02	
1356	Oct-14	0.021	2.7	102.0	5.0	7.53E-02	1.99E-01	
1356	Oct-14	0.04	3.4	102.0	6.3	9.24E-02	2.50E-01	
1274	Oct-14	0.031494	1.386 261	26.6	2.6	1.12E-02	2.66E-02	
456	Oct-14	0.02417	2.284 241	48.5	4.2	3.10E-02	7.99E-02	
YSI 2015								
456	May-15	0.022	1.4	197.2	2.1	6.75E-02	1.60E-01	
456	May-15	0.033	1.2	197.2	1.8	5.98E-02	1.37E-01	
456	May-15	0.025	1	197.2	1.5	5.22E-02	1.14E-01	
456	May-15	0.015	0.7	197.2	1.0	4.08E-02	8.01E-02	
456	May-15	0.029	1.9	197.2	2.8	8.65E-02	2.17E-01	
1350	May-15	0.022	1	87.9	1.5	2.33E-02	5.10E-02	
1350	May-15	0.02	1.4	87.9	2.1	3.01E-02	7.14E-02	

1350	May-15	0.023	0.6	87.9	0.9	1.65E-02	3.06E-02	
1350	May-15	0.022	0.2	87.9	0.3	9.69E-03	1.02E-02	
1350	May-15	0.024	0.7	87.9	1.0	1.82E-02	3.57E-02	
1355	May-15	0.026	0.5	143.6	0.7	2.42E-02	4.17E-02	
1355	May-15	0.021	0.5	143.6	0.7	2.42E-02	4.17E-02	
1355	May-15	0.024	0.5	143.6	0.7	2.42E-02	4.17E-02	
1355	May-15	0.023	-0.1	143.6	-0.1	7.50E-03	-8.33E-03	
456	May-15	0.025	0.8	197.2	1.2	4.46E-02	9.15E-02	
456	May-15	0.022	0.5	197.2	0.7	3.32E-02	5.72E-02	-1.27E-02
456	May-15	0.027	0.8	197.2	1.2	4.46E-02	9.15E-02	
456	May-15	0.021	0.7	197.2	1.0	4.08E-02	8.01E-02	6.67E-03
456	May-15	0.024	0.6	197.2	0.9	3.70E-02	6.86E-02	
456	May-15	0.025	0.7	197.2	1.0	4.08E-02	8.01E-02	
FP 2013								
456	May-13	0.02	0.86	47.3	2.1	1.84E-02	3.86E-02	
1340	May-13	0.03	3.31	64.0	8.1	7.45E-02	2.01E-01	
1341	May-13	0.03	1.19	24.1	2.9	1.19E-02	2.72E-02	
1274	May-13	1.95	1.79	64.0	4.4	4.38E-02	1.09E-01	
1341	Jun-13	0	2.29	24.1	3.8	1.39E-02	3.58E-02	
456	Jun-13	0	0	47.3	0.0	3.78E-03	0.00E+00	
1274	Jun-13	0.01	1.77	64.0	3.0	2.96E-02	7.35E-02	
1350	Jun-13	0.02	0.02	48.4	0.0	4.08E-03	6.28E-04	
1350	Jun-13	0.01	0.09	48.4	0.2	4.82E-03	2.83E-03	
1351	Jun-13	4.57	1.26	14.1	2.1	4.97E-03	1.15E-02	
1344	Jun-13	2.4	1.93	48.7	3.2	2.42E-02	6.10E-02	
FP 2014								
1274	Jun-14	0.02	0.27	26.6	0.7	5.44E-03	6.88E-03	

1274	Jun-14	0.03	0.69	26.6	1.7	9.00E-03	1.76E-02
1353	Jun-14	0	3.31	14.0	8.1	1.64E-02	4.43E-02
1353	Jun-14	0.01	1.75	14.0	4.3	9.46E-03	2.34E-02
1354	Jun-14	0.04	0.98	126.4	2.4	5.44E-02	1.19E-01
1354	Jun-14	0.03	0.39	126.4	1.0	3.07E-02	4.72E-02
1355	Jun-14	0.01	0.28	36.8	0.7	7.63E-03	9.85E-03
1355	Jun-14	0.04	0.27	36.8	0.7	7.51E-03	9.50E-03
1356	Jun-14	0.01	3.65	102.0	9.0	1.31E-01	3.57E-01
1356	Jun-14	0.05	3.32	102.0	8.2	1.20E-01	3.24E-01
1351	Jun-14	0	1.09	4.1	2.7	1.91E-03	4.28E-03
1351	Jun-14	0.02	0.57	4.1	1.4	1.23E-03	2.24E-03
1352	Jun-14	0.01	1.86	40.3	4.6	2.87E-02	7.18E-02
1352	Jun-14	0.04	1.43	40.3	3.5	2.31E-02	5.52E-02
1350	Jun-14	0	0.7	48.6	1.7	1.66E-02	3.26E-02
1350	Jun-14	0.03	1.12	48.6	2.8	2.31E-02	5.21E-02
1349	Jun-14	0	0.31	3.9	0.8	8.41E-04	1.15E-03
1340	Jun-14	0	0.23	125.2	0.6	2.40E-02	2.76E-02
1340	Jun-14	0	0.24	125.2	0.6	2.44E-02	2.88E-02
456	Jun-14	0	1.5	48.5	3.7	2.90E-02	6.97E-02
456	Jun-14	0.05	0.35	48.5	0.9	1.12E-02	1.63E-02
1341	Jun-14	0.03	1.6	8.6	3.9	5.39E-03	1.31E-02
1341	Jun-14	0.01	1.06	8.6	2.6	3.91E-03	8.70E-03
1274	Aug-14	0.03	1.52	26.6	2.9	1.24E-02	3.00E-02
1274	Aug-14	0	0.88	26.6	1.7	8.21E-03	1.73E-02
456	Aug-14	0	0.54	48.5	1.0	1.09E-02	1.94E-02
456	Aug-14	0	1.99	48.5	3.8	2.83E-02	7.15E-02
1353	Aug-14	0	1.29	14.0	2.5	5.73E-03	1.34E-02
1353	Aug-14	0	0.8	14.0	1.5	4.04E-03	8.29E-03
1341	Aug-14	0	1.17	8.6	2.2	3.26E-03	7.43E-03
1341	Aug-14	0.03	6.7	8.6	12.8	1.50E-02	4.25E-02
1356	Oct-14	0	31.65	102.0	58.7	7.85E-01	2.33E+0

							0
1356	Oct-14	0	19.64	102.0	36.4	4.91E-01	1.45E+0
							0
1274	Oct-14	0.02	0.41	26.6	0.8	4.99E-03	7.87E-03
456	Oct-14	0.02	0.46	48.5	0.9	9.68E-03	1.61E-02

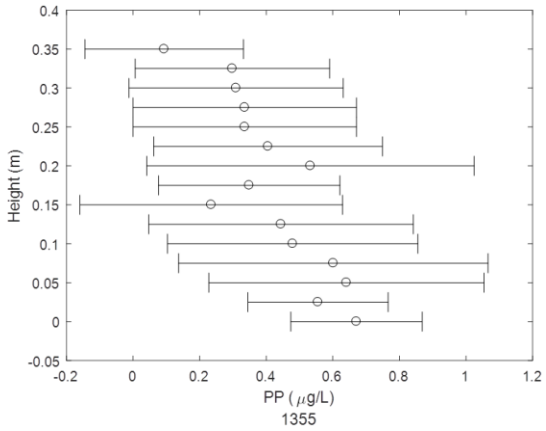
Height (m)
PP (μg/L)
1355

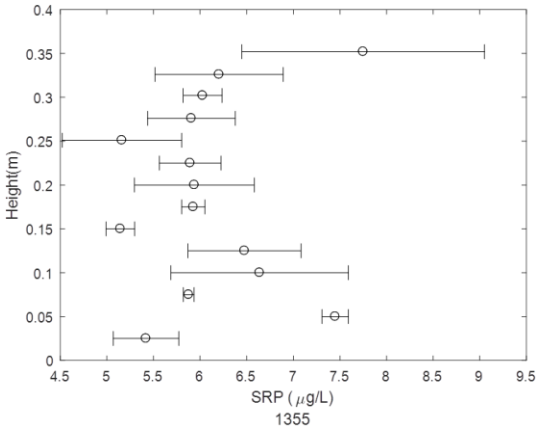
Height(m)
SRP (μg/L)
1355

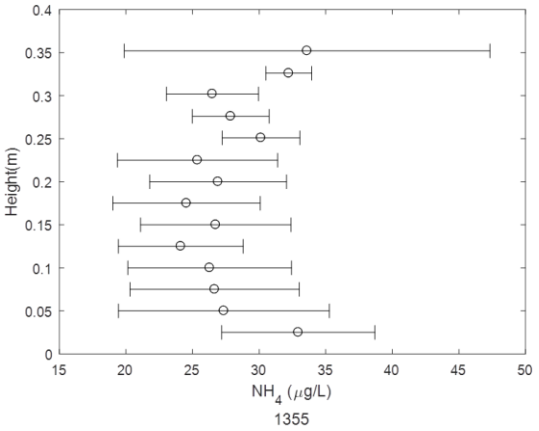
Height(m)
NH_4 (μg/L)
1355

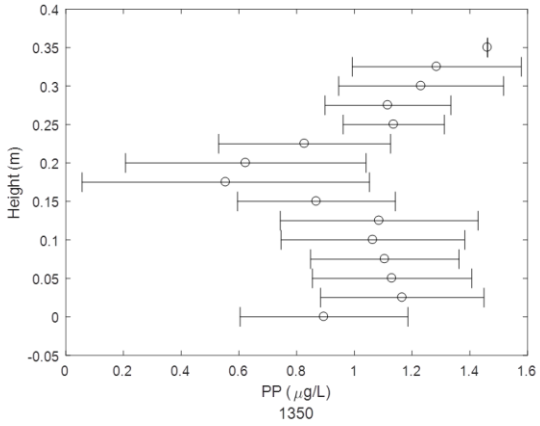
Height (m)
PP (μg/L)
1350

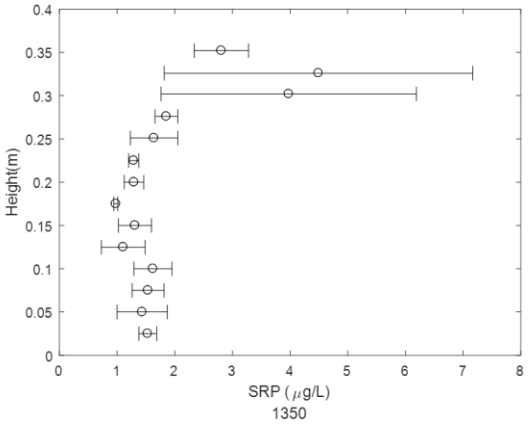
Height(m)
SRP (μg/L)
1350

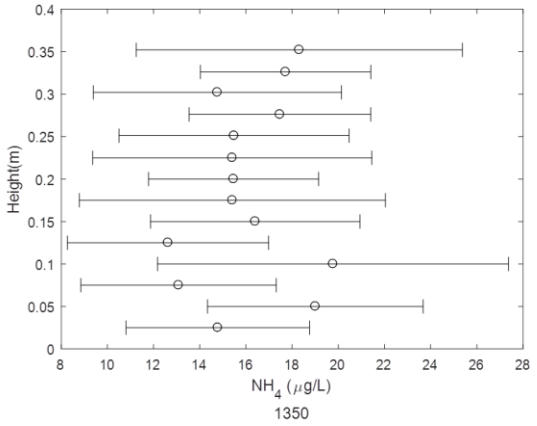
Height(m)
NH_4 (μg/L)
1350

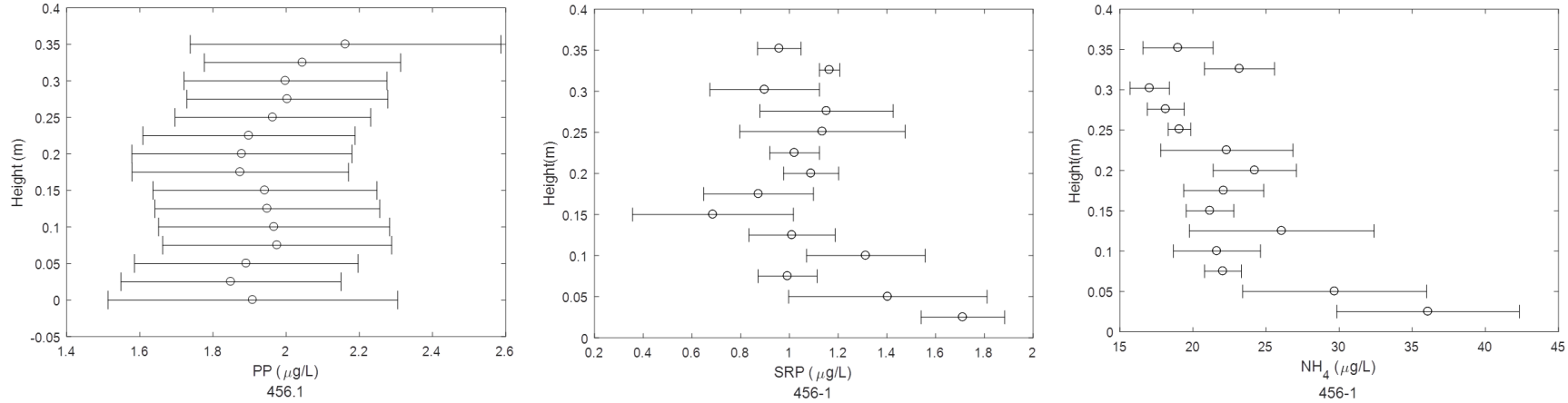

Figure C1. Near-bottom PP, SRP, and NH_4 mean profiles and standard error plots.

Table C2. Station, nominal depth, dreissenid and *Cladophora* biomass

Station	Nominal depth (m)	mean mussel SFDW biomass (g/m^2)	mean *Cladophora* biomass (g/m^2)
1353	3	20.36649	41.31333
1354	5	104.8678	12.29143
1355	10	59.72332	1.672857
1356	18	75.66465	0
1274	3	43.24815	5.580952
1340	5	94.57913	0.509444
456	10	48.02311	0
12	18	22.76635	0
1341	3	16.33493	18.23917
1342	5	65.92922	11.09667
1344	18	51.28257	0
1351	3	11.60655	50.10476
1352	5	41.10243	3.506792
1350	10	48.48469	0.095714
1349	18	20.2147	0

Table C3. Estimates of early season mean PP flux down to and mean SRP flux upward from the bed using Vanderploeg and Dayton estimates. Means are taken from available profile data in May and June 2013-2015.

Station	JPP (g/m2/d)				JSRP (g/m2/d)			
	Vanderploeg		Dayton		Vanderploeg		Dayton	
	Average	SE	Average	SE	Average	SE	Average	SE
1353	1.52×10^{-2}	2.20×10^{-3}	3.23×10^{-2}	4.50×10^{-3}	2.00×10^{-3}	1.00×10^{-4}	1.66×10^{-2}	2.30×10^{-3}
1354	8.10×10^{-2}	2.81×10^{-2}	1.75×10^{-1}	5.83×10^{-2}	1.49×10^{-2}	1.40×10^{-3}	8.94×10^{-2}	2.99×10^{-2}
1355	1.89×10^{-2}	4.40×10^{-3}	3.17×10^{-2}	5.90×10^{-3}	7.70×10^{-3}	1.90×10^{-3}	1.62×10^{-2}	3.00×10^{-3}
1356	1.48×10^{-1}	9.40×10^{-3}	3.12×10^{-1}	1.95×10^{-2}	1.63×10^{-2}	5.00×10^{-4}	1.60×10^{-1}	1.00×10^{-2}
1274	2.49×10^{-2}	8.60×10^{-3}	4.76×10^{-2}	1.54×10^{-2}	4.50×10^{-3}	1.00×10^{-3}	2.44×10^{-2}	7.90×10^{-3}
1340	6.72×10^{-2}	2.70×10^{-2}	1.45×10^{-1}	5.58×10^{-2}	1.31×10^{-2}	1.50×10^{-3}	7.42×10^{-2}	2.86×10^{-2}
456	7.19×10^{-2}	1.04×10^{-2}	1.09×10^{-1}	1.62×10^{-2}	1.53×10^{-2}	1.50×10^{-3}	5.58×10^{-2}	8.30×10^{-3}
1341	1.64×10^{-2}	4.10×10^{-3}	3.18×10^{-2}	7.80×10^{-3}	1.90×10^{-3}	3.00×10^{-4}	1.63×10^{-2}	4.00×10^{-3}
1344	4.21×10^{-2}	0	6.10×10^{-2}	0	5.60×10^{-3}	0.0+00	3.12×10^{-2}	0
1351	3.30×10^{-3}	1.20×10^{-3}	6.00×10^{-3}	1.50×10^{-3}	7.00×10^{-4}	2.00×10^{-4}	3.10×10^{-3}	8.00×10^{-4}
1352	2.96×10^{-2}	1.70×10^{-3}	6.36×10^{-2}	3.50×10^{-3}	5.00×10^{-3}	1.00×10^{-4}	3.25×10^{-2}	1.80×10^{-3}
1350	1.75×10^{-2}	5.30×10^{-3}	2.75×10^{-2}	7.20×10^{-3}	5.60×10^{-3}	9.00×10^{-4}	1.41×10^{-2}	3.70×10^{-3}
1349	1.60×10^{-3}	6.00×10^{-4}	3.50×10^{-3}	1.20×10^{-3}	4.00×10^{-4}	0	1.80×10^{-3}	6.00×10^{-4}

Table C4. Estimates of late season mean PP flux down to and mean SRP flux upward from the bed using Vanderploeg and Dayton estimates. Means are taken from available profile data in August and October 2013-2014.

Station	JPP (g/m2/d)				JSRP(g/m2/d)			
	Vanderploeg		Dayton		Vanderploeg		Dayton	
	Average	SE	Average	SE	Average	SE	Average	SE
1353	1.84×10^{-2}	4.80×10^{-3}	4.51×10^{-2}	1.67×10^{-2}	2.80×10^{-3}	7.00×10^{-4}	2.31×10^{-2}	8.60×10^{-3}
1354	6.01×10^{-2}	4.00×10^{-3}	1.81×10^{-1}	1.43×10^{-2}	1.06×10^{-2}	4.00×10^{-4}	9.29×10^{-2}	7.30×10^{-3}
1355	1.08×10^{-1}	7.90×10^{-3}	3.11×10^{-1}	2.22×10^{-2}	1.48×10^{-2}	5.00×10^{-4}	1.59×10^{-1}	1.14×10^{-2}
1356	3.57×10^{-1}	1.93×10^{-1}	5.90×10^{-1}	2.96×10^{-1}	2.60×10^{-2}	7.90×10^{-3}	3.02×10^{-1}	1.52×10^{-1}
1274	3.92×10^{-2}	1.13×10^{-2}	9.50×10^{-2}	3.43×10^{-2}	5.60×10^{-3}	1.30×10^{-3}	4.86×10^{-2}	1.76×10^{-2}
1340	7.32×10^{-2}	1.64×10^{-2}	2.14×10^{-1}	4.34×10^{-2}	1.07×10^{-2}	1.10×10^{-3}	1.10×10^{-1}	2.22×10^{-2}
456	7.06×10^{-2}	1.89×10^{-2}	1.67×10^{-1}	5.36×10^{-2}	8.10×10^{-3}	1.30×10^{-3}	8.54×10^{-2}	2.75×10^{-2}
12	3.13×10^{-2}	6.80×10^{-3}	9.74×10^{-2}	2.05×10^{-2}	5.50×10^{-3}	5.00×10^{-4}	4.99×10^{-2}	1.05×10^{-2}
1341	1.58×10^{-2}	5.80×10^{-3}	2.57×10^{-2}	9.20×10^{-3}	1.40×10^{-3}	2.00×10^{-4}	1.31×10^{-2}	4.70×10^{-3}
1351	5.99×10^{-2}	4.53×10^{-2}	1.72×10^{-1}	1.27×10^{-1}	5.40×10^{-3}	3.10×10^{-3}	8.81×10^{-2}	6.50×10^{-2}
1352	1.11×10^{-1}	2.60×10^{-3}	3.17×10^{-1}	7.20×10^{-3}	1.13×10^{-2}	2.00×10^{-4}	1.62×10^{-1}	3.70×10^{-3}
1350	8.21×10^{-2}	3.54×10^{-2}	2.38×10^{-1}	9.82×10^{-2}	9.90×10^{-3}	2.40×10^{-3}	1.22×10^{-1}	5.03×10^{-2}
1349	3.40×10^{-2}	8.50×10^{-3}	1.05×10^{-1}	2.58×10^{-2}	5.40×10^{-3}	6.00×10^{-4}	5.39×10^{-2}	1.32×10^{-2}